

Studies of Bruton's tyrosine kinase inhibitors in B-cell malignancies

Thesis submitted for the degree of
Doctor of Philosophy
At the University of Leicester

Harriet Sarah Walter
MBChB BMedSci MSc MRCP(UK)

February 2018

Abstract

Studies of Bruton's tyrosine kinase inhibitors in B-cell malignancies

Harriet S. Walter

Despite significant advances, the prognosis in relapsed/refractory (R/R) B-cell malignancies remains poor. In the Phase I study of the selective Bruton's Tyrosine Kinase inhibitor (BTKi) tirabrutinib in R/R B-cell malignancies, I showed that targeting BTK demonstrated remarkable clinical responses and tolerability in Chronic Lymphocytic Leukaemia and Mantle Cell Lymphoma. Targeted DNA sequencing demonstrated that no mutations were associated with a lack of response in CLL. However, in activated B-cell like diffuse large B-cell lymphoma (ABC DLBCL), only 35% of patients responded to treatment and median duration of response was 12 weeks. This prompted my laboratory studies to explore mechanisms of resistance to BTKi in ABC DLBCL. Using BTKi resistant cell lines TMD8 RO and TMD8 RI, I undertook biological and genetic studies. BTK expression and subcellular localisation was not altered in the resistant cell lines. Apoptosis induced by the BTKi ibrutinib and tirabrutinib occurred 24 hours following drug exposure. A decrease in the expression of the anti-apoptotic proteins MCL1, BCLxL and BCL2A1 was observed in TMD8 but not TMD8 RO following treatment with tirabrutinib, consistent with modulation of the BCR pathway. No significant change was identified in apoptotic gene expression. Study of the BCR signalling pathway showed an increase in cell surface expression of sIgM and CD20 in the resistant cell lines. No change in IgM RNA levels nor CD20 were observed. However, gene expression of *IGJ* was downregulated in the resistant cell lines. Both TMD8 RO and TMD8 RI showed increased basal levels of phosphotyrosine phosphorylation and amplified BCR signalling following BCR ligation. Collectively, these studies indicate hyperactivation of the BCR signalling pathway in the development of resistance to BTKi, with changes occurring upstream of BTK. Further studies to characterise changes at the cell surface are required to identify novel therapeutic approaches to the development of BTKi resistance.

Acknowledgements

I would like to begin by thanking my supervisors, Prof. M.J.S Dyer, Prof. S Wagner and Dr S. Jayne for their guidance, help and encouragement during my PhD studies. I am particularly grateful to Professor Dyer who never seemed to mind being interrupted on his MANY MANY MANY holidays to answer my questions and Dr S. Jayne for her patience, expertise and teaching. I wish to acknowledge and thank The Ernest and Helen-Scott Haematological Research Institute who generously funded my PhD studies and my committee members who provided direction to my studies. I would also like to thank in the Dyer Laboratory, Dr M. Vogler, Mr R. Kozaki, Mr K. Tsumato, Dr Jagdish Mahale and all in Lab 3.42 who helped me throughout my studies, teaching and advising me and helping to collect samples from the clinic. Thank you also to Professor Cain, Mrs B. Juke-Jones and Dr C. Langlais within the MRC Toxicology Unit, University of Leicester, for their expertise, guidance and undertaking of proteomic sample analysis.

I am grateful to the staff within the Departments of Haematology at Leicester Royal Infirmary for their assistance with patient recruitment and advice and to Dr Clare Hutchinson for her initial work on the trial. Thank you to the Hope Clinical Trials Facility for allowing me to hold our trials clinics on the unit, which by the end of the 3 years involved multiple weekly clinics, and in particular our fantastic team of haematology research nursing staff Jayne Denyer, Pam Fermaham, Lydianne Lock and Diane Morris, who looked after all our patients on trial and provided such excellent care. I thank also the referring centres of expertise for their kind referrals.

These studies would not have been possible without our brave patients who entered the clinical trial and generously donated samples to the Haematology Research Tissue Bank. I thank you all. I also thank those in ONO Pharma UK, particularly Dr K. Duffy; Dr T. Yoshizawa at ONO Pharmaceutical Co., Japan; and Drs H. Collins and S. Mitra at Gilead Sciences for their help, review and sharing of data to enable the production of the trial manuscripts.

Finally I would like to thank my family and friends for their support and encouragement to complete my thesis.

Table of Contents

Abstract	1
Acknowledgements	2
Table of Contents	3
List of Tables	9
List of Figures	11
List of Abbreviations	14
Chapter 1 Introduction	19
1.1 Cellular origin of B cell Lymphomas	20
1.2 Epidemiology of Non Hodgkin Lymphoma	21
1.3 Pathogenesis of lymphoid malignancies	23
1.3.1 Diffuse Large B Cell Lymphoma	24
1.3.1.1 DLBCL cell of origin	27
1.3.1.2 Methods for determining COO	30
1.3.1.3 ABC DLBCL	31
1.3.1.4 GCB DLBCL	32
1.3.1.5 Double hit lymphoma	33
1.4 Current therapeutic approaches in DLBCL	33
1.5 Clinical Prognostic Factors in DLBCL	35
1.6 B Cell Receptor Signalling	36
1.6.1 Tonic versus antigen dependent BCR signalling	38
1.6.2 Chronic active BCR signalling	39
1.7 Lipid Rafts	40
1.8 BTK	41
1.8.1 PH domain	42
1.8.2 TH domain	43
1.8.3 SH3 domain	43
1.8.4 SH2 domain	43
1.8.5 Kinase domain	44
1.8.6 BTK phosphorylation	44
1.9 X-Linked Agammaglobulinaemia	44
1.10 BTK inhibitors	45
1.10.1 Preclinical development of Tirabrutinib (ONO/GS-4059)	48

1.10.2 Combination preclinical studies	50
1.11 Clinical activity of BTKi in the treatment of B-cell malignancies	50
1.11.1 Ibrutinib	51
1.11.1.1 Chronic lymphocytic leukaemia	51
1.11.1.2 Mantle cell lymphoma (MCL)	52
1.11.1.3 Waldenstroms Macroglobulinaemia	52
1.11.1.4 DLBCL	52
1.11.1.5 Safety and tolerability of ibrutinib	54
1.11.2 Tirabrutinib	55
1.11.3 CC-292	55
1.11.4 Acalabrutinib (ACP-196)	56
1.11.5 Other BTKi in clinical trials	56
1.12 Resistance to BTKi	56
1.13 Aims of this study	57
Chapter 2 Materials and Methods	58
2.1 Cell Culture	58
2.1.1 Cell lines	58
2.1.2 Cryopreservation and recovery of cell lines	58
2.1.3 Generation of TD8 resistant cell lines	59
2.1.4 Isolation of Peripheral blood mononuclear cells from patient samples	59
2.1.5 Cell viability	60
2.1.6 Cell growth	60
2.2 CellTiter-Glo Luminescent ATP assay	61
2.3 Flow cytometry	61
2.3.1 Apoptosis assays	62
2.3.2 Immunophenotyping	63
2.3.3 Measurement of mitochondrial membrane potential	63
2.4 Western Blotting	64
2.4.1 Whole cell lysis	64
2.4.2 Nuclear and cytoplasmic fractionation and lysis	65
2.4.3 Lipid raft extraction	66

2.4.4 Membrane fractionation discontinuous sucrose density gradients	67
2.4.5 Measurement of protein concentration	68
2.4.6 Protein electrophoresis and western blotting	69
2.5 Immunoprecipitation	71
2.5.1 Preparation of buffers	71
2.5.2 Primary antibody and sample incubation	72
2.5.3 Preparation of protein A sepharose beads and addition to protein and antibody sample	72
2.5.4 Elution of the immunoprecipitate	72
2.6 Mass spectrometry	73
2.7 Cell stimulation assays	74
2.7.1 IgM stimulation	74
2.8 RNA analysis	75
2.8.1 RNA extraction	75
2.8.2 Gene expression profiling	75
2.9 DNA analysis	76
2.9.1 DNA extraction for whole exome sequencing	76
2.9.2 Whole exome sequencing	76
2.9.3 PCR	77
2.10 Analysis of prognostic markers and targeted sequencing using a 36 gene targeted sequencing panel of patients with CLL treated with tirabrutinib on the Phase 1 clinical trial	77
Chapter 3 Clinical Experience of Tirabrutinib	80
3.1 Study objectives and design	81
3.2 Clinical response to the selective BTKi tirabrutinib	82
3.2.1 Chronic Lymphocytic Leukaemia	82
3.2.2 Mantle cell Lymphoma	85
3.2.3 Diffuse Large B cell lymphoma	86
3.3 Safety and Tolerability	86
3.4 Late onset infection-associated driven neutropenia in a patient with CLL receiving 400mg tirabrutinib OD	87

3.5 Discussion	90
3.6 Conclusion	91
Chapter 4 Characterisation of the genomic profile of patients with CLL treated with tirabrutinib on the Phase I clinical trial using a 36 gene targeted sequencing panel	94
4.1 Novel gene mutations and their potential prognostic significance	94
4.2 Clinical Implications of Next Generation Sequencing (NGS) studies in CLL	95
4.3 Impact of BTKi on the treatment of patients with CLL with high risk features	97
4.4 Results	98
4.4.1 Laboratory prognostic factors	98
4.4.2 Targeted sequencing	100
4.5 Discussion	102
4.6 Conclusion	103
Chapter 5 Characterisation of BTKi resistant TMD-8 cell lines	105
5.1 Introduction	105
5.2 Establishment of tirabrutinib and ibrutinib resistant TMD8 cell lines	105
5.2.1 Cell growth and size	106
5.3 BTKi-induced cell death in TMD8 and TMD8 RO and TMD8 RI	108
5.3.1 Ibrutinib and tirabrutinib induce apoptosis in TMD8	108
5.4 Expression of the anti-apoptotic proteins in TMD8 cell lines following exposure to tirabrutinib	115
5.4.1 Role of the BH3-only protein BIM in TMD8	119
5.5 Immunophenotype of TMD8 cell lines	121
5.5.1 Surface IgM (sIgM) expression	121
5.5.2 CD5 expression	122
5.5.3 CD20 expression	123
5.6 A genetic basis to the acquired resistance of TMD8 cells to BTK inhibitors?	126
5.6.1 Changes in gene expression assessed by microarray	127

5.6.2 Changes in gene expression within the BCR signalling pathway	132
5.7 Whole exome sequencing of TMD8 cell lines	134
5.8 Discussion	140
Chapter 6 Proteomic characterisation of the BCR signalling pathway in TMD8 cell lines	143
6.1 Introduction	143
6.2 Subcellular localisation of BTK	143
6.3 BCR signalling	145
6.3.1 Phospho-tyrosine phosphorylation is increased in the BTKi resistant cell lines basally and following IgM stimulation	145
6.3.2 Changes downstream of the BCR	147
6.3.2.1 BTK autophosphorylation following IgM crosslinking in TMD8 cell lines	147
6.3.2.2 Signalling downstream of BTK	148
6.4 BTK immunoprecipitation studies	150
6.5 Lipid rafts	153
6.5.1 Lipid raft proteins identified by mass spectrometry	154
6.5.2 Upregulation of proteins within the resistant cell line lipid rafts	160
6.5.3 Downregulation of proteins within the resistant cell line lipid rafts	161
6.6 Discussion	163
Chapter 7 Discussion	165
7.1 Results from the Phase I clinical trial of tirabrutinib	165
7.2 Characterisation of BTKi resistant TMD8 cell lines	168
7.3 Proteomic characterisation of the BCR signalling pathway in TMD8 cell lines	169
Appendices	170
A.1 National Cancer Institute Common Toxicity Criteria for Adverse Events (CTCAE) Version 4.0 and Criteria for defining Dose Limiting	170

Toxicities (DLTs)	
A.2 Criteria for response	172
A.3 A phase 1 clinical trial of the selective BTK inhibitor ONO/GS-4059 in relapsed and refractory mature B-cell malignancies.	174
A.4 New Agents to Treat Chronic Lymphocytic Leukaemia.	183
A.5 Long-term follow up of patients with CLL treated with the selective Bruton’s tyrosine kinase inhibitor ONO/GS-4059.	185
A.6 List of publications and peer reviewed abstracts	188
References	190

List of Tables

Chapter 1

Table 1.1 DLBCL IHC by Site, and Flow Cytometric Immunophenotype	26
Table 1.2 Identified genetic mutations by next generation sequencing in ABC, GCB, and PMBL DLBCL according to pathway analysis and frequency	29
Table 1.3 The NCCN-IPI	36
Table 1.4 BTKi in pre-clinical and clinical development	48

Chapter 2

Table 2.1 Lysis buffer	65
Table 2.2 Hypotonic Buffer Solution	65
Table 2.3 1x Cell Extraction Buffer Formulation	65
Table 2.4 BSA standard preparation	68
Table 2.5 4x SDS Sample buffer	70
Table 2.6 List of primary antibodies used	70
Table 2.7 Secondary antibodies conjugated to HRP	71
Table 2.8 Immunoprecipitation buffer	71
Table 2.9 Wash buffer	71
Table 2.10 Primers	77
Table 2.11 List of genes on the Sistemas Genomicos CLL NGS panel	79

Chapter 4

Table 4.1 Summary table of the frequency of mutations in different genes identified in studies reporting the results of NGS in CLL treatment naïve and R/R patients	97
Table 4.2 Cytogenetics and IGHV status of CLL patients on study	99
Table 4.3 Targeted mutational analysis of 27 CLL patients at the time of trial entry	101

Chapter 5

Table 5.1 Calculated EC50 values for apoptosis induction in the parental and resistant TMD8 cell lines following exposure to tirabrutinib and ibrutinib	111
Table 5. 2 (a) Genes upregulated > 2 fold in both TMD RO and TMD8 RI (b)	128

Genes downregulated > 2 fold in both TMD RO and TMD8 RI	
Table 5.3 Identified mutations and base pair changes in TMD8 RO and TMD8 RI when compared to TMD8	135
Chapter 6	
Table 6.1 Proteins identified following immunoprecipitation of BTK in TMD8, TMD8 RO and DoHH2	152
Table 6.2 Lipid raft proteins identified within the TMD8 cell line	155
Table 6.3 Lipid raft proteins identified by mass spectrometry in TMD8, TMD8 RO and TMD8 RI	155
Table 6.4 Proteins identified only within the lipid rafts of the resistant cell lines	157
Table 6.5 Pathways associated with proteins upregulated > 2 fold in the lipid rafts of the resistant cell lines (DAVID and KEGG pathway analysis)	161
Table 6.6 Pathways associated with proteins downregulated > 2 fold in the lipid rafts of the resistant cell lines (DAVID and KEGG pathway analysis)	162

List of figures

Chapter 1

Figure 1.1 Cellular origin of human B cell lymphomas	21
Figure 1.2 Age Specific Incidence of DLBCL per 100 000 population and estimated number of new cases per year in the UK (2004-20014).	22
Figure 1.3 50 most mutated genes in diffuse large B-cell lymphoma as registered at the Catalogue of Somatic Mutations in Cancer database).	27
Figure 1.4 Decision tree for IHC classification of DLBCL according to the Hans algorithm).	30
Figure 1.5 Outcome for all patients with DLBCL treated with R-CHOP in British Columbia between 2001 and 2013 and according to stage at diagnosis.	34
Figure 1.6 Structure of the BCR.	38
Figure 1.7 Tonic and chronic active BCR signalling (a) Tonic BCR signalling (b) Chronic BCR signalling.	39
Figure 1.8 Domain structure of BTK showing interaction of binding partners with each domain.	42
Figure 1.9 (a) Structure of Ibrutinib (PCI-32765) (b) Kinome of Ibrutinib: 1000nM Discover RX kinome scan against 442 kinases (c) Ibrutinib inhibits 11 different kinases with an IC50 of about 10nM BTK, BLK, BMX, CSK, FGR, BRK, HCK, EGFR, YES, ErbB2 and ITK.	47
Figure 1.10 (a) Chemical structure of Tirabrutinib (b) Kinomescan dendrogram report of tirabrutinib binding to human kinases. Tirabrutinib was assessed for its ability to interact with 442 kinases using KINOMEscan platform.	49

Chapter 3

Figure 3.1 Patient enrolment by disease subtype and disposition within the trial	82
Figure 3.2 Temporary interruption of tirabrutinib 80 mg OD in a patient with CLL for surgery for resection of a stage I colorectal adenocarcinoma.	84
Figure 3.3 Neutrophil count over time for a patient with a diagnosis of CLL on the Phase I study.	90

Chapter 4

- Figure 4.1 Dose escalation has the potential to re-establish response to therapy: Case study of a patient with TP53 mutation who responded for 31 cycles to 40mg tirabrutinib and for a further 12 months on 600mg tirabrutinib. 100
- Figure 4.2 Cluster diagram of gene mutations 102

Chapter 5

- Figure 5.1 Cell growth of TMD8, TMD8 RO and TMD8 RI cell lines. 107
- Figure 5.2 Cell size of (a) TMD8 (b) TMD8 RO and (c) TMD8 RI cell lines assessed by flow cytometry. 107
- Figure 5.3 Effects of tirabrutinib and ibrutinib on TMD8 and TMD8 RO and TMD8 RI and resistant TMD8 cell lines. 110
- Figure 5.4 Measurement of mitochondrial membrane potential in TMD8 and TMD8 RO cells with and without treatment with tirabrutinib. 112
- Figure 5.5 Effect of Q-VD-OPH on tirabrutinib induced apoptosis in TMD-8 cell lines. 113
- Figure 5.6 PARP and caspase 3 cleavage in the TMD8 cell line following treatment with tirabrutinib in the presence and absence of Q-VD-OPH. 114
- Figure 5.7 Expression of BCL2 family proteins in TMD8 and TMD8 RO cell lines. 116
- Figure 5.8 Effects of TMD8 and TMD8 RO nucleofection with MCL1, BCLxL or BCL2A1 siRNA's on protein expression. 117
- Figure 5.9 TMD8 and TMD8 RO cell lines treated with control, or MCL1, BCLxL or BCL2A1 siRNA prior to addition of 0, 1, 10, 100 and 1000nM tirabrutinib for 24 hrs and assessment of cell viability using the CellTiter-Glo Luminescent Cell Assay. 118
- Figure 5.10 TMD8 nucleofection with BIM small interfering RNA (siRNA). 119
- Figure 5.11 Effect on TMD8 cell viability following nucleofection with BIM siRNA. 120
- Figure 5.12 sIgM expression on the TMD8 and TMD8RO and RI cell lines assessed by flow cytometry. 122
- Figure 5.13 CD5 expression on the TMD8 and TMD8RO and RI cell lines assessed by flow cytometry. 123

Figure 5.14 CD20 by flow cytometry on the TMD8 and TMD8RO and RI cell lines assessed by flow cytometry.	126
Figure 5.15 (a) Venn diagram to show >2 fold gene expression upregulation in the resistant cell lines TMD8 RO and TMD8 RI when compared to the parental cell line TMD8 (b) Venn diagram to show >2 fold gene expression downregulation in the resistant cell lines TMD8 RO and TMD8 RI when compared to the parental cell line TMD8.	127
Figure 5.16 Sanger sequencing to show the BTK C481S and PLCG2 mutations identified within the resistant cell lines.	137

Chapter 6

Figure 6.1 Expression of BTK in TMD8, TMD8 RO and TMD8 RI cell lines.	144
Figure 6.2 Expression of nuclear and cytoplasmic BTK following cellular fractionation in the cell lines TMD8, DoHH2, TMD8 RO and TMD8 RI.	144
Figure 6.3 Total phosphotyrosine levels in TMD8 cells following sIgM crosslinking.	146
Figure 6.4 Protein expression of BTK and pBTKY223 in TMD8 and TMD8 RO following treatment with tirabrutinib +/- sIgM crosslinking.	147
Figure 6.5 Protein expression in TMD8 and TMD8 RO cell lysate following treatment with tirabrutinib +/- sIgM crosslinking.	149
Figure 6.6 Immunoprecipitation of TMD8 cell line with anti IgG or anti-BTK and subject to immunoblot analysis with anti-BTK.	151
Figure 6.7 Venn diagram showing the number of lipid raft proteins identified in the TMD8, TMD8 RO and TMD8 RI cell lines and overlapping distribution.	156

Abbreviations

ABC	Activated B cell-like
ABC DLBCL	Activated B cell-like diffuse large B cell lymphoma
AE	Adverse event
AF	Atrial fibrillation
AID	Activation-induced cytidine deaminase
AIDS	Acquired immunodeficiency syndrome
ALL	Acute lymphoblastic leukaemia
BCL2	B cell leukaemia/lymphoma 2
BCL6	B cell lymphoma 6
BCR	B cell receptor
BID	Twice a day
BLNK	B cell linker
BMX	Bone marrow expressed kinase
BTK	Bruton's tyrosine kinase
BTKi	Bruton's tyrosine kinase inhibitor
CBM	CARD11, BCL10, MALT1 complex
CCND1	Cyclin D1
CD	Cluster of Differentiation
CHOP	Cyclophosphamide, Doxorubicin hydrochloride (Adriamycin), Vincristine (Oncovin), Prednisolone
CLL	Chronic lymphocytic leukaemia
CML	Chronic myeloid leukaemia
CNS	Central nervous system
COO	Cell of origin
CR	Complete response
DAG	Diacylglycerol
dbSNP	Database of single nucleotide polymorphisms
DHL	Double hit lymphomas
DLBCL	Diffuse large B cell lymphoma

DLT	Dose limiting toxicity
DMSO	Dimethylsulphoxide
DNA	Deoxyribonucleic acid
DTT	DL-Dithiothreitol
EBV	Epstein-Barr virus
ECOG	Eastern Cooperative Oncology Group
EGFR	Epidermal growth factor receptor
EMA	European Medicines Agency
EXoc2	Exocyst complex component 2
FC	Fludarabine Cyclophosphamide
FCS	Foetal calf serum
FDA	Federal drugs agency
FFPE	Formalin-fixed, paraffin embedded
FISH	Fluorescence in situ hybridization
FITC	Fluorescein isothiocyanate
FL	Follicular lymphoma
FLIP	FLICE like inhibitory protein
FRET	Fluorescence resonance energy transfer imaging
GC	Germinal centre
GCB	Germinal centre B-cell-like
GEP	Gene expression profiling
HDACs	Histone deacetylases
HIV	Human immunodeficiency virus
HL	Hodgkin Lymphoma
HLA	Human leucocyte antigen
Ig	Immunoglobulin
IgG	Gammaglobulins
IGF-I	insulin-like growth factor I
IGH/IGH@	Immunoglobulin heavy locus
IGHV	Immunoglobulin heavy-chain variable region

IHC	Immunohistochemistry
IPI	International Prognostic Index
IP3	Inositol triphosphate
IRF4	Interferon regulatory factor 4
ITAM	Immune-receptor tyrosine based activation motif
ITK	Inducible T cell kinase
LDH	Lactate dehydrogenase level
MALT	Mucosa-associated lymphoid tissue
MCL	Mantle Cell Lymphoma
MHC	Major Histocompatibility complex
μL	Microlitre
μg	Microgram
μM	Micromolar
mL	Millilitre
mg	Milligram
mM	Millimolar
min	Minutes
MMP	Mitochondrial membrane potential
MRD	Minimal residual disease
MS	Multiple sclerosis
MTD	Maximum tolerated dose
MYD88	Myeloid differentiation primary response 88
MZL	Marginal zone lymphoma
NCCN	National Comprehensive Cancer Network
NF-κB	Nuclear factor kappa beta
NGS	Next generation sequencing
NHL	non-Hodgkin Lymphoma
nM	Nanomolar
OBD	Optimum biological dose
OD	Once daily

ORR	Overall response rate
OS	Overall survival
PBMCs	Peripheral blood mononuclear cells
PCR	Polymerase chain reaction
PD	Pharmacodynamics
PFS	Progression free survival
PH	Pleckstrin homology
PI	Propidium Iodide
PI3K	Phosphatidylinositol-4,5-bisphosphate 3-kinase
PIP2	Phosphatidylinositol 4,5-bisphosphate
PI(4)P2	phosphatidylinositol-4-phosphate
PI(3,4,5)P3	phosphatidylinositol-3,4,5-trisphosphate
PK	Pharmacokinetic
PKC	Protein kinase C
PLCG2	Phospholipase C Gamma 2
PMSF	Phenylmethylsulfonylfluoride
PRDM1	PR/SET Domain 1
RA	Rheumatoid arthritis
R-CHOP	Rituximab, cyclophosphamide, doxorubicin, vincristine and prednisone
RIN	RNA integration number
RLK	Resting lymphocyte kinase
RNA	Ribonucleic acid
RNAi	RNA interference
RP2D	Recommended Phase II dose
R/R	Relapsed/refractory
shRNA	Small hairpin RNAs
SH2	SRC Homology 2
SH3	SRC Homology 3
SLE	Systemic lupus erythematosus
SLL	Small lymphocytic leukaemia

STR	Short tandem repeat
TCR	T cell receptor
TH	Tec homology
TMRE	Tetramethylrhodamine ethyl ester
UK	United Kingdom
WASP	Wiskott–Aldrich syndrome protein
WHO	World Health Organisation
WM	Waldenstroms Macroglobulinaemia
Xid	X linked immunodeficiency
XLA	X-linked agammaglobulinaemia

Chapter 1 Introduction

Approximately 20 new cases of lymphoma are diagnosed per 100 000 population per year (1), of which around 95% are of B cell and 5% of T cell origin. Mature B cell malignancies result from uncontrolled growth of lymphoid B cells during their maturation. They can originate at any stage of mature B cell development, but most commonly occur in B cells following migration to germinal centres, where they undergo proliferation and diversification of immunoglobulin genes through somatic hypermutation and heavy chain class switching. According to the latest World Health Organisation (WHO) classification there are over 30 different subtypes of B cell lymphoma (2). Specific diagnostic entities include chronic lymphocytic leukaemia (CLL), mantle cell lymphoma (MCL), follicular lymphoma (FL), diffuse large B cell lymphoma (DLBCL) and Waldenstrom's Macroglobulinaemia (WM).

Despite significant therapeutic advances in the management of non-Hodgkin lymphoma (NHL) and improvement in prognosis, relapsed/refractory (R/R) disease remains a considerable challenge. In R/R disease, there is no standard of care, and prognosis remains poor. Furthermore chemo-immunotherapy can result in significant toxicity, limiting tolerability; and as a disease that occurs more frequently in the elderly population, many patients are unsuitable for dose intensive regimens. A number of precision medicines that target cell surface receptors, intracellular signalling pathways, transcription factors and epigenetic proteins that provide a mechanism based therapeutic approach are currently being investigated in R/R disease to attempt to improve outcome. However the development of novel and effective therapies in haematological malignancies brings considerable challenges due to the biological and molecular heterogeneity of disease and lack of good preclinical models. Like chemo-immunotherapy, ultimately resistance to precision medicine occurs and it is therefore critical that we improve our understanding of resistance in order to develop more effective targeted therapies.

DLBCL is the most common form of non-Hodgkin lymphoma (NHL) (3) and in the R/R setting there remain significant challenges. Treatment with Rituximab, cyclophosphamide, doxorubicin, vincristine and prednisone (R-CHOP) chemo-

immunotherapy results in a cure rate of approximately 70% (4-6). However, in patient's refractory to R-CHOP or in those who relapse early, prognosis is poor with a median survival of about 6 months. Improving current treatment strategies and developing novel therapeutic approaches to improve the outcome within this relapsed/refractory (R/R) population in DLBCL remains an unmet need and forms the focus for the laboratory work detailed within my thesis.

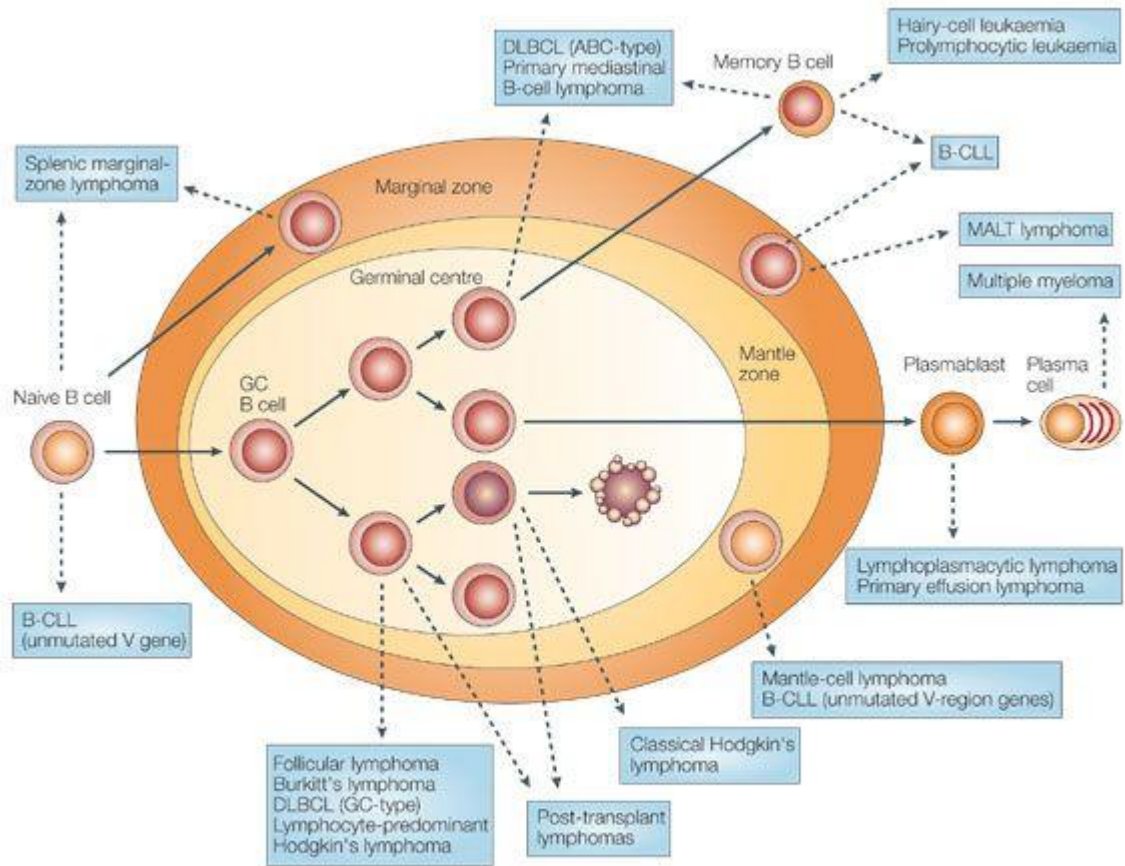
1.1 Cellular Origin of B cell Lymphomas

Normal B cell development and differentiation involves a number of distinct stages (7). Early B cell development occurs in the bone marrow where re-arrangement of immunoglobulin heavy and light chain genes takes place (8). When a B cell precursor expresses a functional B cell receptor (BCR) that is not auto-reactive, it can exit the bone marrow and circulate as a mature B cell in peripheral blood and secondary lymphoid tissues (8).

On contact with antigen, these mature naïve B cells are activated and enter T cell zones of the secondary lymphatic organs (7). Interaction with T helper cells results in proliferation and differentiation into antibody secreting plasma cells. Some B cells however will enter germinal centres (GCs), where clonal expansion and modification of the Ig genes by somatic hypermutation and class switch recombination occurs (9, 10).

When B cell cells undergo malignant change, the stage of B cell differentiation and development through analysis of the BCR structure and differentiation markers has been used to determine the cellular origin of lymphoma (11, 12) (Figure 1.1). Most lymphomas are derived from GC cell or post GC B cells. More recently, gene expression analysis has enabled further clarification and recognition of distinct disease subtypes (13).

Figure 1.1 Cellular origin of human B-cell lymphomas (7).

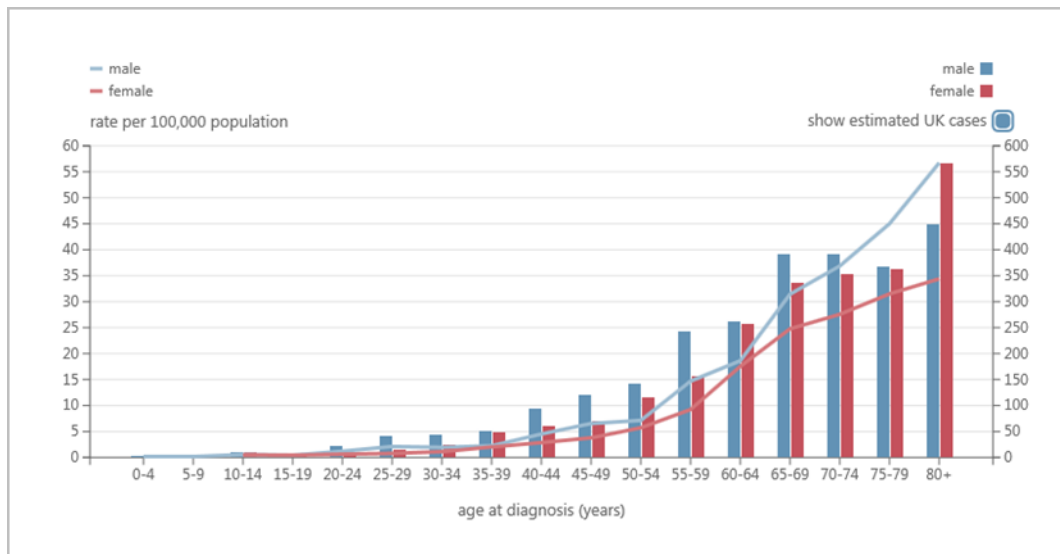


Nature Reviews | Cancer

1.2 Epidemiology of NHL

Of 13,605 new cases of NHL diagnosed in the United Kingdom (UK) in 2014, approximately a third of these cases were classified as DLBCL (14), making this the most common subtype of NHL. Most cases of DLBCL are diagnosed in those over the age of 65, with a median age of diagnosis of 70 years (Figure 1.2). The incidence is greatest in males (8.8 per 100,000 population) with a male to female rate ratio of 1.1:1 (1).

Figure 1.2 Age Specific Incidence of DLBCL per 100 000 population and estimated number of new cases per year in the UK (2004-20014) (1).



Recent understanding of the biology of disease has identified distinct molecular subtypes as described below; it is clear that “DLBCL” comprises a large number of genetically distinct diseases. Typical clinical presentation is with rapidly enlarging nodal disease; however, extranodal disease is present in approximately 40% of patients at diagnosis (7). “B” symptoms of fever, weight loss and drenching night sweats are found in approximately 30% of patients and approximately 60% of patients present with stage III or IV disease (8). Diagnosis is typically made by surgical excision biopsy of an enlarged lymph node, followed by extensive immunohistochemical (IHC) testing, supplemented in some instances by fluorescence in situ hybridization (FISH) and deoxyribonucleic acid (DNA) sequencing analysis.

MCL is comparatively rare, with an incidence of 0.9 per 100, 000 population, and accounting for approximately 5-10% of all NHL (1). It is characterised by the t(11;14)(q13:32) translocation resulting in overexpression of cyclin D1 (15). The median age at diagnosis is 73.9 years and there is a striking male predominance (Male: Female 2:1). Patients typically present with stage III/IV disease with extensive lymphadenopathy, splenomegaly and blood and bone marrow involvement (16). Whilst responsive initially to chemotherapy, it remains an incurable disease.

CLL is the most prevalent form of leukaemia seen within the adult population. In 2014, 3,515 new cases were diagnosed within the UK (17). The incidence increases with age, with a median age at diagnosis of 71.7 years. Approximately 59% of CLL cases in the UK are diagnosed in people aged 70 (17). The incidence per 100,000 population is 7.1 with a male preponderance of 1.8:1 (1).

1.3 Pathogenesis of lymphoid malignancies

Factors contributing to the development of B cell malignancies, can be classified into 3 main groups: hereditary and germ line susceptibilities; acquired immune suppression or immunodeficiency; and immune stimulation.

The risk of DLBCL is increased in individuals with a family history of NHL, with an odds ratio of 1.4 (95% CI 1.1-2.0) (18). In CLL, in approximately 6% of patients, a family history is identified (19). To understand this risk, genome wide association studies have been undertaken. Identified susceptibility loci involve immune response and apoptotic pathways in CLL (20) and include variation in the human leucocyte antigen (HLA) class II region in FL, marginal zone lymphoma (MZL) and DLBCL (20-22). In DLBCL, a susceptibility locus at 6p25.3, which maps near to the gene exocyst complex component 2 (*EXOC2*), is also thought to be important in determining genetic susceptibility (22). *EXOC2* is part of a large multiprotein complex involved in vesicle trafficking and intercellular transfer of viral proteins (23). With most identified susceptibility loci being associated with only low to moderate risk of the development of NHL, screening is not carried out routinely in clinical practice.

Acquired states of immune suppression, for example human immunodeficiency virus (HIV)/ acquired immunodeficiency syndrome (AIDS) and organ transplantation are linked with increased risk of the development of lymphoid malignancies (24). These malignancies are often of DLBCL histology, with extra-nodal involvement, associated with Epstein-Barr virus (EBV) and have an aggressive clinical course. The risk of the development of NHL in HIV-infected individuals in individuals receiving antiretroviral therapy is increased approximately 10 fold (25). Prior to antiretroviral therapy, this risk was increased approximately 100 fold. Similarly this risk is increased by at least 2 fold following organ and stem cell transplantation, with most patients being EBV positive

(2, 26). Intensity, duration of immunosuppression, EBV status of the donor and HLA type and mismatch are thought to be important in determining lymphoma risk post transplantation (27).

An association between both viral and bacterial infections and increased risk of developing lymphoma has been reported (28-30). Bacterial infections have been typically associated with indolent lymphomas, whereas viral infections have been associated with more aggressive diseases. Examples include the association of mucosa-associated lymphoid tissue (MALT) lymphoma of the stomach with *H. Pylori* infection (28), EBV with endemic Burkitt lymphoma (31) and HIV-related lymphomas.

Autoimmune and chronic inflammatory disorders such as rheumatoid arthritis (32) and Crohn's disease (33) have also been linked with increased risk of lymphoma. In rheumatoid arthritis, risk has been linked with disease severity and largely in the development of DLBCL of the activated B cell-like (ABC) subtype (32).

1.3.1 Pathology of DLBCL

DLBCL arises from mature B cells. DLBCL may arise de novo, as a primary disease, or following transformation of a more indolent B-cell malignancy. Lymph nodes typically show complete effacement of the normal architecture by sheets of atypical blastic lymphoid cells. The Kiel classification system subdivides DLBCL based on these morphological findings (34). Centroblastic DLBCL, the most common variant, is composed of cells that resemble the centroblasts found within reactive germinal centres. Immunoblastic morphology is associated with a nongerminal centre B-cell.

DLBCL cells generally express pan-B cell antigens (Cluster of Differentiation 19 (CD19), CD20, CD22, CD79a) (35). Expression of CD45 may be lost. CD30 is present in approximately 25 percent of cases and CD5 is expressed in a small number of cases. The surface immunoglobulin IgM is most frequently expressed. B cell leukaemia/lymphoma 2 (BCL2), B cell lymphoma 6 (BCL6), CD10 and interferon regulatory factor 4 (IRF4) are also expressed in some cases and BCL2 expression has been associated with a worse prognosis (36). The proliferative fraction of cells (Ki-67), is usually higher than 40 percent. CD20 expression, when determined by flow

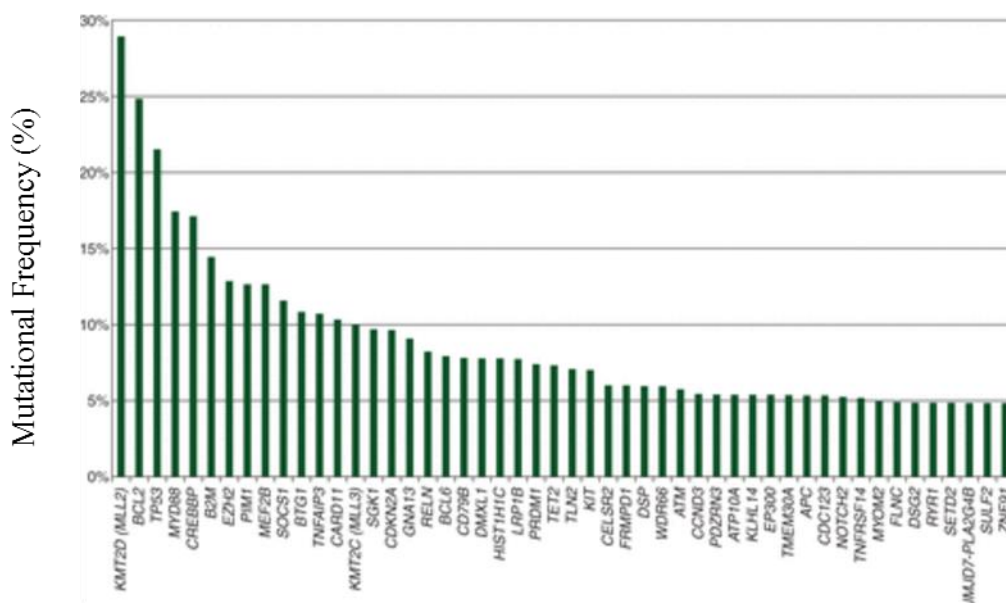
cytometry, has been shown to be heterogeneous. Similar to CLL/small lymphocytic leukaemia (SLL), reduced levels of CD20 have been reported in 16% of diagnostic DLBCL samples by Johnson N., et al (37). 95% of these cases were strongly positive for CD20 by IHC. Importantly patients with reduced levels of CD20 and high CD19 (discordant CD20) by flow cytometry on diagnostic biopsy have been shown to have an inferior overall survival following treatment with either R-CHOP or cyclophosphamide, doxorubicin, vincristine and prednisone (CHOP). Immunophenotype by histological site and flow cytometry in DLBCL is detailed in Table 1.1.

Table 1.1 DLBCL IHC by Site, and Flow Cytometric Immunophenotype (35).

Marker	Function	Lymph node	Mediastinal Subtype	Other Sites	Total	Flow Cytometry
CD20	Membrane bound protein thought to play a role in B cell activation.	92% (166)	93% (43)	96% (318)	94% (527)	94% (50)
CD79a	Required in the initiation of BCR signalling when associated with CD79b and membrane bound immunoglobulin, enabling response to antigen binding.	92% (25)	100% (5)	88% (64)	89% (94)	
PAX5	Critical role in B-cell lineage commitment, differentiation, and function	83% (36)	100% (18)	82% (57)	86% (111)	
CD30	Regulates NF- κ B activity.	52% (40)	64% (44)	40% (41)	52% (125)	
CD23	Role in antibody feedback regulation	50% (10)*	74% (34)	7% (15)	53% (59)	20% (46)
CD5	Negative regulator of T cell and B cell signalling via recruitment of SHP-1	17% (60)*	0% (9)	3% (110)	10% (179)	12% (50)
CD10	Markers of follicular centre B-cell differentiation.	44% (52)	17% (6)	60% (85)	52% (143)	38% (53)
BCL6	Transcriptional repressor.	78% (23)	100% (6)	88% (32)	85% (61)	
CD19	Decreases the threshold for antigen receptor-dependent stimulation.					91% (53)
CD22	Positive regulation of B cell receptor signalling.					97% (35)
Light chain (surface)						57% kappa

Cytogenetic abnormalities are common in DLBCL, but no single genetic abnormality defines DLBCL, reflecting the heterogeneity of this disease. The most commonly mutated genes in DLBCL are shown in Figure 1.3. This is in comparison to MCL where the translocation t(11;14)(q13;q32) between the immunoglobulin heavy locus (*IGH@*) and cyclin D1 (*CCND1*) is found in almost all cases and in FL where 80-90% of cases are associated with the chromosomal translocation t(14;18)(q32;q21) (38, 39). Many however have chromosomal translocations involving the immunoglobulin heavy and light chain genes and somatic mutations of the variable regions of these genes (40).

Figure 1.3 50 most mutated genes in diffuse large B-cell lymphoma as registered at the Catalogue of Somatic Mutations in Cancer database (41).



1.3.1.1 DLBCL cell of origin

Following T cell dependent antigen stimulation, naïve mature B cells enter the GC of secondary lymphoid tissues, where they undergo distinct genetic processes to generate high-affinity antibodies (42). DLBCL arises from either GC cells or B cells that have passed through the GC. Examination of patterns of gene expression in DLBCL, has identified at least three distinct subtypes of DLBCL according to the cell of origin (COO): germinal centre B-cell-like (GCB), which derive from centroblasts; activated B-cell-like (ABC), with features of plasmablastic B cells committed to terminal B cell

differentiation and primary mediastinal, believed to arise from thymic B cells (13). However, this is likely to be an oversimplification of marked diversity and approximately 15% of patients remain unclassifiable according to this molecular classification (43). Furthermore, next generation sequencing (NGS) has enabled driver mutations, including recurrently mutated oncogenes and tumour suppressors, some of which may be common across the subtypes to be identified, highlighting the complexity and heterogeneity in the biology of DLBCL across current classification methods (Table 1.2). For example, the observed downregulation of GC B cell genes (44) and genomic aberrations of PR/SET Domain 1 (*PRDM1*) (45), important in plasmacytic differentiation (46), in ABC DLBCL. Classification according to the COO has significant therapeutic and prognostic implications, with the ABC subtype having a poorer outcome with chemo-immunotherapy and unfavourable prognosis (44-46). Improving our understanding of the molecular heterogeneity of DLBCL is key in improving our understanding of the oncogenic drivers of disease and improving patient outcome using targeted therapies.

Table 1.2 Identified genetic mutations by next generation sequencing in ABC, GCB, and PMBL DLBCL according to pathway analysis and frequency (47).

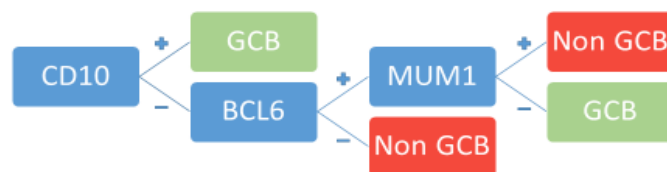
Pathway	ABC (%)	GCB (%)	PMBL (%)
NF-KB			
<i>TNFAIP3</i>	3.6	2.2	9.5
<i>MYD88</i>	7.3	1.8	0
<i>PIM1</i>	20.2	2.2	0
<i>CARD11</i>	3.9	1.6	0
<i>IRF4</i>	4.5	0.9	1.3
<i>PRDM1</i>	5.4	1.1	0
BCR			
<i>CD79A/B</i>	0/6.7	0.4/0.7	0/0
<i>ITPKB</i>	2.4	4.7	8.9
<i>TCF3</i>	0.3	0.4	0
<i>ID3</i>	1.5	0.4	1.9
MAP Kinases			
<i>BRAF</i>	0	0	0
JAK-STAT			
<i>SOCS1</i>	1.5	6.4	15.8
<i>STAT6</i>	0	3.3	13.3
Epigenetic regulation			
<i>EZH2</i>	0	3.3	0.6
<i>KMT2D</i>	10.9	14.4	1.9
<i>EP300</i>	4.2	2.9	1.9
<i>MEF2B</i>	3.3	4.9	1.3
<i>CREBBP</i>	1.8	6.9	1.3
NOTCH			
<i>NOTCH1</i>	1.8	0.2	0.6
<i>NOTCH2</i>	0.6	2.0	0
Apoptosis			
<i>MFHAS1</i>	0.3	2.7	6.3
<i>XPO1</i>	0.3	0.2	4.4
<i>MYC</i>	3.0	4.7	0.6
<i>CDKN2A/B</i>	0.6/0	0.2/0.2	0/0
<i>FOXO1</i>	0.9	2.9	0.6
<i>TP53</i>	4.5	3.3	1.3
<i>GNA13</i>	2.7	4.4	7.6
<i>BCL2</i>	0.3	7.7	0
Immunity			
<i>CIITA</i>	3.0	2.7	8.9
<i>B2M</i>	2.1	4.0	7.0
<i>TNFRSF14</i>	0.6	3.5	0
<i>CD58</i>	1.5	2.9	5.1

1.3.1.2 Methods for determining COO

In the clinical setting, gene expression profiling (GEP) is not routinely conducted outside of the context of a clinical trial. However, this is likely to be of increasing importance clinically, with the current emphasis on development and integration of targeted therapies into clinical practice. Immunohistochemistry (IHC) algorithms are currently used to predict the COO and prognosis based on the use of formalin-fixed, paraffin-embedded (FFPE) tissue. The reproducibility however of these results, is limited by varying laboratory techniques, inter-observer variations and scoring reproducibility (48).

The most commonly used algorithm is the Hans algorithm (49), which stratifies according to GCB or non-GCB subtype based on the protein expression of CD10, BCL6 and IRF4 (Figure 1.4). Evaluation of the concordance of the Hans algorithm with GEP reproduced the gene expression results in 71% of GCB and 88% of non-GCB cases (50). Criticisms made of the Hans criteria are based on its design before the introduction of rituximab into clinical practice and subsequent variable agreement with GEP. Furthermore, the two categories alone identified by the Hans criteria is felt to oversimplify DLBCL and not reflect the clinical variation observed in DLBCL.

Figure 1.4 Decision tree for IHC classification of DLBCL according to the Hans algorithm (49).



1.1.3.3 ABC DLBCL

In the ABC DLBCL subtype, gene expression profiling has shown these cells to have characteristics similar to those of normal B cells activated by cross linking of the B cell receptor (BCR) (13). Cross linking of the B cell receptor is required for the survival and proliferation of mature B cells through activation of downstream tyrosine kinase pathways, including phosphatidylinositol-4,5-bisphosphate 3-kinase (PI3K), RAS-RAF-ERK and nuclear factor kappa beta (NF- κ B) pathways (51). Upregulated genes include *IRF4*, which is transiently induced during normal lymphocyte activation and important in proliferation and *BCL2* and FLICE like inhibitory protein (*FLIP*), inhibitors of apoptosis and important in activation of lymphocytes and peripheral blood B cells.

However, unlike normal B cells in which cross linking of the BCR results in transient activation of the NF- κ B pathway, in ABC DLBCL constitutive activity of the NF- κ B pathway is observed (52). The importance of NF- κ B signalling in ABC DLBCL has been shown by Davies et al., (52) where inhibition of NF- κ B in ABC DLBCL cell lines with a catalytically inactive form of $I\kappa\kappa\beta$ was toxic to ABC DLBCL cell lines but not to GCB DLBCL cell lines.

The CARD11, BCL10, MALT1 (CBM) complex, which is found downstream of the BCR (53), is critical to the activation of the NF- κ B pathway in B cells following BCR stimulation. In the context of normal BCR signalling, phosphorylation of CARD11 by PKC β , results in a conformational change and association with BCL10 and MALT1, forming an active CBM complex (54); in the ABC subtype this complex is active constitutively. This may result from activating mutations of CARD11 in approximately 10% of patients or through chronic active BCR signalling (refer to section 1.6).

Activation of the NF- κ B pathway may also occur through the adaptor protein, myeloid differentiation primary response 88 (MYD88). A ribonucleic acid interference (RNAi) screen, using small hairpin RNAs (shRNAs) targeting *MYD88* in the ABC cell lines, OCI-LY3 and OCI-LY10, have shown that MYD88 and its associated kinases, IRAK1 and IRAK4 are essential for survival (55). Furthermore, the amino acid substitution, L265P, in the MYD88 Toll/IL-1 receptor has been found not only in ABC DLBCL cell

lines but also in 29% of ABC DLBCL tumours, suggesting an important role of MYD88 in the pathogenesis of a significant fraction of ABC DLBCL. Transcriptional feedback through activation of JAK/STAT signalling, which further increases NF- κ B activity with resultant increase in NF- κ B target gene expression such as BCL2A1 may further promote NF- κ B signalling (56). Finally, inactivation of TNFAIP3 (A20), described in MALT and nodular sclerosing Hodgkin's lymphoma, resulting in loss of inhibition of NF- κ B signalling, and inhibition of apoptosis may occur (57).

1.3.1.4 GCB DLBCL

In contrast to ABC DLBCL, the GCB DLBCL subtype does not rely on activation of the NF- κ B pathway nor chronic active BCR signalling for survival (52). Activation of the PI3K/AKT/MTOR pathway however is believed to play an important role in GCB DLBCL, due to inactivation of PTEN, a negative regulator of *PI3K*, seen in 55% of cases (58).

The transcription factor *BCL6*, regulates cell growth and apoptosis (59, 60). In GCB DLBCL, deregulated *BCL6* expression is seen, arising either due to translocation or through somatic mutations, which promotes proliferation. *EZH2* has been reported as a gain of function mutation, with a frequency of 20% in GCB DLBCL (61). The somatic point mutation, in exon 15, affecting a single tyrosine (Tyr461), results in increased methylation of histone 3.

Overexpression of *BCL2* is seen both in ABC and GCB DLBCL. However the mechanism by which overexpression occurs is thought to relate to prognostic outcome. In GCB DLBCL *BCL2* overexpression occurs due to the t(14:18)(q32;q21) translocation, which in the re-rituximab era, was found to be significantly associated with a higher relapse rate, worse disease free and overall survival (OS) (62). With the introduction of rituximab to CHOP chemotherapy, this negative impact, particularly in the ABC subtype seems to have been lessened (63).

1.3.1.5 Double hit lymphomas

Double hit lymphomas (DHL) are characterised by dual chromosomal translocations, the t(14;18)(q32;q21) and t(8;14)(q24;q32) or t(8;22)(q24;q11) with resulting overexpression of both *BCL2* and *MYC* respectively. Typically, these DHL have a very aggressive biological behaviour. They can occur in a number of B cell malignancies including FL, acute lymphoblastic leukaemia (ALL) and DLBCL. Recognition of DHL is important as the median OS has been reported as one year in this subgroup of patients (64). Approximately 5% of DLBCL are DHL and most are of GCB subtype (65).

The t(14;18) juxtaposes the *IGH* and the *BCL2* loci, results in overexpression of the anti-apoptotic protein BCL2 (66) and resistance to chemotherapy (67). Overexpression of the *MYC* oncogene can occur due to its juxtaposition with the immunoglobulin heavy chain (*IGH*) in the t(8;14) or due to the juxtaposition in the t(8;22) and t(2;8) light chain variants (68).

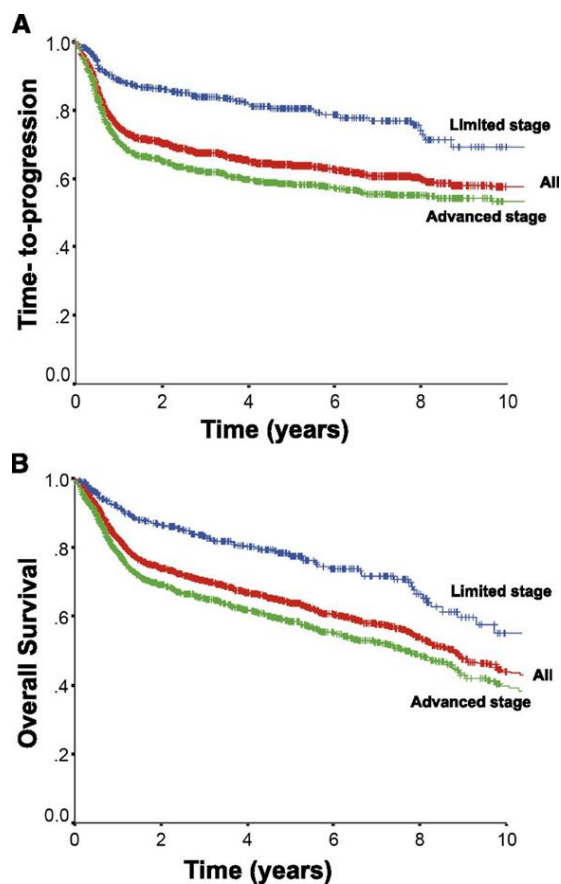
DHL are associated with independent adverse risk factors in DLBCL including B symptoms, high lactate dehydrogenase, advanced age, extra nodal disease, bone marrow involvement, higher Ki-67, Ann Arbor stages III and IV and central nervous system (CNS) disease. Identification of DHL is important in view of the poor outcome associated with R-CHOP chemotherapy.

1.4 Current therapeutic approaches in DLBCL

Untreated, DLBCL follows an aggressive course, with survival measured in months. However for the majority of patients treated with chemo-immunotherapy, cure rates of over 70% are now seen. From the 1970s, until early 2000, the CHOP regimen (cyclophosphamide, doxorubicin, vincristine and prednisone) remained the standard of care, with long term remissions seen in approximately 45% of patients. The addition of further chemotherapy drugs to this standard of care or alternative regimens failed to improve outcomes over CHOP (69-72).

The monoclonal anti-CD20 antibody rituximab showed significant efficacy in low grade lymphomas and was approved for this indication in 1997. Based on these results, rituximab entered clinical trials in DLBCL in combination with CHOP (R-CHOP). Vose et al., conducted a Phase 2 study to determine the safety and efficacy of rituximab in combination with standard-dose CHOP (Rituximab 375mg/m² day 1 for 6 cycles) in previously untreated aggressive NHL (73). The overall response rate (ORR) was 94% (31 of 33 patients) and twenty patients had a complete response (CR) (61%). Importantly, rituximab did not compromise the tolerability of CHOP and all patients completed treatment. Subsequent randomised studies of rituximab in combination with CHOP chemotherapy (R-CHOP) in elderly and young patients alike, confirmed the overall survival benefit seen with rituximab (4-6). Outcome for patients with DLBCL treated with R-CHOP according to stage is shown in Figure 1.5.

Figure 1.5 Outcome for all patients with DLBCL treated with R-CHOP in British Columbia between 2001 and 2013 and according to stage at diagnosis. All, n = 1660; limited stage, n = 433; advanced stage, n = 1227 (74).



The R-CHOP regimen remains today the standard first-line treatment within the UK outside of a clinical trial. Despite the significant survival benefit seen with the addition of rituximab, approximately 30% of all patients will relapse. Currently one of the challenges facing clinicians is the ability to identify those patients who have a poorer prognosis from the outset, using specific biological or clinical factors.

1.5 Clinical Prognostic factors in DLBCL

The International Prognostic Index (IPI), which utilises clinical and biochemical parameters (age >60 years, stage III/IV disease, elevated serum lactate dehydrogenase level (LDH), Eastern Cooperative Oncology Group (ECOG) performance status ≥ 2 , and >1 extranodal site of disease) to stratify patients according to risk has been used for several decades within the clinic.

The addition of rituximab to CHOP, has resulted in the improvement of survival across all risk groups (4, 5). Additional clinical information collected from the National Comprehensive Cancer Network (NCCN) database collected during following the introduction of rituximab into clinical practice, has resulted in the enhanced IPI (75). This relies on the five predictors; age, LDH, sites of involvement, Ann Arbor stage, ECOG performance status (Table 1.3). Four risk groups for 5-year OS: low (L, 0-1 pt), low-intermediate (L-I, 2-3 pts), high-intermediate (H-I, 4-5 pts), and high (H, ≥ 6 pts) were identified. This model shows improved prediction of outcome (both OS and PFS) compared with the original IPI.

Table 1.3 The NCCN-IPI (75).

NCCN-IPI	Score
Age (years)	
>40 to ≤60	1
>60 to ≤75	2
>75	3
LDH, normalized	
>1 to ≤3	1
>3	2
Ann Arbor stage III-IV	1
Extranodal disease (disease in bone marrow, CNS, liver/GI tract or lung)	1
Performance status ≥2	1

However this score does not take into consideration the biological heterogeneity of disease nor guide therapeutic choice. More recently, molecular profiling has enhanced our understanding of DLBCL tumour biology, and identified specific molecular subtypes, and tumour signatures, which have prognostic implications. The ABC subtype exhibits an inferior outcome following R-CHOP (3-year progression-free survival (PFS) of 40% vs 75%. Most importantly, these distinctions and understanding that these subtypes are driven by different oncogenic signalling pathways have informed therapeutic choices in the relapsed/refractory population.

1.6 B Cell Receptor Signalling

The BCR in its inactive state consists of surface membrane immunoglobulin (Ig), associated with two other membrane proteins CD79A and CD79B which form a heterodimer. Naïve B cells express IgM and IgD constant region genes. Class switch recombination to IgG, IgA or IgE constant regions can occur within germinal centres (76). Typically, ABC DLBCL express IgM as they fail to undergo successful class switch recombination due to deletions and recombination events present in the switch μ region and switch γ region of the *IGH* locus (76). Furthermore, constitutive activity of the enzyme activation-induced cytidine deaminase (AID), required for class switch recombination (77), is highly overexpressed in ABC DLBCL (44), leading to mutation and DNA strand breaks that consequently impair class switch recombination (76).

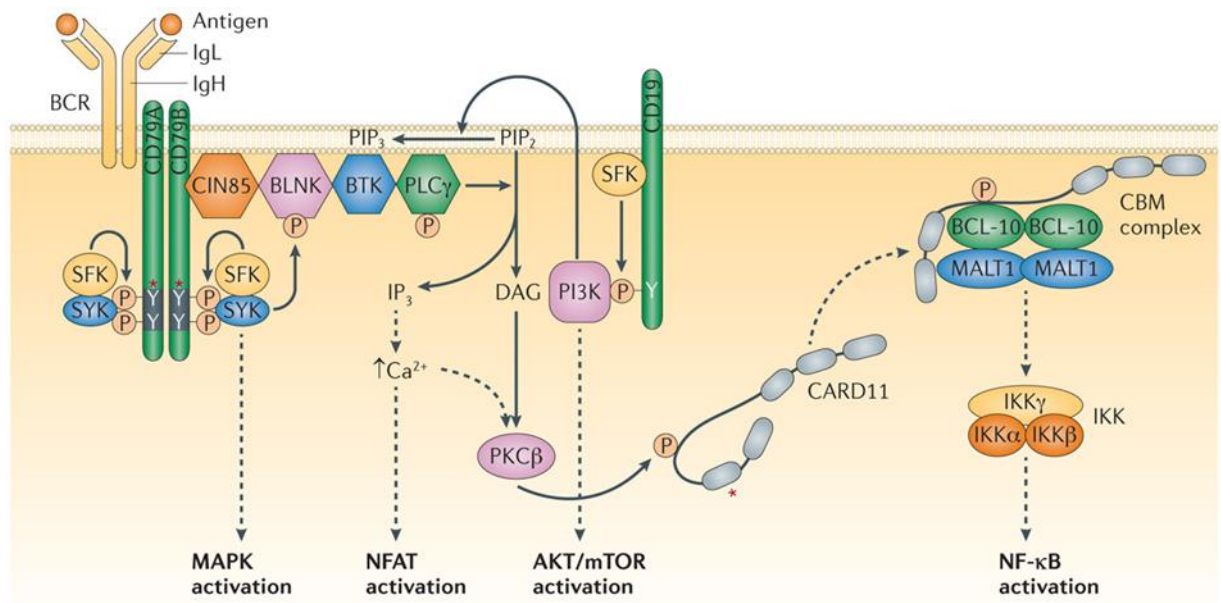
This selective pressure results in the maintenance of an IgM-BCR, with resultant important consequences in signalling, preferentially inducing NF- κ B signalling. The CD79A/B heterodimer contains an immune-receptor tyrosine based activation motif (ITAM). This conserved ITAM motif contains a sequence of four amino acids, containing a tyrosine separated from a leucine or isoleucine by two amino acids, which is repeated twice (78). The surrounding consensus sequence provides the binding site for the SH2 domains of effector proteins.

The organisation of the 'resting BCR' as either a monomer or oligomer continues to be debated. Evidence for the existence as a monomer was provided by Tolar et al., (79) using quantitative fluorescence resonance energy transfer imaging (FRET); FRET measurement between Ig α fused to donor and acceptor fluorophores in unstimulated B cells was low, therefore suggesting that the BR exists as a monomer on the cell surface. In contrast Reth et al., (80) proposed that the BCR exists as a class specific oligomer. This is based on the observation that the BCR of IgM and IgD runs as a large molecular complex during blue native polyacrylamide gel electrophoresis. During its resting state, the BCR exists as an auto inhibitory oligomer on the cell surface (81). Following binding of a multivalent antigen, dissociation of the BCR occurs, which results in exposure of the ITAMS within the Ig domains enabling phosphorylation, and targeting of the BCR cell membrane micro-domain fractions, termed lipid rafts, which contain the tyrosine kinase LYN (82). Phosphorylation of the cytoplasmic domain by LYN occurs within these rafts and results in a subsequent change in the conformation of the ITAM's (Figure 1.6). SYK is then recruited to the phosphorylated ITAMs, where transduction via the Phospholipase C Gamma 2 (PLCG2) and PI3K signalling pathway occurs.

The PLCG2 pathway is initiated by phosphorylation of the B cell linker (BLNK) by SYK (83). BLNK then binds PLCG2 and BTK to form a macromolecular complex in association with LYN and PI3K. Phosphorylation of PLCG2 by BTK occurs at positions Y753 and Y759 (84). PLCG2 then cleaves phosphatidylinositol 4,5-bisphosphate (PIP2) generating inositol triphosphate (IP3) and diacylglycerol (DAG). These second messengers activate a number of downstream pathways including the NF- κ B and MAPK pathways.

LYN also phosphorylates the cytoplasmic tail of CD19, the BCR co-receptor. Subsequent binding and activation of PI3K generates PIP3, which enables BTK to attach to the cell membrane through its PH domain. This allows phosphorylation of BTK by SYK and LYN at Y551, and positive feedback

Figure 1.6 Structure of the BCR (85).

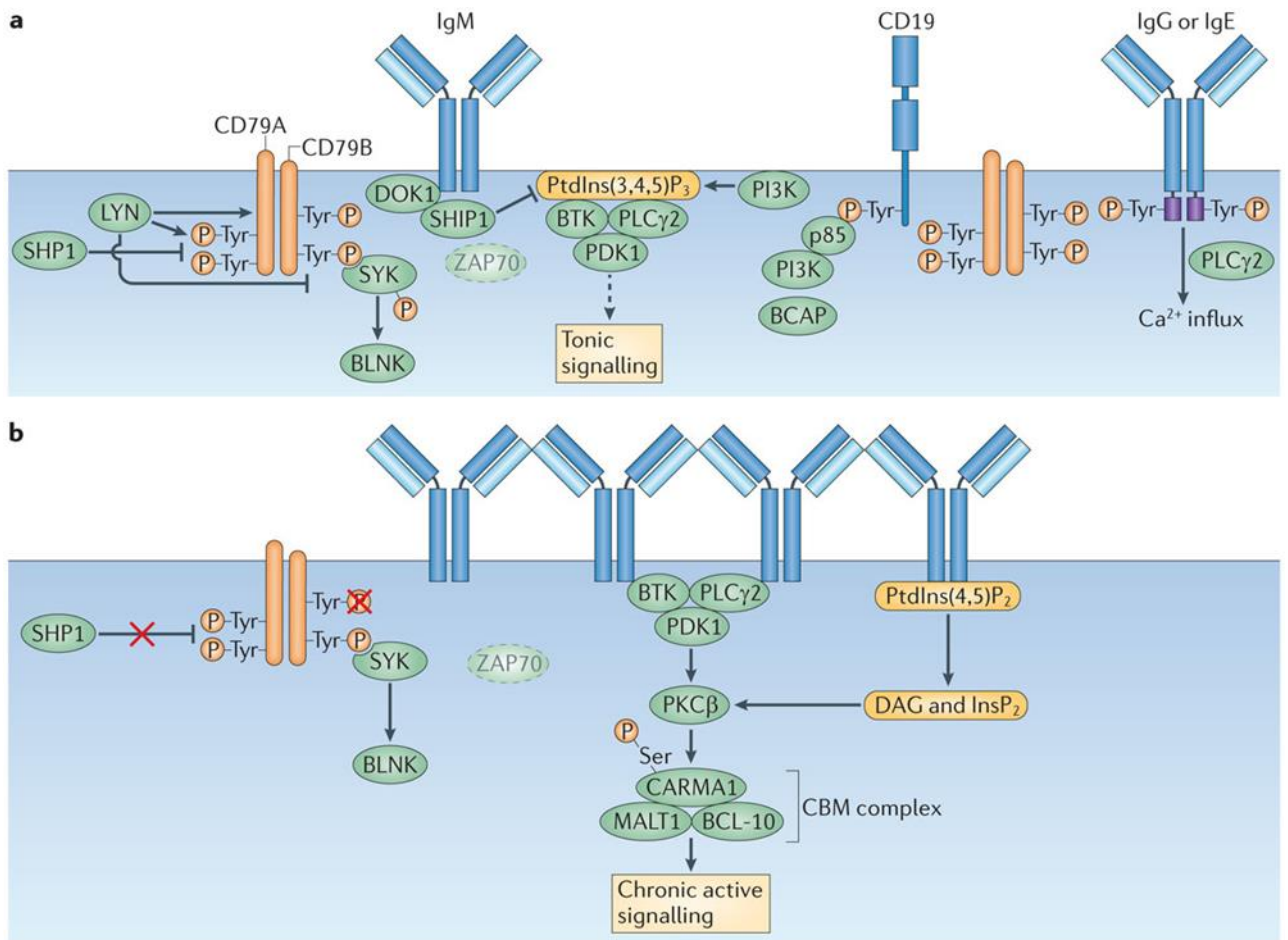


Nature Reviews | Drug Discovery

1.6.1 Tonic versus antigen dependent BCR signalling

Signalling through the BCR may occur *via* antigen independent ('tonic' signalling) or antigen dependent ('active' signalling) mechanisms (Figure 1.7). The importance of tonic signalling for the survival of peripheral B cells was shown by Lam et al., (86) where loss of surface immunoglobulin on mature B cells resulted in apoptotic cell death. Further studies demonstrated that tonic signalling is dependent on the ITAM portion of CD79A, supporting the hypothesis that tonic signalling is antigen independent (87). PI3K signalling has been shown to be critical in delivering the survival signal in tonic signalling (88). However these experiments were done in mice, which may not reflect the biology in humans.

Figure 1.7 Tonic and chronic active BCR signalling (a) Tonic BCR signalling (b) Chronic BCR signalling (89).



1.6.2 Chronic active BCR signalling

Mutations observed in *CD79A* and *CD79B* that result in chronic active BCR signalling occur exclusively within the ITAM region (90). Mutations in the *CD79B* ITAM region occur with greater frequency than in *CD79A* in ABC DLBCL, with a reported frequency of >20% and <3% respectively and most commonly are point mutations observed within the first ITAM tyrosine of *CD79B* (90).

These mutations when introduced into wild type cells, do not result in enhanced NF-κB signalling. However, increased cell surface expression of the BCR occurs, due to impaired endocytosis in the presence of *CD79A* and *CD79B* ITAM mutations (90). A

further mechanism by which NF- κ B activation may be enhanced in ABC DLBCL is through loss of *TNFAIP3* (A20). A20 is a tumour suppressor gene located on chromosome 6q23.3, a region frequently deleted in lymphoma. It encodes an ubiquitin modifying enzyme and is required for termination of NF- κ B responses, thereby exerting a negative feedback effect. It is thought to be important in the pathogenesis of not only ABC DLBCL but also a number of other lymphoma subtypes including Hodgkin Lymphoma (HL) (91).

A role for antigenic drivers in chronic active BCR signalling in ABC DLBCL has been proposed. This stems from studies in CLL, where it has found that CLL BCRs are able to recognise an epitope within the autologous heavy chain V region, thus driving BCR signalling (92).

Recurrent usage of the immunoglobulin heavy-chain variable region (*IGHV*) gene segments *VH4-34*, also frequently used in CLL, has been identified in 15.5% of cohorts of ABC DLBCL studied and may be an important driver (93). This was found exclusively in the ABC DLBCL subtype (93).

1.7 Lipid Rafts

Lipid rafts were first described in the early 1980s following the observation that lipids were not uniformly distributed within the cell membrane. A consensus definition was reached in 2006 at the Keystone Symposium of Lipid Rafts and Cell function, where they were defined as “small (10-200nm), heterogeneous, highly dynamic, sterol- and sphingolipid enriched domains that compartmentalize cellular processes” (94). These small rafts are detergent resistant, forming ordered discrete domains within the plasma membrane. They constitute in total 30-40% of the lymphocyte cell surface. Depending on raft size, the number of protein and phospholipid molecules is variable.

Lipid rafts mediate proximal BCR signal transduction, regulate endocytosis of bound antigen and are the site of formation of major histocompatibility complex (MHC) class II complexes. Moreover, a major role for the development of malignancy and tumour progression has been linked to proteins detected within lipid rafts (95). Engagement of the BCR results in clustering of the BCR and rapid association with lipid rafts. This

association is transient and within 15 minutes after activation, only a small fraction of engaged receptors remain detectable within the rafts (96). Ligation of the BCR, results in disruption of the actin cytoskeleton, enabling both clustering of the BCR and coalescence of the lipid rafts (97). Erin, present in the lipid rafts in unstimulated B cells, which is associated with the transmembrane protein PAG also found within lipid rafts, is believed to limit the mobility of lipid rafts within the membrane and prevent coalescence.

Association within the lipid rafts enables the phosphorylation of the immune-receptor tyrosine-based activation motifs of the BCR by the SRC kinase family members LYN, FYN and BLK present within the rafts (98). Additional recruitment of proximal signalling proteins subsequently occurs including SYK and results in coalescence of lipid rafts (99).

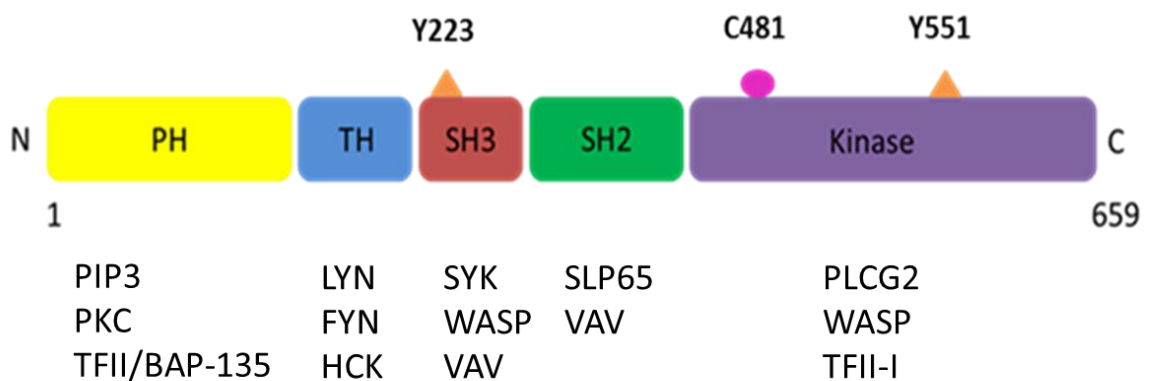
Lipid rafts are important in a number of signalling pathways, including the immune system (BCR and T cell receptor (TCR)) (100), cell survival (insulin-like growth factor I (IGF-I)/phosphatidylinositol 3-kinase (PI3K)/Akt signalling) (101, 102) and apoptotic pathways (103). It is perhaps therefore of no surprise that a number of proteins believed to be important in the development of cancer have been found within lipid rafts, for example MMP-9 in breast cancer (104). Proteins previously identified within lipid rafts include receptors or surface glycoproteins, cytoskeletal or structural proteins, protein kinases, protein phosphatases, small G proteins, motor proteins and vesicle fusion or trafficking proteins (reviewed in (95, 105)).

1.8 BTK

Bruton's tyrosine kinase (BTK) is a cytoplasmic or non-receptor tyrosine kinase that belongs to the Tec family of kinases (106); BTK is expressed broadly throughout the haemopoietic cell lineages, with the exception of T cells (107). It is encoded by the *BTK* gene, located on chromosome Xq22. 5 different kinases belong to the Tec family: bone marrow expressed kinase (BMX), inducible T cell kinase (ITK), TEC, resting lymphocyte kinase (RLK) and BTK (108). Whilst the protein structure of the Tec kinases is broadly similar to the Src family, with an NH₃ domain, SH3 domain, SH2 domain and kinase domain, important differences exist (108). These include the absence

of a myristoylation signal and the COOH terminal tyrosine, which is required for Src attachment to the inner surface of the membrane (109). BTK, ITK and TEC have a highly conserved structure, consisting of an N-terminal pleckstrin homology (PH) domain, a Tec homology domain (TH), a SRC Homology 3 (SH3) and SRC Homology 2 (SH2) domain and a C-terminal kinase domain (110). The PH domain is a unique feature of the Tec family of kinases, which enables tethering to the membrane through binding to specific phospholipids (111). RLK however lacks a PH domain and in place palmitoylated cysteines enable tethering to the membrane (112). The structure of BTK is shown in Figure 1.8. BTK forms an important therapeutic target in B cell malignancies and is a functional rather than a genetically determined therapeutic target.

Figure 1.8 Domain structure of BTK showing interaction of binding partners with each domain (113).



1.8.1 PH domain

The PH domain enables conditional association with the membrane, dependent on PI3-K activity (114). For individual members of the Tec family of kinases, the different specificity of the PH domains to phospholipids enables this conditional association to be tightly controlled. The BTK PH domain preferentially binds to phosphatidylinositol-3,4,5-trisphosphate [PI(3,4,5)P₃] over PI(4,5)P₂ or phosphatidylinositol-4-phosphate [PI(4)P] (115). The roles in cellular function of the PH domain are broad, including cellular signalling, cytoskeletal organisation, and regulation of intracellular membrane transport. The PH domain of BTK also enables association with cellular proteins including the G α and G $\beta\gamma$ subunits of heterotrimeric G-proteins, facilitated by a conserved domain, composed of the PH domain and the adjacent BTK motif (116, 117);

Protein kinase C (PKC) isoforms (118); the transcription factor TFII-I/BAP-135 in either the PH or kinase domain (119) and cytoskeleton (120).

1.8.2 TH domain

The TH domain contains a ‘BTK motif’, which contains only 26 residues and for which the function remains unknown, and proline rich stretch (121). The proline rich stretch has two described functions; interaction with the SH3 region of the SRC family of kinases (122), thus resulting in activation of BTK (123) and regulation of its own kinase activity through intramolecular binding to the SH3 domain (124).

1.8.3 SH3 domain

This domain is important in the autoregulation of the kinase activity, with truncation of the SH3 domain resulting in the constitutive activation of TEC (125) and other kinases for example c-Abl (126). A number of other proteins have been identified which bind to the SH3 region and are important regulators of PTK activity. These include Wiskott–Aldrich syndrome protein (WASP) (127) and VAV (128).

Y223, an autophosphorylation site, is found within the BTK SH3 domain (129), and is an early target for the activated kinase Y551. Phosphorylation of Y223 is thought to be important in intramolecular or intermolecular binding events. For example BTK dependent phosphorylation of BTK associated protein (BAP-135) binding to Y223, is abrogated in the presence of the Y223F mutation (130). Y223 phosphorylation may also be important as a binding site for phosphotyrosine binding protein (131).

1.8.4 SH2 domain

The SH2 domain binds only a small number of proteins, resulting in their phosphorylation and activation. It appears that for some of these proteins at least, phosphorylation is dependent also on interaction with the PH domain (132).

1.8.5 Kinase domain

The kinase domain of BTK contains the BTK regulatory tyrosine residue Y551. In addition to the activation loop, the ATP binding site, the catalytic apparatus, and the allosteric inhibitory segments are also situated in the SH1/TK domain (133).

1.8.6 BTK phosphorylation

Autophosphorylation of BTK occurs at position Y551, within the kinase domain, and is mediated by both LYN and SYK (134). Co-expression of both BTK and LYN in a cell line transformed with EBV resulted in an increase in BTK phosphorylation at two distinct tyrosine residues, with a five to ten fold increase in BTK enzymatic activity (123). Phosphorylation at Y551 was dependent on Lyn, confirming that this was the site of transphosphorylation. Subsequently the site of autophosphorylation was mapped to Y223 within the SH3 domain by Parks et al (129). The autophosphorylation of Y223 is thought to regulate BTK activation, through modulation of protein-protein interactions.

1.9 X-Linked Agammaglobulinaemia

The primary immunodeficiency, X-linked agammaglobulinaemia (XLA) was first described in 1952, by the paediatrician Dr Ogden Bruton in an 8 year old boy, presenting with recurrent episodes of pneumococcal sepsis. Serum protein electrophoresis, showed a lack of gammaglobulins (IgG) (135). These findings were subsequently confirmed in a series of male patients (136), suggesting an X-linked pattern of inheritance. The estimated incidence of XLA is 0.5:100 000 (137). Typically children present at less than 2 years of age with susceptibility to encapsulated bacterial infections, such as *Streptococcus pneumoniae*, *Haemophilus influenza*, *Staphylococcus aureus* and *Pseudomonas*. Placental transmission of IgG antibodies provides protection for the initial few months of life. Patients have low circulating levels of immunoglobulins of all isotypes (~10% of healthy controls) and an impaired cellular immune response to infection and immunisation (138). Replacement intravenous IgG was and continues to remain an effective therapy today.

In XLA, very few circulating mature B cells are present (<1%) (139), due to an inability of pre-B cells in the bone marrow, to develop into mature circulating B cells; suggesting that the protein encoded by the XLA gene is critical in B cell development (107).

However, it was not until 1993, when *BTK* was cloned that the genetic basis of XLA was determined (140, 141). Shortly thereafter, murine X-linked immunodeficiency (Xid) was shown to be the result of a mutation (R28C) within the pleckstrin homology domain (PH) of *Btk* (142, 143). Interestingly, this results in a milder phenotype than XLA patients. In contrast to XLA patients, mature B cells in Xid mice are present but fail to respond to thymus independent type 2 antigens, have an altered response to B cell signalling and an altered surface phenotype (142). Despite these differences, similarities exist between the surface phenotype, both disorders show non-random X chromosome inactivation limited to B cells and shared genetic homology within Xq21.3-Xq22. To date more than 800 different mutations in *BTK* (144) have been described. These occur within all domains of BTK, including noncoding sequences of the gene. The most commonly identified mutation is a missense mutation (accounting for 40% of all mutations), found within all but the SH3 domain (145).

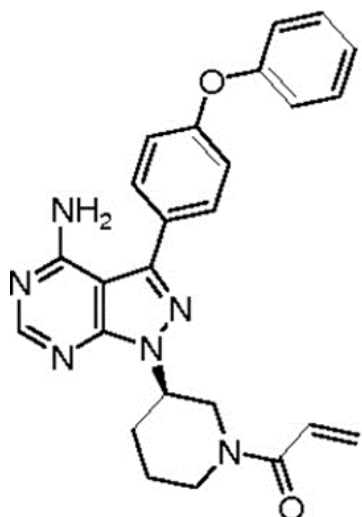
1.10 BTK inhibitors

Despite the broad expression of BTK throughout the haemopoietic lineages except T cells, the primary consequence in XLA, is B cell specific and essential for BCR signalling. BCR signalling is important in the pathogenesis not only of lymphoid malignancies, but also autoimmune diseases such as rheumatoid arthritis (RA) (146), systemic lupus erythematosus (SLE) (147) and multiple sclerosis (MS) (148). Interestingly, targeted disruption of other BCR pathway kinases expressed in mature B cells including Blk (149) and Src family kinases (150) *in vivo* in mice have failed to show inhibition of the B cell humoral immune response, and in some cases resulted in activation of signalling; thus suggesting redundancy and complex roles within the signalling pathway. BTK may therefore be considered an unlikely candidate as a therapeutic target in view of its expression in multiple cell types and signalling pathways and subsequent inference of potential for considerable toxicity. Despite this, a number of BTKi are now used in the clinical setting.

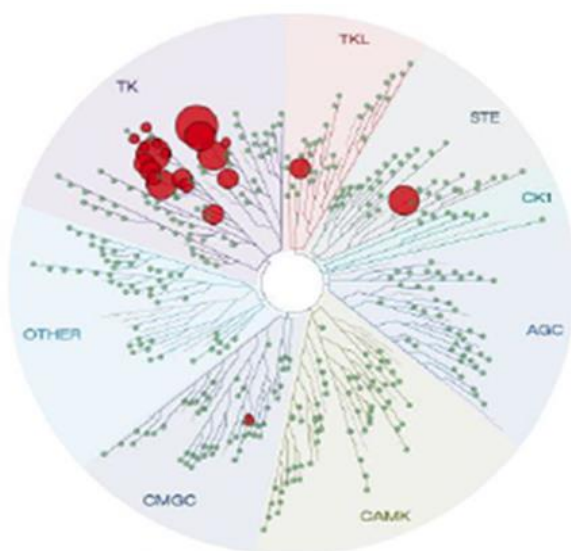
Within the ATP binding pocket of BTK, the presence of a cysteine residue (Cys-481), has enabled the design of a series of specific inhibitors that inhibit the enzymatic activity of BTK with nanomolar potency (151). Cys-481 in BTK is a nucleophilic site, enabling the formation of a covalent complex between BTK and an electrophilic inhibitor. Only ten kinases, including BTK, have been found to have a cysteine at this position (BLK, BTK, BMX, EGFR, ERBB2, ERBB4, ITK, JAK3, TEC, and TXK) (151), enabling highly specific binding of inhibitors to this site. Covalent binding of Cys-481 in the BTK kinase domain, inhibits phosphorylation at Tyr223, thereby inactivating BTK. The compound PCI-32765 (Ibrutinib) was found to have an IC₅₀ of 0.5nM and selectivity for the kinase BTK (152) (Figure 1.9). Honigberg et al., (152) showed that using a fluorescent tag attached to PCI-32765, to form the derivative PCI-33380, binding only occurred in the presence of BTK and Cys-481. In the DoHH2 cell line, PCI-32765 resulted in irreversible inhibition of BTK auto-phosphorylation and the downstream kinase ERK (152). *In vivo* in the arthritic mouse model DBA/1 and MRL-Fas (lpr) lupus model, PCI-32765 resulted in an improvement in clinical arthritis scores and reduction in interstitial nephritis respectively. Furthermore in spontaneous canine B cell lymphomas, partial responses were observed in 3/8 dogs (152). Shortly thereafter PCI-32765 entered clinical trials in B cell malignancies as the first in class inhibitor. Interestingly, despite the broad kinome of ibrutinib and long protein half life of BTK, toxicity is surprisingly low. The structure, kinome and specificity are shown in Figure 1.9.

Figure 1.9 (a) Structure of Ibrutinib (PCI-32765); (b) Kinome of Ibrutinib: 1000nM Discover RX kinome scan against 442 kinases; (c) Ibrutinib inhibits 11 different kinases with an IC₅₀ of about 10nM BTK, BLK, BMX, CSK, FGR, BRK, HCK, EGFR, YES, ErbB2 and ITK (152).

(a)



(b)



(c)

Kinase	IC ₅₀ nM	Btk selectivity, fold
BTK	0.5	-
BLK	0.5	1
BMX	0.8	1.6
CSK	2.3	4.6
FGR	2.3	4.6
BRK	3.3	6.6
HCK	3.7	7.4
EGFR	5.6	11.2
YES	6.5	13
ErbB2	9.4	18.8
ITK	10.7	21.4

Second generation and more specific BTK inhibitors have subsequently been developed and published data is now available for a number of these inhibitors, for example Tirabrutinib (formerly referred to as ONO/GS-4059, ONO-4059 or WG-307), Acalabrutinib (formerly ACP-196), CC-292 and BGB-311 (Table 1.4). The market is becoming increasingly crowded, with each compound seeking to be the best clinically. Of specific interest is the selective BTKi Tirabrutinib, the preclinical and clinical studies of which have been studied in my thesis and will be discussed in detail.

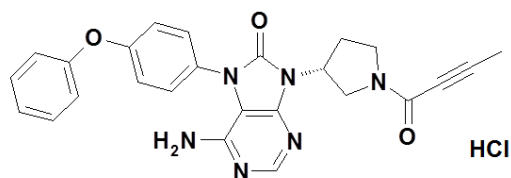
Table 1.4 BTKi in pre-clinical and clinical development

BTK inhibitor	Type of inhibitor	IC50	Development	Reference
Ibrutinib	Covalent, irreversible	0.5nM	CLL/NHL	(152)
GDC-0834	Non covalent, reversible	5.9nM	Rheumatoid Arthritis	(153)
RN-486	Reversible	4.0nM	Rheumatoid Arthritis	(154)
CC-292	Covalent, irreversible	<0.5nM	CLL/NHL	(155)
PRN1008	Covalent, reversible	1.3nM	Rheumatoid Arthritis	(156)
CGI-1746	Reversible	1.9nM	Rheumatoid arthritis	(157)
Acalabrutinib	Irreversible, covalent	3nM	CLL/NHL	(158)
BGB-3111	Irreversible, covalent	1.8nM	CLL/NHL	(159)
Tirabrutinib	Covalent, irreversible	2.2nM	CLL/NHL	(160)
CNX-774	Covalent, irreversible	<1nM	Autoimmune disease/NHL	(155)
LFM-A13	Reversible	17.2 μ M	NHL	(161)
Dasatinib	Reversible	4.6nM	CLL	(162)

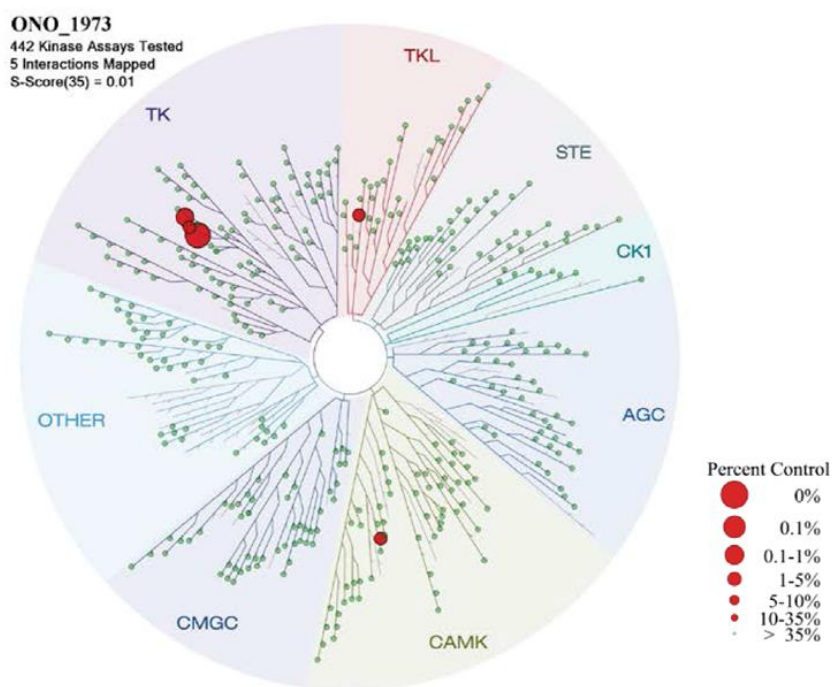
1.10.1 Preclinical development of Tirabrutinib (ONO/GS-4059)

Tirabrutinib is an oral BTK inhibitor being developed by ONO Pharmaceutical Co, Ltd and Gilead Sciences, Inc. (Gilead). The structure and kinome of Tirabrutinib are shown in Figure 1.10. Tirabrutinib inhibits BTK with an IC50 of 2nmol/L and inhibits BTK and ERK phosphorylation (160). *In vitro*, induction of classical apoptosis is seen in the ABC DLBCL cell line TMD8 (163) and in the TMD8 xenograft model in the presence of nanomolar (nM) concentrations of Tirabrutinib, dose dependent inhibition of tumour growth occurred (164). Parallel analysis of pBtk 223, showed complete inhibition.

Figure 1.10 (a) Chemical structure of Tirabrutinib. Tirabrutinib is a potent oral BTK inhibitor that inhibits the autophosphorylation at position Y223 in the BTK SH3 domain after being transphosphorylated at position Y551 by tyrosine protein kinase Lyn (LYN) and spleen tyrosine kinase (SYK) (165).



(b) Kinomescan dendrogram report of tirabrutinib binding to human kinases. Tirabrutinib was assessed for its ability to interact with 442 kinases using KINOMEScan platform (<http://www.discoverx.com/technologies-platforms/competitive-binding-technology/kinomescan-technology-platform> and unpublished data). At a concentration of 300nM, tirabrutinib bound significantly to 5 kinases as summarised in the dendrogram below. Kinases found to bind are marked with red circles, larger circles representing higher affinity binding. These five kinases included BTK (97% Kd 8.6nM), TEC (92%, Kd 9.6nM), BMX (89% Kd>30,000nM), HUNK (89%, Kd 6800nM) and RIPK2 (67%, Kd>30,000nM).



1.10.2 Combination preclinical studies

Tirabrutinib has been evaluated in combination with idelalisib and shown synergy in the ABC-DLBCL cell lines OCI-LY10 and TMD8 and MCL cell lines Rec-1 and JMV-2 (166). In primary CLL cells, combination of ABT-199 with entospletinib, Tirabrutinib or idelalisib resulted in an additive to synergistic increase in apoptosis in primary CLL cells (167). In the TMD8 xenograft model, Tirabrutinib combined with Obinutuzumab or Rituximab showed improved efficacy over respective monotherapy with tumour growth inhibition of 90% for the Obinutuzumab combination and 86% for the Rituximab combination (168).

1.11 Clinical activity of BTKi in the treatment of B-cell malignancies

BTKi have changed the treatment paradigm for patients with R/R B cell malignancies, achieving long term disease control in patients with no other treatment options, with remarkably low levels of toxicity. Success has been most marked in the treatment of CLL, and the indolent B cell malignancies MCL and WM. In CLL, MCL and WM, BTK is over-expressed and constitutively activated, providing a rational therapeutic target (169-172). Inhibiting BTK in both CLL and MCL inhibits a number of pathways, including AKT and NF- κ B, believed to be important in the survival, proliferation and migration of cells (173). In WM, the L265P mutation in *MYD88*, results in constitutive activity of MYD88, a key regulator of BTK activity with BTK inhibition resulting in inhibition of the NF- κ B pathway (172).

Following the success of the first in class inhibitor, ibrutinib, a number of second generation more selective inhibitors have now entered the clinical setting and the search for more effective combination strategies continues to improve on response and duration seen with monotherapy.

1.11.1 Ibrutinib

Ibrutinib, the first in class irreversible inhibitor of BTK, has shown considerable activity in CLL (174), MCL (175), WM (176) and some cases of non-GCB DLBCL (177). Results from the most recent studies are discussed below.

1.11.1.1 Chronic lymphocytic leukaemia

Ibrutinib has now been evaluated in a number of Phase II and Phase III clinical trials in CLL, both in the first line setting and R/R population. It is approved for use both by the Federal drug agency (FDA) and European medicines agency (EMA). In previously untreated patients aged ≥ 65 years, without del(17p), the RESONATE-2 trial compared ibrutinib monotherapy with chlorambucil (178). The response rate was significantly greater in the ibrutinib arm (86% vs 35% chlorambucil treated patients) and following a median follow up of 18.4 months, PFS in the ibrutinib arm was significantly longer than patients receiving chlorambucil irrespective of poor risk factors such as Rai stage III or IV, the presence of bulky disease, del(11q) or unmutated *IGHV*. Importantly, rates of discontinuation due to adverse events were lower in the ibrutinib arm and quality of life assessments significantly improved with ibrutinib.

In patients with R/R CLL, RESONATE compared ibrutinib with ofatumumab, an anti-CD20 antibody in patients not suitable for purine analogue therapy (179). 32.5% of patients had del(17p) and 49.4% had already received at least 3 prior treatment lines. Response rates, PFS and OS rates at 18 months were significantly higher in the ibrutinib treated patient group (180). In combination studies with chemo-immunotherapy in the HELIOS placebo controlled study, ibrutinib in combination with bendamustine and rituximab in prior treated patients has improved response rates, 18 month PFS and continued to be well tolerated with a manageable safety profile (181). Ongoing studies continue to evaluate the role of ibrutinib in combination with chemo-immunotherapy and other targeted therapies.

1.11.1.2 Mantle cell lymphoma (MCL)

The pivotal Phase II study of ibrutinib in 111 patients with R/R MCL led to FDA approval of single agent ibrutinib. The ORR was 67% and median duration of response of 17.5 months in the long term follow up in the extension study (175). The magnitude of these results is reflected by the recognition that these results are the highest reported for a single agent in R/R MCL. Response rates were independent of the number of prior treatment lines.

In an attempt to improve on single agent activity, ibrutinib has been trialled in combination with chemo-immunotherapy and other targeted therapies many of which are ongoing or in varying stages of trial development. Outcomes after ibrutinib failure however remain poor, with the development of aggressive disease and blastoid transformation, and poor response rates to salvage therapy (182). The median reported overall survival following progression on ibrutinib is reported as less than 9 months (183).

1.11.1.3 Waldenstrom's Macroglobulinaemia

In 63 patients with R/R disease, treated with ibrutinib 420mg daily, a 91 % response rate was observed, with higher response rates observed in the presence of *MYD88* (L265P) and either *CXCR4* wild type or *CXCR4*^{WHIM} mutations (176). In Waldenstrom's macroglobulinaemia, activating somatic mutations in *CXCR4* are similar to those detected in patients with the WHIM syndrome of warts, hypogammaglobulinaemia, infections and myelokathexis (184). Expression of *CXCR4*^{WHIM} receptors in tumour cells has been associated with enhanced activation of AKT and ERK and ibrutinib resistance (185). A study of ibrutinib first line is ongoing in the US (NCT02604511). Approval for use has been obtained from both the FDA and EMA.

1.11.1.4 DLBCL

In the Phase I and Phase II study of 80 patients with R/R DLBCL treated with ibrutinib, higher response rates were observed in the ABC subtype (177). Baseline characteristics were similar between groups with a median number of 3 prior therapies in both ABC

and GCB subtypes and poor R-IPi in 63% and 59% of those with ABC and GCB subtypes respectively. 13% of patients with ABC subtype and 30% of patients with GCB subtype had undergone a prior autologous stem cell transplant. 37% (14/38) patients with ABC subtype as determined by GEP, responded to ibrutinib. 6 patients achieved a CR (16%). Response rates in GCB were predictably very much lower at 5% (1/20). The role of BTK in BCR signalling and link with NF- κ B activation on this pathway in ABC DLBCL, where chronic active BCR signalling occurs, supports these clinical findings. *CD79B* gain of function mutations were observed in 9 patients (23%) of ABC DLBCL biopsy samples and response rates were higher in this subgroup at 55.5%. 31% of patients with wild type *CD79B* on tumour testing also responded. Response rates in patients with wild type *MYD88* or *MYD88* mutations were similar but in those with both *MYD88* and *CD79B* mutations, responses were seen in 80% (4/5). In patients with *CARD11* or *TNFAIP3* mutations, no response was observed. Interestingly mutational analysis suggests that in patients with ABC DLBCL, in whom responses to ibrutinib are seen, not all patients have an identified mutation within the BCR signalling pathway and may implicate processes other than genetic mechanisms in defining sensitivity to ibrutinib. In responders, the median duration of response was just 4.83 months and median PFS and OS just 2.02 and 10.32 months respectively in the ABC DLBCL subtype. In those that had a complete response, PFS was significantly longer than those patients who achieved a CR ($P = 0.0039$). All complete responses were associated with a response duration of more than 12 months. Responses were seen in patients with primary chemotherapy refractory disease. In total 18 patients with chemotherapy refractory disease were enrolled in the trial and responses were seen in 22% (4/18).

Whilst these results show promise in a patient group with a poor clinical outcome, there remains the need for the development of more effective treatments and a further understanding of the biology of disease. Currently there are 21 combination studies recruiting or active listed on clinicaltrials.gov (186) for patients with a diagnosis of DLBCL assessing ibrutinib in combination with chemotherapy (e.g NCT02955628) or in combination with other small molecule inhibitors and antibodies (e.g. NCT03136497).

1.11.1.5 Safety and tolerability of ibrutinib

Whilst ibrutinib has shown remarkable efficacy across a range of B cell malignancies, real world data from the Swedish CLL group and the UK CLL forum for patients treated on the named patient scheme, have suggested that the rates of discontinuation and requirement for dose reduction may be greater than those observed in the earlier clinical trials (187, 188). From the UKCLL data 73.7% (232/315) of patients were still on therapy at 1 year with a one year survival rate of 83.8% (264/315). 55/83 patients discontinued treatment permanently due causes other than refractory disease, progression, or Richter's transformation: 15 due to infection; 9 due to haemorrhage/bleeding or anticoagulation related events; 6 due to general debility; 6 due to the development of secondary cancers; 3 due to GI toxicity; 2 due to cytopenias; 2 due to cardiac complications; 1 dermatological; 1 neuropathy and 10 patients for which no reason was provided. 75 patients had a treatment break of up to 6 months and 82 patients (26%) had a dose reduction.

The broad kinome may account for the increased frequency of adverse events observed with ibrutinib, including bleeding, arthralgia, diarrhoea and atrial fibrillation. Conversely, however, this lack of selectivity may have implications for the treatment of solid tumours and T cell malignancies. For example Ibrutinib has demonstrated activity in EGFR driven lung cancer cell lines (189, 190) and *in vivo* in the H1975 mouse xenograft model (190); breast cancer cell lines with HER2 amplification, MDA-MB-453, SK-BR-3 and UACC-893 and xenograft studies with the HER2⁺ cell lines BT-474 and MDA-MB-453 (191); and is currently being investigated as an inhibitor of ITK in relapsed and refractory T cell lymphoma (NCT02309580).

More selective BTKi have therefore been developed and a number have entered clinical trials in haematological malignancies, including tirabrutinib (ONO/GS-4059), acalabrutinib (ACP-196), BGB-3111 and CC-292, all of which target the cysteine residue (Cys481) within the active site. All four inhibitors have entered the clinical setting and have improved selectivity over the other TEC kinase family members and EGFR. Interestingly, however CC-292 showed an inferior outcome when compared to both ibrutinib and other more selective BTK inhibitors with an overall response rate in

CLL/SLL of 53% patients receiving twice-daily dosing; clinical development of this molecule has therefore been abandoned (192).

1.11.2 Tirabrutinib

Tirabrutinib has been evaluated in the Phase I study of 90 patients, ‘A phase I clinical trial of the selective BTK inhibitor ONO/GS-4059 in relapsed and refractory mature B-cell malignancies’ (NCT01659255) and long term extension study (NCT02457559), the results of which are presented in Chapter 3 and 4. A Phase I clinical trial evaluating the combination of tirabrutinib with either idelalisib or entospletinib in relapsed and refractory mature B-cell malignancies is ongoing (NCT02457598).

1.11.3 CC-292

CC-292, whilst a selective BTKi that also targets the cysteine residue within the active site of BTK, has shown an inferior outcome when compared to both ibrutinib and other more selective BTK inhibitors in the Phase I study in patients with R/R CLL/small lymphocytic lymphoma (SLL), B-cell non-Hodgkin lymphoma (B-NHL), and WM (NCT 01351935) (192). 113 patients received daily dosing with CC-292 at doses ranging from 125 mg to 1000 mg once daily, and 375 mg and 500 mg twice daily in the dose escalation phase. In the dose expansion cohorts, patients received 750 mg once daily or 500 mg twice daily. A dose limiting toxicity was not reached. The most frequent grade 3–4 adverse events (AEs) were neutropenia (16%) and thrombocytopenia (8%). Diarrhoea, of any grade occurred in 68% of patients. With twice-daily administration of CC-292 90% BTK receptor was greater than 90%. In the CLL treated population the ORR was 53% in patients receiving twice daily dosing. Therefore whilst well tolerated, an inferior response was seen compared to other BTKi. The inferior outcome seen is postulated to be related to the highly variable PK and PD seen in patients.

1.11.4 Acalabrutinib (ACP-196)

Acalabrutinib binds covalently to C481 within the kinase domain of BTK (158). However acalabrutinib did not inhibit EGFR, ITK, or TEC kinases (158, 193). Acalabrutinib, unlike ibrutinib, in the *in vivo* VWFHA1 mouse thrombosis model did not inhibit thrombus formation. In the Phase I trial (NCT02029443), in R/R CLL, after a median follow-up of 14.3 months, the ORR was 95%. Acalabrutinib requires twice daily dosing. Currently a Phase 3 study (NCT02477696) comparing acalabrutinib with ibrutinib in high-risk patients with relapsed CLL is ongoing. Acalabrutinib is also being evaluated in ABC DLBCL, MCL, WM and other B cell malignancies.

1.11.5 Other BTKi in clinical trials

A number of other BTKi are either in pre-clinical development or entering Phase I trials. Preliminary results from the first in human study of BGB-3111 (NCT02343120), has shown clinical activity in various B cell malignancies, with a safe toxicity profile (194).

1.12 Resistance to BTKi

Ibrutinib and other BTKi have shown considerable efficacy in the treatment of R/R CLL, MCL and WM. However in R/R ABC DLBCL where responses are seen, these are short lived and often discordant. Understanding these acquired mechanisms of resistance are key to improving the prognosis for this patient group and informing rational therapeutic choices. Wilson et al., (177) have shown that in primary resistance to ibrutinib, activating mutations in *CARD 11* conferred resistance, as well as *MYD88* mutations in the absence of *CD79B* mutations. More recently, analysis of primary refractory cell lines have shown increased CD79B protein expression and increased levels of AKT and MAPK signalling (195). This sustained signalling, in the presence of ibrutinib, supported the investigation of preclinical investigation of ibrutinib with AKT and MAPK inhibitors, which showed synergistic activity.

1.13 Aims of this study

The aims of my thesis were:

1. To assess the safety, tolerability and efficacy of the selective BTKi, tirabrutinib, in NHL and CLL in the Phase I clinical trial.
2. To describe the genomic profile of patients with CLL treated with tirabrutinib on the Phase I clinical trial using a targeted sequencing panel and impact of identified mutations on clinical outcome with tirabrutinib.
3. To characterise and compare the BTKi resistant cell lines TMD8 RO and TMD8 RI to the parental cell line TMD8. Experiments were designed to identify whether changes in the immunophenotype, mechanisms of cell death, gene expression and WES occurred in the resistant cell lines and resulted in resistance to BTKi.
4. To characterise and compare the BCR signalling pathway in BTKi resistance in the TMD8 RO and TMD8 RI cell line with the parental cell line TMD8 through proteomic studies.

Chapter 2 Materials and Methods

2.1 Cell Culture

2.1.1 Cell lines

All cell lines were obtained from the Dyer cell bank (<http://www2.le.ac.uk/departments/csmm/research/the-ernest-and-helen-scott-haematological-research-institute>). Cell line authentication was confirmed by genetic profiling using polymorphic short tandem repeat (STR) loci at the University of Kiel, Germany.

The suspension cell lines TMD8, TMD8 RO, TMD8 RI and DoHH2 were cultured in RPMI 1640 Medium containing L-Glutamine (Invitrogen Life Sciences 21875-091) and supplemented with 10% foetal calf serum (FCS) and 50U/ml penicillin and 50µg/ml streptomycin. The TMD8 cell line is an EBV negative ABC DLBCL cell line established in 1999 from a bone marrow sample, donated by a 62 year old gentleman newly diagnosed with ABC DLBCL (196). The TMD8 RO and TMD8 RI cell lines, TMD8 cells resistant to tirabrutinib and ibrutinib respectively, were generated by Mr R. Kozaki as described in section 2.1.3. The DoHH2 cell line was established from pleural fluid cells in 1990 in a 60 year old gentleman with refractory transformed follicular lymphoma (197).

Cell density was determined using a Bio-Rad TC-20 Automated cell counter. The resistant cell lines TMD8 RO and TMD8 RI were maintained in the presence of 1.0µM tirabrutinib and 0.1µM Ibrutinib respectively in culture. All cells were maintained in cell culture flasks (Corning Life Sciences) and stored in an incubator at 37°C in humidified 5% CO₂. Cell lines were passaged twice weekly when cell density reached 1x10⁶/ml. No more than 20 passages were performed per cell line.

To passage a confluent cell culture T75 flask, the required volume of cell suspension was transferred to a sterile falcon tube and centrifuged at 200g for 3 minutes. The medium was removed and the cell pellet re-suspended in fresh supplemented pre-warmed media at a density of 1x10⁵/ml and transferred to a new cell culture flask.

2.1.2 Cryopreservation and recovery of cell lines

Cell lines were stored long term in liquid nitrogen. For cryopreservation, cells were re-suspended in 1ml freezing media (cell density 1×10^7 /ml), containing 90% FCS and 10% dimethylsulphoxide (DMSO) and transferred to 1.5ml cryovials (Greiner BioOne Ltd.). Cryovials were frozen slowly in Mr. Frosty™ (Thermo Scientific) freezing containers, designed to achieve a rate of optimal cooling of $-1^\circ\text{C}/\text{minute}$ by placing in a -80°C freezer. Cryovials were subsequently transferred to liquid nitrogen for long term storage.

On retrieval from liquid nitrogen, cells were thawed briefly in a water bath set at 37°C and transferred to a falcon tube containing 9ml of warm media supplemented as above and washed once. The cell pellet was then re-suspended in 10ml pre warmed supplemented media and transferred to a 25cm surface area cell culture flask (Corning Life Sciences). Normal cellular division was restored prior to use.

2.1.3 Generation of TD8 resistant cell lines

Resistant TMD8 cell lines to ibrutinib and tirabrutinib were established by Mr R. Kozaki. The TMD8 cell line was chosen to develop resistant cell lines as this line was established from a chemotherapeutic and radiation naïve patient and is highly sensitive to treatment with BTKi. In the clinical setting, BTKi are administered daily in a continuous manner and therefore a continuous treatment strategy, whereby the cells were cultures constantly in the presence of the drug, was adopted. Supplemented media and drug were replaced twice weekly according to cell density and viability. Over a period of 9 months, TMD8 cells were continuously treated with either Ibrutinib or tirabrutinib at increasing drug concentrations of up to $0.1\mu\text{M}$ and $1\mu\text{M}$ respectively to achieve resistant cell lines. Cell viability following the development of resistance was consistently $>80\%$.

2.1.4 Isolation of Peripheral blood mononuclear cells from patient samples

Peripheral blood mononuclear cells (PBMCs) were isolated from whole blood using density gradient centrifugation. Approximately 20ml of whole blood kindly donated by

consented patients on the Phase I Study of ONO-4059 (ONO/GS-4059) Given as Monotherapy in Patients With Relapsed/Refractory NHL and CLL at the Leicester Royal Infirmary was collected in lithium heparin 9ml tubes and stored at room temperature. Heparinised blood was transferred to a 50ml falcon tube. 15ml of Histopaque density medium was measured into a separate falcon tube. Using a 10ml pipette the heparinised blood was carefully layered onto the Histopaque density medium. The sample was centrifuged at 400g for 30 minutes at 20°C without acceleration or deceleration using a 5810R Eppendorf centrifuge. PBMCs were collected from the white blood cell interphase using a Pasteur pipette and transferred to a new 50ml falcon tube. The volume was made up to 30ml with supplemented media. The sample was centrifuged at 200g for 10 minutes at room temperature and the supernatant discarded. The resulting pellet was resuspended in 10-50ml of suspended media and the cell counted using the BioRad Cell counter. Cells were then spun down, media removed and re-suspended in freezing media at a density of 2×10^7 /ml. 1ml aliquots were transferred to cryovials and cryopreserved as described in section 2.1.2.

2.1.5 Cell viability

Cells were counted and viability assessed using the Trypan blue exclusion assay (Biorad #145-0021). 10 μ L of cellular suspension was added to 10 μ L of Trypan blue and mixed. 10 μ L was then transferred to a counting slide and cells were counted using a TC-20 Automated cell counter. Viable and non-viable cells counts were obtained and the % of live cells estimated. Viability of cells used for all experiments was greater than 80%.

2.1.6 Cell growth

The growth rate of the cell lines TMD8, TMD8 RO and TMD8 RI were measured. Cells were plated at a density of 1×10^5 /ml in 48 well plates (volume of cell suspension used 250 μ L) and live cells counted every 24 hours for 4 consecutive days using the Trypan blue exclusion assay as described above. Each experiment was performed in triplicate. The growth of these cell lines, is predominantly clumped and therefore prior to counting, cells were gently pipetted to disperse aggregates and provide reproducible results.

2.2 CellTiter-Glo Luminescent ATP assay

Cell viability assays were performed using the cell lines TMD8, TMD8 RO, TMD8 RI, REC and OCI-LY10 using CellTiter-Glo Luminescent Cell Viability Assay (Promega #G7573). This assay measures ATP, a marker of metabolically active and thus viable cells.

Cell suspensions were prepared at a final concentration of 5×10^5 /ml and 50 μ l plated in white walled 96 well plates (Greiner Cell Star #MO187). TMD8, TMD8 RO, and TMD8 RI cells were incubated at 37°C in 5 % CO₂ with a range of concentrations of tirabrutinib and ibrutinib (0, 1, 3, 10, 30, 100, 300, 1000 and 3000nM). All drug concentrations were prepared from a 10 μ M stock (prepared in DMSO) and diluted in RPMI to give a 2x final desired concentration. 50 μ l of the 2x final desired drug concentration was added to wells containing the suspension cells as required. A DMSO control was performed for each experiment. Each condition was carried out in triplicate for each experiment and each experiment repeated three times. Viability assays were performed at 24, 48 and 72 hours. At the desired time point 50 μ L of CellTiter-Glo reagent was added to each well (prepared as per manufactures instructions and stored at -20°C until use. Treated cells were incubated in the dark at room temperature for 30 minutes prior to measurement of the luminescent signal. Measurement was carried out on a Perkin Elmer 2030 plate reader and luminescence was calculated relative to DMSO treated cells.

2.3 Flow cytometry

Flow cytometry is a process that enable the physical and chemical characteristics of single cells to be measured from a fluid stream (198). Cells pass through a laser beam and emitted light signals are detected and analysed. Forward angle light scatter provides information on physical properties of a cell such as size and side scatter information on the internal complexity of a cell. This allows the detection of different cell populations. Labelled cells with fluorescent dyes or antibodies allow information on different cellular components and intracellular and cell surface proteins to be gathered.

2.3.1 Apoptosis assays

TMD8, TMD8 RO and RI cells were plated in 48 well plates at a density of 5×10^5 /ml. 250 μ L of cell suspension was used per condition. Dilutions of tirabrutinib and ibrutinib were prepared from 10mM stocks in media at twice the desired final concentration and 250 μ L of prepared drug concentration was added to 250 μ L of cell suspension to give a 1x final concentration. Treated cell plates were returned to the incubator and incubated for the desired time, up to 72 hours. A DMSO control was used for each experiment.

At the required time point, 200 μ L of cell suspension was added to labelled FACS tubes containing 200 μ L of 1x Annexin buffer (10mM HEPES, 150mM NaCl, 5mM KCL, 1mM MgCl₂, 1.8mM CaCl₂, pH 7.4) and 5 μ L Propidium iodide (PI) and 0.1 μ L Annexin-V fluorescein isothiocyanate (FITC). The Annexin-V assay detects phosphatidylserine (PS) present on the cell surface, an event which occurs early in apoptotic cells (199). In normal physiological conditions, PS distribution is normally restricted to the inner leaflet of the plasma membrane. During apoptosis, when lipid asymmetry within the plasma membrane is lost, PS is translocated from the cytosolic aspect to the cell surface. Annexin V, a calcium binding protein, can thus bind to PS exposed on the outer plasma membrane. PI is a membrane impermeant dye, that acts through binding to double stranded DNA through intercalating between base pairs. It is therefore excluded from viable cells and can be used as a marker of late apoptosis, when the cell membrane integrity is lost.

Cells were incubated at room temperature for ten minutes in the dark prior to analysis and pipetted a number of times to ensure a single cell suspension and circumvent clumping of the cells. Flow cytometry was performed using a BD FACSCanto. Cells were categorised as being either non-apoptotic (both PI and Annexin-V negative), early apoptosis (Annexin V positive only) and late apoptosis/necrotic (Annexin V positive and PI positive). Experiments were repeated on three occasions.

2.3.2 Immunophenotyping

Suspension cells TMD8, TMD8 RO and TMD8 RI were washed once and resuspended in RPMI media. Cell count was determined using the Trypan blue exclusion assay and a total of 1.5×10^6 cells used. Cells were pelleted at 200g for 5 minutes and re-suspended in 1.5ml of FACS (buffer (1x PBS with 2% FCS stored at 4°C). 1×10^5 cells per condition were used. The following antibodies were used to assess the phenotype: IgM (PE Serotec MCA1662), CD19 (PE BD 555413), CD20 (FITC Miltenyi 5070604005), CD3 (FITC BD 555332), CD4 (APC BD 555349), CD5 (APC BD 555355), CD8 (Cy-Chrome Pharmingen 555636), CD56 (PE BD 555516), CD45 (APC BD 555485), CD27 (PE Dako R7179), CD38 (FITC Immunotech PN IM0775), IgG1k isotype control (BDPharm 555748). An unstained sample for each cell line was also run (no antibody). For each of the condition 10 μ L as per manufacturer's instructions was used. The antibody and cell suspension were incubated for 30 minutes on ice in the dark. Following incubation, the stained cells were pelleted (5 minutes at 200g 4°C). The supernatant was then removed and the cells washed once with 300 μ L FACS buffer. Cells were subsequently re-suspended in 300 μ L FACS buffer and transferred to labelled FACS tubes. Cells were kept on ice and subject to analysis by flow cytometry immediately. For each condition, data for 10,000 events was collected. Mean fluorescence intensity and % staining were recorded for each condition.

2.3.3 Measurement of mitochondrial membrane potential

Mitochondria play an important role in apoptosis. During apoptosis, the pro-apoptotic proteins BAX and BAK are activated and undergo conformational change, resulting in disruption of the outer mitochondrial membrane and alteration in the mitochondrial membrane potential (MMP). MMP can be measured using the red-orange dye tetramethylrhodamine ethyl ester (TMRE). TMRE is a cell permeable, positively charged dye that accumulates in active mitochondria due to their negative charge. If the mitochondria are depolarised or inactive, then TMRE cannot be sequestered within the mitochondria.

Typically, 5×10^5 cells were used for each experimental condition. Cells were collected following treatment and resuspended in 1ml fresh supplemented RPMI media. $1 \mu\text{l}$ of $50 \mu\text{M}$ of TMRE (Sigma-Aldrich) was added to each sample and incubated at 37°C for 10 minutes prior to FACS analysis. A 25mM stock solution of TMRE was prepared in DMSO and stored at -20°C and protected from light. To make a working dilution, prepared fresh prior to each experiment, of $50 \mu\text{M}$, $1 \mu\text{l}$ of stock solution of 25mM TMRE was added to $499 \mu\text{l}$ of RPMI supplemented media. Analysis was conducted using a BD FACSCanto flow cytometer and FACS Diva 6.0 software to measure uptake of the dye. 10,000 events per sample were recorded and mean fluorescence intensity of 3 separate experiments calculated. Loss of MMP, results in failure to retain TMRE within the mitochondria and lower fluorescence intensity.

2.4 Western Blotting

2.4.1 Whole cell lysis

Protein was extracted from whole cells by lysis. Suspension cells for lysis were centrifuged at 1000rpm for 5 minutes. The supernatant was removed and the cell pellet resuspended in 1 ml PBS and transferred to a 1.5ml Eppendorf. The resuspended pellet was centrifuged for 5 minutes at 1000rpm. The supernatant was removed and the cell volume estimated. To the cell pellet, 5 x the estimated cell pellet volume of lysis buffer prepared as below, was added directly and the pellet re-suspended and incubated on ice for 20 minutes. Lysis buffer (Table 2.1) was made immediately before use. Centrifugation was carried out at 4°C at 10 000rpm for 10 minutes. The supernatant was transferred to a fresh pre-chilled Eppendorf and the protein concentration determined using the Pierce BSA Protein Assay Kit (Thermo-Scientific), methodology described below. Protein was stored at -80°C until required.

Table 2.1 Lysis buffer.

Reagent	Final Concentration
Tris (pH 8.0)	50mM
NaCl	125mM
NP40	0.5%
Phenylmethylsulfonylfluoride (PMSF)	1mM
DL-Dithiothreitol (DTT)	0.5mM
Phosphatase Inhibitor (Sigma 50x)	1x
Protease Inhibitor Cocktail (Sigma 100x)	1x
Glycerol	10%
Ultrapure water to make up to a final volume of 2ml	

2.4.2 Nuclear and cytoplasmic fractionation and lysis

Hypotonic buffer and 1x cell extraction buffer were prepared as below (Table 2.2 & 2.3).

Table 2.2 Hypotonic Buffer Solution.

Reagent	Final Concentration
Tris-HCl (pH 7.4)	20mM
NaCl	10mM
MgCl ₂	3mM

Table 2.3 1x Cell Extraction Buffer Formulation.

Reagent	Final Concentration
Tris-HCl (pH 7.4)	100mM
NaCl	100mM
Triton X-100	1%
EDTA	1mM
Glycerol	10%
Phosphatase Inhibitor (Sigma 50x)	1x
Protease Inhibitor Cocktail (Sigma 100x)	1x
EGTA	1mM
SDS	0.1%
Deoxycholate	0.5%
Na ₄ P ₂ O ₇	20mM

5×10^6 cells were collected and pelleted at 200g for 4 minutes. The supernatant was removed and the pellet re-suspended in 10 ml cold PBS. Repeat centrifugation 200g for 4 minutes was carried out. The cell pellet following discarding of the supernatant was re-suspended in 200 μ L 1 x hypotonic buffer and transferred to a pre-chilled

microcentrifuge tube and incubated on ice for 15 minutes. 10 μ L of 10% NP40 was then added and the sample vortexed for 10 seconds. The homogenate was centrifuged for 10 minutes at 3000rpm for 10 minutes at 4°C. The supernatant which contains the cytoplasmic fraction was saved. The pellet, which constitutes the nuclear fraction was washed twice with 1ml cold PBS and centrifuged for 10 minutes at 3000rpm at 4°C. The nuclear pellet was then resuspended in 80 μ L extraction buffer and incubated on ice for 40 minutes with vortexing at 10 minute intervals. The sample was centrifuged for 10 minutes at 14 000g at 4°C. The supernatant (nuclear fraction) was then transferred to a clean prechilled microcentrifuge tube and stored at -80°C. The protein concentration was determined before use and immunoblotting was performed using antibodies to parp and alpha tubulin to check for nuclear and cytoplasmic fractionation.

2.4.3 Lipid raft extraction

From a total of 1x10⁹ cells, lipid rafts were isolated from the cell lines TMD8 and TMD8 RO using methods previously described (105). Sucrose containing solutions were prepared the day prior to use to ensure solubilisation and stored at 4°C.

Buffers used:

Buffer A: 50 mM Tris-HCl [pH 7.4], 150 mM NaCl, 80% Sucrose. Check with a refractometer.

Buffer B: 50 mM Tris-HCl [pH 7.4], 150 mM NaCl, 1% Triton X-100 + protease inhibitor.

Buffer C: 50 mM Tris-HCl [pH 7.4], 150 mM NaCl, 30% Sucrose.

Buffer D: 50 mM Tris-HCl [pH 7.4], 150 mM NaCl, 5% Sucrose.

Buffer E: 50 mM Tris-HCl [pH 7.4] + protease inhibitor.

1x10⁹ cells were harvested by centrifugation for 5 minutes at 300g at 4°C and the subsequent pellet resuspended in 10ml of ice cold PBS to wash and centrifuged as previously described. The supernatant was removed and the cell pellet stored on ice. The cell pellet was solubilised in buffer B to give a final volume of 3ml for 30 minutes on ice. Gentle mixing was carried out every five minutes. 3 ml of Buffer A was added to the solubilised cell pellet, to give a final sucrose concentration of 40%. 2ml was added to a pre-chilled ultracentrifuge tube (Thermo Scientific PET Thin-walled Tube #06752

Volume fill 12.2ml and suitable for a Sorvall TH641 rotor). To this 5ml of buffer C (containing 30% sucrose) was carefully layered onto the lysate using a Pasteur pipette. 5ml of Buffer D (containing 5% sucrose) was carefully layered on top using a Pasteur pipette. Centrifuge tubes were carefully balanced and loaded into prechilled buckets suitable for the TH641 rotor. The discontinuous sucrose gradient was subject to ultracentrifugation for 17 hours at 100,000g at 4°C using a Sorvall OTD65B ultracentrifuge. Lipid rafts were harvested from the interphase of the 30% and 5% sucrose bands using Pasteur pipette at 4°C. Care was taken to minimise the volume of sucrose solution sampled. The lipid rafts were added to clean prechilled centrifuge tube and to this 10ml of Buffer E added. The lipid rafts were subject to ultra-centrifugation at 100 000g for 1 hour at 4°C using the same rotor. Following centrifugation, the supernatant removed and the lipid raft pellet solubilised in 1% SDS in PBS at room temperature (approximate final volume of 0.5ml).

The protein concentration was calculated and for the purposes of mass spectrometry analysis or immunoprecipitation samples were not frozen prior to use. For western blots, samples were stored at -80°C until required.

2.4.4 Membrane Fractionation by discontinuous sucrose density gradients

From a total of 1×10^9 cells of TMD8 and TMD8 RO, membrane fractionation by discontinuous sucrose density gradients was carried out. The following buffers were used and prepared as described below. Buffers containing sucrose were made the day before use to enable solubilisation and then stored at 4°C overnight.

Buffers used:

MBS lysis buffer: 25mM 2-(N-morpholino)ethanesulfonic acid (Mes), 150mM NaCl, 1% Triton X-100, protease inhibitor (pH 6.5)

90% sucrose in MBS: MBS: 25mM Mes, 150mM NaCl (pH 6.5); 90% sucrose

35% sucrose in MBS: MBS: 25mM Mes, 150mM NaCl (pH 6.5), 250mM Na₂CO₃; 35% sucrose

5% sucrose in MBS: MBS: 25mM Mes, 150mM NaCl (pH 6.5), 250mM Na₂CO₃; 5% sucrose

Cells were pelleted and washed in 10ml ice cold PBS (pH 7.3) twice (centrifuge 300g for 5 minutes at 4°C). The resultant pellet was lysed in 2ml ice cold MBS lysis buffer for 30 minutes on ice. Lysates were subject to 3 20sec bursts of sonification on ice. To the lysate, an equal volume of 90% sucrose in MBS was added (2ml) and loaded in a prechilled ultracentrifuge tube (Thermo Scientific PET Thin-walled Tube #06752 Volume fill 12.2ml and suitable for a Sorvall TH641 rotor). 4ml of 35% sucrose prepared in MBS (containing 250mM Na₂CO₃) was carefully layered on top using a Pasteur pipette and then 4ml of 5% sucrose prepared in MBS (containing 250mM Na₂CO₃) layered on this to form a discontinuous sucrose density gradient. The gradient was centrifuged at 39,000 rpm on a TH-641 rotor in a Sorvall OTD65B ultracentrifuge for 16 hours at 4°C. 12 fractions of 1 ml from the top to the bottom of each tube were collected using a Pasteur pipette. The protein concentration was calculated as previously described. Samples were stored at -80°C prior to use.

2.4.5 Measurement of Protein Concentration

Protein concentration in the cellular extract was determined according to the Pierce BSA Protein Assay Kit (Thermo Scientific). BSA standards were prepared from a stock concentration of 2mg/ml as shown in Table 2.4.

Table 2.4 BSA standard preparation.

Vial	Volume of Diluent (μL)	Volume and Source of BSA (μL)	Final BSA Concentration (μg/mL)
A	0	300 of Stock	2000
B	125	375 of Stock	1500
C	325	325 of Stock	1000
D	175	175 of vial B dilution	750
E	325	325 of vial C dilution	500
F	325	325 of vial E dilution	250
G	325	325 of vial F dilution	125
H	400	100 of vial G dilution	25
I	400	0	0 = Blank

Using a microplate, 10μl of the protein sample or standard were added to each well in duplicate. 200μL of the working reagent (prepared as per manual) was added to each well and the plate mixed on a plate shaker for 30 seconds. The plate was covered and

incubated at 37°C for 30 minutes prior to reading at an absorbance of 562nm on the TECAN plate reader. A standard curve was prepared by plotting the average Blank-corrected 562nm measurement for each BSA standard vs. its concentration in µg/mL. The standard curve was used to determine the protein concentration of each unknown sample.

2.4.6 Protein Electrophoresis and Western Blotting

Between 20-50µg of total protein was used per sample for analysis. The desired amount of protein was boiled at 95°C for 5 minutes with 4x SDS sample buffer (Table 2.5) and loaded onto a polyacrylamide gel (8-15% as dictated by protein size). A molecular weight marker (2.5µL) obtained from Geneflow (S6-0024) was used to determine molecular weights. This is a protein standard with 12 pre-stained proteins covering a range of molecular weights from 10 to 245 kDa, with two reference bands at 25 kDa and 75 kDa when separated on SDS-PAGE. The gel was allowed to run for approximately 45 minutes at 40mA until protein separation was achieved.

The separated proteins were transferred onto a nitrocellulose membrane using a BioRad Mini transfer (100V for 90 minutes). Following transfer, the membrane was washed 1x with 0.1% TBS-T and then blocked in 15ml 5% skimmed milk in TBST for 1 hour. The membrane was then probed with the primary antibody (Table 2.6) of choice at its desired concentration (diluted in 0.1% TBS-T) in a total volume of 5ml and incubated overnight at 4°C. The membrane was washed for 10 minutes 3 times with 15ml 0.1% TBS-T and subsequently incubated with a secondary antibody (Table 2.7) to the primary antibody conjugated to horseradish peroxidase (diluted in 15ml 0.1% TBS-T) for 1 hour at room temperature. Washing was repeated 3 times again with 15ml 0.1% TBS-T. For detection of immunoreactive bands the detection Reagent, Amersham ECL Prime Western Blotting Detection Reagent or Bio-Rad ECL reagent was used. The membrane was drained of excess developing solution, wrapped in cling film and then exposed to x-ray film (Fuji Film). Images were developed using a Konica x-ray processor. For a loading control, membranes were reprobed with GAPDH.

Table 2.5 4x SDS Sample buffer.

4x SDS Sample buffer
200nM Tris-HCL (pH 6.8)
40% glycerol (v/v)
8% SDS (v/v)
400nM Dithiothreitol
0.4% bromophenol blue (v/v)

Table 2.6 List of primary antibodies used.

Antibody with epitopes recognised where known	Host	Monoclonal or polyclonal?	Source	Catalogue number	Concentration used
BTK	Rabbit	Monoclonal	Cell signalling	8547	1:2000
pBTK (Tyr223)	Rabbit	Monoclonal	Cell signalling	5082	1:1000
BTK/ITK (Y551/Y511)	Mouse	Monoclonal	eBioscience	46-9015	1:1000
Flotillin	Rabbit	Polyclonal	Cell signalling	3253	1:1000
Lyn (H6)	Mouse	Monoclonal	Santa-Cruz	sc-7274	1:2000
Raftlin (N14)	Goat	Polyclonal	Santa-Cruz	sc-103139	1:1000
PAG	Rabbit	Monoclonal	Abcam	ab128286	1:1000
5-LO (C49G1)	Rabbit	Monoclonal	Cell signalling	3289	1:1000
GAPDH (D16H11)	Rabbit	Monoclonal	Cell signalling	5174	1:5000
pERK (Thr202/Tyr204)	Rabbit	Polyclonal	Cell signalling	9001	1:1000
ERK	Rabbit	Polyclonal	Cell signalling	9102	1:1000
pAKT S473	Rabbit	Monoclonal	Cell signalling	4058	1:1000
AKT	Rabbit	Monoclonal	Cell signalling	9272	1:1000
Alpha tubulin	Mouse	Monoclonal	Calbiochem	CP06	1:1000
Parp C2-10	Mouse	Polyclonal	Enzo	BML-SA249	1:1000
Total phosphotyrosine protein (4G-10)	Mouse	Monoclonal	Millipore	05-321	1:1000
PLCy2	Rabbit	Polyclonal	Cell	3872	1:1000

			signalling		
pPLCy2	Rabbit	Polyclonal	Cell signalling	3871	1:1000
IgG	Rabbit	Polyclonal	Cell signalling	2729S	1:1000

Table 2.7 Secondary antibodies conjugated to HRP.

Antibody	Host	Source	Catalogue number	Concentration
Anti-rabbit	goat	Dako	P0448	1:5000
Anti-Mouse	goat	Dako	P0447	1:5000
Anti-Goat	rabbit	Dako	P0449	1:2000

2.5 Immunoprecipitation

2.5.1 Preparation of buffers

Table 2.8 Immunoprecipitation buffer.

20 mM Tris HCl, pH 8

120 mM NaCl

0.5% NP40

Protease Inhibitor Cocktail

PMSF

MilliQ H₂O

Table 2.9 Wash buffer.

20 mM Tris HCl, pH 8

120 mM NaCl

0.5% NP40

MilliQ H₂O

2.5.2 Primary antibody and sample incubation

All stages were carried out on ice unless otherwise specified. For mass spectrometry samples, 1500µg of protein was used and for western blot 500µg of protein was used. For every 500µg of protein, 5ul of antibody was used.

The antibody and protein concentration required were added to a 1.5ml pre-chilled Eppendorf. For every 500µg of protein, the volume was made up to 500µl with cold IP buffer, prepared as above. The sample was then incubated at 4°C for 6 hours on a daisy wheel.

2.5.3 Preparation of protein A sepharose beads and addition to protein and antibody sample

60µl of the resultant bead suspension were used per 500µg of protein. To prepare the beads (Protein A Sepharose 4, GE Healthcare, #17-5280-01), the required amount was centrifuged at 1000rpm for 2 minutes at 4°C. The supernatant was carefully discarded and 1 ml of wash buffer added and the Eppendorf shaken. This was repeated a further two times. The beads were then re-suspended in 2x the size of the bead pellet with wash buffer. 60ul of the sepharose bead suspension was added per 500µg of protein and the each sample centrifuged for 30s at 1000rpm 4°C to ensure equal distribution. Samples were incubated overnight at 4°C. Following overnight incubation, samples were again centrifuged at 4°C for 2 minutes at 1000rpm. The supernatant was removed (flow through sample stored from the supernatant) and 1 ml of wash buffer added to the sample. This was repeated a further 2 times. Care was taken to remove as much supernatant as possible.

2.5.4 Elution of the immunoprecipitate

20µl of 2x sample buffer was added to the beads per 500µg of protein used. This was boiled at 100°C for 5 minutes to release the immunoprecipitate. Samples were centrifuged at room temperature for 2 minutes at 13 000 rpm and the supernatant directly loaded onto a polyacrylamide gel or stored at -80°C.

2.6 Mass spectrometry

Samples were prepared by running 3cm into mini-bolt gels (4-12%) (Invitrogen life sciences) and stained with safeblue stain overnight. Protein identification by mass spectrometry was carried out by Professor Cain's group (MRC Toxicology, University of Leicester). The gel was submitted and samples prepared by Dr C. Langlais and Mrs B. Juke- Jones. The methods shown below were written and provided by the group and reproduced with their permission within my thesis.

'Sample Preparation for Mass Spectrometry: Coomassie stained gels were prepared for mass spectrometry analysis by cutting lanes into slices (~24 slices per lane). Gel sections were transferred to the wells of a 96-well PCR plate and alternately washed in 80ul of 50 mM ammonium bicarbonate and 80ul of 100% acetonitrile at least three times to remove the stain. Samples were reduced with 10 mM dithiothreitol (20 min at 56°C) and alkylated with 100 mM iodoacetamide (20 min in the dark), followed by washes with 50 mM ammonium bicarbonate / 100% acetonitrile. Gel slices were resuspended with 15 µl Trypsin digestion buffer (11.11 µg / ml in 25 mM ammonium bicarbonate; Sequencing Grade Modified Trypsin, Promega Corporation, Madison, Wisconsin, USA). The plate was sealed, incubated at 30°C overnight, 80 µl extraction buffer (0.2% trifluoroacetic acid) added to each well and the plate incubated for 1 h at room temperature. Extracted samples were transferred to 0.5 ml Eppendorf tubes and dried for 1 h with a Savant DNA Speed Vac (Thermo Scientific, Waltham, MA, USA). Dried peptide samples were resuspended with 5% formic acid / acetonitrile (9:1), vortexed, and transferred to glass vials by combining two samples into one vial. Samples were spiked with two internal standards, ADH1 from yeast (accession: P00330) and bovine serum albumin (accession: P02769), to a final concentration of 40fmol / µl (MassPREP standards, Waters Corporation, Manchester, UK).'

'Mass spectrometry analysis: Peptide mixtures were analysed by nanoflow liquid chromatography coupled to a Synapt G2S mass spectrometer (NanoAcquity UPLC system and Synapt G2S mass spectrometer, Waters Corporation, Manchester, UK) using a 25 cm X 75 µm I.D., 1.7 µm, BEH130 C18 column. Samples (2 µl injections) were separated using a reversed phase 50 minute solvent gradients (3% to 40% acetonitrile) at 0.3 µl / min. Mass spectrometry analysis was performed in a data-

independent manner using ion mobility (HDMSE), with IMS wave velocity set to 650 m/s in the helium cell. The mass spectrometer was programmed to step between low energy (4 eV) and elevated collision energies (20-50 eV) in the gas cell, using a scan time of 1 sec and a mass range of 50-2000 m/z.'

'Database Search and Protein Identification: Raw data files were analysed using ProteinLynx Global SERVER (PLGS version 3, Waters Corporation, Manchester, UK) in combination with Scaffold software (version 4, Proteome Software, Inc., Oregon, USA) and the human UniProt database, including reverse sequences (release 2014_05, 11.06.14, 20265 entries). Data processing was performed with the low energy threshold set to 135 and elevated / high energy threshold set to 30. For database searching in PLGS, peptide mass tolerance and fragment mass tolerance was set to auto, with a maximum of one missed cleavage allowed and variable modifications for carbamidomethylation of cysteine and methionine oxidation included. Ion matching requirements were set to one or more fragments per peptide, three or more fragments per protein and one or more peptides per protein (1:3:1) with a false discovery rate (FDR) of 100%. Processed/searched PLGS data files were then loaded into Scaffold for further analysis and visualisation of the data.'

'Spiked ADH1 (yeast) and BSA (bovine) tryptic digests were used for quality control purposes.'

2.7 Cell stimulation assays

2.7.1 IgM stimulation

Suspension cells were cultured in RPMI 1640 containing 10% FCS and 1% PS at a density of 1×10^6 /ml in 6 well plates. 1 μ g/ml of Goat F(ab')₂ Anti-Human IgM was added to all wells aside from the control and cells were incubated for time periods up to 24 hours at 37°C. Following incubation cells were pelleted (200g for 5 minutes 4°C) and washed in 1 ml PBS. The pelleted cells were then subject to lysis and following protein quantification stored at -80°C until use. EGFR cell stimulated lysate was used as a positive control.

2.8 RNA analysis

2.8.1 RNA extraction

Total RNA was extracted from the suspension cell lines TMD8, TMD8 RO and TMD8 RI and from patient samples stored at -80°C pre, during and post the development of resistance to tirabrutimib. 1×10^7 cells were removed from culture and pelleted at 300g for 5 minutes. The supernatant was removed and cells re-suspended in 1ml sterile PBS prior to repeat centrifugation (300g for 5 minutes) to ensure all media was removed. RNA was then extracted using the Quiagen RNeasy mini kit as per manufacturer's instructions (#74104). Homogenisation was achieved using a QIA shredder spin column. The lysate was homogenised on passing through the spin column, preventing cross contamination. Genomic DNA is removed during RNA extraction and therefore an additional process for elimination was not required.

The concentration and A_{260}/A_{280} ratio of extracted RNA was measured using the NanoDrop Lite Spectrometer (Thermo Scientific). RNA was stored at -80°C prior to use.

2.8.2 Gene expression profiling

Gene expression profiling was undertaken within the University of Leicester Nucleus Genomics facility. The RNA was purified from TMD8 cell lines on a Maxwell® 16 Research Instrument (Promega). RNA quality was checked on a Bioanalyzer 2100 (Agilent). All the RNA samples passed the quality control with a RNA Integration Number (RIN) > 7.

A total of 250ng of total RNA were reverse-transcribed and the cRNA was labelled with biotin using the TargetAmp™- Nano Labeling Kit for Illumina® Expression BeadChip (Epicentre) according to manufacturer instructions. Initially first-strand cDNA was synthesised from Poly(A) RNA contained in the total RNA extracted and the reaction primed from an oligo(dT)-primer containing a phage T7 RNA Polymerase promoter sequence at its 5' end. First strand cDNA synthesis was catalysed by SuperScript III Reverse Transcriptase. Second strand cDNA synthesis was then carried out by

converting the cDNA produced in step 1 to a soluble stranded cDNA containing a T7 transcription promoter to generate an anti-sense RNA. In vitro transcription of Biotin-aRNA (or Biotin-cRNA) were produced at high yields using the double stranded cDNA produced as a template. The labelled cRNA was purified using the Qiagen RNeasy MiniElute Cleanup Kit.

cRNA was analysed using the HumanHT-12 v4 Expression BeadChip Kit, allowing quantification of about 47,000 transcripts. The beadchips were then scanned using an Illumina iScan. The raw microarray data were normalized by quantile normalization using the Illumina Genome Studio V2011.1. The probes with a signal intensity below the background level of 140 were considered as not confidently detected and were excluded from the downstream analysis. All further analyses were done using MS excel. The genes were ranked according to fold change of expression between the parental cell line TMD8 and the resistant cell lines TMD8 RO and TMD8 RI. A 2-fold change was used as a cut-off for significance.

2.9 DNA analysis

2.9.1 DNA extraction for whole exome sequencing

Genomic DNA was extracted from the cell lines TMD8, TMD8 RO and TMD8 RI and patient sample pre and post development of resistance to tirabrutinib using the Quiagen DNeasy blood and tissue kit (#69504). 1×10^7 cells were removed from culture and pelleted at 300g for 5 minutes. Cells were re-suspended in 1ml PBS to wash following discarding of the supernatant and again pelleted. DNA was then extracted as per manufacturers' instructions. The yield of DNA was measured using the NanoDrop Lite Spectrometer (Thermo Scientific). Extracted DNA was stored at -20°C .

2.9.2 Whole exome sequencing

Extracted DNA was sent for whole exome sequencing by Oxford Gene Technology. Sequencing reads were aligned to the human reference genome (1000 Genomes Project human assembly GRCh37) with the use of Burrows–Wheeler Aligner.

2.9.3 PCR

Using extracted DNA from TMD8, TMD8 RO and TMD8 RI, PCR was performed. Primers were prepared to a 100µM stock as per manufactures instructions. Table 2.10 shows the custom primers used (Purchased from Sigma Life Sciences).

Table 2.10 Primers.

Gene	Mutation	Forward	Reverse
BTK	C481S	GCCTCTCTACGTCTTCTCCC	TGCTGGCTCAGGCGGTAGTG
PLCG2	R665	GCTGAGGTGCCTTTGTCTGG	GAAGTCCCCCTTGTCTCTC
PLCG2	T706I	GGCCACCAGGATCTTGGCATG	GTATCCCCAGGACCTACAGCAG
PLCG2	S941	GAGAGGAAGAAACGAGAGGG	GAGAGAATGCACTCTCTGC

For the PCR reaction, a total volume of 25µL was used. 1µL of each of the forward and reverse primers (10µM) were used. 1µL of DNA was added at a concentration of 100ng/µL). 12.5µL of the extensor and 9.5µL of ultrapure water was used. For the control, in place of DNA, 1µL of ultrapure water was added. For the PCR reaction: 95°C for 5 minutes, 30 cycles- repeat 95°C 30 seconds, 60°C for 30 seconds and 72°C for 45 seconds followed by 72°C at 20 minutes. This was performed in a G storm labtech PCR machine.

PCR clean up was performed using a nucleospin gel and PCR clean up column as per manufacturers instructions (Quiagen kit). DNA content was checked using the NanoDrop Lite and 20µL at > 10ng/µl was sent for Sanger Sequencing by Beckman Coulter.

2.10 Analysis of prognostic markers and targeted sequencing using a 36 gene targeted sequencing panel of patients with CLL treated with tirabrutinib on the Phase 1 clinical trial

Analysis of prognostic markers was undertaken: interphase FISH to detect 17p13.1, 11q, 13q, trisomy 12, *TP53* and *IGHV* mutational status was performed centrally and confirmed locally. A cutoff of 98 % homology to the germline sequence to discriminate between mutated (<98 %) and unmutated (≥98 %) cases. For NGS analysis, a 36 gene

panel was designed in collaboration with Dr S. Macip (Department of Molecular and Cell Biology, University of Leicester) and Sistemas Genomicos (Valencia, Spain). These are shown in Table 2.11. These span the different Gene Ontology pathways identified as containing genes commonly mutated in CLL with a focus of those actionable by specific precision medicines.

DNA was extracted from peripheral blood from 27 patients prior to trial entry by Dr Sandrine Jayne. Targeted sequencing was performed using the Illumina next generation sequencing (NGS) platform at Sistemas Genomicos, Valencia, Spain. Reads were aligned against the human genome version GRCh37/hg19. Filtering was performed using Picard tools (<http://picard.sourceforge.net>) and SAMtools (<http://samtools.sourceforge.net>). Confirmatory Sanger sequencing was performed by Dr Sandrine Jayne on identified sequence variants and were annotated using the Ensembl database (www.ensembl.org). Only sequence variants leading to a change in amino acid composition and not reported in the database of single nucleotide polymorphisms (dbSNP) were scored as mutations. These mutations were checked against the COSMIC database. Sanger sequencing was used to determine *IGHV* status; this was performed locally in Leicester.

Table 2.11 List of genes on the Sistemas Genomicos CLL NGS panel.

Gene		Location	
Genes for stratified therapies (existing inhibitors)	<i>BRAF</i>	Chromosome 7: 140,719,327-140,924,764	Exonic
	<i>MEK</i>	Chromosome 15: 66,386,817-66,492,312	
	<i>KIT</i>	Chromosome 4: 54,657,918-54,740,715	
	<i>NRAS</i>	Chromosome 1: 114,704,469-114,716,894	
	<i>EGFR</i>	Chromosome 7: 55,019,021-55,211,628	
	<i>ROS1</i>	Chromosome 6: 117,288,300-117,425,855	
	<i>JAK2</i>	Chromosome 9: 4,984,390-5,128,183	
	<i>MAP3K14 (NIK)</i>	Chromosome 17: 45,263,121-45,317,040	
	<i>RIPK1</i>	Chromosome 6: 3,063,991-3,115,187	
	<i>TLR2</i>	Chromosome 4: 153,701,500-153,705,699	
	<i>RYR2</i>	Chromosome 1: 237,042,205-237,833,988	
Genes with mutations that may lead to resistance to therapies	<i>PLCG2</i>	Chromosome 16: 81,739,097-81,962,693	Exonic
	<i>PI3KCD</i>	Chromosome 3: 138,652,699-138,834,938	
	<i>BTK</i>	Chromosome X: 101,349,447-101,390,796	
	<i>CXCR4</i>	Chromosome 2: 136,114,349-136,118,165	
	<i>CD79B</i>	Chromosome 17: 63,928,740-63,932,354	
	<i>MYD88</i>	Chromosome 3: 38,138,478-38,143,022	
	<i>CARD11</i>	Chromosome 7: 2,906,141-3,043,945	
Genes identified as prognostic factors	<i>TP53</i>	Chromosome 17: 7,661,779-7,687,550	Exonic
	<i>ATM</i>	Chromosome 11: 108,222,484-108,369,102	
	<i>NOTCH1</i>	Chromosome 9: 136,494,444-136,545,862	
	<i>SF3B1</i>	Chromosome 2: 197,389,784-197,435,091	
	<i>POT1</i>	Chromosome 7: 124,822,386-124,929,983	
Genes involved in the Wnt signalling pathway	<i>RSPO4</i>	Chromosome 20: 958,452-1,002,264	Exonic
	<i>WNT1</i>	Chromosome 12: 48,978,453-48,981,676	
	<i>FZD5</i>	Chromosome 1: 64,730,558-64,737,751	
	<i>CHD8</i>	Chromosome 14: 21,385,194-21,456,126	
	<i>BCL9</i>	Chromosome 1: 147,541,412-147,626,216	
	<i>CREBBP</i>	Chromosome 16: 3,725,054-3,880,726	
	<i>PRICKLE1</i>	Chromosome 12: 42,456,757-42,590,355	
	<i>RYK</i>	Chromosome 3: 134,065,303-134,250,744	
	<i>BRD7</i>	Chromosome 16: 50,313,487-50,368,934	
	<i>CSNK1E</i>	Chromosome 22: 38,290,691-38,318,084	
	<i>DKK2</i>	Chromosome 4: 106,921,802-107,283,806	

Chapter 3 Clinical Experience of Tirabrutinib

The first in class BTKi, ibrutinib, has shown remarkable efficacy in clinical trials in CLL, MCL, WM and ABC DLBCL. It is generally well tolerated and long term therapy is possible in most patients. However, the broad kinome of ibrutinib, with inhibition of several other kinases at low nanomolar concentrations in addition to BTK, may limit its clinical utility in some patients (188, 200, 201). In the 3 year follow up of 132 patients with CLL receiving ibrutinib, including treatment naïve and relapsed/refractory patients, 27% of all patients experienced a grade ≥ 3 haematological adverse event, 77% a non-haematological grade ≥ 3 event and 42% experienced a grade ≥ 3 infection AE (202). Grade ≥ 3 AEs occurring in $>5\%$ of patients over the 3 years were hypertension (20%), pneumonia (20%), neutropenia (14%), thrombocytopenia (8%), atrial fibrillation (6%), diarrhoea (6%), fatigue (5%) and sepsis (5%) (202).

In vitro, tirabrutinib has been shown to be a more selective tyrosine kinase inhibitor of BTK than ibrutinib, thus warranting its clinical evaluation. Tirabrutinib entered the clinical setting in the Phase I clinical trial of tirabrutinib (NCT01659255) in R/R B cell malignancies in September 2012. This was a multicentre trial with 6 sites selected within the UK and France (University Hospitals Leicester, Plymouth Hospitals NHS Trust, University Hospitals of Wales, Centre Hospitalier Lyon Sud, Centre Hospitalier Régional Universitaire de Lille, Centre Hospitalier Régional Universitaire de Montpellier). My role in this study was in the recruitment and management of patients on trial as sub-investigator. Twice weekly Phase I clinics were conducted on the Hope Clinical Trials Facility at University Hospitals Leicester. Following completion of the study, I played a leading role in extracting and interpreting data from the trial database at ONO Pharmaceuticals in London.

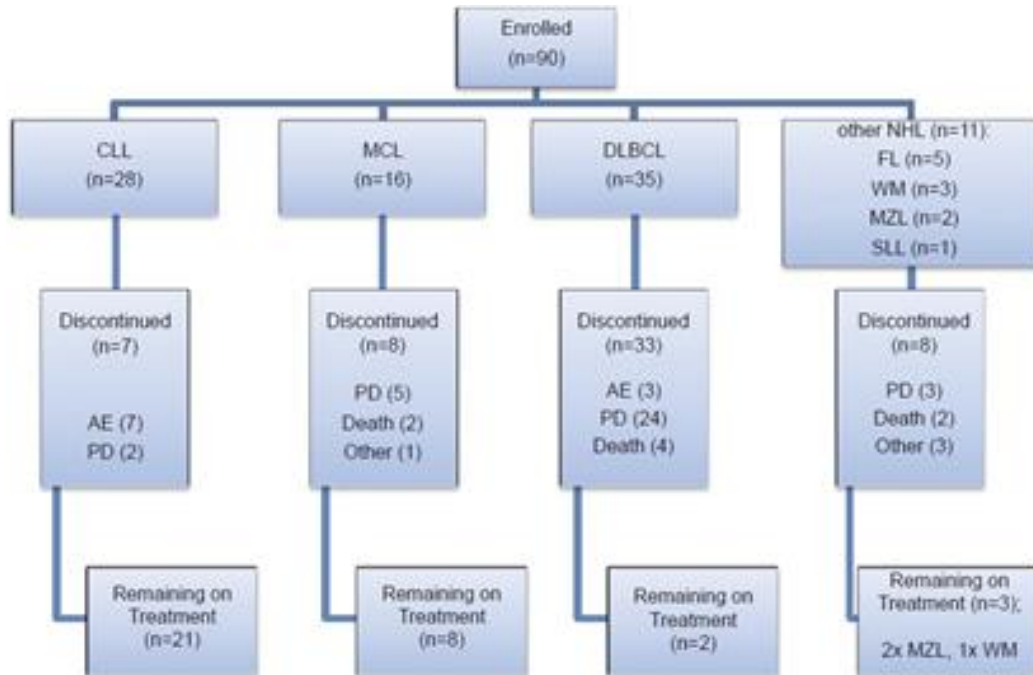
3.1 Study Objectives and design

The primary objectives of the study were to determine the safety and tolerability of escalating oral doses of tirabrutinib given as monotherapy in patients with R/R NHL and R/R CLL (Please refer to Appendix A.1 for definition of DLT and grading of toxicity according to the NCI-CTCAE version 4.0). Secondary objectives were to examine peripheral blood lymphocytosis and recovery with increasing doses of tirabrutinib and to obtain preliminary data on the anti-tumour efficacy of tirabrutinib given as monotherapy in patients with R/R NHL and CLL (Please refer to Appendix A.2 for definition of response to tirabrutinib).

The study was conducted using a 3+3 clinical trial design with two parallel dose escalation groups in CLL and NHL. This rule-based design of dose escalation is the most common method of study design adopted in Phase I cancer clinical trials and is based on the assumption that toxicity of cytotoxic drugs increases with dose (203). Cohorts of three patients were recruited, with the first cohort being treated with a dose of 20mg once daily (OD). In the absence of the occurrence of a dose limiting toxicity (DLT), 3 patients were recruited at the next dose level until a maximum predefined dose of 600mg OD. This was determined from pre-clinical toxicity studies in rats and monkeys, where pancreatitis and central nervous system toxicity were dose limiting toxicities (*ONO Pharmaceuticals, personal communication/unpublished data*).

DLTs were defined as a drug related toxicity occurring within the first 28 days of treatment. All NCI-CTCAE Version 4 Grade 3 and Grade 4 tirabrutinib related adverse events with the exception of lymphocytosis were considered DLTs. In the event of a DLT, a further 3 patients were recruited to that dose level. A dose limiting toxicity was defined if $\geq 33\%$ of patients experienced a dose limiting toxicity at that dose level. Dosing for subsequent CLL cohorts was 40mg, 80mg, 160mg, 320mg, 400mg, 500mg, 600mg OD and 300mg twice a day (BID). Dosing for subsequent NHL was 40mg, 80mg, 160mg, 320mg, 480mg, 600mg OD and 240mg BD. Intra-patient dose escalation was permitted. A summary of patients recruited according to the different diagnostic categories and their disposition in the trial is shown in Figure 3.1.

Figure 3.1 Patient enrolment by disease subtype and disposition within the trial (165).



This research has been published (165) and an updated survival analysis of the CLL cohort was published in June 2016 (204) (Appendices A.3 and A.4). Long term follow up of the CLL cohort was subsequently published (205) (Appendix A.5).

3.2 Clinical response to the selective BTKi tirabrutinib

3.2.1 Chronic Lymphocytic Leukaemia

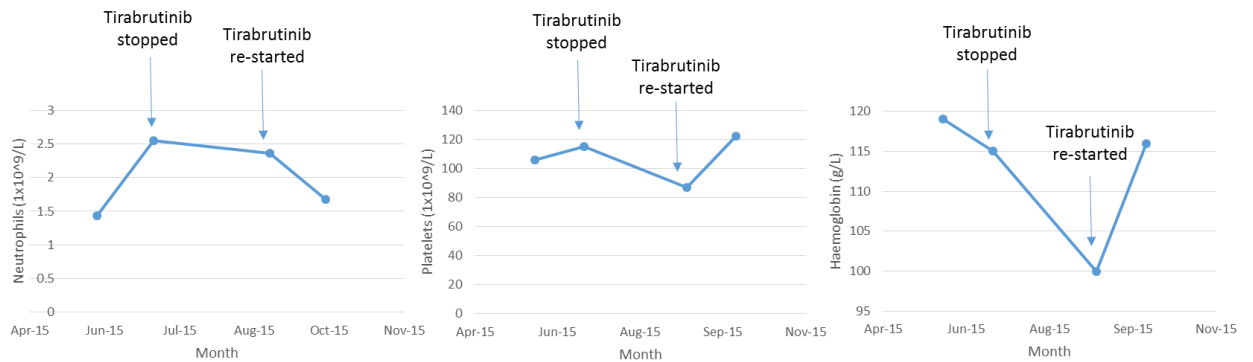
Of the 28 patients with CLL enrolled, 25 were evaluable for disease response. 24/25 (96%) responded and the median length of treatment with tirabrutinib at the time of analysis (December 2015) was 29.9 months. A maximum tolerated dose was not reached and no dose response was observed. Lymphocytosis was observed in 23 patients which resolved within 6 months. Interestingly, whilst major lymph nodal responses occurred rapidly, continued nodal responses were seen up to 18 months following treatment initiation, albeit at a much lower rate of response. Non-evaluable patients included 1 patient who had not reached cycle 3 at the time of data analysis, 1 patient with early progressive disease in cohort 1 (20mg OD) and possible

transformation to DLBCL and 1 patient who was withdrawn due to the development of idiopathic thrombocytopenia.

Four of the 25 evaluable CLL patients were withdrawn due to adverse events, of which one patient had concomitant progressive disease. Adverse events included neutropenic sepsis, purpura, spontaneous psoas hematoma in the presence of a normal platelet count, and idiopathic thrombocytopenia. 3 patients discontinued due to progressive disease and one patient died from pneumonia. In the CLL cohort, no MTD of tirabrutinib was identified. In one patient with *TP53* mutant CLL who initially received 40mg OD and responded for 21 cycles, a further response was seen following dose escalation to 600mg OD for a further year. This case is described in detail in chapter 4. Similar to acalabrutinib, no confirmed cases of Richter syndrome have been reported.

In Leicester, in order to assess the depth of responses obtained with tirabrutinib, minimal residual disease (MRD) analysis to detect residual CLL cells (performed using multicolour flow cytometry with a sensitivity of at least 10^{-4} (206) from peripheral blood and bone marrow samples of patients with CLL treated at Leicester) was undertaken. Three four-color antibody combination (CD5/CD19 with CD20/CD38; CD81/CD22; and CD79b/CD43) is used for the detection of MRD by flow cytometry in CLL (206). All 8 patients with CLL treated within our centre remained MRD positive on peripheral blood analysis during study treatment, despite 5 patients achieving a complete response radiologically. As with ibrutinib, long term continuous therapy with tirabrutinib is necessary to maintain disease control. Temporary interruption of tirabrutinib, for example in a patient whom proceeded to surgery for resection of a stage I colorectal adenocarcinoma resulted in rapid recurrence of nodal disease and a fall in haemoglobin and platelet count was observed (Figure 3.2). Restarting of tirabrutinib again resulted in disease control.

Figure 3.2 Temporary interruption of tirabrutinib 80 mg OD in a patient with CLL for surgery for resection of a stage I colorectal adenocarcinoma. The figure shows the change in neutrophil count, platelet count and haemoglobin over time following interruption of tirabrutinib.



These observations are consistent with reported results with ibrutinib and idelalisib, where MRD negative complete remissions were rare with single agent treatment (202, 207). Following treatment with ibrutinib in treatment naïve CLL patients, 4 patients achieved a complete response (13%) in the phase 1b/2 trial of Ibrutinib in those aged at least 65 years (208) and 23% treatment naïve patients in the PCYC-1102 (NCT01105247) and the ongoing extension study PCYC-1103 (NCT01109069) (202). In the R/R population, 7% of patients achieved a CR (202).

Patients with CLL have been reported to have an increased incidence of second malignancies. This has been attributed to an impaired immune system, an inherent predisposition to malignancy, and prior treatment with chemotherapy (209, 210). The risk of second malignancies reported with ibrutinib in the full prescribing information ranges from 3 to 16%; the most frequent second primary malignancy was non-melanoma skin cancer.

Interestingly, BTK has also been shown to be involved in tumour suppressor pathways in solid tumours, through regulation of p53 activity (211). High expression of BTK in breast and lung cancer has been identified as a marker of good prognosis. BTK has been shown to phosphorylate p53 in vitro in response to DNA damage, implicating BTK

inhibition in the possible development of malignancies in patients receiving BTKi. To date, an increased rate of second malignancies in this population with ibrutinib and acalabrutinib has not been reported, but longer term follow up will be important to ascertain whether an increased incidence is seen.

Secondary solid tumour malignancies, were observed in 2 patients with CLL treated at Leicester; in one patient receiving 80mg OD and a further patient receiving 600mg OD. Patient 1 developed a Stage I colorectal cancer, 2 years into study treatment, which was treated radically with surgery. This was detected *via* the National Bowel Cancer Screening Programme. Drug was interrupted for 6 weeks peri-operatively. In patient 2, squamous cell carcinoma of the lung occurred, which was detected radiologically, a year into treatment. Initially staging was IIA (TNM 7th Edition). This patient had been a heavy smoker in the past. Initially, this was treated with radical stereotactic radiotherapy, however recurrence of the primary, a year later warranted radical surgery, which was successfully completed. Both patients remain without further recurrence of their second malignancies. Due to the early stage at diagnosis of both second malignancies, no adjuvant therapy was required.

3.2.2 Mantle cell Lymphoma

Sixteen patients with MCL were enrolled. 12 patients were evaluable for disease response, of which 11/12 (92%) responded to tirabrutinib. Eight patients remain on study. Four patients failed to respond and three had progressive disease on tirabrutinib following an initial short-lived clinical response. The estimated median treatment duration was 40 weeks.

Two patients had received previous autologous stem cell transplant, whereas a further 2 patients had received allogeneic stem cell transplants in first remission. Both MCL patients post allograft were recruited from Leicester; 1 of whom became MRD negative on bone marrow examination after receiving treatment with tirabrutinib 480mg OD for 3 years. This patient remains the only reported MRD negative response. Interestingly, he developed hypogammaglobulinaemia and loss of CD19 positive peripheral blood B cells at this stage, consistent with the phenotype observed in XLA. Increased

susceptibility to infection was marked by recurrent *E.Coli* urinary tract and upper respiratory tract infections.

The second MCL patient post allograft treated here in Leicester showed an initial rapid response to initiation of treatment. Prior to commencing on study, he developed gross ascites and pancytopenia, requiring frequent transfusions and granulocyte colony stimulating factor support. Within 24 hours of initiating 600mg tirabrutinib, his ascites had resolved and 7 days into study, he was no longer dependent on transfusions. He has recently developed progressive disease, marked by the onset of leukemic phase, anaemia and new retroperitoneal nodal disease on CT scan. He has now been commenced on Venetoclax on a compassionate basis.

3.2.3 Diffuse Large B cell lymphoma

31/35 patients with relapsed or refractory DLBCL were classified as non-GCB. Subtype was determined locally by Hans criteria. 2 patients were classified as GCB subtype and 1 primary mediastinal and 1 plasmablastic DLBCL were enrolled; no responses were seen in these 4 patients. Of the non-GC B-cell diffuse large B-cell lymphoma (DLBCL) 11/31 (35%) patients responded. This included one patient with primary chemo-refractory ABC DLBCL in leukaemic phase. Responses, where seen, were of rapid onset but short duration, with all patients subsequently progressing within 12 months of commencing on study. In some patients, this initial response lasted less than 4 weeks. The median treatment duration was 12 weeks. Interestingly, mixed responses were frequently observed, with progression and response observed in different nodal areas. This likely reflects ongoing acquisition of mutations and intra-tumoral clonal heterogeneity, common features observed in DLBCL and other solid tumours (212, 213). In the NHL cohort, a maximum tolerated dose was reached of 480mg OD.

3.3 Safety and Tolerability

Tirabrutinib was very well tolerated with 75% of adverse events being CTCAE V4.0 Grade 1 or Grade 2. Grade 3/4 adverse events, considered to be drug related occurred in 14.3% of those with CLL and 16.1% of those with NHL. These were mainly

haematological (neutropenia (10%), thrombocytopenia (13.3%) and anaemia (13.3%)), occurred early during treatment and recovered spontaneously during ongoing therapy. There was one grade 3 episode of drug-related haemorrhage, in a CLL patient. Importantly, and in contrast to ibrutinib no clinically significant diarrhoea, cardiac dysrhythmias or arthralgia were observed. Diarrhoea and arthralgia where seen were grade 1-2 in toxicity. Also 31.1% of patients received anticoagulation during the study period, including warfarin, with no resulting increased risk of bleeding. In the five patients with atrial fibrillation (AF), in four this was a pre-existing medical condition. One patient developed AF considered unrelated to treatment whilst on tirabrutinib during an episode of pneumonia, which resolved spontaneously with resolution of infection.

3.4 Late onset infection-associated driven neutropenia in a patient with CLL receiving 400mg tirabrutinib OD

Despite the broad expression of BTK in haemopoetic cells and long protein half-life (214), targeting with small molecule covalent inhibitors usually results in remarkably little toxicity. In our experience, selective BTKi are generally very well tolerated, including in those heavily pre-treated, of poor performance status and in the elderly populations. Toxicities when they do occur are often mild and rapidly resolve.

With ibrutinib, Grade 3-4 neutropenia was reported in 15% of patients in the Phase I study (174). Similarly, in the Phase 3 trial, neutropenia occurred in 16% of patients (179). In the 3 year follow up of patients receiving single agent ibrutinib in either the relapsed/refractory setting or untreated cohort, neutropenia occurred in 16% and in 4% of patients respectively (202). The frequency of grade ≥ 3 neutropenia occurring during years 1, >1-2, and >2-3 on therapy generally decreased with time (11%, 1%, 2%). Over the 3 year follow up period, 5 R/R patients experienced febrile neutropenia (5%) during this period and 18 R/R patients received growth factor support for neutropenia. One episode of grade 3 and one of grade 4 neutropenia resulted in a dose reduction but neutropenia did not result in discontinuation of ibrutinib. Greater haematological toxicity in relapsed/refractory disease and early occurrence, may suggest that prior therapy and disease status may contribute to this risk and timing and that BTK is not required for most myeloid functions.

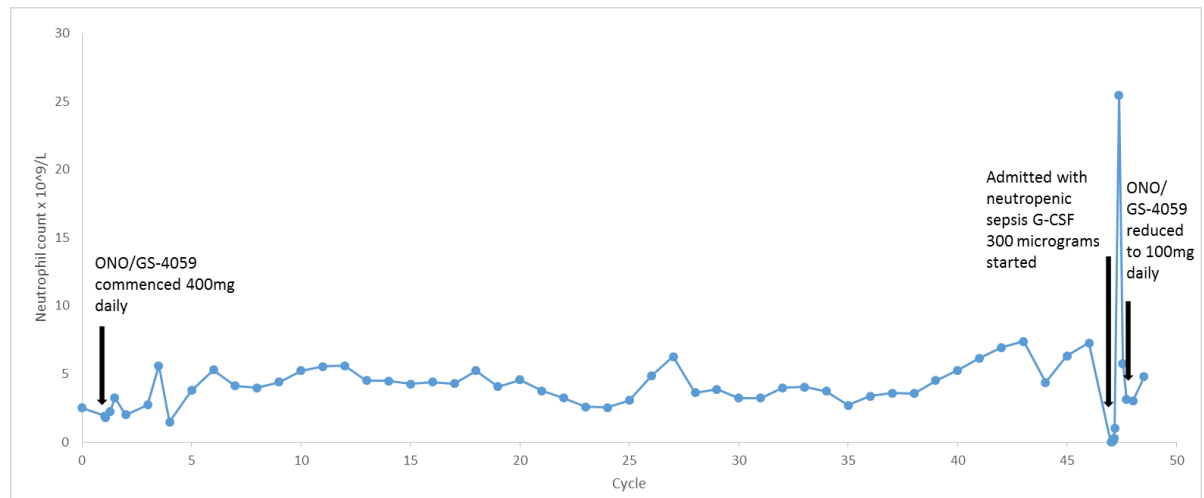
In comparison, long term follow up of patients receiving tirabrutinib, reported events of grade 1-2 neutropenia in 10.7% of patients and grade 3-4 events in 25%, with an overall frequency of 35.7% (205). However numbers of patients treated were small in comparison to patients receiving ibrutinib on the RESONATE and long-term follow-up study. In the phase 1-2 study of Acalabrutinib in relapsed CLL, grade 4 neutropenia was observed in 1/61 (1.6%) patients at a median follow up of 14.3 months (193). No grade 2 or 3 treatment emergent events of neutropenia occurred and similarly the median number of prior treatments in this population was 3 (range 1-13).

Reports of infection driven neutropenia in patients receiving BTKi have not been described. However in patients with a diagnosis of XLA, neutropenia is present in 11-30% of patients and is induced by infection (215, 216), unlike that observed in common variable immunodeficiency. Previous reports had provided evidence for a maturation arrest of neutrophils at the myelocyte/promyelocyte stage within the bone marrow, in samples obtained from some XLA patients, to account for reduced peripheral circulating neutrophil numbers (217). Subsequent studies in Xid-mice, where the R28C mutation within the Btk gene results in functionally inactive Btk protein and in Btk-deficient mice, where Btk expression is lost through gene targeting, have shown that in granulocyte-monocyte-progenitors (GMP), Btk is important in the expression of transcription factors, including C/EBPB, which are important in late and emergency granulopoiesis (218). In neutrophils deficient in Btk, impaired expression of granule proteins and functional impairment in the Arthus reaction, an acute inflammatory response, was found. These findings suggested Btk to be important in neutrophil development and function. However these findings in mouse models failed to explain why infection driven neutropenia occurs in XLA.

Here, I describe the case of a patient with a diagnosis of CLL, diagnosed in 2013, treated with tirabrutinib from 2013 to present. Interestingly, he was diagnosed with Follicular Lymphoma stage IVa in 2003, and treated initially with chlorambucil (refractory disease) followed by 6 cycles of CVP, to which he responded. He subsequently relapsed 6 months later and received 4 cycles of R-CHOP achieving a partial response, followed by 2 cycles of IVE with peripheral blood stem cell harvest, prior to proceeding to an autologous stem cell transplant in 2006. He subsequently received maintenance rituximab. He developed new nodal disease and splenomegaly in

September 2013 with bone marrow failure, and was surprisingly diagnosed with chronic lymphocytic leukaemia. Cytogenetics revealed no aberrations. He commenced on the Phase 1 dose-escalation study of tirabrutinib in November 2013 within the cohort of 400mg OD, achieving a complete clinical and radiological response but with residual disease within the bone marrow on MRD analysis. His neutrophil count is shown in Figure 3.3 over the course of treatment. In March 2017, having received continuous therapy on study with 400mg tirabrutinib he presented in clinic feeling unwell with a sore throat and symptoms of a lower respiratory tract infection. On examination he was febrile, with signs consistent with a lower respiratory tract infection. His neutrophil count was $0.0 \times 10^9/L$. He was admitted for treatment of neutropenic sepsis and received IV meropenem and filgrastim 300 micrograms. Tirabrutinib was continued during his admission. He received 5 days of intravenous antibiotics. Following normalisation of his neutrophil count and improvement of symptoms, he was discharged home. Repeat bone marrow examination following resolution of neutropenic sepsis, was normocellular with over-representation of granulocytes, with full maturation and plentiful neutrophils. Lymphocytes were of normal number with one aggregate observed on trephine of small mature lymphocytes. Megakaryocyte and erythroid colonies were normal in number and appearance. There was no evidence of impaired myeloid differentiation and no evidence of residual CLL. Tirabrutinib was dose reduced to 100mg OD to reduce the risk of recurrent neutropenic sepsis. Since the initial Phase I trial, studies of BTK occupancy have shown that 80mg daily of tirabrutinib achieves maximum receptor occupancy (Gilead unpublished data). He remains well with no recurrence of infection nor neutropenia.

Figure 3.3 Neutrophil count over time for a patient with a diagnosis of CLL on the Phase I study.



The occurrence of neutropenia and rapid resolution described above, occurred following over 3 years of treatment with tirabrutinib. This episode coincided with the development of an upper respiratory tract infection. Whilst grade 3 and 4 neutropenia has been observed in patients treated with ibrutinib and the more selective second generation inhibitors, no specific reports of infection induced neutropenia have been reported. Furthermore reported long term follow up with ibrutinib, shows the incidence of treatment emergent neutropenia to decrease over time.

Honda et al., evaluated the role of BTK in the production of ROS and apoptosis in human neutrophils. They found that in BTK deficient neutrophils, ROS production was increased following stimulation via Toll like receptors (TLRs), TNF receptors or PMA. This was not observed in monocytes (207). An increase in ROS production results in neutrophils primed to undergo apoptosis, consistent with reduced numbers of neutrophils observed in XLA patients during concurrent periods of infection. It is possible that this reported mechanism of apoptosis secondary to an increase in ROS production, occurred here, resulting in neutropenia occurring late during treatment.

3.5 Discussion

One of the advantages of tirabrutinib, is the remarkable tolerability and lack of toxicity observed to date. Ibrutinib discontinuation has been reported to occur in up to 20% of patients for reasons other than disease progression treated outside of the context of a

clinical trial (187, 188). Importantly, data from the UK and Ireland have shown that dose reductions were required in 26% of patients and in patients whom discontinued Ibrutinib, the main reason was due to the development of an Ibrutinib-related AE (56/83 patients) (188). The most common identified reasons for drug cessation were infection, haemorrhage/ bleeding related events, cytopenias, lower gastro-intestinal toxicity and cardiac toxicity. Some of these events may be due to inhibition of specific kinases. For example, gastrointestinal toxicity with ibrutinib may be directly due to inhibition of EGFR. Diarrhoea induced through inhibition of EGFR is thought to result from excessive chloride secretion, thus resulting in a secretory form of diarrhoea (219). Since tirabrutinib does not inhibit this kinase, the GI toxicity is correspondingly much less. The incidence of AF in a randomised controlled trial of ibrutinib versus ofatumumab, has been reported to occur in 6% of patients versus 1% respectively (179). The reported incidence in long term follow up, suggests that this risk may continue to increase over time (220). The mechanism of ibrutinib induced atrial fibrillation remains unclear. It has been suggested that inhibition of BTK and TEC kinases, results in inhibition of the PI3K-Akt pathway, which has a cardioprotective role under conditions of stress (221).

In the Phase 1 study with tirabrutinib, no dose reductions were required and discontinuation occurred in less than 10% of patients for reasons other than progression. This supports a more favourable toxicity profile. Similarly with acalabrutinib, most adverse events were grade 1 or 2 and resolved over time (193). The most common adverse events were headache, diarrhoea, increased weight, pyrexia and upper respiratory tract infection. No major bleeding events nor atrial fibrillation were seen.

3.6 Conclusion

Tirabrutinib has shown at least comparable efficacy in CLL and MCL to ibrutinib (165, 204, 205). Its more selective kinome, may confer significant clinical advantages over ibrutinib. The estimated mean PFS was 874 and 341 days in CLL and MCL respectively receiving tirabrutinib. In the recently reported 5 year follow up of ibrutinib in R/R patients with CLL, median PFS was 51 months and in a pooled analysis of 370 patients with MCL treated with ibrutinib, median PFS was 12.8 months (222, 223). Long term responses in CLL and MCL patients with chemotherapy refractory disease,

chromosome 17p deletion and/or p53 mutant disease and in patients having received prior stem cell transplants are seen here with tirabrutinib and previously reported with ibrutinib. However it is not possible to directly compare the results of this Phase I study of tirabrutinib in CLL and NHL with results from trials with ibrutinib, as this trial was not a head to head comparison, includes smaller patient numbers and a shorter duration of follow up. Thus while the results presented here show promising activity, a randomised Phase III trial of tirabrutinib versus ibrutinib would be required to allow a direct comparison to be made of the efficacy and tolerability.

It is somewhat surprising that patients treated with tirabrutinib and other BTKi do not develop an XLA like phenotype with a block of B cell differentiation at the B cell precursor stage. Results with ibrutinib, acalabrutinib and with tirabrutinib show that Immunoglobulin levels are maintained following long term treatment (193, 205, 224) and in fact an increase in IgA is seen in patients treated with ibrutinib. One hypothesis for this is that the effects of BTK kinase inhibition are observed on mature B cells, where the role of BTK is in intracellular signalling. Furthermore once daily dosing may not be sufficient to induce complete kinase inhibition. BTK occupancy studies within the lymph nodes and bone marrow in addition to peripheral blood would need to be conducted to assess this further.

A criticism of this study is the use of MTD as an endpoint. The usefulness of this endpoint in the era of targeted and immunotherapies is debated, as these agents may not have dose dependent toxicities (225). Rather, pharmacokinetic, pharmacodynamics or functional imaging may be more valuable in determining the recommended Phase II dose (RP2D). This establishment of dose, based on a pre-specified biomarker threshold is termed optimal biological dosing (OBD). Several agents utilised in the clinical setting such as imatinib and bevacizumab, did not rely on establishment of a MTD during Phase I trials, but rather PK and or PD endpoints were used to determine the RP2D.

Increased understanding of the molecular drivers of cancer have enabled us to select patients for treatment with specific targeted therapies in selected tumour types; for example the use of imatinib in BCR-ABL1 in chronic myeloid leukaemia (CML) (226); erlotinib and gefinitib in EGFR mutated lung cancer (227, 228) and vemurafenib for BRAF mutant tumours (229). However, responses to single agent targeted therapies are

often short lived. Resistance may occur through a variety of mechanisms including: occurrence of activating mutations; activation of downstream targets and recruitment of compensatory signalling pathways.

It is clear that responses when seen with BTKi in R/R ABC DLBCL, unlike in CLL and MCL, are not durable and as demonstrated with ibrutinib tend to occur in approximately one third of patients treated, with median durations of response of less than 3 months (177). Therefore additional strategies are required to improve outcome in this group which address the heterogeneity of disease seen within R/R DLBCL. Rational combinations of small molecule inhibitors are currently being explored in an attempt to improve outcome in this population. This requires an improved understanding of signalling pathways and molecular drivers of disease. More recently, immunotherapy has shown promising activity in R/R DLBCL, where CAR T cells have shown durable responses in almost half of all patients treated at 6 months (230). The use of CAR T cells in this population is likely to become an increasingly important treatment strategy with the possibility of long lasting remissions.

Chapter 4: Characterisation of the genomic profile of patients with CLL treated with tirabrutinib on the Phase I clinical trial using a 36 gene targeted sequencing panel

4.1 Novel gene mutations and their potential prognostic significance

Assessment of the mutation status of immunoglobulin heavy chain variable gene segments (*IGHV*) and evaluation of cytogenetic aberrations by FISH are important in understanding of the biological heterogeneity of CLL and enable improved disease stratification and prognostic information over clinical staging systems (231). Mutational analysis can provide additional information, including assessment of *TP53* and *ATM* (232). Mutations in the absence of deletion, provides further prognostic impact beside FISH cytogenetic stratification (233, 234). Improved understanding of the molecular genetics of CLL allows for a more refined prognostic stratification of patients and has important implications for the clinical management of patients with CLL (235).

Gene mutations of clinical relevance in the outcome of patients with CLL have been identified by next generation sequencing. *NOTCH1*, *SF3B1* *POT1* and *BIRC3* mutations have been associated with a more aggressive phenotype and are more prevalent in advanced disease (236-239). *NOTCH1* and *SF3B1* are among the most frequent and are detected in 5-20% of patients (236, 237, 240-242). Currently, whilst their presence does not guide choice of therapy within the clinic, a number of key observations have been made, which have significant clinical ramifications.

The addition of rituximab to fludarabine and cyclophosphamide (FC) has been shown to improve clinical outcome of CLL patients (243, 244). Analysis of the German CLL8 trial (NCT00281918) identified that patients with *NOTCH1* mutation (c.7541_7542delCT) did not benefit from the addition of rituximab to FC (PFS in the presence of *NOTCH1* mutations 33.9 months and 34.2 months with FC and FCR respectively P 0.996; unmutated *NOTCH1* PFS 32.8 months and 57.3 months with FC and FCR respectively P <0.001) (245). Subsequent analysis of *NOTCH1* mutated CLL cells has shown low CD20 expression, consistent with lower sensitivity to rituximab *in vitro* (246). This effect is specific to the presence of *NOTCH1* c.7541_7542delCT mutation and other truncating mutations, which may be mediated by epigenetic downregulation of CD20 by histone deacetylases (HDACs).

Chemorefractory disease is defined as either a failure to respond to treatment or disease progression within 6 months of the last anti-leukaemic therapy (247). *SF3B1* and *BIRC3* mutations are associated with a chemorefractory phenotype (239, 248). *SF3B1* is a component of the major and minor spliceosomes. Mutations can result in alternatively spliced transcripts and gene expression (249). Splice variants in mutated *SF3B1* CLL cells, have been identified in multiple CLL pathways including genes linked to Notch signalling, e.g. *DVL2*, *DNAJC3*, *TRIP12* and *HDAC7*. Differential expression of genes such as *KLF3* and *KLF8*, which are involved in the DNA damage response pathway, oncogenic transformation, cell cycle regulation and cell differentiation have also been identified.

In the UKCLL 4 trial, *SF3B1* mutations were associated with an inferior PFS and fludarabine refractoriness. *BIRC3* is a negative regulator of *MAP3K14*, and disruption results in constitutive activation of the NF- κ B pathway. *BIRC3* mutations occur in up to 40% patients' refractory to fludarabine and poor outcome when present at diagnosis, independently of *TP53* abnormalities (239, 248). *POT1* mutations are found in a number of human cancers. In CLL, *POT1* is important in the formation of the shelterin complex and is important in the stability of chromosomal telomeres (250). *POT1* is an independent prognostic factor for OS.

4.2 Clinical Implications of Next Generation Sequencing (NGS) studies in CLL

NGS has allowed for the detection and study of previously unidentified mutated genes in CLL, which may have clinical utility as predictive and prognostic biomarkers. Furthermore, NGS allows for the detection and monitoring of small sub-clones during the course of disease and therefore has the potential to refine our current clinical practice.

Prior studies of CLL patients, have largely focused on the use of NGS platforms at diagnosis and association with chemotherapy outcome. For example, NGS analysis of 200 consecutive CLL patients at diagnosis using a 20 gene CLL panel (*ATM*, *BIRC3*, *BRAF*, *CDKN2A*, *PTEN*, *CDH2*, *DDX3X*, *FBXW7*, *KIT*, *KLHL6*, *KRAS*, *MYD88*, *NOTCH1*, *NRAS*, *PIK3CA*, *POT1*, *SF3B1*, *TP53*, *XPO1*, *ZMYM3*) has been reported (251). Using this platform inferior survival was associated with the presence of complex

karyotypes, defined by at least 3 chromosome aberrations by cytogenetic analysis, and was superior in predicting time to first treatment (TTFT) in both complex karyotypes and in the presence of mutations involving *TP53* (6.0%), *NOTCH1* (7.5%), *ATM* (4.0%) and *BRAF* (2.5%) (251) than cytogenetic studies and clinical prognostic factors alone. Targeted NGS was performed in a representative subset of 689 patients (88.2%) at baseline, treated front line in the CLL11 trial (comparison of chlorambucil vs. Rituximab-chlorambucil vs. Obinituzumab-chlorambucil in physically unfit patients) of all coding exons (*TP53*, *ATM*, *MYD88*, *FBXW7*, *BIRC3*, *XPO1*, *POT1*) or hotspots (*NOTCH1* exons 33/34, *SF3B1* exons 14-16/18). Importantly Obinituzumab-chlorambucil improved outcome when compared to Rituximab-chlorambucil irrespective of the presence of specific gene mutations except for *FBXW7* mutations and overcame resistance to Rituximab associated with *NOTCH1* mutations (251). The presence of *ATM* and *TP53* mutations were associated with significantly inferior PFS irrespective of treatment arm (252).

Use of targeted NGS in relapsed/ refractory CLL patients has been less frequently studied and this remains a very useful platform in the prospective evaluation of patients receiving novel targeted therapies. The largest NGS study of 114 patients with relapsed/ refractory CLL recruited prospectively into 3 clinical trials (ICLL01, CLL201, CLL202) treated with conventional chemo-immunotherapy tested for mutations in a panel of 9 genes (*TP53*, *SF3B1*, *ATM*, *NOTCH1*, *XPO1*, *SAMHD1*, *MED12*, *BIRC3*, *MYD88*) (253). A high incidence of concurrent mutations affecting *TP53*, *ATM* and *SF3B1* was identified; associated with a poor response to salvage conventional immunochemotherapy and shorter survival. Enrichment of *TP53*, *NOTCH1* and *SF3B1* was seen within this relapsed/ refractory population as previously reported (250, 254, 255). Considered individually, the presence of mutations either in *TP53* or *BIRC3* were the only mutations found to impact on prognosis, and have been proposed to confer the worst outcome in CLL in a hierarchal model (256).

Table 4.1 Summary table of the frequency of mutations in different genes identified in studies reporting the results of NGS in CLL treatment naïve and R/R patients.

Mutation	References					
	250	251	253	(254)	255	256
<i>TP53</i>	8	22.8	10.4	39.0	30	8.5
<i>SF3B1</i>	5	28.1	11.2	17.5	26	6.8
<i>ATM</i>	4	26.3				
<i>NOTCH1</i>	8.0	14.9	8	13.4	14	11.1
<i>XPO1</i>	1.5	14.9				
<i>BIRC3</i>	4	5.3	2.5			2.7
<i>MYD88</i>	3.5	2.6	2.2			4.1
<i>PTEN</i>	3.5					
<i>FBXW7</i>	3					
<i>POT1</i>	2.5					
<i>BRAF</i>	2.5					
<i>ZMYM3</i>	2.5					
<i>KRAS</i>	2					
<i>NRAS</i>	1.5					
<i>CHD2</i>	2					
<i>CDKN2A</i>	1.5					
<i>PIK3CA</i>	1.5					
<i>KLHL6</i>	1					
<i>DDX3X</i>	0.5					
<i>KIT</i>	0					
<i>SAMHD</i>		9.6				
<i>MED12</i>		8.8				

4.3 Impact of BTKi on the treatment of patients with CLL with high risk features

The Phase 1b-2 study of ibrutinib in CLL, found response rates were similar irrespective of the presence of 17p13.1 (174). However disease progression was more frequently observed in patients with 17p13.1 and del11q (202). Interestingly, patients with unmutated *IGHV* status had a higher response rate to ibrutinib, than those with mutated *IGHV* status (202). This finding was also shown in a subsequent study of ibrutinib in the elderly population, with a response rate seen of 86.7% in the *IGHV* unmutated group *versus* 56.3% in the mutated group to ibrutinib (208). Furthermore in untreated patients, those with unmutated *IGHV* status achieved a higher rate of response at 3 years than those with mutated *IGHV* status, 40% *versus* 6% respectively (202). *In vitro*, unmutated CLL has been demonstrated to have higher levels of BTK protein,

increased BTK phosphorylation (Y223); higher cellular proliferation, that is dependent on BTK, in addition to increased activity of downstream kinases from BTK, all of which appear to confer increased sensitivity to ibrutinib (257). Increased BCR signalling in unmutated CLL, may therefore explain this difference in response.

Of the selective BTKi, CLL patients treated with tirabrutinib in the Phase I study, who had 17p13.1 deletion or *TP53* mutations, all 12 patients responded. At the time of initial data analysis, 9 patients remained on therapy (165). Equally, acalabrutinib has shown comparable efficacy in relapsed CLL in the Phase I/2 single arm study, in this high-risk population (193). Among the 18 patients with chromosome 17p13.1 deletion, the response rate was 100%. Only 1 patient with chromosome 17p13.1 deletion had disease progression during therapy.

We sought to interrogate the mutational spectrum of patients with CLL entered into the Phase 1 study with tirabrutinib using a targeted NGS panel (please refer to Chapter 2 Methods Table 2.11) to assess whether specific subgroups of disease might be associated with a worse outcome.

4.4 Results

4.4.1 Laboratory prognostic factors

Laboratory prognostic factors were available for 25 patients (Table 4.2). Twenty-one of 25 patients exhibited unmutated *IGHV* gene segments; seven with unmutated *IGHV* and 2 with mutated *IGHV* have discontinued treatment. One patient with mutated *IGHV* utilizing VH3-21 has progressed on treatment. Mutated VH3-21 has been associated with an inferior overall survival when compared to other mutated VH genes (258). This patient also had a *TP53* mutation and *SF3B1* mutation.

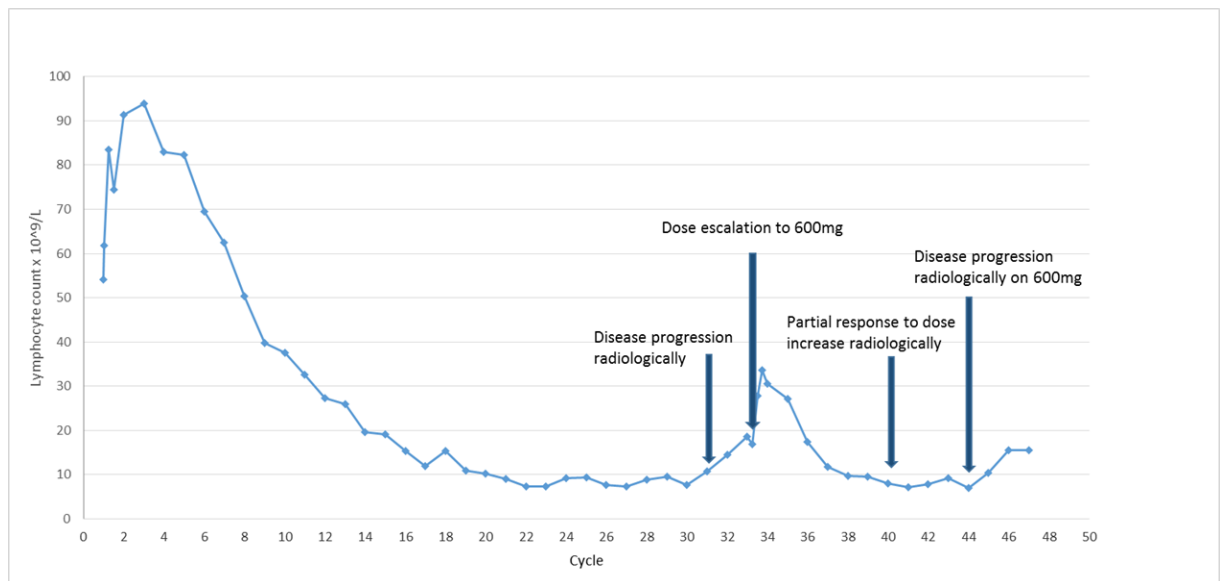
Although no formal correlative analysis was possible due to small sample size, no differences in response or PFS according to chromosome 17p13.1 deletion or *TP53* mutation were observed. 17p13.1 deletion was determined by FISH and *TP53* mutations by Sanger DNA sequencing. All 12 evaluable patients with 17p13.1 or *TP53* mutation without chromosome 17p13.1 deletion responded to therapy; 9 remain on treatment.

Seven of 9 patients with *TP53* mutation remain on therapy; of the 2 that discontinued study treatment, 1 progressed and 1 died from septicemia. One patient with a *TP53* mutation in the DNA binding domain (DeltaL252T253) had an initial response for 31 cycles on a dose of 40mg OD tirabrutinib but then progressed. Sanger sequencing confirmed this patient lacked *BTK* and *PLCG2* mutations, and the dose of tirabrutinib was increased to 600mg OD. The patient responded for a further 12 months, associated with a second lymphocytosis comparable in size and duration to that seen initially (1.74-fold increase; initial 1.81-fold increase) and lymph nodal response (Figure 4.1) before further progression.

Table 4.2 Cytogenetics and IGHV status of CLL patients on study.

	Progressed (N=3)	Patients continuing on study (N=19)	All CLL patients (%)
IGHV sequence			
Mutated	1	3	5
Unmutated	2	15	22
Not available	0	1	1
Interphase cytogenetic abnormalities (N=25)			
N (%) with del (13)(q14.3)	0	10	12 (48)
N (%) with del (11)(q22.3)	0	0	0 (0)
N (%) with del (17)(q13.1)	2	6	9 (36)
N (%) with Trisomy 12	1	4	5 (20)
N (%) with ATM deletion	1	5	7 (28)
No cytogenetics available		1	3 (10.71)

Figure 4.1 Dose escalation has the potential to re-establish response to therapy: Case study of a patient with TP53 mutation who responded for 31 cycles to 40mg tirabrutinib and for a further 12 months on 600mg tirabrutinib(205).



4.4.2 Targeted sequencing

Results from targeted sequencing on 27 patients, using the custom designed NGS panel, are shown in Table 4.3. 5 patients had no detectable mutations; 9 had 1 mutation; 8 had 2 mutations and 4 patients 3 mutations (Figure 4.2). Mutations in *TP53* were the most frequently observed, identified in 9 patients (33.3%). Eight patients had *SF3B1* mutations, 5 of whom have discontinued treatment (1 due to progression). *NOTCH1* mutations were found in 7 patients, 3 of whom have come off study (1 due to progression). As previously reported, *NOTCH1* and *SF3B1* were mutually exclusive (232). 3 patients were found to have *ATM* mutations, one has progressed on study (930 days). Mutations not previously identified in CLL include a mutation in *MEK1* (E203K) in 1 patient with early progression, previously reported in metastatic melanoma resistant to vemurafenib (259) and a *POT1* mutation E67K. No mutations in *MYD88*, *PLCG2*, or *BRAF* were observed within the cohort.

Table 4.3 Targeted mutational analysis of 27 CLL patients at the time of trial entry.

	Progressed (N=3)	Patients continuing on study (N=19)	All CLL patients (%)
Targeted mutational analysis (N=27)			
N (%) with <i>TP53</i>	1	7	9 (33)
N (%) with <i>ATM</i>	1	2	3 (11.1)
N (%) with <i>MAP2K1 (MEK1)</i>	1	0	1 (3.7)
N (%) with <i>MAP3K14 (NIK)</i>	0	1	1 (3.7)
N (%) with <i>NOTCH 1</i>	1	4	7 (25.9)
N (%) with <i>PLCG2</i>	0	0	0 (0)
N (%) with <i>POT1</i>	0	1	1 (3.7)
N (%) with <i>SF3B1</i>	1	3	8 (29.6)
N (%) with <i>RYR</i>	0	1	1 (3.7)
N (%) with <i>RYK</i>	2	0	2 (7.4)
N (%) with <i>WNT1</i>	0	1	1 (3.7)
N (%) with <i>ROS1</i>	0	2	3 (11.1)
N (%) with <i>BRAF</i>	0	0	0 (0)

4.7 Conclusion

Increasingly, emerging data demonstrate that in most cases of relapsed/refractory CLL, patients will have more than 1 recurrently mutated gene, and complex karyotype is associated with a poor outcome. Use of a validated CLL gene panel has the potential to change clinical practice, allowing for reproducible and actionable results. The value of NGS methods over current techniques including FISH analysis and Sanger sequencing, is also increasingly recognised in its ability to detect smaller clones, relevant for disease progression and assessment of treatment response, predicting clinical response to chemo-immunotherapy and predicting prognosis. Therefore NGS is required to describe the individual molecular complexity, which cannot be fully described with conventional single gene analysis. Whilst whole genome and exome sequencing enables full characterisation of the mutational landscape, using a targeted sequencing panel that is actionable, enables a more economic and user friendly dataset applicable to current clinical practice. Results presented here support the panel reliability to detect mutations and provide information on known clinically relevant mutations. However due to the small number of patients and lack of longer term follow up, we are unable to draw conclusions in terms of response or time to progression with tirabrutinib. It is also important to recognise that we detected mutations not previously described in the literature either in CLL or in other cancers and therefore the significance of these mutations remains unknown and cannot as yet be used to inform our clinical practice.

The panel designed in collaboration with Dr Macip and Sistemas Genomicos in early 2014 includes commonly mutated genes which are of prognostic value in CLL such as *TP53*, *ATM*, *NOTCH1*, *BIRC3* and *SF3B1* and mutations that are therapeutically tractable. It is recognised that with increasingly knowledge and insight into the biology of CLL as well as novel therapeutic targets, that this panel will require careful revision to ensure that it remains clinically relevant. For example *SAMHD1* has more recently been identified in 11% of relapsed/refractory patients, where it has a role in DNA repair (260). The presence of *SAMHD1* mutations in CLL are thought to promote leukaemia development and confer a poor prognosis. Furthermore it will be important to assess this panel in both newly diagnosed treatment naïve patients and across a wider cohort of patients with disease to allow for correlation of mutations with prognosis and treatment outcome.

Efforts to design an optimal gene panel that could be widely used in the NHS and is affordable are still ongoing. It is likely that NGS in prognostication and predicting response to treatment, will become widespread in the future. However the rapid progress in this field, requirement for validation of new prognostic and predictive markers and ensuring harmonisation across the UK are significant challenges to be met. Therefore the adoption of this panel into routine clinical practice would require consensus amongst treating clinicians, ensuring sequencing is conducted in ISO accredited laboratories and adequate access to skilled bioinformaticians to deliver results in a clinic ready format.

Chapter 5 Characterisation of BTKi resistant TMD-8 cell lines

5.1 Introduction

During the course of the Phase 1 clinical study of tirabrutinib in B cell malignancies outlined above, it became apparent that whilst the efficacy of selective BTK inhibition in CLL and MCL was usually profound, in non-GCB DLBCL it was much less; some responses were observed, but these were usually short-lived with rapid progression. Similar data have been reported with other BTKi (177). Response to ibrutinib in ABC DLBCL was correlated with the presence of BCR mutations (*CD79A* and *CD79B* ITAM mutations) and especially in the presence of concomitant *MYD88* mutations. Patients with *CARD11* mutations, downstream of BTK within the BCR signalling pathway or mutations within *TNFAIP3*, a negative regulator of NF- κ B, failed to respond to ibrutinib. Median duration of response was 4.83 (1.02–9.26) months. However it is clear that response to ibrutinib is not confined to the presence of mutations within *CD79A* or *CD79B*. The Phase I clinical trial of acalabrutinib in ABC DLBCL (NCT02112526) has completed accrual and the results are awaited.

Collectively, these data suggest that BTK inhibition in non-GCB DLBCL can result in rapid emergence of resistance following a prior responses are seen. However, in nearly two thirds of patients primary resistance was observed. Whilst resistance to BTK inhibition in CLL is associated with mutation of *BTK* itself and one of its immediate downstream targets, *PLCG2*, the mechanisms of resistance in DLBCL are much less clear. In collaboration with others in the Dyer laboratory in Leicester, I therefore sought to establish *in vitro* models of BTK resistance. Here I report the preliminary genetic and biological characterisation of models that exploited the extreme sensitivity of the ABC-cell line TMD8 to BTK inhibition (261, 262).

5.2 Establishment of tirabrutinib and ibrutinib resistant TMD8 cell lines

Tirabrutinib and ibrutinib resistant TMD8 cell lines were established *via* long term culturing of the parental TMD8 cell line with gradually increasing concentrations of tirabrutinib and ibrutinib respectively by Mr R. Kozaki in our laboratories in Leicester.

Once established, BTKi resistant TMD8 cell lines were maintained in RPMI media containing 1 μ M tirabrutinib and 0.1 μ M ibrutinib respectively. These concentrations of tirabrutinib and ibrutinib readily induce apoptosis in the parental cell line, as shown in Figure 5.3. The resistant cells for all experiments were passaged once prior to use in all experiments, to prevent changes observed being seen due to effect of drug on the resistant cell lines. It should be noted however that these resistant cell lines were not single cell cloned at the time my experiments were performed. Single cell cloning has proved difficult to achieve as the TMD8 cell line preferentially grows in clumps.

5.2.1 Cell growth and size

Growth rates of the parental TMD8 and BTKi resistant lines, TMD8 RO and TMD8 RI, (resistant to tirabrutinib and ibrutinib respectively) were assessed every 24 hours over a 96-hour period. All cell lines proliferated predominantly in small clumps, with some single cells. To increase the accuracy of cell counting, clumps were gently dispersed by pipetting. Doubling time was approximately 24 hours and there were no significant differences in growth rates between the resistant and parental cell lines (Figure 5.1). However, the resistant cell lines were found to have a statistically significant greater cell diameter than the parental cell line (mean 11 μ m (range 10-12 μ m) versus 9 μ m (range 7-10 μ m) $P=0.01$), measured using a TC20TM cell counter (Biorad), to gate the live cell population. A larger cell diameter was confirmed by flow cytometry, where it was observed that forward scatter profile of the resistant cell lines was consistently greater than the parental TMD8, supporting a larger cell size (Figure 5.2). Average forward scatter for the resistant cell lines was 8.5×10^4 and for the parental cell line 5.5×10^4 ($P=0.001$).

Figure 5.1 Cell growth of TMD8, TMD8 RO and TMD8 RI cell lines. Cells were plated at a density of $1 \times 10^5/\text{ml}$ in 48 well plates and cells counted every 24 hours for 4 consecutive days using the trypan blue exclusion assay. Viable cell count was plotted against time. Each point represents the mean \pm the standard deviation of three experiments. Viability was consistently greater than 80% for all cell lines at each time point.

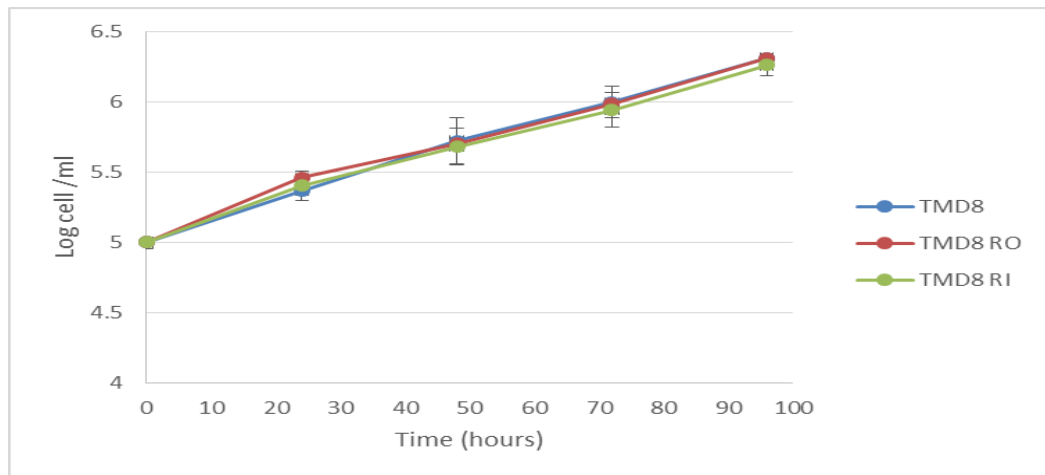
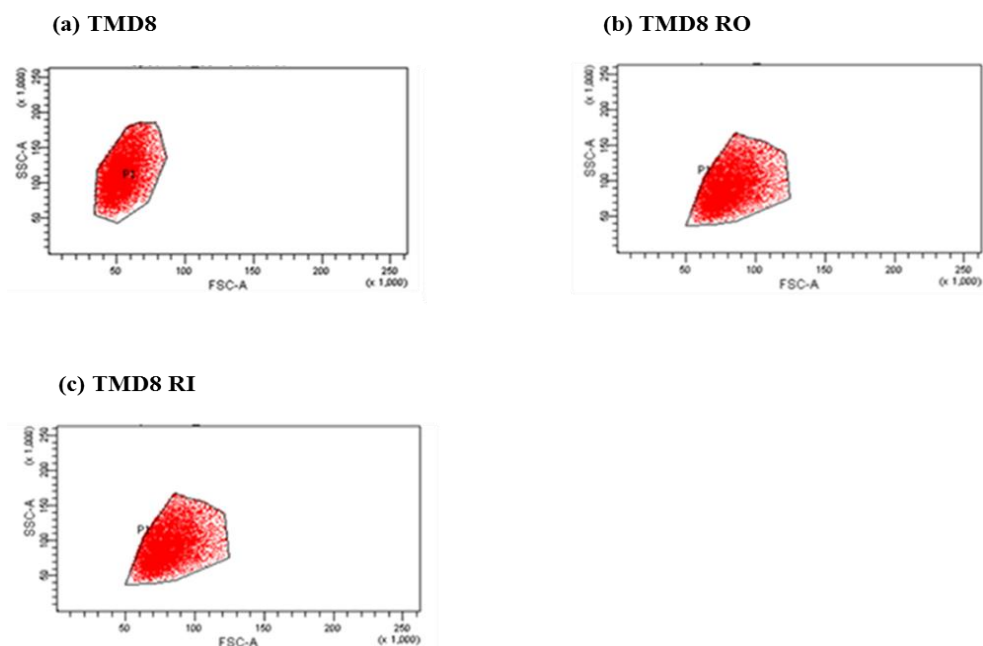


Figure 5.2 Forward scatter and side scatter density plots of all live cells are shown for the cell lines (a) TMD8, (b) TMD8 RO and (c) TMD8 RI assessed by flow cytometry.



5.3 BTKi-induced cell death in TMD8 and TMD8 RO and TMD8 RI

The ABC DLBCL cell lines OCI-LY10 and TMD8, have been shown to be sensitive to Ibrutinib induced cell death (263). Using short hairpin RNAs (shRNAs) targeting BTK, cell death was observed after 24 hours and at 2 weeks no viable cells could be detected in the TMD8 cell line. Interestingly, and in comparison, in the OCILY10 cell line, cell death was observed after 4 days and at 12 days approximately 50% of cells remained viable (90). I confirmed and extended these observations in parental and BTKi resistant cell lines using both tirabrutinib and ibrutinib. Viability of the parental and resistant cell lines was assessed using the Cell Titer-Glo cell viability assay following exposure to tirabrutinib and ibrutinib at concentrations from 1-3000nM and was determined at 24, 48 and 72 hours. The parental TMD8 cell line was sensitive to both tirabrutinib and ibrutinib with an EC₅₀ of 4.5nM and 4.6nM respectively, measured at 72 hours (Table 5.1). In the tirabrutinib resistant cell line TMD8 RO, an EC₅₀ value was not obtained at 72 hours following continuous exposure to 3µM tirabrutinib (Figure 5.3). The EC₅₀ of the ibrutinib resistant cell line, TMD8RI, was greater than 1.9µM (Figure 5.3).

Over a range of drug concentrations (1nM-3µM) of ibrutinib and tirabrutinib, cell death occurred at least 24 hours after drug exposure. The mechanisms underlying BTK inhibitor-induced cell death, and linking it with BTK inhibition, have not been described.

5.3.1 Ibrutinib and tirabrutinib induce apoptosis in TMD8

During apoptosis, cells undergo a number of typical morphological and biochemical changes (264). Classical morphological changes include cell shrinkage and membrane blebbing, nuclear condensation and loss of membrane integrity. These changes of apoptosis were shown to occur in TMD8 cells following exposure to tirabrutinib by electron microscopy by Mr R. Kozaki (262).

To measure apoptosis in TMD8 cells, Annexin V/PI staining by flow cytometry was undertaken in the parental and resistant cell lines following exposure to tirabrutinib and ibrutinib. The parental and resistant cell lines were exposed to tirabrutinib and ibrutinib

at concentrations between 1nM and 3 μ M. The percentage of early apoptotic cells (Annexin V positive and PI negative) were measured at 24, 48 and 72 hours (Figure 5.3). Apoptosis was maximal at 72 hours. Little apoptosis was observed before 24 hours. In the TMD8 RO cell line, apoptosis was not observed following continuous exposure to 3 μ M tirabrutinib at 72 hours; however, the TMD8 RI cell line following exposure to concentrations of >300nM ibrutinib underwent apoptosis. These results show that TMD8 cells are highly sensitive to ibrutinib and tirabrutinib, consistent with previously published work and confirm resistance of the derived resistant cell lines. In the resistant cell lines, cross resistance to both BTKi was seen (Table 5.1).

Figure 5.3 Effects of tirabrutinib and ibrutinib on TMD8 and TMD8 RO and TMD8 RI and resistant TMD8 cell lines. TMD8 cell lines (5x10⁵/ml) were treated with increasing concentrations of BTKi or DMSO for 24, 48 and 72 hours. Viability was assessed using the Cell Titer-Glo assay; apoptosis was assessed by staining with Annexin V and PI. Data shown represent the mean +/- SD (n = 3). Panel a) viability of TMD8 cell line exposed to tirabrutinib; b) viability of TMD8 cell line exposed to ibrutinib; c) Annexin V positive and PI negative TMD8 cells following treatment with tirabrutinib (concentration range 0-3000nM); d) Annexin V positive and PI negative TMD8 cells following treatment with ibrutinib (concentration range 0-3000nM); e) viability of TMD8 RO exposed to tirabrutinib; f) viability of TMD8 RI exposed to ibrutinib.

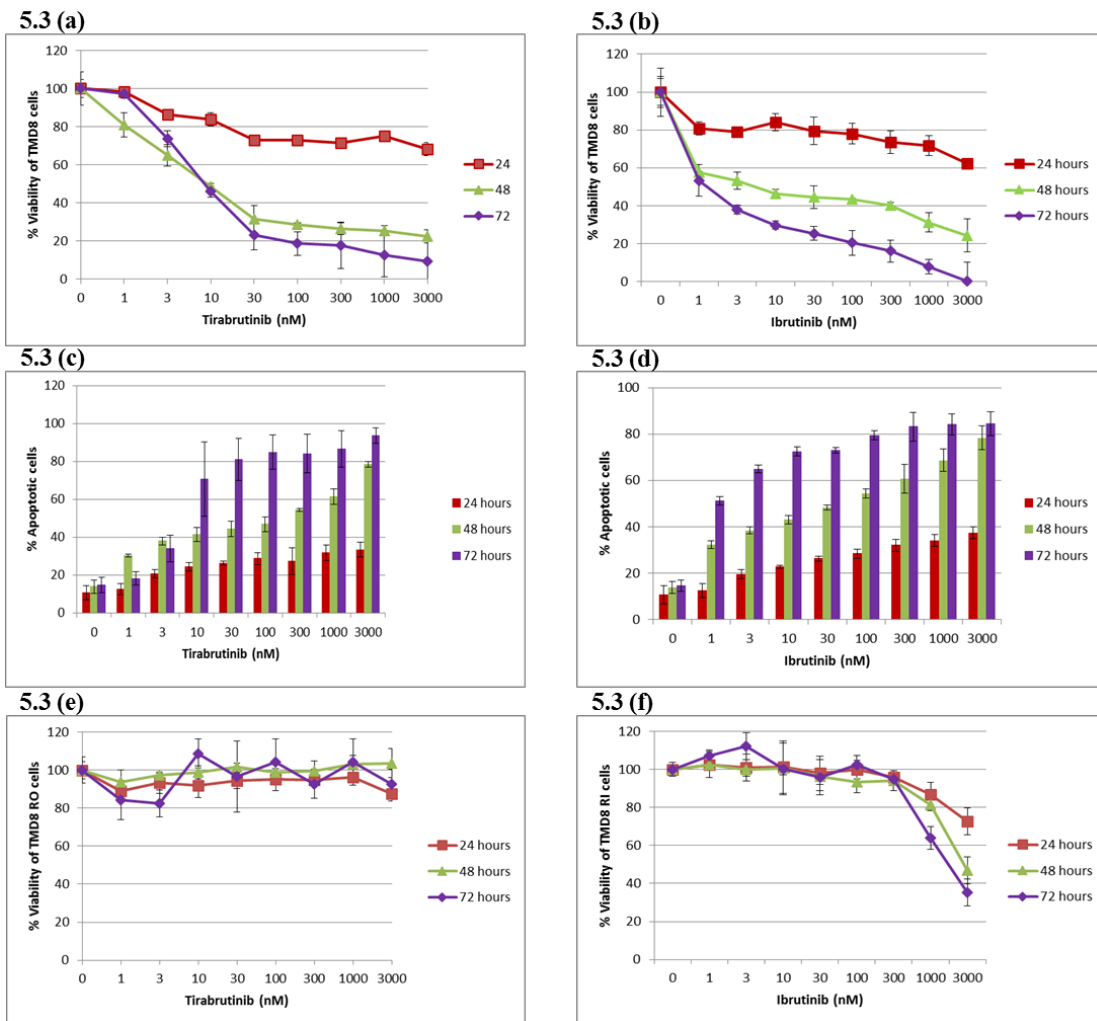


Table 5.1 Calculated EC₅₀ values for apoptosis induction in the parental and resistant TMD8 cell lines following exposure to tirabrutinib and ibrutinib.

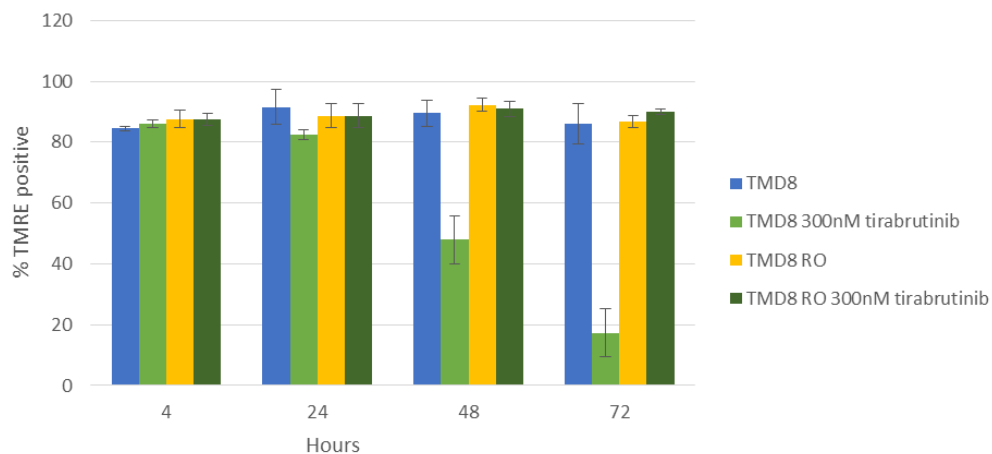
	Tirabrutinib EC₅₀	Ibrutinib EC₅₀
TMD8	4.5nM	4.6nM
TMD8 R0	>3μM	>3μM
TMD8 RI	2.1μM	1.9μM

To confirm these observations, changes in the mitochondrial potential was determined (265). Loss of the mitochondrial transmembrane ($\Delta\Psi_m$) is an early event in apoptosis (264). Loss of $\Delta\Psi_m$ has been shown to occur prior to PS exposure in dexamethasone induced apoptosis in splenocytes or thymocytes (266). However, in other induced apoptotic states, PS has been shown to occur prior to collapse of $\Delta\Psi_m$, for example in 1- β -D-arabinofuranosylcytosine-induced apoptosis in leukemic blast cells (267). Therefore, exposure of PS can constitute an early event in the apoptotic process, which does not necessarily require loss of $\Delta\Psi_m$.

Tetramethylrhodamine ethyl ester perchlorate (TMRE) staining can be used to detect changes in the mitochondrial transmembrane potential. Mitochondrial retention of the dye depends on the maintenance of the mitochondrial inner membrane potential (268). Measurement of change in mitochondrial membrane potential in TMD8 and TMD8 RO cells with and without treatment with tirabrutinib 300nM at 4, 24, 48 and 72 hours was assessed by flow cytometry by measurement of change in TMRE positive cell populations (Figure 5.4). Treatment with tirabrutinib resulted in a greater proportion of TMRE negative TMD8 cells (80.4% +/- SD 5.6 at 72 hours), than TMD8 RO cells (16.4% +/- SD 3.1 at 72 hours), consistent with a larger population of apoptotic cells. The % of TMD8 cells that are TMRE negative and therefore show loss of $\Delta\Psi_m$ appears to be consistent with the % cells that are Annexin V positive and PI negative at these same time points. It could however be anticipated that the % of TMRE negative cells would be greater at these time points as loss of $\Delta\Psi_m$ is thought to reflect the earliest changes in apoptosis. One explanation for this may be that PS has been shown to be expressed spontaneously in the absence of apoptosis on the outer membrane of normal B cells ex vivo on CD-45 deficient B cells (269) and is a marker of B cell activation and altered IgM signalling (270). It is therefore possible that PS

externalisation in TMD8 cells following exposure to tirabrutinib reflects B cell activation rather than apoptosis and therefore this results in a similar timescale for the observed changes in Annexin V positive cells as with TMRE negative cells. However given the classical features of apoptosis observed on light microscopy, this would suggest apoptosis occurs and that more frequent time points for TMRE staining could be conducted to detect earlier changes that occur before 24 hours. Alternative dyes used to detect changes in membrane potential include JC-1 (5,5e6,6e-tetrachloro-1,1e,3,3e-tetraethylbenzimidazol carbo-cyanide iodide) could also be explored.

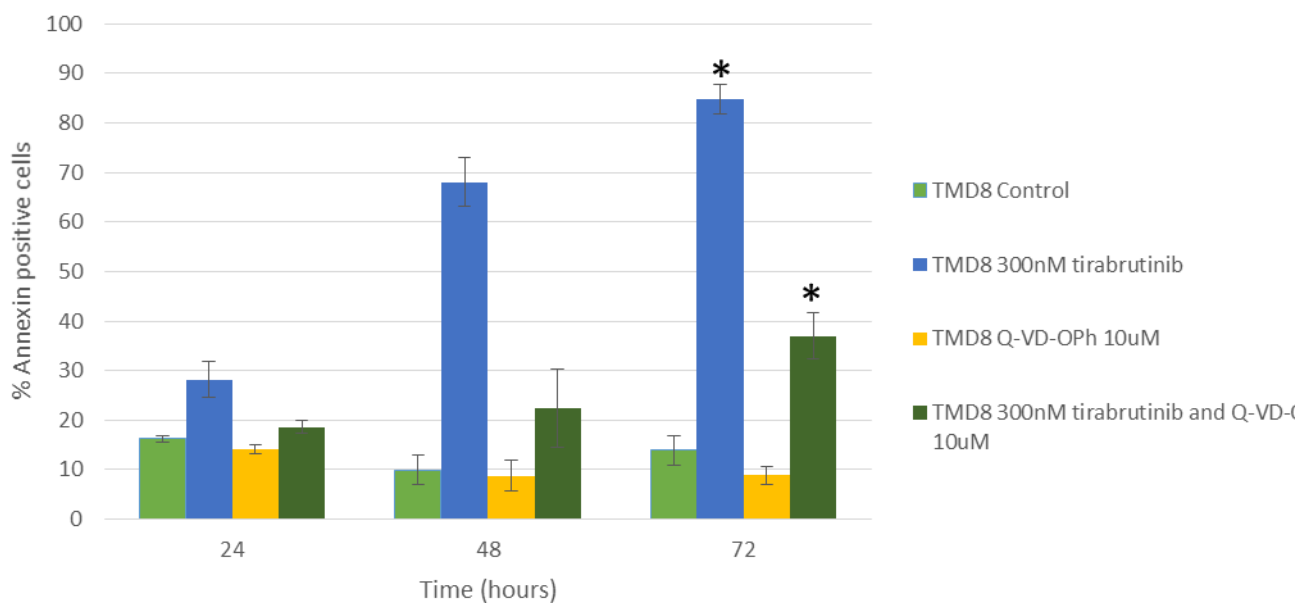
Figure 5.4 Measurement of mitochondrial membrane potential in TMD8 and TMD8 RO cells with and without treatment with tirabrutinib 300nM at 4, 24, 48 and 72 hours by flow cytometry by measurement of TMRE binding. Each point represents the mean +/- SD (n=3).



To confirm that apoptosis in the TMD8 cell line occurred in a caspase dependent manner, cells were treated with tirabrutinib 300nM in the presence or absence of 10 μ M of the pan-caspase inhibitor quinolyl-valyl-O-methylaspartyl-[-2,6-difluorophenoxy]-methyl ketone (Q-VD-OPh). This broad spectrum caspase inhibitor was used as it has been recently shown to be less cytotoxic than the fluoromethylketone-based caspase inhibitors (Boc-D-fmk, Z-VAD-fmk) (271). Furthermore, it has been shown to decrease caspase dependent cell death more significantly than Z-VAD-fmk and Boc-D-fmk (272-274) and inhibits caspase 2 and caspase 6 more effectively (271). The percentage of Annexin-V positive cells in the presence of Q-VD-OPh was assessed by flow cytometry at 24, 48 and 72 hours (Figure 5.5). The percentage of apoptotic cells significantly decreased following treatment with tirabrutinib 300nM in the presence of Q-VD-OPh

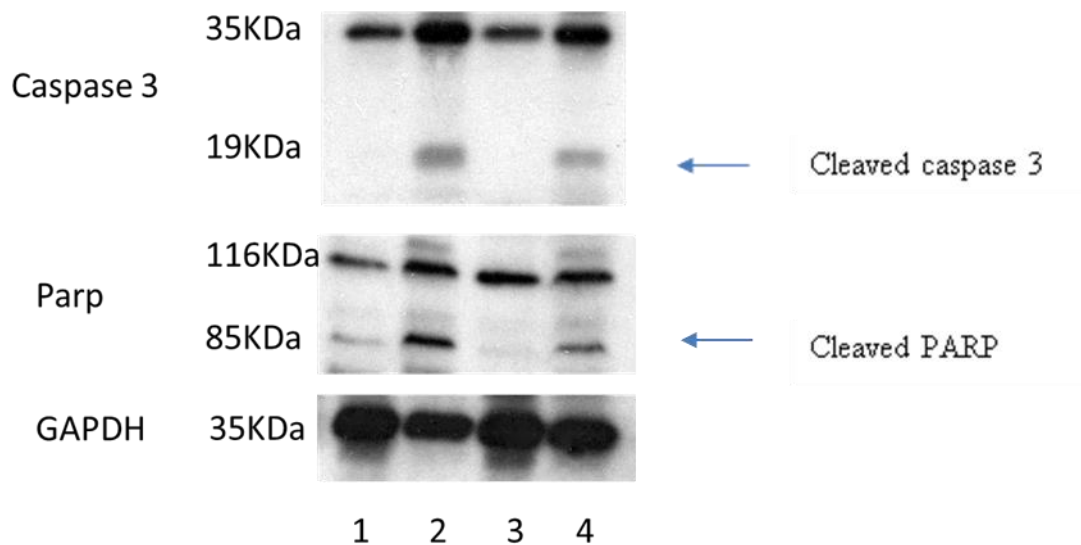
(36.9% +/- SD 4.65 at 72 hours and 84.8% +/- SD 2.9 at 72 hours with tirabrutinib alone; $p < 0.05$). However the use of Annexin V/ PI staining in this protocol to assess apoptosis has limitations in view of my prior findings discussed earlier in this section and therefore may account for the incomplete inhibition of apoptosis observed following treatment with tirabrutinib 300nM in the presence of Q-VD-Oph at 72 hours.

Figure 5.5 Effect of Q-VD-Oph on tirabrutinib induced apoptosis in TMD-8 cell lines. TMD8 cells were plated at a final concentration of 5×10^5 /ml and incubated with tirabrutinib 300nM, Q-VD-Oph 10 μ M or both tirabrutinib 300nM and Q-VD-Oph 10 μ M for up to 72 hours. Cell death was analysed by Annexin V/PI staining measured by flow cytometry. DMSO-treated cells were used as the time-matched control. Data shown represent the mean +/- SD (n = 3). * $P < 0.05$.



Q-VD-Oph suppressed cell death by 50% in TMD8 cells treated with tirabrutinib. Similarly, treatment of TMD8 with tirabrutinib 300nM for 72 hours resulted in the detection of cleavage of caspase 3 and PARP by western blot. PARP and caspase 3 cleavage was not completely suppressed in the presence of Q-VD-Oph, consistent with the results of flow cytometry (Figure 5.6).

Figure 5.6 PARP and caspase 3 cleavage in the TMD8 cell line following treatment with tirabrutinib in the presence and absence of Q-VD-OPH.



Lanes

1. 72 hr TMD8 DMSO control
2. 72 hr TMD8 300nM tirabrutinib
3. 72 hr TMD8 Q-VD-OPH 10 μ M
4. 72 hr TMD8 300nM tirabrutinib and Q-VD-OPH 10 μ M

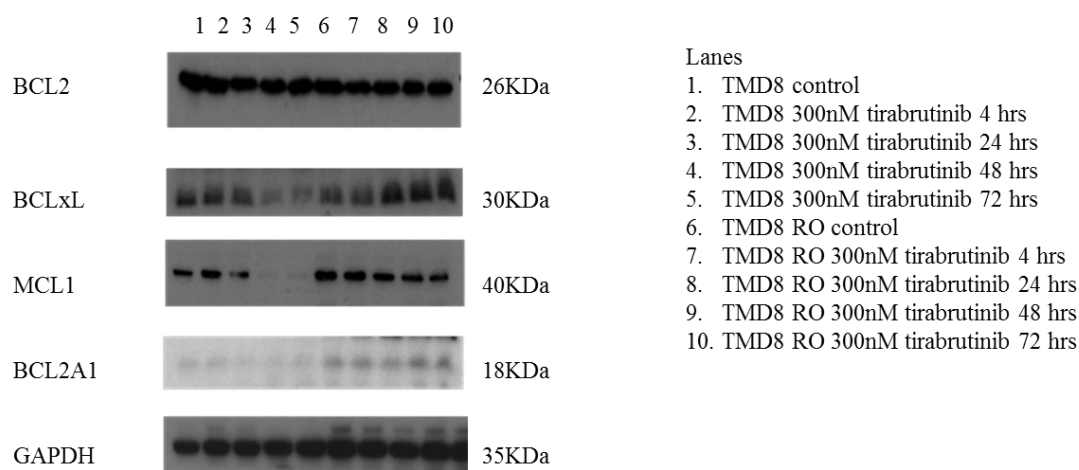
Collectively, these data indicate relatively “late” mitochondrial changes in TMD8 cells following BTK inhibition. A lack of complete inhibition of apoptosis with Q-VD-OPh, using the Annexin V/PI protocol, may be explained by the choice of this protocol to assess apoptosis. As Q-VD-OPh is a pan caspase inhibitor, it is unlikely that caspase inhibition did not occur.

5.4 Expression of the anti-apoptotic proteins in TMD8 cell lines following exposure to tirabrutinib

To investigate the mechanisms of cell death further, I investigated levels of expression of BCL2 family members in TMD8 during cell death. The mitochondrial apoptotic pathway is regulated by the BCL2 family of proteins (275). The expression of BCL2 family members has previously been shown to be altered in response to BTKi. Ibrutinib has been shown to decrease the expression of BCL2, BCLxL and MCL1 anti-apoptotic proteins in the sensitive MCL cell line Mino through direct inhibition (170).

Expression of BCL2 family proteins was assessed by immunoblot before and following treatment with tirabrutinib over 72 hours (Figure 5.7). These experiments showed variable responses in the BCL2 family proteins. Firstly, BCL2 levels were unchanged in TMD8 and TMD8 RO cell lines and did not alter following exposure to tirabrutinib. Interestingly, MCL1, BCLxL and BCL2A1 protein levels decreased in the parental TMD8 but not the resistant TMD8RO following treatment with 300nM tirabrutinib over 72 hours; initial downregulation was seen after 24 hours exposure. Loss of these proteins correlated with the change in TMRE, and therefore loss of membrane potential, for which these anti-apoptotic proteins are responsible.

Figure 5.7 Expression of BCL2 family proteins in TMD8 and TMD8 RO cell lines.



Ibrutinib in both primary CLL cells and the MCL cell line CCMCL1, has previously been shown to reduce protein levels of MCL1 (276), and both MCL1 and BCLxL in CLL (277). mRNA levels of *MCL1* and *BCLxL* were also reduced in CLL (277). The BCR signalling pathway has been shown to directly modulate transcription, translation and post translational modification of MCL1, resulting in over expression of MCL1 (278). Therefore through inhibition of this pathway using a BTKi, an expected outcome would be reduced expression of MCL1. Furthermore, BTK is necessary for BCR-induced phosphorylation of the cAMP-response element-binding protein (CREB) (279). In B cells, phosphorylation of CREB induces BCL2 protein expression upon cross-linking of surface immunoglobulin, resulting in inhibition of apoptosis (280) and therefore providing an explanation for the observed downregulation of anti-apoptotic proteins.

To explore the relative roles of MCL1, BCLxL and BCL2A1 in the development of resistance to cell death, RNA interference experiments were performed. siRNAs against MCL1, BCLxL and BCL2A1, inhibited or reduced protein expression on immunoblot (Figure 5.8). In the TMD8 cell line, siRNAs against MCL1, BCLxL and BCL2A1, resulted in reduced viability at 24 hours, which was further reduced with the addition of tirabrutinib (concentration range 1nM - 1000nM) when compared with the negative control siRNA (Figure 5.9). The reduction in viability was greatest with MCL1 and BCL2A1 siRNAs. In the resistant cell line, TMD8 RO, siRNAs against MCL1, BCLxL

and BCL2A1, resulted in reduced viability at 24 hours, which was not significantly reduced further in the presence of tirabrutinib (concentration range 1nM - 1000nM) (Figure 5.9). It should be noted however that the efficiency of BCL2A1 knockdown in TMD8 RO was poor. Single knockdown failed to restore fully sensitivity to tirabrutinib.

Figure 5.8 Effects of TMD8 and TMD8 RO nucleofection with MCL1, BCLxL or BCL2A1 siRNA's on protein expression after 24 hours.

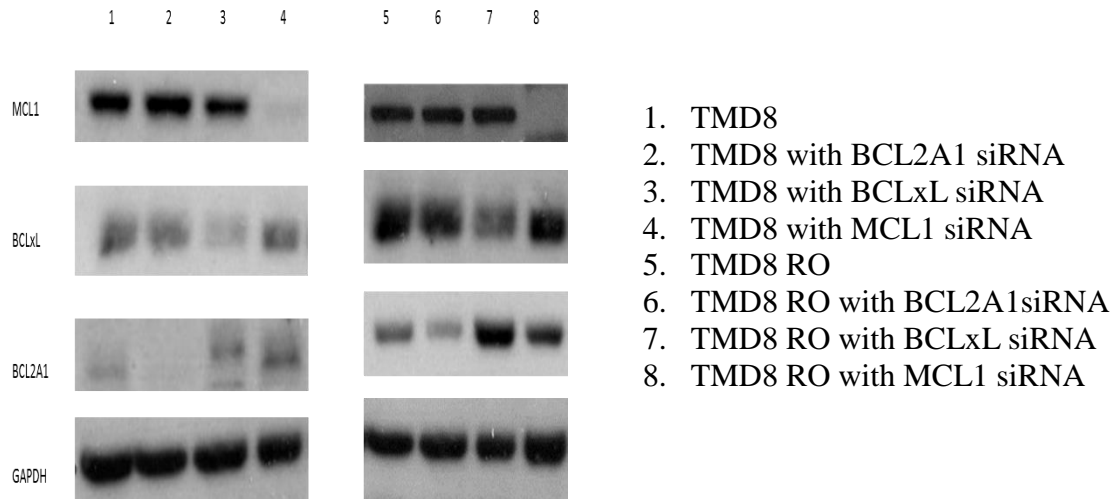
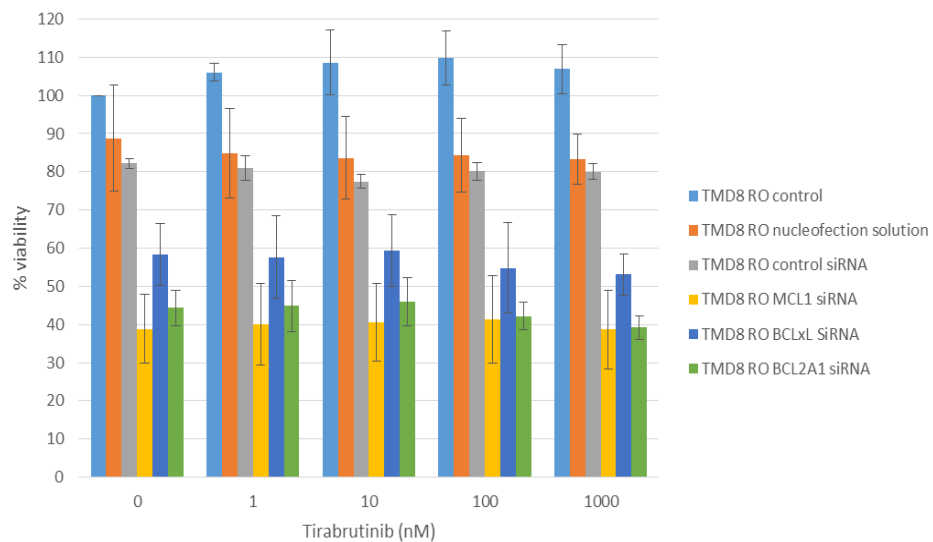
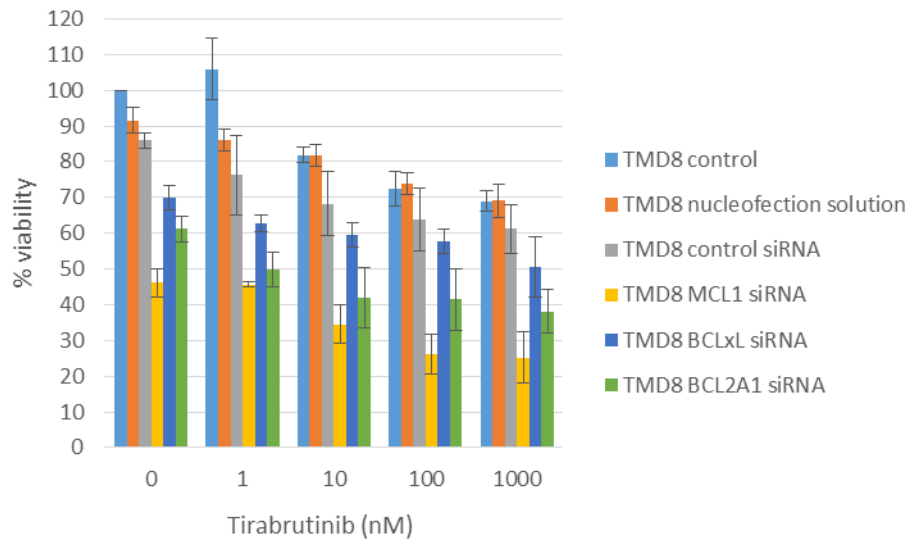


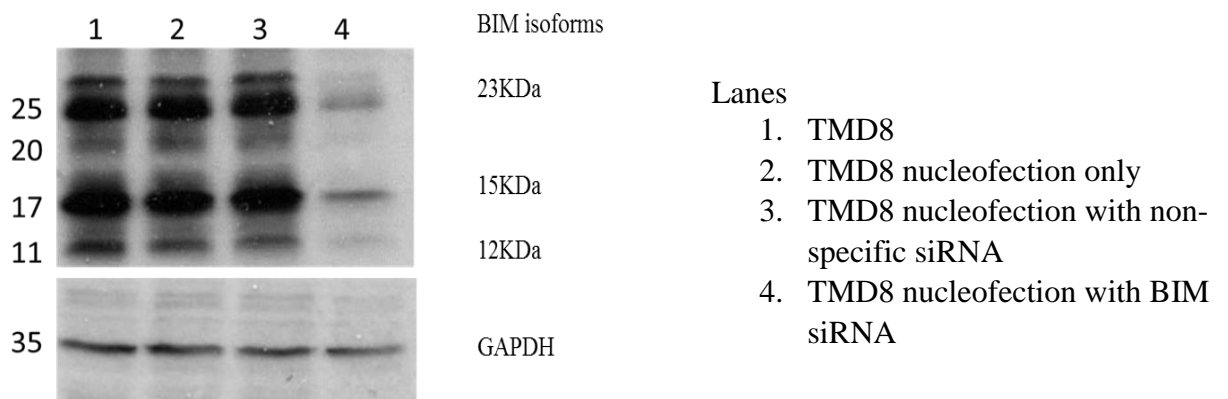
Figure 5.9 TMD8 and TMD8 RO cell lines treated with control, or MCL1, BCLxL or BCL2A1 siRNA prior to addition of 0, 1, 10, 100 and 1000nM tirabrutinib for 24 hrs and assessment of cell viability using the CellTiter-Glo Luminescent Cell Assay. Data shown represent the mean +/- SD (n = 3). Each experiment was performed in triplicate.



5.4.1 Role of the BH3-only protein BIM in TMD8

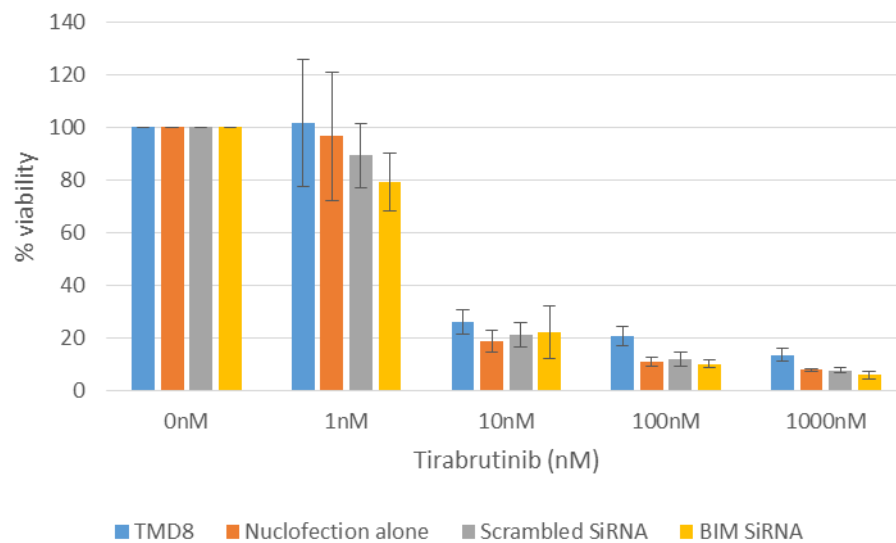
The possible role of pro-apoptotic BH3-only proteins in BTK-mediated apoptosis is unclear. Previous work from our laboratory demonstrated increased BIM expression in TMD8 following suppression of ERK signalling by BTK (262). I therefore knocked down BIM with siRNA, to assess whether this would result in survival of TMD8 cells following treatment with tirabrutinib. Confirmation of knockdown of BIM was confirmed at the protein level by immunoblot (Figure 5.10).

Figure 5.10 TMD8 nucleofection with BIM small interfering RNA (siRNA). Western blotting was performed for BIM at 72 hours post transfection.



However, tirabrutinib resulted in loss of cell viability in BIM knockdown TMD8 cells. (Figure 5.11). This suggests that upregulation of BIM alone does not result in apoptosis in the presence of tirabrutinib in TMD8. As BAX and BAK showed no change in protein expression on immunoblot (262), I did not undertake siRNA experiments with the BIM effectors, BAX and BAK.

Figure 5.11 Effect on TMD8 cell viability following nucleofection with BIM siRNA. TMD8 control, TMD8 following nucleofection alone, TMD8 following nucleofection with scrambled siRNA, TMD8 following nucleofection with BIM small interfering RNA (siRNA) following addition of 0, 1, 10, 100 and 1000nM tirabrutinib for 24 hrs and assessment of cell viability using the CellTiter-Glo Luminescent Cell Assay. Data shown represent the mean \pm SD (n = 3). Each experiment was performed in triplicate.



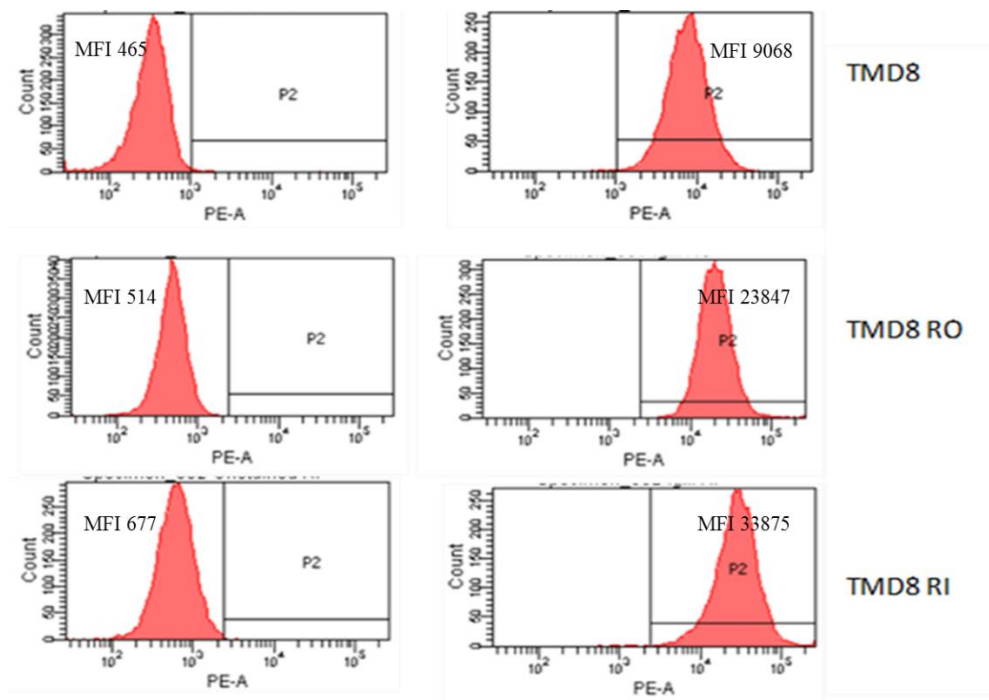
5.5 Immunophenotype of TMD8 cell lines

Both *in vitro* and *in vivo* studies of CLL cells treated with ibrutinib have shown marked changes in cell surface immunophenotype, some of which may have therapeutic implications (281). The effects of selective BTKi on the immunophenotype of CLL and other B cell malignancies has been much less well studied. I therefore used a small panel of MAbs to determine possible changes in TMD8 cell lines.

5.5.1 Surface IgM (sIgM) expression

Altered BCR signalling may shape treatment responses to BCR pathway inhibitors. In ABC DLBCL, gene expression profiling has shown higher expression of the *IGHM* gene (44). This was subsequently shown to correlate with the expression of functional IgM in the ABC DLBCL subtype, in comparison to GCB where in the majority of cases another IG isotype is expressed as a consequence of class switching (282). Expression of sIgM on the parental and resistant cell lines was assessed by flow cytometry and was significantly increased in the resistant cell lines ($P=0.002$) (Figure 5.12). This could reflect inhibition of internalisation of IgM following antigen engagement in the resistant cell line and result in enhanced signalling through the BCR.

Figure 5.12 sIgM expression on the TMD8 and TMD8RO and RI cell lines assessed by flow cytometry. Each experiment was repeated in triplicate. MFI = mean fluorescence intensity.

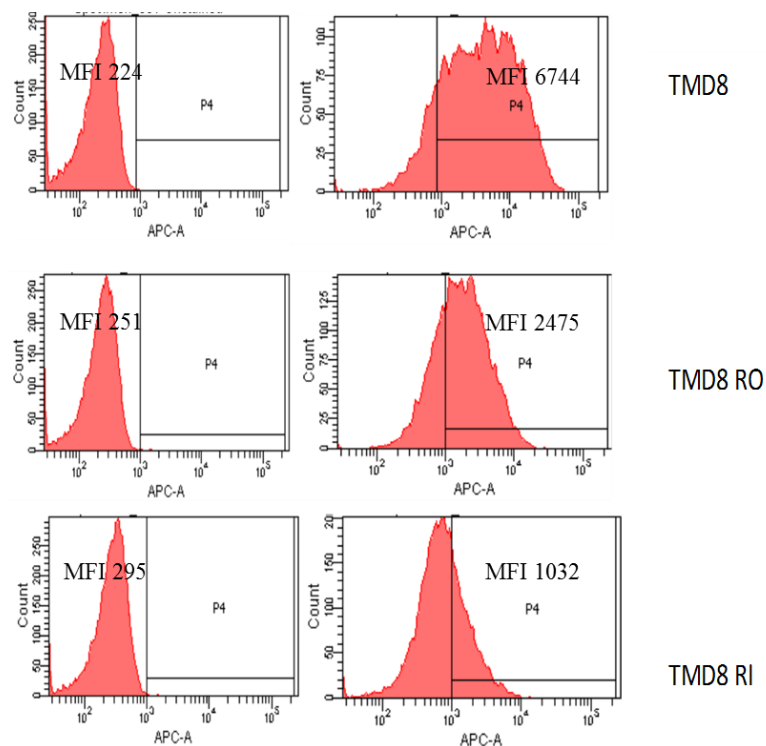


5.5.2 CD5 expression

CD5 is expressed in 5-10% of cases of DLBCL (283); expression is associated with more advanced disease at presentation, ABC DBCL subtype and over-expression of BCL2 (284). It is distinct from CD5+ Richter transformation of CLL (285). CD5 is a negative regulator of B cell receptor signalling (286), inhibiting calcium flux, phosphorylation of PLCG2 and activation of extracellular regulated kinase-2 (287), through recruitment of tyrosine phosphatase-1 (SHP-1) (288, 289). Association of LYN with the BCR permits phosphorylation of the immunoreceptor tyrosine inhibitory motifs (ITIMs) with inhibitory cell surface co-receptors such as CD5 (290). SHP-1 is then able to associate with CD5, through 2 adjacent amino terminal SH2 domains and dephosphorylates key factors that mediate antigen receptor signalling (291). The regulatory role for CD5 in BCR signalling had been shown *in vivo* in CD5 deficient mice (292). CD5⁺ peritoneal B-1 cells proliferate poorly in response to anti-IgM stimulation, which is restored in CD5 negative mice. Calcium flux also increased in CD5 negative mice, suggesting that CD5 may regulate early events in the BCR signalling pathway.

Interestingly, CD5 expression was downregulated in both TMD8 BTKi resistant lines, but to a much greater degree in TMD8 RI than in TMD8 RO, 84.7% and 63.9% respectively (Figure 5.13). The loss of inhibition may lead to enhanced response on crosslinking of the BCR.

Figure 5.13 CD5 expression on the TMD8 and TMD8RO and RI cell lines assessed by flow cytometry. Each experiment was repeated in triplicate. MFI = mean fluorescence intensity.



5.5.3 CD20 expression

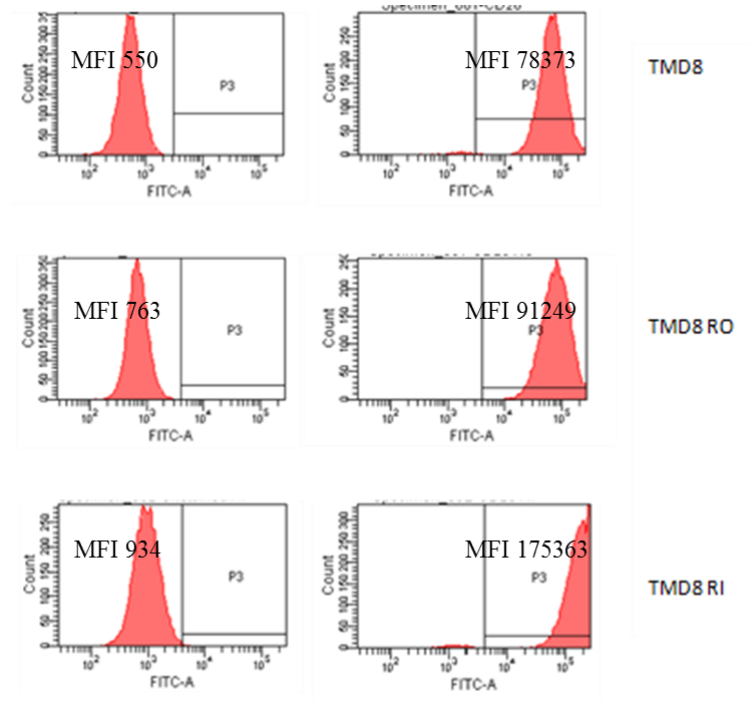
CD20 is a pan B cell molecule and expressed in more than 90% mature B cell lymphomas (293, 294). Its expression is lost following differentiation into plasma cells. It is a non-glycosylated member of the membrane spanning 4-A family (295). The CD20 intracellular regions contain multiple serine and threonine phosphorylation sites (296). Phosphorylation of these sites occurs in response to B cell antigen receptor engagement (BCR). CD20 is thought to play a key role in B-cell activation, differentiation, and cell-cycle progression (297, 298). Co-localisation of the BCR and

CD20 occurs within lipid rafts following BCR stimulation, enabling resultant modulation of the cell cycle (299). CD20-knockout B cells have reduced BCR signalling (300). In humans, complete lack of surface expression of CD20 on B cells due to a homozygous mutation in the *CD20 (MS4A1)* gene, has been reported in an individual of Turkish descent, born to consanguineous parents (301). This resulted in persistent hypogammaglobulinaemia and a reduction in the number of circulating memory cells in the presence of normal B cell numbers, consistent with an impaired ability to mount a response to T cell-independent antibodies. Therefore, whilst the phenotypes of CD20-deficient humans and mice differ, this would suggest that CD20 signals are essential to enable B cells to optimally respond to antigenic stimuli.

CD20 expression is heterogeneous between and within lymphoma subtypes (302). Low CD20 expression has been associated with a poor prognosis in primary DLBCL in both CHOP and R-CHOP treated patients, suggesting that this prognostic effect is important beyond its role as a therapeutic target for rituximab (37). CD20 expression may be modulated by targeted therapies. For example, in bortezomib acquired resistance in JY human B lymphoblastic cells, CD20 expression is upregulated (303). In CLL, expression of CD20 is upregulated through the CXCR4/SDF-1 axis (281). CD20 cell surface expression and mRNA expression is higher on CLL cells that have recently exited the lymph node microenvironment into the peripheral blood and are CXCR4^{dim}CD5^{bright}. CLL cells treated with a ligand for CXCR4, SDF-1 α (CXCL12), produced by stromal cells resulted in an upregulation of CD20, suggesting that the microenvironment is important in the regulation of CD20 expression (281). Ibrutinib *in vivo* also resulted in a reduction of CXCR4^{dim}CD5^{bright} cell populations and lower surface and mRNA expression of CD20, which may have therapeutic implications. Similarly, CLL cells treated with SDF-1 α in the presence of ibrutinib resulted in lower levels of CD20 upregulation. This is likely to occur through inhibition by ibrutinib of CXCR4 phosphorylation and kinases downstream of BTK (304). Loss of CD20 expression may occur as the result of clonal evolution or through epigenetic mechanisms. Alterations in the expression of the transcription factors PU.1, Pip and Oct2, critical for CD20 gene expression may be important in the loss of CD20 expression (305). Loss of CD20 expression may also be observed following the development of resistance to rituximab or other CD20 therapeutic antibodies (306, 307).

CD20 expression following the development of BTKi resistance has not yet been studied. To investigate the changes in CD20 cell surface expression following the development of resistance to tirabrutinib and ibrutinib, the expression of CD20 was determined by flow cytometry. CD20 was upregulated in the resistant cell lines, with greater upregulation observed in the TMD8RI cell line 188 fold increase, versus 120 fold increase in TMD8 RO (Figure 5.14). This finding may have important implications in the use of anti-CD20 therapies in combination with BTKi, suggesting a role for combination therapy in the setting of resistance to BTKi. In a mouse *in vivo* TMD8 xenograft model, tirabrutinib when used in combination with anti-CD20 monoclonal antibodies, resulted in greater anti-tumour effects than either tirabrutinib or anti-CD20 antibody therapy alone (168). Currently, clinical trials are underway, and indeed some have now been reported, with no significant improvement with the addition of rituximab, to assess the effect of the combination of BTKi and anti-CD20 monoclonal antibodies in the clinical setting, e.g. NCT01980654, NCT02682641, NCT02315768, NCT02457598.

Figure 5.14 CD20 by flow cytometry on the TMD8 and TMD8RO and RI cell lines assessed by flow cytometry. Each experiment was repeated in triplicate. MFI = mean fluorescence intensity.



The observed changes in sIgM, CD5 and CD20 in the resistant cell lines are likely to result in increased BCR signalling. Further studies are required to determine the kinetics of change and whether the configuration of the BCR is altered in response to the development of resistance. These findings may explain resistance if loss of the negative regulators of the BCR are observed in the development of resistance.

5.6 A genetic basis to the acquired resistance of TMD8 cells to BTK inhibitors?

Resistance to kinase inhibitors may be defined as either primary or acquired resistance. Acquired resistance may occur as the result of modification of the target gene, activation of compensatory signalling pathways or histological transformation. From the preliminary data presented above, and from other data in the Dyer laboratory, it appeared likely that there was paradoxically enhanced BCR signalling in the BTKi resistant cell lines TMD8 RO and RI. However, the mechanisms underlying this were unclear. I therefore sought to investigate these changes by studying changes in global gene expression and whole exome sequencing.

5.6.1 Changes in gene expression assessed by microarray

Global gene expression analysis was performed using the Illumina HumanHT-12 v4 Expression Array (308) and comparison made between the resistant and parental cell lines before treatment. An arbitrary level of equal to or greater than two fold change was considered to be significant. A small number of genes were found to be coordinately regulated. 55 genes were upregulated ≥ 2 fold in TMD8 RO and 45 in TMD8RI when compared to the parental cell line (Figure 5.15); 16 were common to both TMD8 RO and TMD8 RI (Table 5.2 (a)). 139 genes were downregulated by ≥ 2 fold when TMD8 RO and 178 in TMD8 RI when compared to the parental cell line (Figure 5.15). 79 of these were common to both TMD8 RO and TMD8 RI (Table 5.2 (b)).

Figure 5.15 (a) Venn diagram to show ≥ 2 fold gene expression upregulation in the resistant cell lines TMD8 RO and TMD8 RI when compared to the parental cell line TMD8.

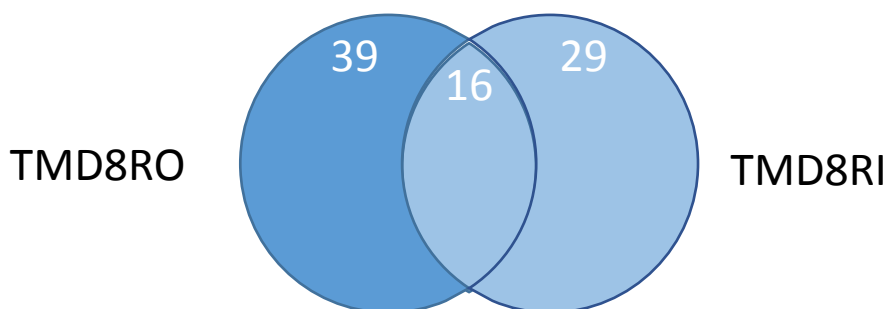
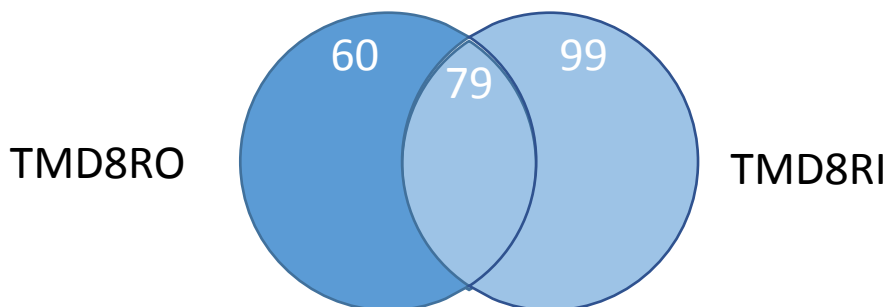


Figure 5.16 (b) Venn diagram to show ≥ 2 fold gene expression downregulation in the resistant cell lines TMD8 RO and TMD8 RI when compared to the parental cell line TMD8.



Gene Ontology (GO) enrichment analysis and KEGG pathway analysis of the common upregulated and downregulated genes of both resistant cell lines was performed (309-311) to determine genes involved in pathways related to B cell signalling.

Table 5. 2 (a) Genes upregulated ≥ 2 fold in both TMD RO and TMD8 RI

Genes upregulated ≥ 2 fold in TMD8 RO and TMD8 RI when compared to TMD8	Fold upregulated in TMD8 RO	Fold upregulated in TMD8 RI	GO biological/ KEGG pathways identified of relevance to B cell signalling
<i>IFI44L</i>	3.80	2.59	
<i>FOXC1</i>	3.52	3.08	negative regulation of transcription
<i>IFIT1</i>	3.32	2.80	
<i>LOC728835</i>	2.58	3.27	MAPK cascade
<i>GBP1</i>	2.48	3.03	negative regulation of T cell receptor signalling pathway
<i>CCL4L1</i>	3.63	3.28	chemokine-mediated signalling pathway
<i>CCL3L3</i>	5.69	4.18	chemokine-mediated signalling pathway
<i>STAT1</i>	2.60	2.03	JAK-STAT cascade
<i>MX1</i>	4.52	2.41	apoptotic process
<i>RMI1</i>	2.29	2.28	DNA synthesis involved in DNA repair
<i>EGR2</i>	3.79	2.59	transcription
<i>HIST1H2BK</i>	2.51	2.89	protein ubiquitination
<i>ISG15</i>	2.66	2.44	type I interferon signalling pathway
<i>MAD2L1</i>	2.07	2.35	cell cycle progression
<i>TPRG1</i>	2.56	2.20	
<i>IFI27</i>	8.36	2.39	apoptotic signalling pathway

Table 5. 2 (b) Genes downregulated ≥ 2 fold in both TMD RO and TMD8 RI

Genes downregulated ≥ 2 fold in TMD8 RO and TMD8 RI	Fold down-regulated in TMD8 RO	Fold down-regulated in TMD8 RI	GO biological/ KEGG pathways identified of relevance to B cell signalling
<i>ENO3</i>	-2.31	-2.63	glycolytic process
<i>RNU1-5</i>	-2.71	-6.31	
<i>HPCAL1</i>	-2.45	-2.71	
<i>FLJ10916</i>	-2.35	-2.01	
<i>NXPH4</i>	-2.03	-2.20	
<i>P4HA1</i>	-2.81	-3.84	oxidation-reduction process
<i>PLAC8</i>	-2.10	-2.49	cell proliferation
<i>CEACAM1</i>	-2.35	-2.13	T cell mediated cytotoxicity
<i>PFKFB4</i>	-4.86	-7.73	fructose metabolic process
<i>KIAA1370</i>	-2.48	-2.80	
<i>FAM65A</i>	-2.10	-2.03	Rho protein signal transduction
<i>FSTL5</i>	-5.14	-3.07	
<i>VTRNA1-1</i>	-3.56	-2.84	
<i>BNIP3</i>	-2.37	-3.58	apoptotic process
<i>RNU6ATAC</i>	-2.61	-4.81	
<i>SNORA12</i>	-3.52	-4.47	
<i>RNF144B</i>	-2.01	-2.61	apoptotic process
<i>TMEM119</i>	-2.45	-2.61	cell differentiation
<i>PAM</i>	-2.64	-4.00	negative regulation of transcription
<i>KIAA1407</i>	-2.77	-2.20	
<i>RNY1</i>	-2.80	-2.54	
<i>CD72</i>	-3.63	-2.21	BCR signalling pathway
<i>P4HA2</i>	-2.77	-2.88	oxidation-reduction process
<i>CECR1</i>	-3.18	-2.97	cellular protein metabolic process
<i>FGFBP2</i>	-2.52	-2.67	
<i>WNT10A</i>	-2.01	-2.49	Wnt signalling pathway
<i>FAM113B</i>	-3.30	-2.40	

<i>EVI2B</i>	-2.21	-2.07	
<i>MKNK2</i>	-2.36	-2.02	cell surface receptor signalling pathway
<i>GAS7</i>	-2.75	-4.01	transcription regulation
<i>CAMK2N1</i>	-2.35	-2.34	negative regulation of protein kinase activity
<i>RNU6-1</i>	-3.14	-4.01	
<i>MTSS1</i>	-2.20	-2.04	transmembrane receptor protein tyrosine kinase signalling
<i>YPEL5</i>	-2.39	2.42	
<i>PTPRE</i>	-2.85	-3.38	
<i>RNU1G2</i>	-3.02	-7.41	B cell receptor signalling
<i>APBB1IP</i>	-2.95	-9.80	
<i>SNORA57</i>	-2.01	-2.54	
<i>RNU1-3</i>	-2.84	-7.51	
<i>TNFRSF21</i>	-2.29	-2.25	Apoptosis
<i>RNASET2</i>	-2.65	-3.00	
<i>TSC22D3</i>	-2.32	-2.07	negative regulation of transcription
<i>SSPN</i>	-2.71	-2.27	
<i>SLC16A3</i>	-4.84	-8.05	metabolism
<i>LTB</i>	-2.98	-2.20	NF-kappa B signalling pathway
<i>FCRL3</i>	-2.53	-2.13	regulation of B cell proliferation
<i>MYOM1</i>	-2.53	-3.67	
<i>SNORD13</i>	-2.49	-2.90	
<i>RNY4</i>	-2.90	-2.44	
<i>HINT3</i>	-3.27	-2.41	
<i>SPINT2</i>	-2.36	-4.12	
<i>SNORD46</i>	-2.49	-2.90	
<i>BNIP3L</i>	-2.37	-3.58	Apoptosis
<i>GPER</i>	-4.48	-3.82	
<i>CRYM</i>	-2.42	-3.01	negative regulation of transcription
<i>SLC47A1</i>	-3.90	-2.70	
<i>LY96</i>	-2.19	-3.38	toll-like receptor signalling pathway
<i>HRK</i>	-2.45	-2.30	apoptosis
<i>TXNIP</i>	-2.62	-2.42	negative regulation of transcription

<i>CA9</i>	-2.26	-2.39	
<i>ALDOC</i>	-7.29	-7.51	glycolysis/gluconeogenesis
<i>SEL1L3</i>	-2.01	-2.94	
<i>MYL5</i>	-2.08	-2.82	
<i>TRIM8</i>	-2.50	-2.05	
<i>FCRL2</i>	-2.43	-2.87	BCR signalling
<i>SNORA79</i>	-2.80	-3.30	
<i>BIVM</i>	-2.11	-2.25	
<i>PQLC3</i>	-2.05	-2.09	
<i>CCR7</i>	-2.02	-3.21	Chemokine signalling pathway
<i>BTG1</i>	-2.10	-2.31	regulation of transcription
<i>RNU6-15</i>	-3.10	-4.01	
<i>FAM46C</i>	-2.03	-2.01	
<i>SCARNA14</i>	-2.30	-2.59	
<i>KLHL24</i>	-2.58	-2.22	
<i>MS4A6A</i>	-2.30	-3.92	
<i>SULF2</i>	-2.07	-3.57	
<i>PTPRO</i>	-2.41	-3.03	BCR signalling
<i>LOC100130179</i>	-2.51	-3.83	protein phosphorylation
<i>MIR1978</i>	-2.01	-2.11	

5.6.2 Changes in gene expression within the BCR signalling pathway

Given the importance of BCR signalling in the TMD8 cell lines, my analysis initially focused on this pathway. BTK gene expression was non-significantly altered in the resistant cell lines; this was confirmed at the level of protein expression and in terms of subcellular localisation as described earlier in chapter 5. Also, there were no significant changes in gene expression levels of nearly all genes directly implicated in BCR signalling. However, some interesting changes in expression were identified in genes that may influence BCR signalling.

Firstly, as noted above, sIgM protein expression was increased in the BTKi resistant cell lines, but surprisingly there were no change in IgM RNA levels in either resistant cell lines. How this increased level of sIgM arises therefore remains unclear. Interestingly, expression of two genes that may indirectly affect sIgM levels were significantly altered. Gene expression of *IGJ* was downregulated in TMD8 RI (4.05 fold downregulation) and RO (1.81 fold downregulation) when compared to TMD8. IGJ protein links IgM monomers and forms a nucleating unit for the IgM pentamer (312), suggesting that BTKi resistant cell lines may have increased monomeric IgM rather than pentameric IgM at the cell surface. Also, a non-coding RNA (*RNUIG2*) (313) that controls the switch between membrane and secreted forms of IgM was significantly decreased (more than 2 fold in both resistant cell lines), thereby potentially increasing membrane expression in TMD8 RO and TMD8 RI.

Several B-cell specific signalling cell surface receptors showed diminished expression. Notably, both *CD5* and *CD72* were down-regulated in the resistant cell lines. *CD5* downregulation was downregulated more strongly in TMD8 RI (fold change -2.98) than in TMD8 RO (fold change -1.73). *CD5* and *CD72* are binding partners and the expression of both molecules on the cell surface of TMD8 leads to the suggestion of an auto-stimulatory pathway, which would be therapeutically targetable. The possible functional significance of loss of these molecules in the resistant cell line is not clear. *CD5* however is a known inhibitor of BCR signalling and thus its loss might be anticipated to lead to enhanced BCR function.

Downstream of the BCR, gene expression of *LYN*, *SYK*, *PLCG2* and the CBM complex were unaltered. However both *PTPRO*, a protein tyrosine phosphatase receptor-type O that functions as a tumour suppressor (314, 315), and *FAIM3*, a BCL6 target gene (316), were > 2 fold downregulated. Overexpression of a lymphoid PTP termed PTP receptor-type O truncated (PTPROt), has been found to inhibit BCR triggered SYK phosphorylation and activation of associated adaptor proteins and downstream signalling events, DLBCL proliferation and apoptosis (315). Therefore *PTPRO* is likely an important regulator of BCR signalling and survival and upregulation in the resistant cell lines may account for the modulation in SYK activity observed on immunoblot. Further studies of targeting SYK with a specific inhibitor in the BTKi resistant cell lines have been undertaken by Mr Tsukamoto (Dyer laboratory).

> 2 fold upregulation of *CCL3L3* and *CCL4L1*, members of the *CCL3* chemokine and *CCL4* chemokine gene families respectively, was observed. *CCL3* and *CCL4* are increased through BCR signalling in DLBCL (317) and ibrutinib *in vitro* as well as other BCR inhibitors inhibited *CCL3* and *CCL4* secretion. High levels of serum *CCL3* and *CCL4* in pre-treatment samples obtained from DLBCL patients was also found to correlate with higher IPI scores and higher levels of *CCL3* associated with poorer OS (317). This data suggests that exploration of serum levels of *CCL3* and *CCL4* from patients receiving tirabrutinib and potential exploration as a biomarker of resistance should be undertaken.

Upregulation of *STAT1* mRNA was identified in both resistant cell lines, suggesting a role for JAK/STAT signalling pathways in the development of resistance. Cerdulatinib, a dual inhibitor of SYK and JAK kinases (318), has been shown to inhibit proliferation of ibrutinib-resistant primary CLL cells and BTK^{C481S} transfected TMD8 cells (319).

5. 7 Whole exome sequencing of TMD8 cell lines

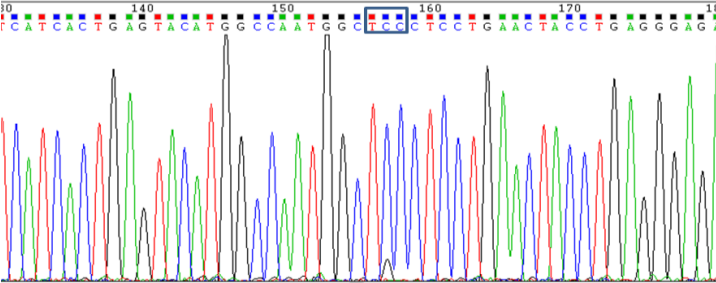
To investigate mutational changes associated with BTKi resistance, whole exome sequencing (WES) was carried out on the TMD8 cell lines. WES was undertaken by the Oxford Gene Technology, with a mean coverage of 52x and 81% of bases at >20x coverage. The median tumour variant allele frequency was just under 50%. The number of nonsynonymous mutations detected in TMD8 RO was 24 and in TMD8 RI was 28, of which 15 were common to both cell lines. The identified mutations and base pair change are show in table 7.2. *MYD88* and *CD79B* mutations were found on WES within the parental TMD8 cell line as previously identified within the literature (90), and resistant cell lines. These mutations are believed to confer sensitivity to BTKi as previously described (177). Mutational analysis was undertaken through collaboration with Professor Claude Chelala at the Barts Cancer Institute and presented in Table 5.3.

Table 5.3 Identified mutations and base pair changes in TMD8 RO and TMD8 RI when compared to TMD8.

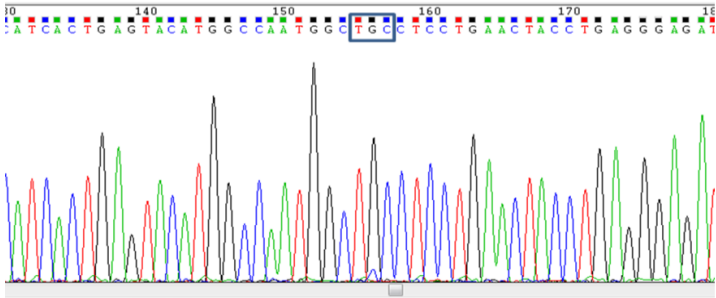
Cell line	Chromosome	Gene	Expression in TMD8 cell line	Genomic co-ordinates (GRCh37)	Type	Reference	Alternative	Genotype	Severity of mutation	Mutation	Previously identified
TMD8RO	10	ENTPD7	Yes	10:101439080..101439080	SNP	G	T	Heterozygous	Serious	Non synonymous coding	
	15	FAN1	Yes	15:31197273..31197273	Intron					Non synonymous coding	
	16	PLCG2	Yes	16:81946260..81946260	SNP	C	T	Heterozygous	Serious	Non synonymous coding	COSMIC
	19	NLRP12	No	19:54314078..54314078							
	6	SEC63	Yes	6:108214751..108214751	SNP	T	C	Heterozygous	Serious	Mutation downstream	COSMIC
	7	LRCH4	Yes	7:100175319..100175319	SNP	G	T	Heterozygous	Other	5 Prime UTR	
	7	CASP2	Yes	7:142997044..142997044	Intron						
	9	RASEF	No	9:85677605..85677605							
X	BTK	Yes	X:100611163..100611164	SNP	C	G	Homozygous	Serious	Non synonymous coding	COSMIC	
TMD8RI	10	CC2D2B	No	10:97775979..97775979							
	11	ATG2A	Yes	11:64675344..64675344	SNP	G	A	Heterozygous	Serious	Non synonymous coding	
	14	TEP1	Yes	14:20854732..20854732	SNP	C	T	Heterozygous	Serious	Non synonymous coding	COSMIC
	16	PLCG2	Yes	16:81953151..81953151	SNP	C	T	Heterozygous	Serious	Non synonymous coding	
	16	PLCG2	Yes	16:81968117..81968117	SNP	C	A	Heterozygous	Serious	Non synonymous coding	
	18	DSC2	No	18:28672169..28672169							
	18	BCL2	Yes	18:60985810..60985810	SNP	G	C	Heterozygous	Serious	Missense	COSMIC
	19	S1PR5	No	19:10624963..10624963							
	19	KIR3DL1	No	19:55341433..55341433							
	19	PEG3	No	19:57325540..57325540							
	2	COBLL1	Yes	2:165600378..165600378	SNP	G	A	Heterozygous	Serious	Non synonymous coding	
3	ZNF717	No	3:75790787..75790787								
8	RP11-463D19.2	No	8:74742615..74742615								

TMD8RO and RI												
	11	MRGPRG	No	11:3239530..3239530								
	11	NUP160	Yes	11:47824989..47824989	SNP	C	T	Heterozygous	Serious	Essential splice site		
	12	PLCZ1	No	12:18876362..18876362								
	12	BEST3	No	12:70088197..70088197								
	12	OTOGL	No	12:80761503..80761503								
	15	FSD2	No	15:83451638..83451638								
	19	ZNF583	Yes	19:56935671..56935671	Intron							
	2	UNC80	No	2:210791676..210791676								
	2	SMARCAL1	Yes	2:217311879..217311879	SNP	C	T	Heterozygous	Other	Non synonymous coding	COSMIC	
	22	FBLN1	No	22:45929752..45929752								
	3	VIPR1	Yes	3:42576544..42576544	SNP	A	C	Heterozygous	Serious	Non synonymous coding		
	5	EBF1	Yes	5:158523410..158523410	SNP	G	A	Heterozygous	Serious	Non synonymous coding		
	7	EPHA1	No	7:143098605..143098605								
	9	LCN2	No	9:130912634..130912634								
	X	ZDHC15	No	X:74725654..74725654								

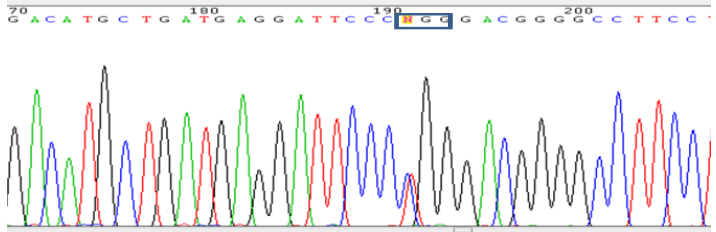
Figure 5.16 Sanger sequencing to show the *BTK* C481S and *PLCG2* mutations identified within the resistant cell lines.



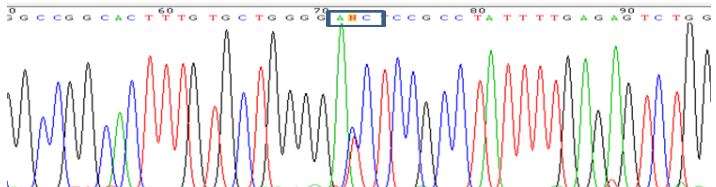
TMD8 RO
C481S
mutation in
BTK



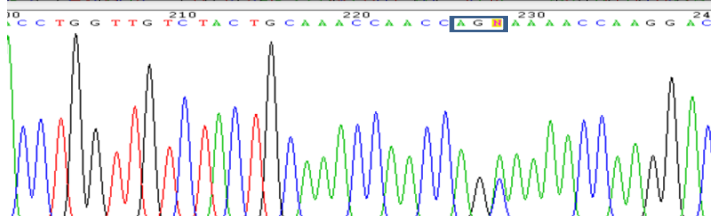
TMD8 RI
C481S
mutation in
BTK



TMD8 RO R665W
mutation in
PLCG2



TMD8 RI T7061
mutation in
PLCG2



TMD8 RI S941R
mutation in
PLCG2

The number of nonsynonymous mutations observed in both cell lines was low, 28 in TMD8RI and 24 in TMD8RO. Of the mutations identified in the resistant cell lines on WES, only a small proportion of these genes are expressed within the TMD8 cell line, according to the gene expression atlas (320). Consistent with prior reports of resistance to BTKi, mutations within the cysteine binding site of *BTK* (C481S) and *PLCG2* (R665W) in CLL were identified in TMD8 RO, however these mutations were not present in TMD8 RI on WES, suggesting an alternative mechanism of resistance in TMD8 RI. These results in TMD8 RO were confirmed by Sanger Sequencing (Figure 5.16). However, on Sanger sequencing of TMD8 RI, the *BTK* mutation was present at a frequency of less than 5%, which may represent an emerging subclone (Figure 5.16). The C481S mutation has been previously reported to confer resistance in CLL, MCL and WM. Additionally in the *MYD88* mutated ABC DLBCL cell lines TMD8 and HBL-1, transduction with the lentiviral vector expressing BTK with C481S, resulted in a 1-3 log fold increase in EC50 for ibrutinib versus BTK WT transduced cells or vector only (321). A TMD8 cell line model of acquired BTK inhibitor resistance, developed through continuous exposure to ibrutinib at 10 or 20nM, showed complete resistance to ibrutinib and WES demonstrated the presence of the *BTK* C481F homozygous mutation in all clones treated with 20nM ibrutinib (322).

The *PLCG2* mutations detected on WES in TMD8 RI, T7061 and S941R, within exon 26 and intronic respectively, have not previously been described. In CLL, the P664S, R665W, L845F and S707Y, non-synonymous mutations and 6 nucleotide deletion leading to the deletion of S707 and A708 in *PLCG2* have previously been identified in ibrutinib resistant patients (200, 323, 324). The function of R665W and L845F has been characterised following expression in the *PLCG2* deficient DT40 B cells (323). In the presence of the mutant *PLCG2* isoenzyme, autonomous signalling did not occur, but rather relied on BCR ligation. In the absence of BTK, BCR mediated activation of R665W mutant

PLCG2 was increased, suggesting a bypass of BCR mediated BTK activation and capability of mediating ibrutinib resistance in CLL (324).

The previously described mutation in *TNF α -induced protein 3 (TNFAIP3 Q143*mutation, A20 protein)* identified in a 10nM clonal TMD8 ibrutinib resistant cell line was not identified in our resistant cell line (322); consistent with NF- κ B pathway activation. Interestingly *EBF1* mutations were identified in both resistant cell lines, which has been associated with transformation of follicular lymphoma (325). Additional mutations in the *NF κ B*, *MAPK* or *AKT* signalling pathways were not identified.

Interestingly, a missense mutation, in *SMARCAL1* R617W was identified in both resistant cell lines, which has previously been described in COSMIC (COSM1241760) in colorectal and oesophageal adenocarcinoma (326, 327). *SMARCAL1* is important in the DNA damage repair response and cell cycle progression (328). Mutations in *SMARCAL1* or knockdown has been shown to result in more double stranded breaks and to enhance sensitivity to chemotherapy (328) and references within. This may suggest a role for targeting the DNA damage response repair mechanism in BTKi resistance. In primary CLL cells, synergism between the ATR inhibitor, AZD6738 and ibrutinib in DNA damage response defective cells has been observed (329) and provided rationale for the proposed clinical trial of acalabrutinib with AZD6738 (NCT03328273). However most chromatin modifying gene mutations in DLBCL, for example *EZH2* and *CREBBP*, are found within the GCB subtype of DLBCL (330).

Results from WES and prior published reports of ibrutinib resistance confirm that resistance to BTKi is not limited to the presence of either *PLCG2* mutations or *BTK* mutations within the ATP binding pocket. The subclonal heterogeneity (identified here on Sanger sequencing and also following single cell cloning by

Mr K. Tsukamoto (unpublished data)) and absence of presence of the *BTK* C418S mutation in all cases of BTKi resistance has important therapeutic implications. Whilst SNS-062, a reversible BTK inhibitor, that does not interact with C481 may offer an alternative treatment option for patients who have developed a mutation in *BTK* within the ATP binding pocket (331).

5.8 Discussion

R/R ABC DLBCL, despite recent treatment advances, remains difficult to treat, with a poor prognosis. Response to tirabrutinib, where seen, is often of short duration. The establishment of the BTKi resistant cell lines TMD8 RO and TMD8 RI provides an *in vitro* model for the study of development of drug resistance. The TMD8 parental cell line was developed from a chemotherapy and radiotherapy naïve patient thus allowing studies to be relevant to the development of resistance to BTKi. High level drug resistance within the resistant cell lines allowed the development of a stable resistant phenotype. To mimic the clinical setting, cells were maintained continuously in the presence of either ibrutinib or tirabrutinib. However the degree to which the generated resistant cell lines provide a clinically relevant model to study drug resistance is uncertain. One of the main considerations is that the resistant cell lines were not single cell cloned. However it is well described that tumours are heterogeneous and that resistance to ibrutinib is not the result of a single mutation in BTK in all settings of resistance. Therefore a heterogeneous cell population may be more reflective of the clinical scenario.

Characterisation of the gene and protein expression of the resistant cell lines has suggested that changes in BTKi resistance occur proximal to BTK. Notably gene expression of *BTK* and the downstream target *PLCG2* were not altered between the two cell lines. Similarly, the levels of expression of known BTK interacting proteins were not altered significantly. Collectively the changes in gene

expression in the BCR signalling pathway and protein expression, appear to occur predominantly at the cell surface membrane and/or lipid rafts result in restoration of BCR signalling and upregulation of downstream signalling pathways on immunoblot. The significance of these changes are not known and further studies are required to assess the structure and function of IgM on the resistant cell lines. These changes prompted detailed proteomic studies to be conducted, including BTK immunoprecipitation and proteomic analysis of lipid rafts in both the parental and resistant cell lines, described in chapter 6.

The finding of a C481S mutation within the cysteine binding site of *BTK* and *PLCG2* R665W mutation in TMD8 RO on WES, supports the hypothesis that disruption of binding of tirabrutinib to BTK and concomitant mutation in *PLCG2* enables resistance to develop. The ability to detect the C481S mutation in TMD8 RI on Sanger Sequencing only, but at a low frequency may reflect the presence of a small subclone. It remains unknown whether these mutations are present in TMD8 subclones before the development of resistance or whether these mutations are acquired during BTKi treatment. Targeted deep sequencing and droplet based methods for the detection of resistant subclones at treatment initiation of ibrutinib in patients with a diagnosis of CLL have shown that these clones may be present at very low levels prior to commencing therapy with a BTKi and subsequently evolve during treatment to enable a selection advantage (332).

It is clear however that not all cases of resistance to ibrutinib occur as a result of the development of mutations in *BTK* and *PLCG2*. For example the detection of a *SMARCAL1* R617W mutation in both resistant cell lines may suggest a role for targeting the DNA damage response repair mechanism in BTKi resistance. However functional studies are required to assess the significance of this mutation. Therefore strategies to target BTKi resistance need to consider that resistance may involve pathways independent of the BCR. Sequential monitoring for the development of resistant subclones during BTKi treatment may provide

further understanding of the development of resistance and enable earlier relapse to be detected.

Chapter 6: Proteomic characterisation of the BCR signalling pathway in TMD8 cell lines

6.1 Introduction

Regulation of the activity of BTK is partially influenced through its subcellular localisation (333). BTK is predominantly cytoplasmic. However, following crosslinking of the BCR, BTK translocates to the plasma membrane, and is recruited to lipid rafts, where it associates with PIP3 through its PH domain (99, 334), and activates downstream targets. BTK also has a nuclear distribution, where it may play a role in transcription (335). I sought to determine whether resistance to BTKi in TMD8 cell lines was firstly associated with a change in the subcellular localisation of BTK and secondly undertook proteomic studies, to determine interactions of BTK in different subcellular compartments, including lipid rafts.

6.2 Subcellular localisation of BTK

Initially, expression of BTK in whole cell lysates was examined in both the parental TMD8 and resistant cell lines. Immunoblot of BTK in the parental and both resistant cell lines showed similar expression levels (Figure 6.1). Through subcellular fractionation, I investigated whether a difference in BTK localisation was seen between the parental and resistant cell lines. BTK was detected within the cytoplasm and nucleus in both TMD8 and the resistant cell lines on immunoblot. As previously described, the predominant proportion of BTK was cytoplasmic and the distribution and quantity of BTK within the nucleus and cytoplasm appeared similar between the cell lines (336). A comparison was also made with the primary BTKi resistant GCB DLBCL (transformed follicular lymphoma) cell line DoHH2, which showed again a predominantly cytoplasmic distribution of BTK (Figure 6.2).

Figure 6.1 Expression of BTK in TMD8, TMD8 RO and TMD8 RI cell lines.

Expression of BTK in whole cell lysate from the cell lines detected by immunoblot.

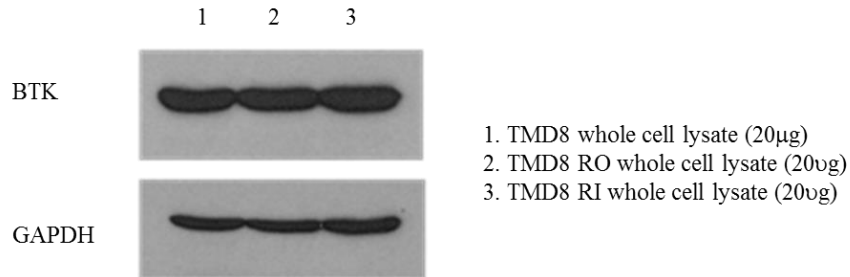
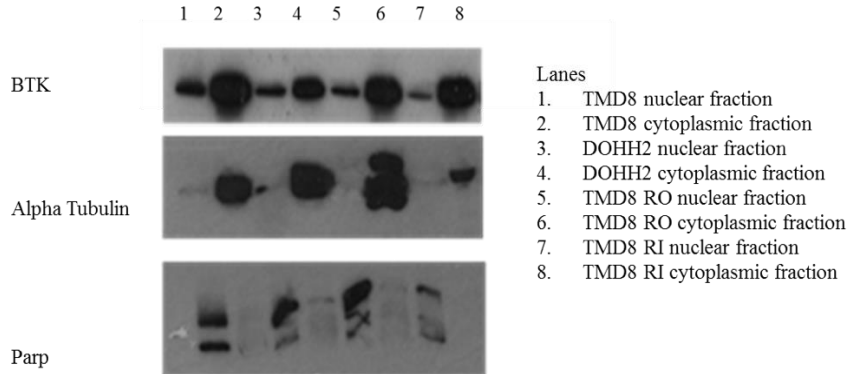


Figure 6.2 Expression of nuclear and cytoplasmic BTK following cellular fractionation in the cell lines TMD8, DoHH2, TMD8 RO and TMD8 RI.

Alpha tubulin and PARP were used to confirm that cytoplasmic and nuclear fractionation was achieved respectively. Percentage of BTK in each compartment was determined by densitometry using ImageJ.



Cell Line	BTK Nuclear fraction (%)	BTK Cytoplasmic fraction (%)
TMD8	9.5	90.5
DOHH2	13.5	86.5
TMD8 RO	7.8	92.2
TMD8 RI	12.4	87.6

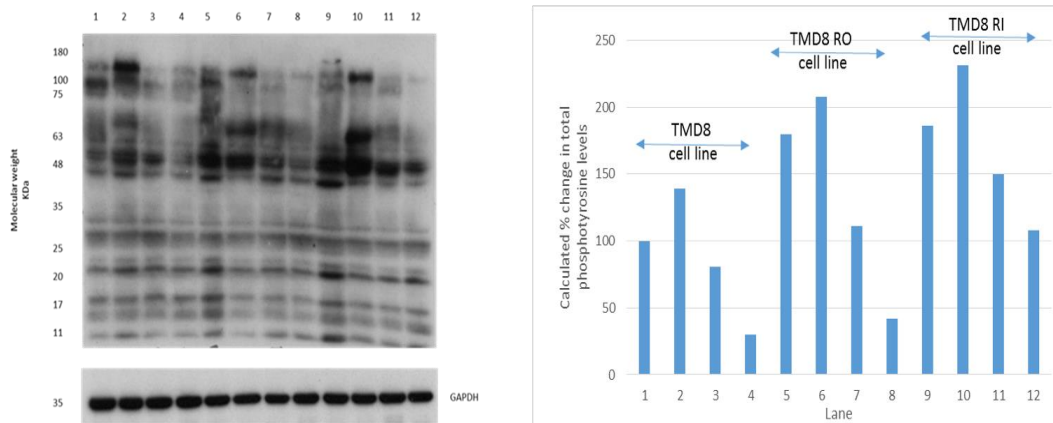
6.3 BCR signalling

6.3.1 Phospho-tyrosine phosphorylation is increased in the BTKi resistant cell lines basally and following IgM stimulation

To determine if tyrosine kinases are hyperactivated in the resistant cell lines, I evaluated levels of pan-phosphotyrosine proteins in the parental and BTKi resistant cell lines using the antibody total phospho-tyrosine protein (4G-10). As shown in Figure 6.3, phosphotyrosine levels were increased in the resistant cell lines in the absence of BCR ligation and increased further following BCR ligation. In both the parental and resistant cell lines phosphotyrosine levels following BCR ligation were maximal 15 minutes after stimulation and returned to basal levels by 24 hours. Densitometric analysis confirmed phospho-tyrosine basal levels were greater in the resistant cell lines, when compared with the parental cell line and are shown in Figure 6.3.

These data suggest that development of resistance to BTKi is firstly associated with increased tyrosine kinase activity and secondly (and unexpectedly) amplified BCR signalling despite BTK inhibition (Figure 6.5).

Figure 6.3 Total phosphotyrosine levels in TMD8 cells following sIgM crosslinking. Whole cell lysates from the cell lines TMD8, TMD8 RO and TMD8 RI were prepared after treatment with 1ug/ml of Goat F(ab')₂ Anti-Human IgM for 15 minutes, 4 hours and 24 hours. Total phospho-tyrosine protein expression was detected by immunoblot. Results from densometric analysis are shown as a % of TMD8 control.



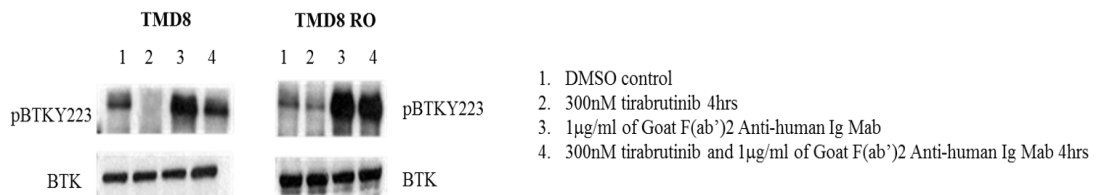
1. TMD8 control
2. TMD8 Goat F(ab')₂ Anti-Human IgMab 15 minute stimulation
3. TMD8 Goat F(ab')₂ Anti-Human IgMab 4 hour stimulation
4. TMD8 Goat F(ab')₂ Anti-Human IgMab 24 hour stimulation
5. TMD8 RO control
6. TMD8 RO Goat F(ab')₂ Anti-Human IgMab 15 minute stimulation
7. TMD8 RO Goat F(ab')₂ Anti-Human IgMab 4 hour stimulation
8. TMD8 RO Goat F(ab')₂ Anti-Human IgMab 24 hour stimulation
9. TMD8 RI control
10. TMD8 RI Goat F(ab')₂ Anti-Human IgMab 15 minute stimulation
11. TMD8 RI Goat F(ab')₂ Anti-Human IgMab 4 hour stimulation
12. TMD8 RI Goat F(ab')₂ Anti-Human IgMab 24 hour stimulation

6.3.2 Changes downstream of the BCR

6.3.2.1 BTK autophosphorylation following IgM crosslinking in TMD8 cell lines

Tyrosine residue 223 in BTK is a marker of BTK autophosphorylation and is considered to be a marker of BTK activity (129). Tyrosine residue 551, located within the activation loop of the kinase domain is phosphorylated by Src family kinases (123, 337). Assessment of pBTKY551 on immunoblot was not successful due to the occurrence of non-specific binding despite modification of conditions and trial of different antibodies. I assessed levels of expression of pBTKY223 in TMD8 and TMD8RO cell lines basally and after exposure to tirabrutinib +/- sIgM crosslinking. Following exposure to tirabrutinib decreased levels of pBTKY223 were seen in the parental line, but not in TMD8 RO (Figure 6.4). sIgM crosslinking resulted in increased pBTKY223 phosphorylation in both cell lines (TMD8RO > TMD8), which was much higher than observed basal levels. This was reduced by tirabrutinib in TMD8 but not TMD8RO. Increased tyrosine phosphorylation of multiple proteins following anti-IgM induced BCR signalling in ABC DLBCL cell lines has been previously shown (338).

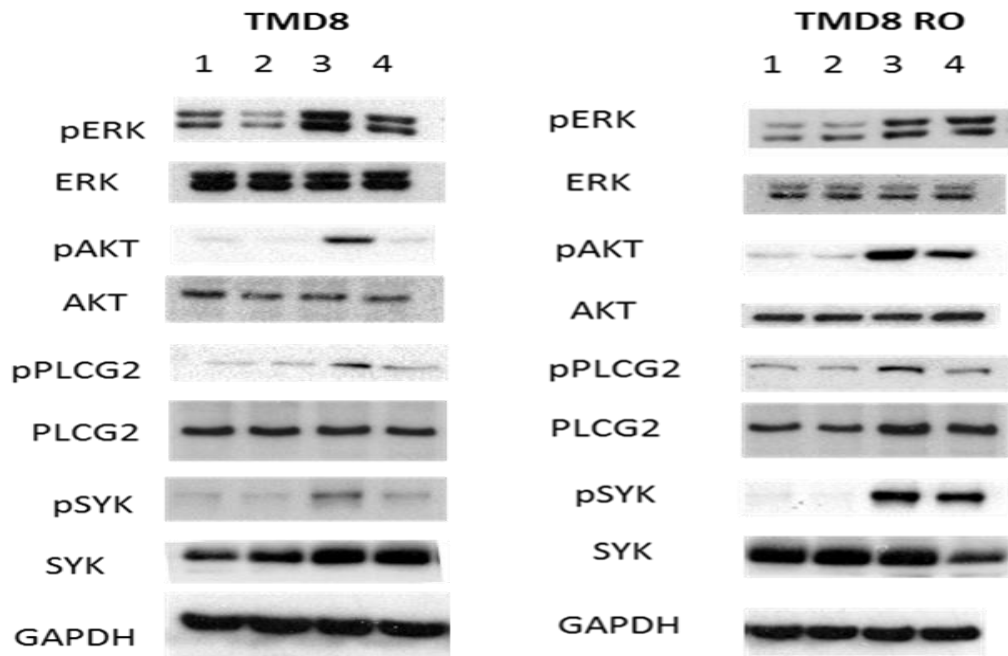
Figure 6.4 Protein expression of BTK and pBTKY223 in TMD8 and TMD8RO following treatment with tirabrutinib +/- sIgM crosslinking.



6.3.2.2 Signalling downstream of BTK

I investigated whether signalling downstream of BTK is altered in TMD8 RO. I assessed AKT, ERK/p44/42 MAP kinase, PLCG2 and SYK activation in the parental and resistant cell line (Figure 6.5). Basal expression of SYK and AKT was increased in TMD8 RO in comparison to TMD8. Levels were not altered following exposure to tirabrutinib or following sIgM crosslinking. Basal expression of ERK and PLCG2 was not increased in TMD8 RO. In TMD8 and TMD8 RO sIgM crosslinking results in increased phosphorylation of ERK, AKT, PLCG2 and SYK. This observed increase is greater in TMD8 RO. Following exposure to tirabrutinib, without sIgM crosslinking, downregulation of pERK and pAKT is seen in TMD8, whilst levels are unchanged in TMD8 RO. Levels of pSYK and pPLCG2 are unchanged in the presence of tirabrutinib in both TMD8 and TMD8 RO. Following sIgM crosslinking levels of pERK, pAKT, pPLCG2 and pSYK were increased in both TMD8 and TMD8 RO. sIgM crosslinking in the presence of tirabrutinib resulted in downregulation of pERK, pAKT, pPLCG2 and pSYK in TMD8, whilst levels of ERK, AKT, PLCG2 and SYK were unaltered. In comparison in TMD8 RO, following sIgM crosslinking, downregulation of pAKT and pPLCG2 was observed but pERK and pSYK were unaltered.

Figure 6.5 Immunoblot to show ERK, pERK, AKT, pAKT, PLCG2, pPLCG2, SYK, and pSYK protein expression in TMD8 and TMD8 RO following treatment with tirabrutinib +/- sIgM crosslinking. Cell lysates (20 µg per lane) were separated by SDS-PAGE gel and immunoblotted with indicated antibodies.



1. DMSO control
2. 300nM tirabrutinib 4hrs
3. 1mg/ml Goat F(ab')₂ Anti-human IgMab
4. 300nM tirabrutinib 4 hrs and 1mg/ml Goat F(ab')₂ Anti-Human IgMab

Sensitivity to ibrutinib has been associated with the inhibition of AKT, ERK and NF-κB signalling pathways. BTK has previously been shown to be required for BCR induced activation of AKT (339) and enhanced AKT activation in ibrutinib resistant CLL, MCL and WM has been described (323, 340, 341). Increased expression of SYK on immunoblot and consistent with increased sIgM detected by flow cytometry may suggest that resistance to BTKI occurs upstream of BTK. Consistent with this hypothesis, CD79B upregulation in ABC DLBCL, has been associated with ibrutinib resistance and increased AKT and MAPK activation.

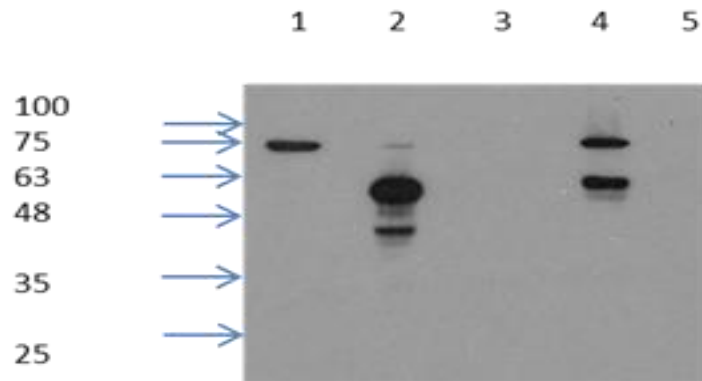
Interestingly, whilst in TMD8 RO, increased total as well as phosphorylation of ABT and SYK are observed comparative to TMD8, total BTK and ERK are not increased on immunoblot in TMD8 RO. The SYK/JAK inhibitor cerdulatinib has shown activity in ibrutinib resistant CLL and in ibrutinib resistant DLBCL cell lines with MYD88, CARD11 or A20 mutations (319, 342). Currently, the clinical trial NCT02983617 is investigating combination therapy with the SYK inhibitor, entospletinib, with tirabrutinib in B cell NHL.

SYK has a complex role in cancer, with reports of activity as a tumour suppressor in some solid tumour but also as a promoter in other cancers. In haematological malignancies, it has an important survival function and inhibition frequently results in apoptosis. Whilst increased gene expression of SYK is not observed in TMD8 RO, downregulation of PTPRO or amplification of BCR signalling, may result in a positive feedback loop and increased phosphorylation (343).

6.4 BTK immunoprecipitation studies

Whilst the importance of BTK in BCR signalling is well described, what confers sensitivity to BTK inhibition (and resistance to BTKi) remains unclear. I sought to test the hypothesis that there might be differences in the proteins that interact with BTK in the sensitive cell line TMD8, primary resistant cell line DoHH2 and acquired resistant cell line TMD8 RO. Initially I used whole cell lysates. BTK was immunoprecipitated. After elution, samples were run on an SDS-PAGE gel and immunoblotted with anti BTK Mab (Figure 6.6). This showed a band at the predicted size of 77KDa in lane 4 from the BTK immunoprecipitation, indicating successful immunoprecipitation.

Figure 6.6 Immunoprecipitation of TMD8 cell line with anti IgG or anti-BTK and subject to immunoblot analysis with anti-BTK. Lane 1 whole cell lysate, anti-BTK 77KDa, consistent with BTK. Lane 2 shows the heavy and light chains of IgG, immunoprecipitated on protein A sepharose beads. Lane 3 shows IgG flow through the supernatant removed from the sepharose beads, following overnight incubation. Lane 4 immunoprecipitation of BTK and co-immunoprecipitation of the heavy chain of IgG. Lane 5 shows BTK flow through, immunoblot of the supernatant removed from the sepharose beads following overnight incubation with BTK.



- Lanes:**
1. 10% input (50ug protein)
 2. IgG
 3. IgG flow through
 4. BTK
 5. BTK flow through

To identify potential interacting proteins with BTK using a whole cell approach, immunoprecipitate samples from all 3 cell lines were analysed by mass spectrometry. From this initial screen I identified 16 BTK-specific interacting proteins in TMD8, 20 in TMD8RO and 61 in DoHH2, of which relevant proteins are shown in table 6.1. Proteins identified are found in all cellular locations. The most abundant classes were nucleic acid binding proteins and cytoskeletal proteins.

Table 6.1 Proteins of interest identified following immunoprecipitation of BTK in TMD8, TMD8 RO and DoHH2. Proteins common to all 3 cell lines are highlighted in yellow and those common to both TMD8 and DoHH2 in green. Proteins present only in the BTK immunoprecipitate of TMD8 are highlighted in blue; those present only in DoHH2 in pink and those only in TMD8 RO in orange.

BTK TMD8 IP	BTK DoHH2 IP	BTK TMD8 RO IP
Tyrosine-protein kinase BTK	Tyrosine-protein kinase BTK	Tyrosine-protein kinase BTK
Treacle protein	Treacle protein	UPF0585 protein C16orf13
T-complex protein subunit delta	T-complex protein 1 subunit delta	Calmodulin
General transcription factor II-I	General transcription factor II-I	Glutathione S-transferase
	Endoplasmic	Mu 4
Drebrin	Polyadenylate-binding protein 1	NEDD8-conjugating enzyme
Bifunctional aminoacyl-tRNA synthetase	Probable ATP-dependent RNA helicase DDX17	Ubc12
Phostensin	Transitional endoplasmic reticulum ATPase	
Sorting nexin-18	ATP-dependent RNA helicase A	
Pro-interleukin-16	Heterogeneous nuclear ribonucleoprotein U-like protein 1	
Isoform 4 of Protein phosphatase 1 regulatory subunit 12C	Proliferation-associated protein 2G4	
Heterogeneous nuclear ribonucleoprotein M	Ubiquitin-like modifier-activating enzyme 1	
Brain acid soluble protein 1	Aspartyl-tRNA synthetase, cytoplasmic	
RuvB-like 2	ATP-dependent DNA helicase 2 subunit 2	
Lymphocyte-specific protein 1	Isoform Short of Heterogeneous nuclear ribonucleoprotein U	
Myosin-Ig	Heterogeneous nuclear ribonucleoproteins A2/B1	
Caprin-1	Coronin-1A	
Phenylalanyl-tRNA synthetase beta chain	Eukaryotic initiation factor 4A-I	
Insulin-like growth factor 2 mRNA-binding protein 3	Tyrosyl-tRNA synthetase, cytoplasmic	
Insulin-like growth factor 2 mRNA-binding protein 1	T-complex protein 1 subunit zeta	
	Eukaryotic initiation factor 4A-III	
	T-complex protein 1 subunit eta	
	RuvB-like 2	
	T-complex protein 1 subunit beta	
	Poly(rC)-binding protein 2	
	Phosphatidylethanolamine-binding protein 1	

Results from immunoprecipitation with whole cell lysate identified a bewilderingly large number of potential interacting proteins from all cellular compartments especially from the DoHH2 cell line. The only protein identified in all three immunoprecipitations was BTK itself. General Transcription Factor II-I (a previously identified BTK-interacting protein (119, 130, 344)) was immunoprecipitated from parental TMD8 and DoHH2 but not from TMD8RI. Similarly, the Treacle protein (TCOF1 expressed in the nucleolus) (345) and T-complex protein 1 subunit delta (a molecular chaperone, assisting the folding of proteins upon ATP hydrolysis) (346) were only immunoprecipitated from TMD8 and DoHH2. It therefore seemed likely that this approach was unlikely to identify any crucial interactions. I therefore sought to immunoprecipitate BTK specifically from lipid rafts, which form a platform for BCR signalling and therefore might contain constitutively active BTK, in the hope that this would reduce “contamination” by other proteins. Given the low levels of lipid rafts in B cells, these were technically demanding experiments requiring large numbers of cells as the starting materials (1×10^9). These experiments proved unsuccessful. I therefore compared the proteomes of purified lipid rafts from the three cell lines, TMD8, TMD8 RO and TMD8 RI.

6.5 Lipid rafts

Lipid rafts play an important role in a number of cellular functions, such as cell signalling, proliferation and apoptosis. A number of receptor tyrosine kinases and surface antigens have been identified within lipid rafts, including BTK (347). Due to their functional importance and the potential for identification of mechanisms of resistance and new drug targets, I sought to characterise the lipid raft proteome in TMD8, TMD8 RO and TMD8 RI. The presence of the lipid raft marker, flotillin was confirmed on immunoblot to ensure that isolation had been successful prior to mass spectrometry (data not shown).

6.5.1 Lipid raft proteins identified by mass spectrometry

Across all three cell lines a total of 989 proteins were identified by mass spectrometry; 949 were identified in TMD8 derived lipid rafts, 907 from TMD8 RI and 566 from TMD8 RO. On review of the literature of proteomic analysis of B cell lipid rafts, proteins commonly identified include receptor or surface glycoproteins, cytoskeletal or structural proteins, protein kinases, small G proteins, motor proteins and vesicle fusion or trafficking proteins. In table 6.2, proteins identified within the TMD8 isolated lipid rafts that have been previously described in this compartment are shown (94, 105). CD79b was not identified on purification of lipid rafts by mass spectrometry. However on immunoblot this was detected following membrane fractionation by discontinuous sucrose density gradients, thereby suggesting that this may be the result of the methods employed to isolate lipid rafts.

Table 6.2 Previously identified lipid raft proteins identified within the TMD8 cell line (94, 105).

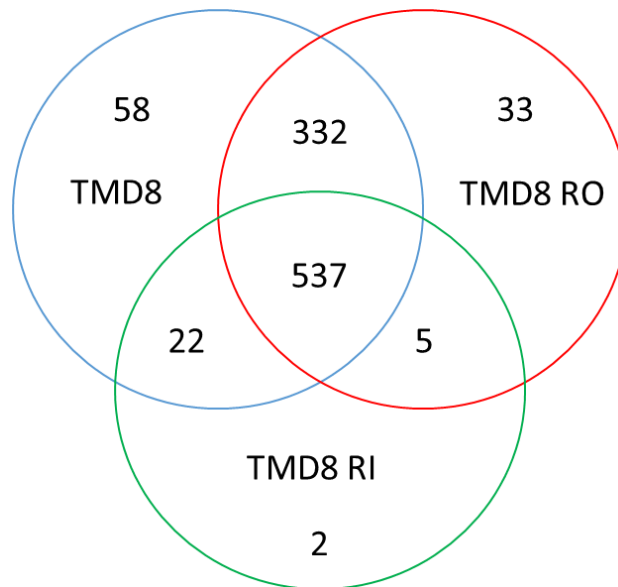
Lipid raft protein groups	Identified proteins within the TMD8 cell line lipid rafts
Receptor or surface glycoproteins	BCR, CD20, CD36, CD42, CD44, CD48, CD59, CD72, HLA-A, HLA-g, HLA-Drab, CBP/PAG, CD79a.
Cytoskeletal or structural proteins	Actin, B tubulin, Flotillin-1 and 2, Raftlin, Ezrin
Protein kinases	LYN, CSK, SYK, BTK, BLK
Small G proteins	RhoG, RhoF, Rap1A, Rap2A,B,C
Motor proteins	Myh9, Myh10. Myo1C,D,E and G, Myosin light chain, Myosin regulatory light chain
Vesicle fusion or trafficking proteins	Clathrin heavy chain

A total of 537 proteins were common to all cell line lipid rafts, whilst only 40 were found in either TMD8 RO or TMD8 RI (Table 6.3 and Figure 6.7).

Table 6.3 Lipid raft proteins identified by mass spectrometry in TMD8, TMD8 RO and TMD8 RI. Unique proteins are proteins identified exclusively in the lipid rafts of that cell line and total proteins are proteins identified in that cell line and overlapping with other cell lines.

	TMD8	TMD8 RO	TMD8 RI
Unique	58	33	2
Total proteins	949	907	566

Figure 6.7 Venn diagram showing the number of lipid raft proteins identified in the TMD8, TMD8 RO and TMD8 RI cell lines and overlapping distribution.



Of the 40 proteins identified within the lipid rafts present only within the resistant cell lines, 5 were common to both TMD8 RO and TMD8 RI. These are shown in table 6.4.

Table 6.4 Proteins identified only within the lipid rafts of the resistant cell lines.

Cell line	Protein
TMD8 RO and RI	IgM Large neutral amino acids transporter small subunit 1 Peroxiredoxin-6 Pantetheinase Keratin, type I cytoskeletal 9
TMD8 RO	Proto-oncogene vav Ubiquitin carboxyl-terminal hydrolase 5 NEDD8-conjugating enzyme Ubc12 Ubiquitin-conjugating enzyme E2 variant 2 Thymidine phosphorylase Aspartate--tRNA ligase, mitochondrial Superkiller viralicidic activity 2-like 2 U2 small nuclear ribonucleoprotein B'' Rho GTPase-activating protein 17 Ras-related protein Rab-3B Proteasome subunit beta type-8 Peptidyl-prolyl cis-trans isomerase H Phosphatidylethanolamine-binding protein 1 Ubiquitin thioesterase OTUB1 Niban-like protein 2 Merlin DNA replication licensing factor MCM3 NAD-dependent malic enzyme, mitochondrial Leukotriene A-4 Luc7-like protein 3 Keratin, type I cytoskeletal 13 Eukaryotic translation initiation factor 4B Hypoxanthine-guanine phosphoribosyltransferase Fibronectin Eukaryotic translation initiation factor 3 subunit K Dihydropyrimidinase-related protein 2 DnaJ homolog subfamily C member ATP-dependent RNA helicase DDX1 Calcium and integrin-binding protein 1 Putative L-aspartate dehydrogenase ADP-ribosylation factor-like protein 2 Aconitate hydratase, mitochondrial Very long-chain specific acyl-CoA dehydrogenase, mitochondrial
TMD8 RI	Lysophosphatidylcholine acyltransferase 1 Keratin, type II cytoskeletal 2 oral

Of the proteins found specifically in lipid rafts in both resistant cell lines, a striking finding was the presence of IgM, which was not detected in lipid rafts from parental TMD8 cells. Over and above the increased levels of IgM seen in the resistant cell lines, the presence of IgM in lipid rafts may account for the increased BCR signalling seen in the resistant cell lines; how this recruitment to lipid rafts is mediated, however, remains to be determined. The possible roles of the other proteins in mediating resistance to BTKi are less obvious. Pantetheinase (VNN1) is a membrane associated protein that catalyses the hydrolysis of D-pantetheine into cysteamine and pantothenate (vitamin B5) is involved in CoA biosynthesis and may be involved in response to metabolic and oxidative stress (348). Peroxiredoxin 6 is similarly involved in protecting against oxidative stress by detoxifying peroxides; it catalyses the reduction of peroxides including H₂O₂ as well as oxidised lipids (349). Large neutral amino acids transporter small subunit 1 (SLC7A5) acts as a high affinity transporter for neutral amino acids, and may be involved in activation of mTORC1 (350). Collectively these data suggest a role of activation of metabolic and oxidative stress pathways in the BTKi resistant cell lines.

The identified proteins most commonly affected metabolic pathways, carbon metabolism, the spliceosome and the PI3K-AKT signalling pathway. Upregulation of PI3K has previously been identified following the development of ibrutinib resistance, thereby suggesting a potential therapeutic option following the development of BTKi resistance (340). The MCL ibrutinib resistant Jeko-1 and PF-1 cell lines have been associated with increased protein expression of PI3K/AKT/mTOR/MCL-1 pathway components (351) and sensitivity of these ibrutinib resistant MCL cell lines and patient derived xenograft (PDX) models to the PI3K inhibitors duvelisib (PI3K- δ/γ Inhibitor) and idelalisib (PI3K- δ) has been shown (352). Similarly in CLL, duvelisib killed CLL cells *in vitro* resistant to ibrutinib (353). In a Phase I study of duvelisib, in patients with R/R CLL and R/R NHL previously treated with ibrutinib, a median of 4.1 treatment cycles (28 days;

range 3.0-9.2) in patients with R/R CLL and 2.5 treatment cycles (range 1.8-5.4) in patients with R/R NHL was seen (354). Similarly, a real world experience of patients with R/R CLL treated with idelalisib following progression showed an ORR of 28% (355). In ABC DLBCL, the rationale for the use of idelalisib in BTKi resistance has been studied in acquired ibrutinib resistant TMD8 cell lines (322). In both the TMD8 cell line, resistant to ibrutinib through loss of *A20* and the presence of the *BTK* C481F mutation, cell viability was not reduced through exposure to single agent idelalisib and tirabrutinib at 96 hours. However the TMD8^{A20-Q143} cell line, with loss of *A20*, showed partial sensitivity to the combination of tirabrutinib and idelalisib.

The ubiquitin conjugating enzyme E2N (UBE2N) was identified within the TMD8 RO lipid rafts. The cellular location of UBE2N has been described as nuclear and cytoplasmic, but it has also been identified previously in lipid rafts in human mesenchymal stem cells (356, 357). UBE2N is important in NF- κ B activation, DNA double-strand break repair, nuclear localisation of p53 and MAPK activation (358-363). These functions, have prompted the investigation of small molecule inhibitors that inhibit the ubiquitin pathway. NSC697923, an inhibitor of UBE2N and one of its cofactors UBE2V1, has been shown to inhibit NF- κ B activation in vitro in ABC DLBCL and inhibit both proliferation and survival of ABC-DLBCL and GCB-DLBCL cell lines and survival of primary DLBCL cells (364). Further studies will be undertaken to assess whether this compound shows activity in the TMD8 BTKi resistant cell lines.

6.5.2 Upregulation of proteins within the resistant cell line lipid rafts

In the lipid rafts of the TMD8 RO resistant cell line, 74 proteins were upregulated at least 2 fold when compared to the parental cell line and 71 in the TMD8 RI resistant cell line. Functional pathway analysis (DAVID and KEGG pathway analysis), identified 13 pathways associated with the upregulation of these proteins in TMD8 RO lipid rafts and 9 associated with the upregulated proteins in TMD8 RI (Table 6.5). 2 KEGG pathways were common to both resistant cell lines, oxidative phosphorylation and metabolism.

Table 6.5 Pathways associated with proteins upregulated ≥ 2 fold in the lipid rafts of the resistant cell lines (DAVID and KEGG pathway analysis). Lipid raft pathway analysis of proteins was undertaken in proteins upregulated ≥ 2 fold compared to the parental cell line TMD8. Each experiment was repeated twice.

TMD8 RO upregulated	TMD8 RI upregulated
Biosynthesis of antibiotics	Pancreatic secretion
Carbon metabolism	Mineral absorption
Biosynthesis of amino acids	Oxidative phosphorylation
Glycolysis/gluconeogenesis	Measles
Metabolism	Metabolism
Pentose pathway	Phagosome
Prion diseases	Cardiac muscle contraction
Pyruvate metabolism	Insulin secretion
Glucagon signalling pathway	Herpes simplex infection
Pathognomic E.Coli infection	
Platelet activation	
Regulation of actin cytoskeleton	
Oxidative Phosphorylation	

6.5.2 Downregulation of proteins within the resistant cell line lipid rafts

In the lipid rafts of the TMD8 RO resistant cell line, 43 proteins were downregulated at least 2 fold when compared to the parental cell line and 141 in the TMD8 RI resistant cell line. Functional pathway analysis (DAVID and KEGG pathway analysis), identified 7 pathways associated with the downregulation of these proteins in TMD8 RO lipid rafts and 15 associated with the downregulated proteins in TMD8 RI (Table 6.6). 3 KEGG pathways were common to both resistant cell lines, oxidative phosphorylation, spliceosome and ribosome.

Table 6.6 Pathways associated with proteins downregulated ≥ 2 fold in the lipid rafts of the resistant cell lines (DAVID and KEGG pathway analysis). Lipid raft pathway analysis of proteins was undertaken in proteins downregulated ≥ 2 fold compared to the parental cell line TMD8. Each experiment was repeated twice.

TMD8 RO downregulated	TMD8 RI downregulated
Oxidative phosphorylation	Ribosome
Non alcoholic fatty acid disease	Endocrine/other factor regulating calcium reabsorption
Cardiac muscle contraction	Spliceosome
Metabolic pathways	Non alcoholic fatty acid disease
Spliceosome	Oocyte meiosis
Proximal tubule bicarbonate reclamation	Viral carcinogenesis
Ribosome	Proteasome
	Cell cycle
	Gap junction
	Oxidative phosphorylation
	E.coli
	Epstein Barr Virus
	MAPK signalling
	Proteoglycans in cancer

6.6 Discussion

BTK was present in the nuclear and cytoplasm in sensitive, primary resistant and acquired resistant cell lines, tested. The tyrosine kinases are hyperactivated in the resistant cell lines, suggesting a higher level of kinase activity and amplified BCR signalling even in the absence of stimulation.

Using whole cell lysate, BTK immunoprecipitation resulted in the identification of a number of proteins, confounding analysis. I therefore sought to study lipid rafts in order to attempt to further clarify differences within the BCR signalling pathway between the resistant and sensitive cell lines. The lipid raft proteome is known to contain proteins of clinical relevance in the aetiology of cancer (365, 366) and their study may allow further understanding of the pathogenesis of cancer and identification of novel therapeutic targets. They have previously been profiled in solid tumours, for example melanoma and colorectal cancer, as well as haematological malignancies such as CLL and MCL (105, 367-369). One of the recognised difficulties in their study is that lipid rafts are often co-purified with other cellular proteins. To overcome this, one method employed is to identify and deplete the cholesterol proteins present in the detergent resistant membrane fractions, which are not actual components of the lipid rafts themselves but co-purify with the raft proteins (370). This is carried out through the use of methyl β -cyclodextrin (M β CD), as a cholesterol deleting agent.

Within the lipid rafts, a number of proteins important in cell survival, apoptosis and signalling were identified. The development of resistance to either ibrutinib or tirabrutinib resulted in changes in the protein content of lipid rafts and their quantities. The proteins identified in the lipid rafts of the resistant cell lines varied according to whether the cells were generated using ibrutinib or tirabrutinib, which may reflect their different kinomes. For example in the resistant cell line lipid rafts, a non-significant reduction in the lymphocyte specific protein 1 (LSP1)

was seen, which is a protein that is important in signalling and apoptosis (371, 372). Identified proteins of interest in the lipid rafts and changes in their expression should be confirmed by immunoblot and RT-PCR.

Of particular interest, was the finding of IgM within the resistant cell line lipid rafts. This together with increased phosphotyrosine levels in the resistant cell lines both in the absence and presence of BCR ligation, may suggest alteration in the structure of the BCR in the development of BTKi resistance. Further studies should include sequencing of the BCR in both the parental and resistant cell lines, to investigate this hypothesis. Further exploration and validation using paired biopsy samples from patients who develop resistance to BTKi and in leukaemic patients will be undertaken.

Further understanding of changes that occur upstream of BTK are of key importance in understanding resistance to BTKi, to develop new therapeutic strategies for patients who develop resistance and for identifying rational targets for combination studies, that may prevent the emergence of resistance and deepen response.

Chapter 7 Discussion

7.1 Results from the Phase I clinical trial of tirabrutinib

The introduction of BTKi has transformed the management of some B cell malignancies, most notably CLL and MCL. My thesis reports both clinical and laboratory studies on the selective BTKi, tirabrutinib.

In the clinical studies, I reported the data from the first clinical trial of a selective BTKi; not only was I involved in the management of patients recruited into the trial in Leicester but also, in collaboration with ONO Pharmaceuticals London, in collating all the data from the primary sources, which turned out to be a considerable undertaking. Overall, the results obtained with tirabrutinib were broadly comparable to those seen with ibrutinib. In patients with MCL and CLL, monotherapy with tirabrutinib resulted in high rates of disease control and remarkably improved quality of life, although this was not formally assessed in this phase 1 study. Strikingly, tirabrutinib was associated with markedly reduced toxicities in comparison with ibrutinib; similar results have also been reported with other selective BTKi including acalabrutinib, although it should be noted that tirabrutinib does not appear to be associated with the headache and diarrhoea commonly seen with acalabrutinib. These differences likely reflect the broad kinome of ibrutinib (151, 152), resulting in toxicities arising from structurally-related kinases.

In terms of efficacy, the data are too preliminary to allow any formal comparison, which will have to await ongoing comparative studies. Broadly speaking, the efficacies of ibrutinib and tirabrutinib appear to be similar, indicating that the efficacy of ibrutinib is dependent primarily on BTK inhibition rather than any other target. There may be some interesting differences though. Firstly, the responses in some patients with MCL may be deeper with tirabrutinib, achieving

MRD negativity in both peripheral blood and within the bone marrow in heavily pre-treated patients. We have observed ongoing improvements in response up to four years following initiation of therapy, with four of our MCL patients now having achieved a normal CT scan along with MRD negativity as determined by multicolour flow cytometry (HMDS, Leeds) in the blood and bone marrow (MJSD and HSW unpublished results and MS in preparation). In this small cohort, there does appear (uniquely) to be a possible dose response with patients receiving doses of >320mg daily making very good durable responses. Confirmation of these data would require larger clinical trials. Another potential area of difference with ibrutinib is the apparently reduced incidence of Richter's transformation in patients with CLL. In this study, no patients treated with tirabrutinib developed Richter's, a trend seen with acalabrutinib. However, it was also observed that temporary interruption of therapy in patients with CLL can result in rapid loss of disease control. Therefore, continuous therapy is required. This has implications from a number of perspectives: quality of life, continuous grade 1 or 2 therapies ongoing for years can be difficult to tolerate; financial implications for the NHS and lastly that for the main, patients will likely relapse at some time point with potentially rapidly progressive and difficult to treat disease.

We have shown using a targeted sequencing panel of genes commonly mutated in CLL in R/R CLL patients treated with tirabrutinib with long term follow up, that no mutations appeared to predict for a shorter PFS nor lack of response with tirabrutinib. However, the sample sizes were too small for formal statistical analysis. Importantly, the presence of 17p13.1/*TP53* mutations did not in this small analysis predict for poor response, nor shorter PFS as shown with ibrutinib (373). Mutations in *TP53*, *SF3B1*, *NOTCH1* and *ATM* were the most commonly identified, similar to large data set analysis within the COSMIC database. This may suggest an important difference between ibrutinib and tirabrutinib and

support the preferential use of tirabrutinib in all genetic subtypes of CLL, however this requires further validation in a larger clinical trial.

Results of tirabrutinib in non GCB DLBCL were much less satisfactory. The prognosis of those with R/R DLBCL remains extremely poor. Strategies aimed at improving outcome from standard chemotherapy, including shortening the interval of R-CHOP to 14 days, or use of intensification strategies such as dose adjusted rituximab plus etoposide, prednisone, vincristine, cyclophosphamide, doxorubicin have failed to show a significant difference in overall survival (374, 375). Obinutuzumab, a type II anti-CD20 antibody, whilst showing superior results to rituximab in CLL (NCT01010061) (376), failed to show an improvement in treatment naïve CD20 positive DLBCL in the Phase III GOYA trial (377). Treatment outcome at 3 years showed no significant improvement of obinutuzumab over rituximab in PFS, disease free survival (DFS) or time to next treatment (TTNT). Additional strategies based on an improved understanding of the biology of DLBCL, through the addition of additional agents to RCHOP to target specific oncogenic pathways (R(X)CHOP) are ongoing for example the addition of bortezomib to RCHOP in DLBCL (NCT01324596) (378). Molecular characterisation and the development of biomarkers is of critical importance in identifying prospectively patients whom may benefit from this approach.

Based principally on the understanding that constitutive activity of BCR signalling in ABC DLBCL contributes to the pathogenesis of this subtype of disease, inhibitors of the BCR pathway signalling pathways have been evaluated. In 80 subjects with R/R DLBCL, ibrutinib demonstrated an ORR of 25%, with a median PFS and OS of 1.64 and 6.41 months respectively (177). However in patients with ABC DLBCL, the response rate was 37%, providing clinical evidence that chronic active BCR signalling is important in ABC DLBCL. Similarly, with tirabrutinib, we saw a response rate of 35% in those diagnosed with non-GCB DLBCL, a median treatment duration of 12 weeks and no

responses lasting beyond 12 months. Interestingly, some responses were rapid and profound but of only short duration, suggesting rapid development of resistance, which is in stark contrast to the results obtained in other more indolent B cell malignancies. Clinically, I also observed in some cases a mixed response to tirabrutinib in ABC DLBCL, with some nodal regions regressing and others continuing to progress.

An urgent unmet need is therefore to define mechanisms of primary and acquired resistance to BTK inhibitors in order to facilitate identification of mechanism-based synergistic combinations to take into the clinic.

7.2 Characterisation of BTKi resistant TMD-8 cell lines

Establishing an *in vitro* model of BTKi resistance using the TMD8 cell line provided a relevant laboratory model to study cellular changes that occur with resistance to ibrutinib and tirabrutinib. Characterisation of the gene and protein expression of the resistant cell lines suggested that changes in BTKi resistance occur proximal to BTK. Notably, gene expression of *BTK* and the downstream target *PLCG2* were not altered between the two cell lines. Similarly, the levels of expression of known BTK interacting proteins were not altered significantly. Collectively the changes in gene expression in the BCR signalling pathway and protein expression, assessed by flow cytometry and immunoblot, appear to occur predominantly at the cell surface membrane, with or without changes in RNA levels. How this “cell surface remodelling” is mediated and how it contributes to resistance to BTKi remains unclear.

7.3 Proteomic characterisation of the BCR signalling pathway in TMD8 cell lines

Results from immunoprecipitation studies and lipid raft analysis have identified proteins and pathways that may be involved in the development of resistance, for example UBE2N. It is also apparent from proteomic analysis that a number of proteins that were identified are not reported to be localised to lipid rafts and that published results in the literature using different techniques have shown discordance in proteins identified within lipid rafts (369). The protein composition of lipid rafts remains contentious and contaminants are often co-purified. Therefore these results require validation using techniques such as immunoblot and RT-PCR. Investigation of paired biopsy samples from patients progressing on tirabrutinib would provide further validation, however to undertake lipid raft analysis large numbers of cells would be required, which may limit the feasibility of this approach.

Overall, results from immunophenotyping, RNA profiling, changes in protein expression identified on immunoblot and in lipid raft analysis all suggest hyperactivation of the BCR signalling pathway occurring at the cell surface. Further studies will focus therefore upstream of BTK in the development of resistance to BTKi. Initially I will undertake NGS of the BCR, total internal reflection fluorescence (TIRF) microscopy to assess the spatial organisation of the BCR, assess IgM internalisation by flow cytometry and undertake studies of co-immunoprecipitation of IgM.

Together these additional studies may elude not only to the unravelling of the mechanisms of resistance but also identify rationale therapeutic targets for the treatment of BTKi resistance or for the design of rational combination studies.

Appendix A.1

National Cancer Institute Common Toxicity Criteria for Adverse Events (CTCAE) Version 4.0

In the Phase I clinical trial of tirabrutinib, toxicities were graded according to the National Cancer Institute Common Terminology Criteria for Adverse Events (CTCAE), version 4.0. In CTCAE, an adverse event is defined as an abnormal clinical finding, associated with the use of a cancer therapy. These criteria form the basis for the management of drug administration and dosing in clinical trials to allow standardisation of reporting and consistency in the definition of a treatment related toxicity. Version 4.0 was published in 2009. The scale of grading used is Grade 1 to Grade 5 and for each grade, specific conditions and symptoms may be described. Broadly speaking patients will be hospitalised for a toxicity Grade ≥ 3 . The general principle for the severity of each grade is:

Grade 1 Mild; asymptomatic or mild symptoms; clinical or diagnostic observation only; intervention not indicated.

Grade 2 Moderate; minimal, local or non-invasive intervention indicated; limiting age-appropriate instrumental Activities of Daily Living (ADL).

Grade 3 Severe or medically significant but not immediately life threatening; hospitalisation or prolongation of hospitalisation indicated; disabling; limiting self-care ADL.

Grade 4 Life-threatening consequences; urgent intervention indicated.

Grade 5 Death related to AE.

The full CTCAE document is available on the NCI web site, at https://ctep.cancer.gov/protocolDevelopment/electronic_applications/ctc.htm.

Dose Limiting Toxicities (DLTs)

DLTs occurring during the first 28 days of treatment, with the exception of lymphocytosis, that cannot be clearly attributed to an alternative cause, other than tirabrutinib were defined as (NCI-CTCAE Version 4.0):

- All CTC Grade 4 tirabrutinib related adverse events
- All CTC Grade 3 tirabrutinib related adverse events, with the exception of the following:
 - CTC Grade 3 lymphocytosis which is considered an expected outcome of therapy.

Any toxicity which in the opinion of the Investigator is attributed to a patient's underlying disease, was not considered a DLT.

Appendix A.2

Criteria for response

Standardised response criteria are essential for the conduct of clinical research, enabling comparison of results across patient groups within a study and a framework for the assessment for evaluating new therapies.

Response Criteria for Non Hodgkin Lymphomas

Consensus guidelines were published in 1999 for the response assessment in adult patients with indolent and aggressive NHL (379). These criteria, shown below were used within the Phase I trial of tirabrutinib.

Response criteria for NHL used within the Phase I trial of tirabrutinib in NHL.

Response Category	Physical Examination	Lymph Nodes	Lymph Node Masses	Bone Marrow
Complete Response	Normal	Normal	Normal	Normal
Complete Response Unconfirmed	Normal	Normal	Normal	Indeterminate
	Normal	Normal	> 75% decrease	Normal or indeterminate
Partial Response	Normal	Normal	Normal	Positive
	Normal Decrease in liver/spleen	$\geq 50\%$ decrease $\geq 50\%$ decrease	$\geq 50\%$ decrease $\geq 50\%$ decrease	Irrelevant Irrelevant
Relapse/ progression	Enlarging liver/spleen; new sites	New or increased	New or increased	Reappearance

Response Criteria for patients with CLL

The international Workshop on CLL (IWCLL) guidelines for the definition of response following treatment in patients with CLL, shown below, were used within the Phase I trial of tirabrutinib (247).

Response definition after treatment for patients with CLL used within the Phase I trial of tirabrutinib in CLL.

	Complete Response	Partial Response	Progressive Disease
Group A			
Lymphadenopathy	None > 1.5 cm	Decrease \geq 50%	Increase \geq 50%
Hepatomegaly	None	Decrease \geq 50%	Increase \geq 50%
Splenomegaly	None	Decrease \geq 50%	Increase \geq 50%
Blood Lymphocytes	< 4000/ μ L	Decrease \geq 50% from baseline	Increase \geq 50% over baseline
Marrow	Normocellular, < 30% lymphocytes, no B-lymphoid nodules. Hypocellular marrow defines complete response with incomplete bone marrow recovery.	50% reduction in marrow infiltrate, or B-lymphoid nodules	-
Group B			
Platelet Count	> 100 000/ μ L	> 100 000/ μ L or increase \geq 50% over baseline	Decrease of \geq 50% from baseline secondary to CLL
Haemoglobin	> 11.0 g/dL	> 11 g/dL or increase \geq 50% over baseline	Decrease of > 2 g/dL from baseline secondary to CLL
Neutrophils	> 1500/ μ L	> 1500/ μ L or > 50% improvement over baseline	-

Appendix A.3

Walter HS, Rule SA, Dyer MJ et al. A phase 1 clinical trial of the selective BTK inhibitor ONO/GS-4059 in relapsed and refractory mature B-cell malignancies. *Blood*. 2016; 127(4): 411-9 (165).

Appendix A.4

Walter HS, Salles GA, Dyer MJ. New agents to treat chronic lymphocytic leukemia. *N Engl J Med.* 2016; 374(22): 2185-2186 (204).

Appendix A.5

Walter HS, Jayne S, Rule SA, Cartron G, Morschhauser F, Macip S, et al. Long-term follow-up of patients with CLL treated with the selective Bruton's tyrosine kinase inhibitor ONO/GS-4059. *Blood*. 2017 May 18;129(20):2808-10 (205).

Appendix A.6

Publications

Publications resulting from work during my thesis are listed below:

Journal Publications

Vogler M, Walter HS, Dyer MJS. Targeting anti-apoptotic BCL2 family proteins in haematological malignancies - from pathogenesis to treatment. *Br J Haematol.* 2017 Apr 27. doi: 10.1111/bjh.14684.

Walter HS, Jayne S, Rule SA et al. Long-term follow-up of patients with CLL treated with the selective Bruton's tyrosine kinase inhibitor ONO/GS-4059. *Blood.* 2017; 129(20):2808-2810

Walter HS, Jayne S, Mensah P et al. Obinutuzumab-induced coagulopathy in chronic lymphocytic leukemia (CLL) with trisomy 12. *Blood Cancer Journal* (2016) 6, e435; doi:10.1038/bcj.2016.42.

Walter HS, Salles GA, Dyer MJ. New agents to treat chronic lymphocytic leukemia. *N Engl J Med.* 2016; 374(22): 2185-2186.

Walter HS, Rule SA, Dyer MJ et al. A phase 1 clinical trial of the selective BTK inhibitor ONO/GS-4059 in relapsed and refractory mature B-cell malignancies. *Blood.* 2016; 127(4): 411-9.

Walter HS, Webster A, Kennedy B., et al. Transformation of follicular lymphoma (FL) to diffuse large B-cell lymphoma (DLBCL) within the bone marrow detected by 18FDG-PET/CT. <http://www.bloodjournal.org/content/125/7/1078.e-letters> .

Selected peer reviewed abstracts

Tsukamoto K, Walter HS, Jayne S, Dyer MJ. Activation of SYK tyrosine kinase plays a role in resistance against the selective BTK inhibitor ONO/GS-4059 in diffuse large B cell lymphoma (DLBCL). *Haematologica*. 2017 JUN 26;102(2):563-564.

Walter HS, Sandrine J, Rule SA et al. Long-Term Follow-up with GS-4059, a Selective Irreversible BTK Inhibitor, in Patients with Relapsed and Refractory Chronic Lymphocytic Leukemia. *Blood*. 2017 DEC 2;128(22):3233.

Walter HS, Visser J, Barnes C et al. Refractory atypical Rosai-Dorfman disease (RDD) successfully treated according to a Langerhans cell histiocytosis regimen. *Br J Haematol*. 2015 APR 20;169(S1):38-38.

Walter HS, Ladani S, Miall F et al. Outcome of transplantation in mantle cell lymphoma at University Hospitals Leicester - a single centre experience. *Br J Haematol*. 2015 APR 20;169(S1):57-58.

Walter HS, Hutchinson CV, Sharpe J et al. Single centre experience of a Bruton's tyrosine kinase (BTK) specific inhibitor (ONO-4059) in relapsed mantle cell lymphoma (MCL). *Br J Haematol*. 2015 APR 20;169(S1):58-59.

Fegan C, Bagshawe J, Salles G et al. The Bruton's Tyrosine Kinase (BTK) Inhibitor ONO-4059: Promising Single Agent Activity and Well Tolerated in Patients with High Risk Chronic Lymphocytic Leukaemia (CLL). *BLOOD*. 2014 DEC 6;124(21).

References

1. Haematological Malignancy Research Network: Haematological Malignancy Research. Incidence statistics. Available from: <https://www.hmrn.org/statistics/incidence> (Accessed 02.12.2017).
2. Swerdlow SH, Campo E, Pileri SA, Harris NL, Stein H, Siebert R, et al. The 2016 revision of the World Health Organization classification of lymphoid neoplasms. *Blood*. 2016 May 19;127(20):2375-90.
3. Cancer Research UK. Non-hodgkin-lymphoma Incidence Statistics. Available from: <http://www.cancerresearchuk.org/about-cancer/non-hodgkin-lymphoma/types/high-grade> (Accessed 02.12.2017).
4. Coiffier B, Lepage E, Briere J, Herbrecht R, Tilly H, Bouabdallah R, et al. CHOP chemotherapy plus rituximab compared with CHOP alone in elderly patients with diffuse large-B-cell lymphoma. *N Engl J Med*. 2002 Jan 24;346(4):235-42.
5. Habermann TM, Weller EA, Morrison VA, Gascoyne RD, Cassileth PA, Cohn JB, et al. Rituximab-CHOP versus CHOP alone or with maintenance rituximab in older patients with diffuse large B-cell lymphoma. *J Clin Oncol*. 2006 Jul 1;24(19):3121-7.
6. Pfreundschuh M, Trumper L, Osterborg A, Pettengell R, Trneny M, Imrie K, et al. CHOP-like chemotherapy plus rituximab versus CHOP-like chemotherapy alone in young patients with good-prognosis diffuse large-B-cell lymphoma: a randomised controlled trial by the MabThera International Trial (MInT) Group. *Lancet Oncol*. 2006 May;7(5):379-91.
7. Kuppers R. Mechanisms of B-cell lymphoma pathogenesis. *Nat Rev Cancer*. 2005 Apr;5(4):251-62.
8. Rajewsky K. Clonal selection and learning in the antibody system. *Nature*. 1996 Jun 27;381(6585):751-8.
9. Kuppers R, Zhao M, Hansmann ML, Rajewsky K. Tracing B cell development in human germinal centres by molecular analysis of single cells picked from histological sections. *EMBO J*. 1993 Dec 15;12(13):4955-67.
10. Liu YJ, Arpin C, de Bouteiller O, Guret C, Banchereau J, Martinez-Valdez H, et al. Sequential triggering of apoptosis, somatic mutation and isotype switch during germinal center development. *Semin Immunol*. 1996 Jun;8(3):169-77.
11. Kuppers R, Klein U, Hansmann ML, Rajewsky K. Cellular origin of human B-cell lymphomas. *N Engl J Med*. 1999 Nov 11;341(20):1520-9.

12. Stevenson FK, Sahota SS, Ottensmeier CH, Zhu D, Forconi F, Hamblin TJ. The occurrence and significance of V gene mutations in B cell-derived human malignancy. *Adv Cancer Res.* 2001;83:81-116.
13. Alizadeh AA, Eisen MB, Davis RE, Ma C, Lossos IS, Rosenwald A, et al. Distinct types of diffuse large B-cell lymphoma identified by gene expression profiling. *Nature.* 2000 Feb 3;403(6769):503-11.
14. Cancer Research UK. Non-hodgkin-lymphoma Incidence Statistics. Available from: <http://www.cancerresearchuk.org/health-professional/cancer-statistics/statistics-by-cancer-type/non-hodgkin-lymphoma> (Accessed 02.12.2017).
15. Berton F, Rinaldi A, Zucca E, Cavalli F. Update on the molecular biology of mantle cell lymphoma. *Hematol Oncol.* 2006 Mar;24(1):22-7.
16. Tiemann M, Schrader C, Klapper W, Dreyling MH, Campo E, Norton A, et al. Histopathology, cell proliferation indices and clinical outcome in 304 patients with mantle cell lymphoma (MCL): a clinicopathological study from the European MCL Network. *Br J Haematol.* 2005 Oct;131(1):29-38.
17. Chronic lymphocytic leukaemia (CLL) incidence statistics. [Internet]. [].
18. Wang SS, Slager SL, Brennan P, Holly EA, De Sanjose S, Bernstein L, et al. Family history of hematopoietic malignancies and risk of non-Hodgkin lymphoma (NHL): a pooled analysis of 10 211 cases and 11 905 controls from the International Lymphoma Epidemiology Consortium (InterLymph). *Blood.* 2007 Apr 15;109(8):3479-88.
19. Yuille MR, Matutes E, Marossy A, Hilditch B, Catovsky D, Houlston RS. Familial chronic lymphocytic leukaemia: a survey and review of published studies. *Br J Haematol.* 2000 Jun;109(4):794-9.
20. Law PJ, Berndt SI, Speedy HE, Camp NJ, Sava GP, Skibola CF, et al. Genome-wide association analysis implicates dysregulation of immunity genes in chronic lymphocytic leukaemia. *Nat Commun.* 2017 Feb 6;8:14175.
21. Vijai J, Wang Z, Berndt SI, Skibola CF, Slager SL, de Sanjose S, et al. A genome-wide association study of marginal zone lymphoma shows association to the HLA region. *Nat Commun.* 2015 Jan 8;6:5751.
22. Cerhan JR, Berndt SI, Vijai J, Ghesquieres H, McKay J, Wang SS, et al. Genome-wide association study identifies multiple susceptibility loci for diffuse large B cell lymphoma. *Nat Genet.* 2014 Nov;46(11):1233-8.
23. Mukerji J, Olivieri KC, Misra V, Agopian KA, Gabuzda D. Proteomic analysis of HIV-1 Nef cellular binding partners reveals a role for exocyst complex proteins in

- mediating enhancement of intercellular nanotube formation. *Retrovirology*. 2012 Jun 22;9:33.
24. Grulich AE, Vajdic CM. The epidemiology of cancers in human immunodeficiency virus infection and after organ transplantation. *Semin Oncol*. 2015 Apr;42(2):247-57.
25. van Leeuwen MT, Vajdic CM, Middleton MG, McDonald AM, Law M, Kaldor JM, Grulich AE. Continuing declines in some but not all HIV-associated cancers in Australia after widespread use of antiretroviral therapy. *AIDS* [- 16]. 2009 Oct 23;23(16):2183-90.
26. Opelz G, Dohler B. Lymphomas after solid organ transplantation: a collaborative transplant study report. *Am J Transplant*. 2004 Feb;4(2):222-30.
27. Hussain SK, Makgoeng SB, Everly MJ, Goodman MT, Martinez-Maza O, Morton LM, et al. HLA and Risk of Diffuse Large B cell Lymphoma After Solid Organ Transplantation. *Transplantation*. 2016 Nov;100(11):2453-60.
28. Dreyling M, Thieblemont C, Gallamini A, Arcaini L, Campo E, Hermine O, et al. ESMO Consensus conferences: guidelines on malignant lymphoma. part 2: marginal zone lymphoma, mantle cell lymphoma, peripheral T-cell lymphoma. *Ann Oncol*. 2013 Apr;24(4):857-77.
29. Ferreri AJ, Govi S, Pasini E, Mappa S, Bertoni F, Zaja F, et al. Chlamydia psittaci eradication with doxycycline as first-line targeted therapy for ocular adnexae lymphoma: final results of an international phase II trial. *J Clin Oncol*. 2012 Aug 20;30(24):2988-94.
30. Zignego AL, Ramos-Casals M, Ferri C, Saadoun D, Arcaini L, Roccatello D, et al. International therapeutic guidelines for patients with HCV-related extrahepatic disorders. A multidisciplinary expert statement. *Autoimmun Rev*. 2017 May;16(5):523-41.
31. Grywalska E, Rolinski J. Epstein-Barr virus-associated lymphomas. *Semin Oncol*. 2015 Apr;42(2):291-303.
32. Baecklund E, Iliadou A, Askling J, Ekbom A, Backlin C, Granath F, et al. Association of chronic inflammation, not its treatment, with increased lymphoma risk in rheumatoid arthritis. *Arthritis Rheum*. 2006 Mar;54(3):692-701.
33. van den Heuvel, T R, Wintjens DS, Jeuring SF, Wassink MH, Romberg-Camps MJ, Oostenbrug LE, et al. Inflammatory bowel disease, cancer and medication: Cancer risk in the Dutch population-based IBDSL cohort. *Int J Cancer*. 2016 Sep 15;139(6):1270-80.

34. Engelhard M, Brittinger G, Huhn D, Gerhartz HH, Meusers P, Siegert W, et al. Subclassification of diffuse large B-cell lymphomas according to the Kiel classification: distinction of centroblastic and immunoblastic lymphomas is a significant prognostic risk factor. *Blood*. 1997 Apr 1;89(7):2291-7.
35. Boyd SD, Natkunam Y, Allen JR, Warnke RA. Selective immunophenotyping for diagnosis of B-cell neoplasms: immunohistochemistry and flow cytometry strategies and results. *Appl Immunohistochem Mol Morphol*. 2013 Mar;21(2):116-31.
36. Iqbal J, Neppalli VT, Wright G, Dave BJ, Horsman DE, Rosenwald A, et al. BCL2 expression is a prognostic marker for the activated B-cell-like type of diffuse large B-cell lymphoma. *J Clin Oncol*. 2006 Feb 20;24(6):961-8.
37. Johnson NA, Boyle M, Bashashati A, Leach S, Brooks-Wilson A, Sehn LH, et al. Diffuse large B-cell lymphoma: reduced CD20 expression is associated with an inferior survival. *Blood*. 2009 Apr 16;113(16):3773-80.
38. Campo E, Swerdlow SH, Harris NL, Pileri S, Stein H, Jaffe ES. The 2008 WHO classification of lymphoid neoplasms and beyond: evolving concepts and practical applications. *Blood*. 2011 May 12;117(19):5019-32.
39. Macintyre E, Willerford D, Morris SW. Non-Hodgkin's Lymphoma: Molecular Features of B Cell Lymphoma. *Hematology Am Soc Hematol Educ Program*. 2000:180-204.
40. Dyer MJ, Oscier DG. The configuration of the immunoglobulin genes in B cell chronic lymphocytic leukemia. *Leukemia*. 2002 Jun;16(6):973-84.
41. Forbes SA, Tang G, Bindal N, Bamford S, Dawson E, Cole C, et al. COSMIC (the Catalogue of Somatic Mutations in Cancer): a resource to investigate acquired mutations in human cancer. *Nucleic Acids Res*. 2010 Jan;38(Database issue):652.
42. Zhang Y, Garcia-Ibanez L, Toellner KM. Regulation of germinal center B-cell differentiation. *Immunol Rev*. 2016 Mar;270(1):8-19.
43. Li S, Young KH, Medeiros LJ. Diffuse large B-cell lymphoma. *Pathology*. 2018 Jan;50(1):74-87.
44. Wright G, Tan B, Rosenwald A, Hurt EH, Wiestner A, Staudt LM. A gene expression-based method to diagnose clinically distinct subgroups of diffuse large B cell lymphoma. *Proc Natl Acad Sci U S A*. 2003 Aug 19;100(17):9991-6.
45. Pasqualucci L, Compagno M, Houldsworth J, Monti S, Grunn A, Nandula SV, et al. Inactivation of the PRDM1/BLIMP1 gene in diffuse large B cell lymphoma. *J Exp Med*. 2006 Feb 20;203(2):311-7.

46. Shaffer AL, Lin KI, Kuo TC, Yu X, Hurt EM, Rosenwald A, et al. Blimp-1 orchestrates plasma cell differentiation by extinguishing the mature B cell gene expression program. *Immunity*. 2002 Jul;17(1):51-62.
47. Dubois S, Viailly PJ, Mareschal S, Bohers E, Bertrand P, Ruminy P, et al. Next-Generation Sequencing in Diffuse Large B-Cell Lymphoma Highlights Molecular Divergence and Therapeutic Opportunities: a LYSA Study. *Clin Cancer Res*. 2016 Jun 15;22(12):2919-28.
48. de Jong D, Rosenwald A, Chhanabhai M, Gaulard P, Klapper W, Lee A, et al. Immunohistochemical prognostic markers in diffuse large B-cell lymphoma: validation of tissue microarray as a prerequisite for broad clinical applications--a study from the Lunenburg Lymphoma Biomarker Consortium. *J Clin Oncol*. 2007 Mar 1;25(7):805-12.
49. Hans CP, Weisenburger DD, Greiner TC, Gascoyne RD, Delabie J, Ott G, et al. Confirmation of the molecular classification of diffuse large B-cell lymphoma by immunohistochemistry using a tissue microarray. *Blood*. 2004 Jan 1;103(1):275-82.
50. Visco C, Li Y, Xu-Monette ZY, Miranda RN, Green TM, Li Y, et al. Comprehensive gene expression profiling and immunohistochemical studies support application of immunophenotypic algorithm for molecular subtype classification in diffuse large B-cell lymphoma: a report from the International DLBCL Rituximab-CHOP Consortium Program Study. *Leukemia*. 2012 Sep;26(9):2103-13.
51. Niuro H, Clark EA. Regulation of B-cell fate by antigen-receptor signals. *Nat Rev Immunol*. 2002 Dec;2(12):945-56.
52. Davis RE, Brown KD, Siebenlist U, Staudt LM. Constitutive nuclear factor kappaB activity is required for survival of activated B cell-like diffuse large B cell lymphoma cells. *J Exp Med*. 2001 Dec 17;194(12):1861-74.
53. Thome M, Charton JE, Pelzer C, Hailfinger S. Antigen receptor signaling to NF-kappaB via CARMA1, BCL10, and MALT1. *Cold Spring Harb Perspect Biol*. 2010 Sep;2(9):a003004.
54. Rawlings DJ, Sommer K, Moreno-Garcia ME. The CARMA1 signalosome links the signalling machinery of adaptive and innate immunity in lymphocytes. *Nat Rev Immunol*. 2006 Nov;6(11):799-812.
55. Ngo VN, Young RM, Schmitz R, Jhavar S, Xiao W, Lim KH, et al. Oncogenically active MYD88 mutations in human lymphoma. *Nature*. 2011 Feb 3;470(7332):115-9.
56. Lam LT, Davis RE, Ngo VN, Lenz G, Wright G, Xu W, et al. Compensatory IKKalpha activation of classical NF-kappaB signaling during IKKbeta inhibition

identified by an RNA interference sensitization screen. *Proc Natl Acad Sci U S A*. 2008 Dec 30;105(52):20798-803.

57. Kato M, Sanada M, Kato I, Sato Y, Takita J, Takeuchi K, et al. Frequent inactivation of A20 in B-cell lymphomas. *Nature*. 2009 Jun 4;459(7247):712-6.

58. Pfeifer M, Grau M, Lenze D, Wenzel SS, Wolf A, Wollert-Wulf B, et al. PTEN loss defines a PI3K/AKT pathway-dependent germinal center subtype of diffuse large B-cell lymphoma. *Proc Natl Acad Sci U S A*. 2013 Jul 23;110(30):12420-5.

59. Basso K, Saito M, Sumazin P, Margolin AA, Wang K, Lim WK, et al. Integrated biochemical and computational approach identifies BCL6 direct target genes controlling multiple pathways in normal germinal center B cells. *Blood*. 2010 Feb 4;115(5):975-84.

60. Huang C, Geng H, Boss I, Wang L, Melnick A. Cooperative transcriptional repression by BCL6 and BACH2 in germinal center B-cell differentiation. *Blood*. 2014 Feb 13;123(7):1012-20.

61. Beguelin W, Popovic R, Teater M, Jiang Y, Bunting KL, Rosen M, et al. EZH2 is required for germinal center formation and somatic EZH2 mutations promote lymphoid transformation. *Cancer Cell*. 2013 May 13;23(5):677-92.

62. Gascoyne RD, Adomat SA, Krajewski S, Krajewska M, Horsman DE, Tolcher AW, et al. Prognostic significance of Bcl-2 protein expression and Bcl-2 gene rearrangement in diffuse aggressive non-Hodgkin's lymphoma. *Blood*. 1997 Jul 1;90(1):244-51.

63. Iqbal J, Meyer PN, Smith LM, Johnson NA, Vose JM, Greiner TC, et al. BCL2 predicts survival in germinal center B-cell-like diffuse large B-cell lymphoma treated with CHOP-like therapy and rituximab. *Clin Cancer Res*. 2011 Dec 15;17(24):7785-95.

64. Green TM, Young KH, Visco C, Xu-Monette ZY, Orazi A, Go RS, et al. Immunohistochemical double-hit score is a strong predictor of outcome in patients with diffuse large B-cell lymphoma treated with rituximab plus cyclophosphamide, doxorubicin, vincristine, and prednisone. *J Clin Oncol*. 2012 Oct 1;30(28):3460-7.

65. Sesques P, Johnson NA. Approach to the diagnosis and treatment of high-grade B-cell lymphomas with MYC and BCL2 and/or BCL6 rearrangements. *Blood*. 2017 Jan 19;129(3):280-8.

66. Hanahan D, Weinberg RA. The hallmarks of cancer. *Cell*. 2000 Jan 7;100(1):57-70.

67. Schmitt CA, Lowe SW. Bcl-2 mediates chemoresistance in matched pairs of primary E(mu)-myc lymphomas in vivo. *Blood Cells Mol Dis*. 2001;27(1):206-16.

68. Cai Q, Medeiros LJ, Xu X, Young KH. MYC-driven aggressive B-cell lymphomas: biology, entity, differential diagnosis and clinical management. *Oncotarget*. 2015 Nov 17;6(36):38591-616.
69. Gaynor ER, Unger JM, Miller TP, Grogan TM, White LA, Jr, Mills GM, et al. Infusional CHOP chemotherapy (CVAD) with or without chemosensitizers offers no advantage over standard CHOP therapy in the treatment of lymphoma: a Southwest Oncology Group Study. *J Clin Oncol*. 2001 Feb 1;19(3):750-5.
70. Meyer RM, Quirt IC, Skillings JR, Cripps MC, Bramwell VH, Weinerman BH, et al. Escalated as compared with standard doses of doxorubicin in BACOP therapy for patients with non-Hodgkin's lymphoma. *N Engl J Med*. 1993 Dec 9;329(24):1770-6.
71. Sertoli MR, Santini G, Chisesi T, Congiu AM, Rubagotti A, Contu A, et al. MACOP-B versus ProMACE-MOPP in the treatment of advanced diffuse non-Hodgkin's lymphoma: results of a prospective randomized trial by the non-Hodgkin's Lymphoma Cooperative Study Group. *J Clin Oncol*. 1994 Jul;12(7):1366-74.
72. Fisher RI, Gaynor ER, Dahlborg S, Oken MM, Grogan TM, Mize EM, et al. Comparison of a standard regimen (CHOP) with three intensive chemotherapy regimens for advanced non-Hodgkin's lymphoma. *N Engl J Med*. 1993 Apr 8;328(14):1002-6.
73. Vose JM, Link BK, Grossbard ML, Czuczman M, Grillo-Lopez A, Gilman P, et al. Phase II study of rituximab in combination with chop chemotherapy in patients with previously untreated, aggressive non-Hodgkin's lymphoma. *J Clin Oncol*. 2001 Jan 15;19(2):389-97.
74. Sehn LH, Gascoyne RD. Diffuse large B-cell lymphoma: optimizing outcome in the context of clinical and biologic heterogeneity. *Blood*. 2015 Jan 1;125(1):22-32.
75. Zhou Z, Sehn LH, Rademaker AW, Gordon LI, Lacasce AS, Crosby-Thompson A, et al. An enhanced International Prognostic Index (NCCN-IPI) for patients with diffuse large B-cell lymphoma treated in the rituximab era. *Blood*. 2014 Feb 6;123(6):837-42.
76. Lenz G, Nagel I, Siebert R, Roschke AV, Sanger W, Wright GW, et al. Aberrant immunoglobulin class switch recombination and switch translocations in activated B cell-like diffuse large B cell lymphoma. *J Exp Med*. 2007 Mar 19;204(3):633-43.
77. Muramatsu M, Sankaranand VS, Anant S, Sugai M, Kinoshita K, Davidson NO, et al. Specific expression of activation-induced cytidine deaminase (AID), a novel member of the RNA-editing deaminase family in germinal center B cells. *J Biol Chem*. 1999 Jun 25;274(26):18470-6.
78. Reth M. Antigen receptor tail clue. *Nature*. 1989 Mar 30;338(6214):383-4.

79. Tolar P, Sohn HW, Pierce SK. The initiation of antigen-induced B cell antigen receptor signaling viewed in living cells by fluorescence resonance energy transfer. *Nat Immunol.* 2005 Nov;6(11):1168-76.
80. Schamel WW, Reth M. Monomeric and oligomeric complexes of the B cell antigen receptor. *Immunity.* 2000 Jul;13(1):5-14.
81. Yang J, Reth M. The dissociation activation model of B cell antigen receptor triggering. *FEBS Lett.* 2010 Dec 15;584(24):4872-7.
82. Cheng PC, Dykstra ML, Mitchell RN, Pierce SK. A role for lipid rafts in B cell antigen receptor signaling and antigen targeting. *J Exp Med.* 1999 Dec 6;190(11):1549-60.
83. Goitsuka R, Fujimura Y, Mamada H, Umeda A, Morimura T, Uetsuka K, et al. BASH, a novel signaling molecule preferentially expressed in B cells of the bursa of Fabricius. *J Immunol.* 1998 Dec 1;161(11):5804-8.
84. Kim YJ, Sekiya F, Poulin B, Bae YS, Rhee SG. Mechanism of B-cell receptor-induced phosphorylation and activation of phospholipase C-gamma2. *Mol Cell Biol.* 2004 Nov;24(22):9986-99.
85. Young RM, Staudt LM. Targeting pathological B cell receptor signalling in lymphoid malignancies. *Nat Rev Drug Discov.* 2013 Mar;12(3):229-43.
86. Lam KP, Kuhn R, Rajewsky K. In vivo ablation of surface immunoglobulin on mature B cells by inducible gene targeting results in rapid cell death. *Cell.* 1997 Sep 19;90(6):1073-83.
87. Kraus M, Alimzhanov MB, Rajewsky N, Rajewsky K. Survival of resting mature B lymphocytes depends on BCR signaling via the Igalphabeta heterodimer. *Cell.* 2004 Jun 11;117(6):787-800.
88. Srinivasan L, Sasaki Y, Calado DP, Zhang B, Paik JH, DePinho RA, et al. PI3 kinase signals BCR-dependent mature B cell survival. *Cell.* 2009 Oct 30;139(3):573-86.
89. Rickert RC. New insights into pre-BCR and BCR signalling with relevance to B cell malignancies. *Nat Rev Immunol.* 2013 Aug;13(8):578-91.
90. Davis RE, Ngo VN, Lenz G, Tolar P, Young RM, Romesser PB, et al. Chronic active B-cell-receptor signalling in diffuse large B-cell lymphoma. *Nature.* 2010 Jan 7;463(7277):88-92.
91. Compagno M, Lim WK, Grunn A, Nandula SV, Brahmachary M, Shen Q, et al. Mutations of multiple genes cause deregulation of NF-kappaB in diffuse large B-cell lymphoma. *Nature.* 2009 Jun 4;459(7247):717-21.

92. Duhren-von Minden M, Ubelhart R, Schneider D, Wossning T, Bach MP, Buchner M, et al. Chronic lymphocytic leukaemia is driven by antigen-independent cell-autonomous signalling. *Nature*. 2012 Sep 13;489(7415):309-12.
93. Sebastian E, Alcoceba M, Balanzategui A, Marin L, Montes-Moreno S, Flores T, et al. Molecular characterization of immunoglobulin gene rearrangements in diffuse large B-cell lymphoma: antigen-driven origin and IGHV4-34 as a particular subgroup of the non-GCB subtype. *Am J Pathol*. 2012 Nov;181(5):1879-88.
94. Pike LJ. Rafts defined: a report on the Keystone Symposium on Lipid Rafts and Cell Function. *J Lipid Res*. 2006 Jul;47(7):1597-8.
95. Patra SK. Dissecting lipid raft facilitated cell signaling pathways in cancer. *Biochim Biophys Acta*. 2008 Apr;1785(2):182-206.
96. Petrie RJ, Schnetkamp PP, Patel KD, Awasthi-Kalia M, Deans JP. Transient translocation of the B cell receptor and Src homology 2 domain-containing inositol phosphatase to lipid rafts: evidence toward a role in calcium regulation. *J Immunol*. 2000 Aug 1;165(3):1220-7.
97. Gupta N, Wollscheid B, Watts JD, Scheer B, Aebersold R, DeFranco AL. Quantitative proteomic analysis of B cell lipid rafts reveals that ezrin regulates antigen receptor-mediated lipid raft dynamics. *Nat Immunol*. 2006 Jun;7(6):625-33.
98. DeFranco AL. The complexity of signaling pathways activated by the BCR. *Curr Opin Immunol*. 1997 Jun;9(3):296-308.
99. Guo B, Kato RM, Garcia-Lloret M, Wahl MI, Rawlings DJ. Engagement of the human pre-B cell receptor generates a lipid raft-dependent calcium signaling complex. *Immunity*. 2000 Aug;13(2):243-53.
100. Pierce SK. Lipid rafts and B-cell activation. *Nat Rev Immunol*. 2002 Feb;2(2):96-105.
101. Patra SK, Bettuzzi S. Epigenetic DNA-methylation regulation of genes coding for lipid raft-associated components: a role for raft proteins in cell transformation and cancer progression (review). *Oncol Rep*. 2007 Jun;17(6):1279-90.
102. Simons K, Toomre D. Lipid rafts and signal transduction. *Nat Rev Mol Cell Biol*. 2000 Oct;1(1):31-9.
103. Oh HY, Lee EJ, Yoon S, Chung BH, Cho KS, Hong SJ. Cholesterol level of lipid raft microdomains regulates apoptotic cell death in prostate cancer cells through EGFR-mediated Akt and ERK signal transduction. *Prostate*. 2007 Jul 1;67(10):1061-9.

104. Raghu H, Sodadasu PK, Malla RR, Gondi CS, Estes N, Rao JS. Localization of uPAR and MMP-9 in lipid rafts is critical for migration, invasion and angiogenesis in human breast cancer cells. *BMC Cancer*. 2010 Nov 24;10:647.
105. Boyd RS, Jukes-Jones R, Walewska R, Brown D, Dyer MJ, Cain K. Protein profiling of plasma membranes defines aberrant signaling pathways in mantle cell lymphoma. *Mol Cell Proteomics*. 2009 Jul;8(7):1501-15.
106. Bolen JB. Protein tyrosine kinases in the initiation of antigen receptor signaling. *Curr Opin Immunol*. 1995 Jun;7(3):306-11.
107. de Weers M, Verschuren MC, Kraakman ME, Mensink RG, Schuurman RK, van Dongen JJ, et al. The Bruton's tyrosine kinase gene is expressed throughout B cell differentiation, from early precursor B cell stages preceding immunoglobulin gene rearrangement up to mature B cell stages. *Eur J Immunol*. 1993 Dec;23(12):3109-14.
108. Mano H. Tec family of protein-tyrosine kinases: an overview of their structure and function. *Cytokine Growth Factor Rev*. 1999;10(3-4):267-80.
109. Brown MT, Cooper JA. Regulation, substrates and functions of src. *Biochim Biophys Acta*. 1996 Jun 7;1287(2-3):121-49.
110. Bradshaw JM. The Src, Syk, and Tec family kinases: distinct types of molecular switches. *Cell Signal*. 2010 Aug;22(8):1175-84.
111. Harlan JE, Hajduk PJ, Yoon HS, Fesik SW. Pleckstrin homology domains bind to phosphatidylinositol-4,5-bisphosphate. *Nature*. 1994 Sep 8;371(6493):168-70.
112. Smith CI, Baskin B, Humire-Greiff P, Zhou JN, Olsson PG, Maniar HS, et al. Expression of Bruton's agammaglobulinemia tyrosine kinase gene, BTK, is selectively down-regulated in T lymphocytes and plasma cells. *J Immunol*. 1994 Jan 15;152(2):557-65.
113. Hendriks RW, Yuvaraj S, Kil LP. Targeting Bruton's tyrosine kinase in B cell malignancies. *Nat Rev Cancer*. 2014 Apr;14(4):219-32.
114. August A, Sadra A, Dupont B, Hanafusa H. Src-induced activation of inducible T cell kinase (ITK) requires phosphatidylinositol 3-kinase activity and the Pleckstrin homology domain of inducible T cell kinase. *Proc Natl Acad Sci U S A*. 1997 Oct 14;94(21):11227-32.
115. Salim K, Bottomley MJ, Querfurth E, Zvelebil MJ, Gout I, Scaife R, et al. Distinct specificity in the recognition of phosphoinositides by the pleckstrin homology domains of dynamin and Bruton's tyrosine kinase. *EMBO J*. 1996 Nov 15;15(22):6241-50.

116. Jiang Y, Ma W, Wan Y, Kozasa T, Hattori S, Huang XY. The G protein G alpha12 stimulates Bruton's tyrosine kinase and a rasGAP through a conserved PH/BM domain. *Nature*. 1998 Oct 22;395(6704):808-13.
117. Tsukada S, Simon MI, Witte ON, Katz A. Binding of beta gamma subunits of heterotrimeric G proteins to the PH domain of Bruton tyrosine kinase. *Proc Natl Acad Sci U S A*. 1994 Nov 8;91(23):11256-60.
118. Yao L, Suzuki H, Ozawa K, Deng J, Lehel C, Fukamachi H, et al. Interactions between protein kinase C and pleckstrin homology domains. Inhibition by phosphatidylinositol 4,5-bisphosphate and phorbol 12-myristate 13-acetate. *J Biol Chem*. 1997 May 16;272(20):13033-9.
119. Novina CD, Kumar S, Bajpai U, Cheriya V, Zhang K, Pillai S, et al. Regulation of nuclear localization and transcriptional activity of TFII-I by Bruton's tyrosine kinase. *Mol Cell Biol*. 1999 Jul;19(7):5014-24.
120. Yao L, Janmey P, Frigeri LG, Han W, Fujita J, Kawakami Y, et al. Pleckstrin homology domains interact with filamentous actin. *J Biol Chem*. 1999 Jul 9;274(28):19752-61.
121. Hyvonen M, Saraste M. Structure of the PH domain and Btk motif from Bruton's tyrosine kinase: molecular explanations for X-linked agammaglobulinaemia. *EMBO J*. 1997 Jun 16;16(12):3396-404.
122. Cheng G, Ye ZS, Baltimore D. Binding of Bruton's tyrosine kinase to Fyn, Lyn, or Hck through a Src homology 3 domain-mediated interaction. *Proc Natl Acad Sci U S A*. 1994 Aug 16;91(17):8152-5.
123. Rawlings DJ, Scharenberg AM, Park H, Wahl MI, Lin S, Kato RM, et al. Activation of BTK by a phosphorylation mechanism initiated by SRC family kinases. *Science*. 1996 Feb 9;271(5250):822-5.
124. Andreotti AH, Bunnell SC, Feng S, Berg LJ, Schreiber SL. Regulatory intramolecular association in a tyrosine kinase of the Tec family. *Nature*. 1997 Jan 2;385(6611):93-7.
125. Yamashita Y, Miyazato A, Ohya K, Ikeda U, Shimada K, Miura Y, et al. Deletion of Src homology 3 domain results in constitutive activation of Tec protein-tyrosine kinase. *Jpn J Cancer Res*. 1996 Nov;87(11):1106-10.
126. Backesjo CM, Vargas L, Superti-Furga G, Smith CI. Phosphorylation of Bruton's tyrosine kinase by c-Abl. *Biochem Biophys Res Commun*. 2002 Dec 6;299(3):510-5.

127. Guinamard R, Aspenstrom P, Fougereau M, Chavrier P, Guillemot JC. Tyrosine phosphorylation of the Wiskott-Aldrich syndrome protein by Lyn and Btk is regulated by CDC42. *FEBS Lett.* 1998 Sep 4;434(3):431-6.
128. Guinamard R, Fougereau M, Seckinger P. The SH3 domain of Bruton's tyrosine kinase interacts with Vav, Sam68 and EWS. *Scand J Immunol.* 1997 Jun;45(6):587-95.
129. Park H, Wahl MI, Afar DE, Turck CW, Rawlings DJ, Tam C, et al. Regulation of Btk function by a major autophosphorylation site within the SH3 domain. *Immunity.* 1996 May;4(5):515-25.
130. Yang W, Desiderio S. BAP-135, a target for Bruton's tyrosine kinase in response to B cell receptor engagement. *Proc Natl Acad Sci U S A.* 1997 Jan 21;94(2):604-9.
131. Wahl MI, Fluckiger AC, Kato RM, Park H, Witte ON, Rawlings DJ. Phosphorylation of two regulatory tyrosine residues in the activation of Bruton's tyrosine kinase via alternative receptors. *Proc Natl Acad Sci U S A.* 1997 Oct 14;94(21):11526-33.
132. Ohya K, Kajigaya S, Kitanaka A, Yoshida K, Miyazato A, Yamashita Y, et al. Molecular cloning of a docking protein, BRDG1, that acts downstream of the Tec tyrosine kinase. *Proc Natl Acad Sci U S A.* 1999 Oct 12;96(21):11976-81.
133. Oppermann FS, Gnad F, Olsen JV, Hornberger R, Greff Z, Keri G, et al. Large-scale proteomics analysis of the human kinome. *Mol Cell Proteomics.* 2009 Jul;8(7):1751-64.
134. Kurosaki T, Kurosaki M. Transphosphorylation of Bruton's tyrosine kinase on tyrosine 551 is critical for B cell antigen receptor function. *J Biol Chem.* 1997 Jun 20;272(25):15595-8.
135. BRUTON OC. Agammaglobulinemia. *Pediatrics.* 1952 Jun;9(6):722-8.
136. BRUTON OC, APT L, GITLIN D, JANEWAY CA. Absence of serum gamma globulins. *AMA Am J Dis Child.* 1952 Nov;84(5):632-6.
137. Vihinen M, Mattsson PT, Smith CI. Bruton tyrosine kinase (BTK) in X-linked agammaglobulinemia (XLA). *Front Biosci.* 2000 Dec 1;5:917.
138. Conley ME, Parolini O, Rohrer J, Campana D. X-linked agammaglobulinemia: new approaches to old questions based on the identification of the defective gene. *Immunol Rev.* 1994 Apr;138:5-21.
139. Conley ME. B cells in patients with X-linked agammaglobulinemia. *J Immunol.* 1985 May;134(5):3070-4.

140. Vetrie D, Vorechovsky I, Sideras P, Holland J, Davies A, Flinter F, et al. The gene involved in X-linked agammaglobulinaemia is a member of the src family of protein-tyrosine kinases. *Nature*. 1993 Jan 21;361(6409):226-33.
141. Tsukada S, Saffran DC, Rawlings DJ, Parolini O, Allen RC, Klisak I, et al. Deficient expression of a B cell cytoplasmic tyrosine kinase in human X-linked agammaglobulinemia. *Cell*. 1993 Jan 29;72(2):279-90.
142. Rawlings DJ, Saffran DC, Tsukada S, Largaespada DA, Grimaldi JC, Cohen L, et al. Mutation of unique region of Bruton's tyrosine kinase in immunodeficient XID mice. *Science*. 1993 Jul 16;261(5119):358-61.
143. Thomas JD, Sideras P, Smith CI, Vorechovsky I, Chapman V, Paul WE. Colocalization of X-linked agammaglobulinemia and X-linked immunodeficiency genes. *Science*. 1993 Jul 16;261(5119):355-8.
144. Shared database BTK (Bruton tyrosine kinase) [Internet]. []. Available from: <https://databases.lovd.nl/shared/variants/BTK/unique>.
145. Valiaho J, Smith CI, Vihinen M. BTKbase: the mutation database for X-linked agammaglobulinemia. *Hum Mutat*. 2006 Dec;27(12):1209-17.
146. Edwards JC, Szczepanski L, Szechinski J, Filipowicz-Sosnowska A, Emery P, Close DR, et al. Efficacy of B-cell-targeted therapy with rituximab in patients with rheumatoid arthritis. *N Engl J Med*. 2004 Jun 17;350(25):2572-81.
147. Favas C, Isenberg DA. B-cell-depletion therapy in SLE--what are the current prospects for its acceptance? *Nat Rev Rheumatol*. 2009 Dec;5(12):711-6.
148. Hauser SL, Waubant E, Arnold DL, Vollmer T, Antel J, Fox RJ, et al. B-cell depletion with rituximab in relapsing-remitting multiple sclerosis. *N Engl J Med*. 2008 Feb 14;358(7):676-88.
149. Texido G, Su IH, Mecklenbrauker I, Saijo K, Malek SN, Desiderio S, et al. The B-cell-specific Src-family kinase Blk is dispensable for B-cell development and activation. *Mol Cell Biol*. 2000 Feb;20(4):1227-33.
150. Lowell CA. Src-family kinases: rheostats of immune cell signaling. *Mol Immunol*. 2004 Jul;41(6-7):631-43.
151. Pan Z, Scheerens H, Li SJ, Schultz BE, Sprengeler PA, Burrill LC, et al. Discovery of selective irreversible inhibitors for Bruton's tyrosine kinase. *ChemMedChem*. 2007 Jan;2(1):58-61.
152. Honigberg LA, Smith AM, Sirisawad M, Verner E, Lounsbury D, Chang B, et al. The Bruton tyrosine kinase inhibitor PCI-32765 blocks B-cell activation and is efficacious in

models of autoimmune disease and B-cell malignancy. *Proc Natl Acad Sci U S A*. 2010 Jul 20;107(29):13075-80.

153. Liu L, Di Paolo J, Barbosa J, Rong H, Reif K, Wong H. Antiarthritis effect of a novel Bruton's tyrosine kinase (BTK) inhibitor in rat collagen-induced arthritis and mechanism-based pharmacokinetic/pharmacodynamic modeling: relationships between inhibition of BTK phosphorylation and efficacy. *J Pharmacol Exp Ther*. 2011 Jul;338(1):154-63.

154. Xu D, Kim Y, Postelnek J, Vu MD, Hu DQ, Liao C, et al. RN486, a selective Bruton's tyrosine kinase inhibitor, abrogates immune hypersensitivity responses and arthritis in rodents. *J Pharmacol Exp Ther*. 2012 Apr;341(1):90-103.

155. Labenski M, Chaturvedi P, Evans E, Mazdiyazni H, Sheets M, Aslanian S, et al. In vitro reactivity assessment of covalent drugs targeting Bruton's tyrosine kinase. *Drug Metab Rev*. 2011 NOV;43:140-1.

156. Smith PF, Krishnarajah J, Nunn PA, Hill RJ, Karr D, Tam D, et al. A phase I trial of PRN1008, a novel reversible covalent inhibitor of Bruton's tyrosine kinase, in healthy volunteers. *Br J Clin Pharmacol*. 2017 Nov;83(11):2367-76.

157. Di Paolo JA, Huang T, Balazs M, Barbosa J, Barck KH, Bravo BJ, et al. Specific Btk inhibition suppresses B cell- and myeloid cell-mediated arthritis. *Nat Chem Biol*. 2011 Jan;7(1):41-50.

158. Covey T, Barf T, Gulrajani M, Krantz F, van Lith B, Bibikova E, et al. ACP-196: a novel covalent Bruton's tyrosine kinase (Btk) inhibitor with improved selectivity and in vivo target coverage in chronic lymphocytic leukemia (CLL) patients. *Cancer Res*. 2015 AUG 1;75.

159. Tam C, Grigg AP, Opat S, Ku M, Gilbertson M, Anderson MA, et al. The BTK Inhibitor, Bgb-3111, Is Safe, Tolerable, and Highly Active in Patients with Relapsed/Refractory B-Cell Malignancies: Initial Report of a Phase 1 First-in-Human Trial. *Blood*. 2015 DEC 3;126(23).

160. Yoshizawa T, Ariza Y, Ueda Y, Hotta S, Narita M, Kawabata K. Development of a Bruton's Tyrosine Kinase (Btk) Inhibitor, ONO-4059: Efficacy in a Collagen Induced Arthritis (CIA) Model Indicates Potential Treatment for Rheumatoid Arthritis (RA). *Arthritis Rheum*. 2012 OCT;64(10):S709.

161. Mahajan S, Ghosh S, Sudbeck EA, Zheng Y, Downs S, Hupke M, et al. Rational design and synthesis of a novel anti-leukemic agent targeting Bruton's tyrosine kinase (BTK), LFM-A13 [alpha-cyano-beta-hydroxy-beta-methyl-N-(2, 5-dibromophenyl)propenamido]. *J Biol Chem*. 1999 Apr 2;274(14):9587-99.

162. Amrein PC, Attar EC, Takvorian T, Hochberg EP, Ballen KK, Leahy KM, et al. Phase II study of dasatinib in relapsed or refractory chronic lymphocytic leukemia. *Clin Cancer Res*. 2011 May 1;17(9):2977-86.
163. Kozaki, R., Hutchinson, C., Jayne, S., Dyer, M. The BTK-specific inhibitor ONO-4059 synergizes with the BCL2 inhibitor ABT-263. *Haematologica*. 2013;Vol.98(s1).
164. Kozaki R, Yoshizawa T, Tohda S, Yasuhiro T, Hotta S, Ariza Y, et al. Development of a Bruton's Tyrosine Kinase (Btk) Inhibitor, ONO-WG-307: Efficacy in ABC-DLBCL Xenograft Model Potential Treatment for B-Cell Malignancies. *Blood*. 2011 NOV 18;118(21):1593.
165. Walter HS, Rule SA, Dyer MJ, Karlin L, Jones C, Cazin B, et al. A phase 1 clinical trial of the selective BTK inhibitor ONO/GS-4059 in relapsed and refractory mature B-cell malignancies. *Blood*. 2016 Jan 28;127(4):411-9.
166. Tannheimer S, Liu J, Sorensen R, Yahiaoui A, Meadows S, Li L, et al. Combination of Idelalisib and ONO/GS-4059 in Lymphoma Cell Lines Sensitive and Resistant to BTK Inhibitors. *Blood*. 2015 DEC 3;126(23).
167. Jones R, Axelrod MJ, Tumas D, Queva C, Di Paolo J. Combination Effects of B Cell Receptor Pathway Inhibitors (Entospletinib, ONO/GS-4059, and Idelalisib) and a BCL-2 Inhibitor in Primary CLL Cells. *Blood*. 2015 DEC 3;126(23).
168. Yasuhiro T, Sawada W, Klein C, Kozaki R, Hotta S, Yoshizawa T. Anti-tumor efficacy study of the Bruton's tyrosine kinase (BTK) inhibitor, ONO/GS-4059, in combination with the glycoengineered type II anti-CD20 monoclonal antibody obinutuzumab (GA101) demonstrates superior in vivo efficacy compared to ONO/GS-4059 in combination with rituximab. *Leuk Lymphoma*. 2017 Mar;58(3):699-707.
169. Herman SE, Gordon AL, Hertlein E, Ramanunni A, Zhang X, Jaglowski S, et al. Bruton tyrosine kinase represents a promising therapeutic target for treatment of chronic lymphocytic leukemia and is effectively targeted by PCI-32765. *Blood*. 2011 Jun 9;117(23):6287-96.
170. Cinar M, Hamedani F, Mo Z, Cinar B, Amin HM, Alkan S. Bruton tyrosine kinase is commonly overexpressed in mantle cell lymphoma and its attenuation by Ibrutinib induces apoptosis. *Leuk Res*. 2013 Oct;37(10):1271-7.
171. Chang BY, Francesco M, De Rooij MF, Magadala P, Steggerda SM, Huang MM, et al. Egress of CD19(+)CD5(+) cells into peripheral blood following treatment with the Bruton tyrosine kinase inhibitor ibrutinib in mantle cell lymphoma patients. *Blood*. 2013 Oct 3;122(14):2412-24.

172. Yang G, Zhou Y, Liu X, Xu L, Cao Y, Manning RJ, et al. A mutation in MYD88 (L265P) supports the survival of lymphoplasmacytic cells by activation of Bruton tyrosine kinase in Waldenstrom macroglobulinemia. *Blood*. 2013 Aug 15;122(7):1222-32.
173. Jares P, Colomer D, Campo E. Molecular pathogenesis of mantle cell lymphoma. *J Clin Invest*. 2012 Oct;122(10):3416-23.
174. Byrd JC, Furman RR, Coutre SE, Flinn IW, Burger JA, Blum KA, et al. Targeting BTK with ibrutinib in relapsed chronic lymphocytic leukemia. *N Engl J Med*. 2013 Jul 4;369(1):32-42.
175. Wang ML, Rule S, Martin P, Goy A, Auer R, Kahl BS, et al. Targeting BTK with ibrutinib in relapsed or refractory mantle-cell lymphoma. *N Engl J Med*. 2013 Aug 8;369(6):507-16.
176. Treon SP, Tripsas CK, Meid K, Warren D, Varma G, Green R, et al. Ibrutinib in previously treated Waldenstrom's macroglobulinemia. *N Engl J Med*. 2015 Apr 9;372(15):1430-40.
177. Wilson WH, Young RM, Schmitz R, Yang Y, Pittaluga S, Wright G, et al. Targeting B cell receptor signaling with ibrutinib in diffuse large B cell lymphoma. *Nat Med*. 2015 Aug;21(8):922-6.
178. Burger JA, Tedeschi A, Barr PM, Robak T, Owen C, Ghia P, et al. Ibrutinib as Initial Therapy for Patients with Chronic Lymphocytic Leukemia. *N Engl J Med*. 2015 Dec 17;373(25):2425-37.
179. Byrd JC, Brown JR, O'Brien S, Barrientos JC, Kay NE, Reddy NM, et al. Ibrutinib versus ofatumumab in previously treated chronic lymphoid leukemia. *N Engl J Med*. 2014 Jul 17;371(3):213-23.
180. Pagel J, Brown J, Hillmen P, O'Brien S, Barrientos J, Reddy N, et al. Updated efficacy including genetic subgroup analysis and overall safety in the phase 3 RESONATE trial of ibrutinib versus ofatumumab in previously-treated CLL/SLL. *Leuk Lymphoma*. 2015 SEP 1;56:153-4.
181. Chanan-Khan A, Cramer P, Demirkan F, Fraser G, Silva RS, Grosicki S, et al. Ibrutinib combined with bendamustine and rituximab compared with placebo, bendamustine, and rituximab for previously treated chronic lymphocytic leukaemia or small lymphocytic lymphoma (HELIOS): a randomised, double-blind, phase 3 study. *Lancet Oncol*. 2016 Feb;17(2):200-11.
182. Stephens DM, Spurgeon SE. Ibrutinib in mantle cell lymphoma patients: glass half full? Evidence and opinion. *Ther Adv Hematol*. 2015 Oct;6(5):242-52.

183. Cheah CY, Chihara D, Romaguera JE, Fowler NH, Seymour JF, Hagemeister FB, et al. Patients with mantle cell lymphoma failing ibrutinib are unlikely to respond to salvage chemotherapy and have poor outcomes. *Ann Oncol*. 2015 Jun;26(6):1175-9.
184. Dotta L, Tassone L, Badolato R. Clinical and genetic features of Warts, Hypogammaglobulinemia, Infections and Myelokathexis (WHIM) syndrome. *Curr Mol Med*. 2011 Jun;11(4):317-25.
185. Cao Y, Hunter ZR, Liu X, Xu L, Yang G, Chen J, et al. The WHIM-like CXCR4(S338X) somatic mutation activates AKT and ERK, and promotes resistance to ibrutinib and other agents used in the treatment of Waldenstrom's Macroglobulinemia. *Leukemia*. 2015 Jan;29(1):169-76.
186. ClinicalTrials.gov [Internet]. [cited September 2017]. Available from: <https://clinicaltrials.gov/>.
187. Winqvist M, Asklid A, Andersson PO, Karlsson K, Karlsson C, Lauri B, et al. Real-world results of ibrutinib in patients with relapsed or refractory chronic lymphocytic leukemia: data from 95 consecutive patients treated in a compassionate use program. A study from the Swedish Chronic Lymphocytic Leukemia Group. *Haematologica*. 2016 Dec;101(12):1573-80.
188. UK CLL Forum. Ibrutinib for relapsed/refractory chronic lymphocytic leukemia: a UK and Ireland analysis of outcomes in 315 patients. *Haematologica*. 2016 Dec;101(12):1563-72.
189. Gao W, Wang M, Wang L, Lu H, Wu S, Dai B, et al. Selective antitumor activity of ibrutinib in EGFR-mutant non-small cell lung cancer cells. *J Natl Cancer Inst*. 2014 Sep 10;106(9):10.1093/jnci/dju204. Print 2014 Sep.
190. Haura EB, Rix U. Deploying ibrutinib to lung cancer: another step in the quest towards drug repurposing. *J Natl Cancer Inst*. 2014 Sep 10;106(9):10.1093/jnci/dju250. Print 2014 Sep.
191. Chen J, Kinoshita T, Sukbuntherng J, Chang BY, Elias L. Ibrutinib Inhibits ERBB Receptor Tyrosine Kinases and HER2-Amplified Breast Cancer Cell Growth. *Mol Cancer Ther*. 2016 Dec;15(12):2835-44.
192. Brown JR, Harb WA, Hill BT, Gabrilove J, Sharman JP, Schreeder MT, et al. Phase I study of single-agent CC-292, a highly selective Bruton's tyrosine kinase inhibitor, in relapsed/refractory chronic lymphocytic leukemia. *Haematologica*. 2016 Jul;101(7):295.

193. Byrd JC, Harrington B, O'Brien S, Jones JA, Schuh A, Devereux S, et al. Acalabrutinib (ACP-196) in Relapsed Chronic Lymphocytic Leukemia. *N Engl J Med*. 2016 Jan 28;374(4):323-32.
194. Tam C, Grigg AP, Opat S, Ku M, Gilbertson M, Anderson MA, et al. The BTK Inhibitor, Bgb-3111, Is Safe, Tolerable, and Highly Active in Patients with Relapsed/Refractory B-Cell Malignancies: Initial Report of a Phase 1 First-in-Human Trial. *Blood*. 2015 DEC 3;126(23).
195. Kim JH, Kim WS, Ryu K, Kim SJ, Park C. CD79B limits response of diffuse large B cell lymphoma to ibrutinib. *Leuk Lymphoma*. 2016;57(6):1413-22.
196. Tohda S, Sato T, Kogoshi H, Fu L, Sakano S, Nara N. Establishment of a novel B-cell lymphoma cell line with suppressed growth by gamma-secretase inhibitors. *Leuk Res*. 2006 Nov;30(11):1385-90.
197. Kluin-Nelemans HC, Limpens J, Meerabux J, Beverstock GC, Jansen JH, de Jong D, et al. A new non-Hodgkin's B-cell line (DoHH2) with a chromosomal translocation t(14;18)(q32;q21). *Leukemia*. 1991 Mar;5(3):221-4.
198. Brown M, Wittwer C. Flow cytometry: principles and clinical applications in hematology. *Clin Chem*. 2000 Aug;46(8 Pt 2):1221-9.
199. Henry CM, Hollville E, Martin SJ. Measuring apoptosis by microscopy and flow cytometry. *Methods*. 2013 Jun 1;61(2):90-7.
200. Maddocks KJ, Ruppert AS, Lozanski G, Heerema NA, Zhao W, Abruzzo L, et al. Etiology of Ibrutinib Therapy Discontinuation and Outcomes in Patients With Chronic Lymphocytic Leukemia. *JAMA Oncol*. 2015 APR;1(1):80-7.
201. Mato AR, Lamanna N, Ujjani CS, Brander DM, Hill BT, Howlett C, et al. Toxicities and Outcomes of Ibrutinib-Treated Patients in the United States: Large Retrospective Analysis of 621 Real World Patients. *Blood*. 2016 DEC 2;128(22).
202. Byrd JC, Furman RR, Coutre SE, Burger JA, Blum KA, Coleman M, et al. Three-year follow-up of treatment-naïve and previously treated patients with CLL and SLL receiving single-agent ibrutinib. *Blood*. 2015 Apr 16;125(16):2497-506.
203. Hansen AR, Graham DM, Pond GR, Siu LL. Phase 1 trial design: is 3 + 3 the best? *Cancer Control*. 2014 Jul;21(3):200-8.
204. Walter HS, Salles GA, Dyer MJ. New Agents to Treat Chronic Lymphocytic Leukemia. *N Engl J Med*. 2016 Jun 2;374(22):2185-6.

205. Walter HS, Jayne S, Rule SA, Cartron G, Morschhauser F, Macip S, et al. Long-term follow-up of patients with CLL treated with the selective Bruton's tyrosine kinase inhibitor ONO/GS-4059. *Blood*. 2017 May 18;129(20):2808-10.
206. Rawstron AC, Villamor N, Ritgen M, Bottcher S, Ghia P, Zehnder JL, et al. International standardized approach for flow cytometric residual disease monitoring in chronic lymphocytic leukaemia. *Leukemia*. 2007 May;21(5):956-64.
207. Furman RR, Sharman JP, Coutre SE, Cheson BD, Pagel JM, Hillmen P, et al. Idelalisib and rituximab in relapsed chronic lymphocytic leukemia. *N Engl J Med*. 2014 Mar 13;370(11):997-1007.
208. O'Brien S, Furman RR, Coutre SE, Sharman JP, Burger JA, Blum KA, et al. Ibrutinib as initial therapy for elderly patients with chronic lymphocytic leukaemia or small lymphocytic lymphoma: an open-label, multicentre, phase 1b/2 trial. *Lancet Oncol*. 2014 Jan;15(1):48-58.
209. Tsimberidou AM, Wen S, McLaughlin P, O'Brien S, Wierda WG, Lerner S, et al. Other malignancies in chronic lymphocytic leukemia/small lymphocytic lymphoma. *J Clin Oncol*. 2009 Feb 20;27(6):904-10.
210. Molica S. Second neoplasms in chronic lymphocytic leukemia: incidence and pathogenesis with emphasis on the role of different therapies. *Leuk Lymphoma*. 2005 Jan;46(1):49-54.
211. Althubiti M, Rada M, Samuel J, Escorsa JM, Najeeb H, Lee KG, et al. BTK Modulates p53 Activity to Enhance Apoptotic and Senescent Responses. *Cancer Res*. 2016 Sep 15;76(18):5405-14.
212. Gerlinger M, Rowan AJ, Horswell S, Math M, Larkin J, Endesfelder D, et al. Intratumor heterogeneity and branched evolution revealed by multiregion sequencing. *N Engl J Med*. 2012 Mar 8;366(10):883-92.
213. Morin RD, Mungall K, Pleasance E, Mungall AJ, Goya R, Huff RD, et al. Mutational and structural analysis of diffuse large B-cell lymphoma using whole-genome sequencing. *Blood*. 2013 Aug 15;122(7):1256-65.
214. Hutchinson CV, Dyer MJ. Breaking good: the inexorable rise of BTK inhibitors in the treatment of chronic lymphocytic leukaemia. *Br J Haematol*. 2014 Jul;166(1):12-22.
215. Conley ME, Broides A, Hernandez-Trujillo V, Howard V, Kanegane H, Miyawaki T, et al. Genetic analysis of patients with defects in early B-cell development. *Immunol Rev*. 2005 Feb;203:216-34.

216. Winkelstein JA, Marino MC, Lederman HM, Jones SM, Sullivan K, Burks AW, et al. X-linked agammaglobulinemia: report on a United States registry of 201 patients. *Medicine (Baltimore)*. 2006 Jul;85(4):193-202.
217. Kozłowski C, Evans DI. Neutropenia associated with X-linked agammaglobulinaemia. *J Clin Pathol*. 1991 May;44(5):388-90.
218. Fiedler K, Sindrilaru A, Terszowski G, Kokai E, Feyerabend TB, Bullinger L, et al. Neutrophil development and function critically depend on Bruton tyrosine kinase in a mouse model of X-linked agammaglobulinemia. *Blood*. 2011 Jan 27;117(4):1329-39.
219. Pessi MA, Zilembo N, Haspinger ER, Molino L, Di Cosimo S, Garassino M, et al. Targeted therapy-induced diarrhea: A review of the literature. *Crit Rev Oncol Hematol*. 2014 May;90(2):165-79.
220. Farooqui MZ, Valdez J, Martyr S, Aue G, Saba N, Niemann CU, et al. Ibrutinib for previously untreated and relapsed or refractory chronic lymphocytic leukaemia with TP53 aberrations: a phase 2, single-arm trial. *Lancet Oncol*. 2015 Feb;16(2):169-76.
221. McMullen JR, Amirahmadi F, Woodcock EA, Schinke-Braun M, Bouwman RD, Hewitt KA, et al. Protective effects of exercise and phosphoinositide 3-kinase(p110alpha) signaling in dilated and hypertrophic cardiomyopathy. *Proc Natl Acad Sci U S A*. 2007 Jan 9;104(2):612-7.
222. O'Brien S, Furman RR, Coutre S, Flinn IW, Burger JA, Blum K, et al. Single-agent ibrutinib in treatment-naive and relapsed/refractory chronic lymphocytic leukemia: a 5-year experience. *Blood*. 2018 Apr 26;131(17):1910-9.
223. Rule S, Dreyling M, Goy A, Hess G, Auer R, Kahl B, et al. Outcomes in 370 patients with mantle cell lymphoma treated with ibrutinib: a pooled analysis from three open-label studies. *Br J Haematol*. 2017 Nov;179(3):430-8.
224. Advani RH, Buggy JJ, Sharman JP, Smith SM, Boyd TE, Grant B, et al. Bruton tyrosine kinase inhibitor ibrutinib (PCI-32765) has significant activity in patients with relapsed/refractory B-cell malignancies. *J Clin Oncol*. 2013 Jan 1;31(1):88-94.
225. Cook N, Hansen AR, Siu LL, Abdul Razak AR. Early phase clinical trials to identify optimal dosing and safety. *Mol Oncol*. 2015 May;9(5):997-1007.
226. Druker BJ, Talpaz M, Resta DJ, Peng B, Buchdunger E, Ford JM, et al. Efficacy and safety of a specific inhibitor of the BCR-ABL tyrosine kinase in chronic myeloid leukemia. *N Engl J Med*. 2001 Apr 5;344(14):1031-7.
227. Fukuoka M, Yano S, Giaccone G, Tamura T, Nakagawa K, Douillard JY, et al. Multi-institutional randomized phase II trial of gefitinib for previously treated patients

with advanced non-small-cell lung cancer (The IDEAL 1 Trial) [corrected. *J Clin Oncol.* 2003 Jun 15;21(12):2237-46.

228. Shepherd FA, Rodrigues Pereira J, Ciuleanu T, Tan EH, Hirsh V, Thongprasert S, et al. Erlotinib in previously treated non-small-cell lung cancer. *N Engl J Med.* 2005 Jul 14;353(2):123-32.

229. Chapman PB, Hauschild A, Robert C, Haanen JB, Ascierto P, Larkin J, et al. Improved Survival with Vemurafenib in Melanoma with BRAF V600E Mutation. *The New England Journal of Medicine.* 2011 Jun 30;364(26):2507-16.

230. Schuster SJ, Bishop MR, Tam CS, Waller EK, Borchmann P, et al. Primary analysis of JULIET: A global, pivotal, phase 2 trial of CTL019 in adult patients with relapsed or refractory diffuse large B-cell lymphoma. *Blood.* 2017;130(1).

231. Juliusson G, Oscier DG, Fitchett M, Ross FM, Stockdill G, Mackie MJ, et al. Prognostic subgroups in B-cell chronic lymphocytic leukemia defined by specific chromosomal abnormalities. *N Engl J Med.* 1990 Sep 13;323(11):720-4.

232. Foa R, Del Giudice I, Guarini A, Rossi D, Gaidano G. Clinical implications of the molecular genetics of chronic lymphocytic leukemia. *Haematologica.* 2013 May;98(5):675-85.

233. Dicker F, Herholz H, Schnittger S, Nakao A, Patten N, Wu L, et al. The detection of TP53 mutations in chronic lymphocytic leukemia independently predicts rapid disease progression and is highly correlated with a complex aberrant karyotype. *Leukemia.* 2009 Jan;23(1):117-24.

234. Guarini A, Marinelli M, Tavolaro S, Bellacchio E, Magliozzi M, Chiaretti S, et al. ATM gene alterations in chronic lymphocytic leukemia patients induce a distinct gene expression profile and predict disease progression. *Haematologica.* 2012 Jan;97(1):47-55.

235. Fabbri G, Rasi S, Rossi D, Trifonov V, Khiabani H, Ma J, et al. Analysis of the chronic lymphocytic leukemia coding genome: role of NOTCH1 mutational activation. *J Exp Med.* 2011 Jul 4;208(7):1389-401.

236. Rossi D, Rasi S, Fabbri G, Spina V, Fangazio M, Forconi F, et al. Mutations of NOTCH1 are an independent predictor of survival in chronic lymphocytic leukemia. *Blood.* 2012 Jan 12;119(2):521-9.

237. Quesada V, Conde L, Villamor N, Ordonez GR, Jares P, Bassaganyas L, et al. Exome sequencing identifies recurrent mutations of the splicing factor SF3B1 gene in chronic lymphocytic leukemia. *Nat Genet.* 2011 Dec 11;44(1):47-52.

238. Herling CD, Klaumunzer M, Rocha CK, Altmuller J, Thiele H, Bahlo J, et al. Complex karyotypes and KRAS and POT1 mutations impact outcome in CLL after chlorambucil-based chemotherapy or chemoimmunotherapy. *Blood*. 2016 Jul 21;128(3):395-404.
239. Rossi D, Fangazio M, Rasi S, Vaisitti T, Monti S, Cresta S, et al. Disruption of BIRC3 associates with fludarabine chemorefractoriness in TP53 wild-type chronic lymphocytic leukemia. *Blood*. 2012 Mar 22;119(12):2854-62.
240. Villamor N, Conde L, Martinez-Trillos A, Cazorla M, Navarro A, Bea S, et al. NOTCH1 mutations identify a genetic subgroup of chronic lymphocytic leukemia patients with high risk of transformation and poor outcome. *Leukemia*. 2013 Apr;27(5):1100-6.
241. Rossi D, Brusca A, Spina V, Rasi S, Khiabani H, Messina M, et al. Mutations of the SF3B1 splicing factor in chronic lymphocytic leukemia: association with progression and fludarabine-refractoriness. *Blood*. 2011 Dec 22;118(26):6904-8.
242. Wang L, Lawrence MS, Wan Y, Stojanov P, Sougnez C, Stevenson K, et al. SF3B1 and other novel cancer genes in chronic lymphocytic leukemia. *N Engl J Med*. 2011 Dec 29;365(26):2497-506.
243. Robak T, Dmoszynska A, Solal-Celigny P, Warzocha K, Loscertales J, Catalano J, et al. Rituximab plus fludarabine and cyclophosphamide prolongs progression-free survival compared with fludarabine and cyclophosphamide alone in previously treated chronic lymphocytic leukemia. *J Clin Oncol*. 2010 Apr 1;28(10):1756-65.
244. Hallek M, Fischer K, Fingerle-Rowson G, Fink AM, Busch R, Mayer J, et al. Addition of rituximab to fludarabine and cyclophosphamide in patients with chronic lymphocytic leukaemia: a randomised, open-label, phase 3 trial. *Lancet*. 2010 Oct 2;376(9747):1164-74.
245. Stilgenbauer S, Schnaiter A, Paschka P, Zenz T, Rossi M, Dohner K, et al. Gene mutations and treatment outcome in chronic lymphocytic leukemia: results from the CLL8 trial. *Blood*. 2014 May 22;123(21):3247-54.
246. Pozzo F, Bittolo T, Arruga F, Bulian P, Macor P, Tissino E, et al. NOTCH1 mutations associate with low CD20 level in chronic lymphocytic leukemia: evidence for a NOTCH1 mutation-driven epigenetic dysregulation. *Leukemia*. 2016 Jan;30(1):182-9.
247. Hallek M, Cheson BD, Catovsky D, Caligaris-Cappio F, Dighiero G, Dohner H, et al. Guidelines for the diagnosis and treatment of chronic lymphocytic leukemia: a report from the International Workshop on Chronic Lymphocytic Leukemia updating the National Cancer Institute-Working Group 1996 guidelines. *Blood*. 2008 Jun 15;111(12):5446-56.

248. Oscier DG, Rose-Zerilli MJ, Winkelmann N, Gonzalez de Castro D, Gomez B, Forster J, et al. The clinical significance of NOTCH1 and SF3B1 mutations in the UK LRF CLL4 trial. *Blood*. 2013 Jan 17;121(3):468-75.
249. Wang L, Brooks AN, Fan J, Wan Y, Gambe R, Li S, Hergert S, Yin S, Freeman SS, Levin JZ, Fan L, Seiler M, Buonamici S, Smith PG, Chau KF, Cibulskis CL, Zhang W, Rassenti LZ, Ghia EM, Kipps TJ, Fernandes S, Bloch DB, Kotliar D, Landau DA, Shukla SA, Aster JC, Reed R, DeLuca DS, Brown JR, Neuberg D, Getz G, Livak KJ, Meyerson MM, Kharchenko PV, Wu CJ. Transcriptomic Characterization of SF3B1 Mutation Reveals Its Pleiotropic Effects in Chronic Lymphocytic Leukemia. *Cancer Cell*. 2016;30(5):750-63.
250. Baliakas P, Hadzidimitriou A, Sutton LA, Rossi D, Minga E, Villamor N, et al. Recurrent mutations refine prognosis in chronic lymphocytic leukemia. *Leukemia*. 2015 Feb;29(2):329-36.
251. Rigolin GM, Saccenti E, Bassi C, Lupini L, Quaglia FM, Cavallari M, et al. Extensive next-generation sequencing analysis in chronic lymphocytic leukemia at diagnosis: clinical and biological correlations. *J Hematol Oncol*. 2016 Sep 15;9(1):z.
252. Estenfelder S, Tausch E, Robrecht S, Bahlo J, Goede V, Ritgen M, et al. Gene Mutations and Treatment Outcome in the Context of Chlorambucil (Clb) without or with the Addition of Rituximab (R) or Obinutuzumab (GA-101, G) - Results of an Extensive Analysis of the Phase III Study CLL11 of the German CLL Study Group. *Blood*. 2016 DEC 2;128(22).
253. Guieze R, Robbe P, Clifford R, de Guibert S, Pereira B, Timbs A, et al. Presence of multiple recurrent mutations confers poor trial outcome of relapsed/refractory CLL. *Blood*. 2015 Oct 29;126(18):2110-7.
254. Schnaiter A, Paschka P, Rossi M, Zenz T, Buhler A, Winkler D, et al. NOTCH1, SF3B1, and TP53 mutations in fludarabine-refractory CLL patients treated with alemtuzumab: results from the CLL2H trial of the GCLLSG. *Blood*. 2013 Aug 15;122(7):1266-70.
255. Dreger P, Schnaiter A, Zenz T, Bottcher S, Rossi M, Paschka P, et al. TP53, SF3B1, and NOTCH1 mutations and outcome of allotransplantation for chronic lymphocytic leukemia: six-year follow-up of the GCLLSG CLL3X trial. *Blood*. 2013 Apr 18;121(16):3284-8.
256. Rossi D, Rasi S, Spina V, Brusca A, Monti S, Ciardullo C, et al. Integrated mutational and cytogenetic analysis identifies new prognostic subgroups in chronic lymphocytic leukemia. *Blood*. 2013 Feb 21;121(8):1403-12.

257. Guo A, Lu P, Galanina N, Nabhan C, Smith SM, Coleman M, et al. Heightened BTK-dependent cell proliferation in unmutated chronic lymphocytic leukemia confers increased sensitivity to ibrutinib. *Oncotarget*. 2016 Jan 26;7(4):4598-610.
258. Tobin G, Thunberg U, Johnson A, Eriksson I, Soderberg O, Karlsson K, et al. Chronic lymphocytic leukemias utilizing the VH3-21 gene display highly restricted Vlambda2-14 gene use and homologous CDR3s: implicating recognition of a common antigen epitope. *Blood*. 2003 Jun 15;101(12):4952-7.
259. Trunzer K, Pavlick AC, Schuchter L, Gonzalez R, McArthur GA, Hutson TE, et al. Pharmacodynamic effects and mechanisms of resistance to vemurafenib in patients with metastatic melanoma. *J Clin Oncol*. 2013 May 10;31(14):1767-74.
260. Clifford R, Louis T, Robbe P, Ackroyd S, Burns A, Timbs AT, et al. SAMHD1 is mutated recurrently in chronic lymphocytic leukemia and is involved in response to DNA damage. *Blood*. 2014 Feb 13;123(7):1021-31.
261. Kozaki R, Yoshizawa T, Tohda S, Yasuhiro T, Hotta S, Ariza Y, et al. Development of a Bruton's Tyrosine Kinase (Btk) Inhibitor, ONO-WG-307: Efficacy in ABC-DLBCL Xenograft Model Potential Treatment for B-Cell Malignancies. *Blood*. 2011;118(21):1593.
262. Kozaki R, Hutchinson C, Sandrine J, Dyer MJS. Kinome Reprogramming in Dlbcl by the Btk-Specific Inhibitor Ono-4059 Highlights Synergistic Combinations for Clinical Application. *Haematologica*. 2014 JUN 1;99:137-8.
263. Yang Y, Shaffer AL, 3rd, Emre NC, Ceribelli M, Zhang M, Wright G, et al. Exploiting synthetic lethality for the therapy of ABC diffuse large B cell lymphoma. *Cancer Cell*. 2012 Jun 12;21(6):723-37.
264. Kroemer G, Dallaporta B, Resche-Rigon M. The mitochondrial death/life regulator in apoptosis and necrosis. *Annu Rev Physiol*. 1998;60:619-42.
265. Kroemer G. Mitochondrial control of apoptosis: an overview. *Biochem Soc Symp*. 1999;66:1-15.
266. Marchetti P, Castedo M, Susin SA, Zamzami N, Hirsch T, Macho A, et al. Mitochondrial permeability transition is a central coordinating event of apoptosis. *J Exp Med*. 1996 Sep 1;184(3):1155-60.
267. Backway KL, McCulloch EA, Chow S, Hedley DW. Relationships between the mitochondrial permeability transition and oxidative stress during ara-C toxicity. *Cancer Res*. 1997 Jun 15;57(12):2446-51.

268. Jayaraman S. Flow cytometric determination of mitochondrial membrane potential changes during apoptosis of T lymphocytic and pancreatic beta cell lines: comparison of tetramethylrhodamineethyl ester (TMRE), chloromethyl-X-rosamine (H2-CMX-Ros) and MitoTracker Red 580 (MTR580). *J Immunol Methods*. 2005 Nov 30;306(1-2):68-79.
269. Elliott JI, Sardini A, Cooper JC, Alexander DR, Davanture S, Chimini G, et al. Phosphatidylserine exposure in B lymphocytes: a role for lipid packing. *Blood*. 2006 Sep 1;108(5):1611-7.
270. Dillon SR, Mancini M, Rosen A, Schlissel MS. Annexin V binds to viable B cells and colocalizes with a marker of lipid rafts upon B cell receptor activation. *J Immunol*. 2000 Feb 1;164(3):1322-32.
271. Chauvier D, Ankri S, Charriaud-Marlangue C, Casimir R, Jacotot E. Broad-spectrum caspase inhibitors: from myth to reality? *Cell Death Differ*. 2007 Feb;14(2):387-91.
272. Chauvier D, Lecoœur H, Langonne A, Borgne-Sanchez A, Mariani J, Martinou JC, et al. Upstream control of apoptosis by caspase-2 in serum-deprived primary neurons. *Apoptosis*. 2005 Dec;10(6):1243-59.
273. Caserta TM, Smith AN, Gultice AD, Reedy MA, Brown TL. Q-VD-OPh, a broad spectrum caspase inhibitor with potent antiapoptotic properties. *Apoptosis*. 2003 Aug;8(4):345-52.
274. Chen J, Ramos J, Sirisawad M, Miller R, Naumovski L. Motexafin gadolinium induces mitochondrially-mediated caspase-dependent apoptosis. *Apoptosis*. 2005 Oct;10(5):1131-42.
275. Brunelle JK, Letai A. Control of mitochondrial apoptosis by the Bcl-2 family. *J Cell Sci*. 2009 Feb 15;122(Pt 4):437-41.
276. Bojarczuk K, Sasi BK, Gobessi S, Innocenti I, Pozzato G, Laurenti L, et al. BCR signaling inhibitors differ in their ability to overcome Mcl-1-mediated resistance of CLL B cells to ABT-199. *Blood*. 2016 Jun 23;127(25):3192-201.
277. Cervantes-Gomez F, Lamothe B, Woyach JA, Wierda WG, Keating MJ, Balakrishnan K, et al. Pharmacological and Protein Profiling Suggests Venetoclax (ABT-199) as Optimal Partner with Ibrutinib in Chronic Lymphocytic Leukemia. *Clin Cancer Res*. 2015 Aug 15;21(16):3705-15.
278. Petlickovski A, Laurenti L, Li X, Marietti S, Chiusolo P, Sica S, et al. Sustained signaling through the B-cell receptor induces Mcl-1 and promotes survival of chronic lymphocytic leukemia B cells. *Blood*. 2005 Jun 15;105(12):4820-7.

279. Blois JT, Mataraza JM, Mecklenbrauker I, Tarakhovsky A, Chiles TC. B cell receptor-induced cAMP-response element-binding protein activation in B lymphocytes requires novel protein kinase Cdelta. *J Biol Chem*. 2004 Jul 16;279(29):30123-32.
280. Wilson BE, Mochon E, Boxer LM. Induction of bcl-2 expression by phosphorylated CREB proteins during B-cell activation and rescue from apoptosis. *Mol Cell Biol*. 1996 Oct;16(10):5546-56.
281. Pavlasova G, Borsky M, Seda V, Cerna K, Osickova J, Doubek M, et al. Ibrutinib inhibits CD20 upregulation on CLL B cells mediated by the CXCR4/SDF-1 axis. *Blood*. 2016 Sep 22;128(12):1609-13.
282. Ruminy P, Etancelin P, Couronne L, Parmentier F, Rainville V, Mareschal S, et al. The isotype of the BCR as a surrogate for the GCB and ABC molecular subtypes in diffuse large B-cell lymphoma. *Leukemia*. 2011 Apr;25(4):681-8.
283. Jain P, Fayad LE, Rosenwald A, Young KH, O'Brien S. Recent advances in de novo CD5+ diffuse large B cell lymphoma. *Am J Hematol*. 2013 Sep;88(9):798-802.
284. Xu-Monette ZY, Tu M, Jabbar KJ, Cao X, Tzankov A, Visco C, et al. Clinical and biological significance of de novo CD5+ diffuse large B-cell lymphoma in Western countries. *Oncotarget*. 2015 Mar 20;6(8):5615-33.
285. Matolcsy A, Chadburn A, Knowles DM. De novo CD5-positive and Richter's syndrome-associated diffuse large B cell lymphomas are genotypically distinct. *Am J Pathol*. 1995 Jul;147(1):207-16.
286. Lankester AC, van Schijndel GM, Cordell JL, van Noesel CJ, van Lier RA. CD5 is associated with the human B cell antigen receptor complex. *Eur J Immunol*. 1994 Apr;24(4):812-6.
287. Gary-Gouy H, Bruhns P, Schmitt C, Dalloul A, Daeron M, Bismuth G. The pseudo-immunoreceptor tyrosine-based activation motif of CD5 mediates its inhibitory action on B-cell receptor signaling. *J Biol Chem*. 2000 Jan 7;275(1):548-56.
288. Pani G, Fischer KD, Mlinaric-Rascan I, Siminovitch KA. Signaling capacity of the T cell antigen receptor is negatively regulated by the PTP1C tyrosine phosphatase. *J Exp Med*. 1996 Sep 1;184(3):839-52.
289. Sen G, Bikah G, Venkataraman C, Bondada S. Negative regulation of antigen receptor-mediated signaling by constitutive association of CD5 with the SHP-1 protein tyrosine phosphatase in B-1 B cells. *Eur J Immunol*. 1999 Oct;29(10):3319-28.
290. Xu Y, Harder KW, Huntington ND, Hibbs ML, Tarlinton DM. Lyn tyrosine kinase: accentuating the positive and the negative. *Immunity*. 2005 Jan;22(1):9-18.

291. Lorenz U. SHP-1 and SHP-2 in T cells: two phosphatases functioning at many levels. *Immunol Rev.* 2009 Mar;228(1):342-59.
292. Bikah G, Carey J, Ciallella JR, Tarakhovsky A, Bondada S. CD5-mediated negative regulation of antigen receptor-induced growth signals in B-1 B cells. *Science.* 1996 Dec 13;274(5294):1906-9.
293. Anderson KC, Bates MP, Slaughenhaupt BL, Pinkus GS, Schlossman SF, Nadler LM. Expression of human B cell-associated antigens on leukemias and lymphomas: a model of human B cell differentiation. *Blood.* 1984 Jun;63(6):1424-33.
294. Stashenko P, Nadler LM, Hardy R, Schlossman SF. Characterization of a human B lymphocyte-specific antigen. *J Immunol.* 1980 Oct;125(4):1678-85.
295. Teeling JL, Mackus WJ, Wiegman LJ, van den Brakel, J H, Beers SA, French RR, et al. The biological activity of human CD20 monoclonal antibodies is linked to unique epitopes on CD20. *J Immunol.* 2006 Jul 1;177(1):362-71.
296. Tedder TF, Schlossman SF. Phosphorylation of the B1 (CD20) molecule by normal and malignant human B lymphocytes. *J Biol Chem.* 1988 Jul 15;263(20):10009-15.
297. Clark EA, Shu G, Ledbetter JA. Role of the Bp35 cell surface polypeptide in human B-cell activation. *Proc Natl Acad Sci U S A.* 1985 Mar;82(6):1766-70.
298. Golay JT, Clark EA, Beverley PC. The CD20 (Bp35) antigen is involved in activation of B cells from the G0 to the G1 phase of the cell cycle. *J Immunol.* 1985 Dec;135(6):3795-801.
299. Petrie RJ, Deans JP. Colocalization of the B cell receptor and CD20 followed by activation-dependent dissociation in distinct lipid rafts. *J Immunol.* 2002 Sep 15;169(6):2886-91.
300. Uchida J, Lee Y, Hasegawa M, Liang Y, Bradney A, Oliver JA, et al. Mouse CD20 expression and function. *Int Immunol.* 2004 Jan;16(1):119-29.
301. Kuijpers TW, Bende RJ, Baars PA, Grummels A, Derks IA, Dolman KM, et al. CD20 deficiency in humans results in impaired T cell-independent antibody responses. *J Clin Invest.* 2010 Jan;120(1):214-22.
302. Olejniczak SH, Stewart CC, Donohue K, Czuczman MS. A quantitative exploration of surface antigen expression in common B-cell malignancies using flow cytometry. *Immunol Invest.* 2006;35(1):93-114.
303. Verbrugge SE, Al M, Assaraf YG, Niewerth D, van Meerloo J, Cloos J, et al. Overcoming bortezomib resistance in human B cells by anti-CD20/rituximab-mediated

complement-dependent cytotoxicity and epoxyketone-based irreversible proteasome inhibitors. *Exp Hematol Oncol*. 2013 Jan 10;2(1):2.

304. Chen SS, Chang BY, Chang S, Tong T, Ham S, Sherry B, et al. BTK inhibition results in impaired CXCR4 chemokine receptor surface expression, signaling and function in chronic lymphocytic leukemia. *Leukemia*. 2016 Apr;30(4):833-43.

305. Himmelmann A, Riva A, Wilson GL, Lucas BP, Thevenin C, Kehrl JH. PU.1/Pip and basic helix loop helix zipper transcription factors interact with binding sites in the CD20 promoter to help confer lineage- and stage-specific expression of CD20 in B lymphocytes. *Blood*. 1997 Nov 15;90(10):3984-95.

306. Czuczman MS, Olejniczak S, Gowda A, Kotowski A, Binder A, Kaur H, et al. Acquisition of rituximab resistance in lymphoma cell lines is associated with both global CD20 gene and protein down-regulation regulated at the pretranscriptional and posttranscriptional levels. *Clin Cancer Res*. 2008 Mar 1;14(5):1561-70.

307. Hiraga J, Tomita A, Sugimoto T, Shimada K, Ito M, Nakamura S, et al. Down-regulation of CD20 expression in B-cell lymphoma cells after treatment with rituximab-containing combination chemotherapies: its prevalence and clinical significance. *Blood*. 2009 May 14;113(20):4885-93.

308. Illumina. Available from:

https://www.illumina.com/products/humanht_12_expression_beadchip_Kits_v4.html

(Accessed 02.12.2017).

309. Ashburner M, Ball CA, Blake JA, Botstein D, Butler H, Cherry JM, et al. Gene ontology: tool for the unification of biology. The Gene Ontology Consortium. *Nat Genet*. 2000 May;25(1):25-9.

310. The Gene Ontology Consortium. Expansion of the Gene Ontology knowledgebase and resources. *Nucleic Acids Res*. 2017 Jan 4;45(D1):D338.

311. Mi H, Huang X, Muruganujan A, Tang H, Mills C, Kang D, et al. PANTHER version 11: expanded annotation data from Gene Ontology and Reactome pathways, and data analysis tool enhancements. *Nucleic Acids Res*. 2017 Jan 4;45(D1):D189.

312. Max EE, Korsmeyer SJ. Human J chain gene. Structure and expression in B lymphoid cells. *J Exp Med*. 1985 Apr 1;161(4):832-49.

313. Ma J, Gunderson SI, Phillips C. Non-snRNP U1A levels decrease during mammalian B-cell differentiation and release the IgM secretory poly(A) site from repression. *RNA*. 2006 Jan;12(1):122-32.

314. Aguiar RC, Yakushijin Y, Kharbanda S, Tiwari S, Freeman GJ, Shipp MA. PTPROt: an alternatively spliced and developmentally regulated B-lymphoid phosphatase that promotes G0/G1 arrest. *Blood*. 1999 Oct 1;94(7):2403-13.
315. Chen L, Juszczynski P, Takeyama K, Aguiar RC, Shipp MA. Protein tyrosine phosphatase receptor-type O truncated (PTPROt) regulates SYK phosphorylation, proximal B-cell-receptor signaling, and cellular proliferation. *Blood*. 2006 Nov 15;108(10):3428-33.
316. Ci W, Polo JM, Cerchiatti L, Shakhovich R, Wang L, Yang SN, et al. The BCL6 transcriptional program features repression of multiple oncogenes in primary B cells and is deregulated in DLBCL. *Blood*. 2009 May 28;113(22):5536-48.
317. Takahashi K, Sivina M, Hoellenriegel J, Oki Y, Hagemester FB, Fayad L, et al. CCL3 and CCL4 are biomarkers for B cell receptor pathway activation and prognostic serum markers in diffuse large B cell lymphoma. *Br J Haematol*. 2015 Dec;171(5):726-35.
318. Coffey G, Betz A, DeGuzman F, Pak Y, Inagaki M, Baker DC, et al. The novel kinase inhibitor PRT062070 (Cerdulatinib) demonstrates efficacy in models of autoimmunity and B-cell cancer. *J Pharmacol Exp Ther*. 2014 Dec;351(3):538-48.
319. Guo A, Lu P, Coffey G, Conley P, Pandey A, Wang YL. Dual SYK/JAK inhibition overcomes ibrutinib resistance in chronic lymphocytic leukemia: Cerdulatinib, but not ibrutinib, induces apoptosis of tumor cells protected by the microenvironment. *Oncotarget*. 2017 Feb 21;8(8):12953-67.
320. Expression Atlas [updated October 2017]. Available from: <https://www.ebi.ac.uk/gxa/home> (Accessed 02.12.2017).
321. Chen JG, Liu X, Chen J, Xu L, Tsakmaklis N, Demos M, et al. Acquisition of BTK C481S Produces Resistance to Ibrutinib in MYD88 Mutated WM and ABC DLBCL Cells That Is Accompanied By ERK1/2 Hyperactivation, and Is Targeted By the Addition of the ERK1/2 Inhibitor Ulixertinib. *Blood*. 2016 DEC 2;128(22).
322. Yahiaoui A, Meadows SA, Sorensen RA, Cui ZH, Keegan KS, Brockett R, et al. PI3Kdelta inhibitor idelalisib in combination with BTK inhibitor ONO/GS-4059 in diffuse large B cell lymphoma with acquired resistance to PI3Kdelta and BTK inhibitors. *PLoS One*. 2017 Feb 8;12(2):e0171221.
323. Woyach JA, Furman RR, Liu TM, Ozer HG, Zapatka M, Ruppert AS, et al. Resistance mechanisms for the Bruton's tyrosine kinase inhibitor ibrutinib. *N Engl J Med*. 2014 Jun 12;370(24):2286-94.

324. Liu TM, Woyach JA, Zhong Y, Lozanski A, Lozanski G, Dong S, et al. Hypermorphic mutation of phospholipase C, gamma2 acquired in ibrutinib-resistant CLL confers BTK independency upon B-cell receptor activation. *Blood*. 2015 Jul 2;126(1):61-8.
325. Liao D. Emerging roles of the EBF family of transcription factors in tumor suppression. *Mol Cancer Res*. 2009 Dec;7(12):1893-901.
326. Dulak AM, Stojanov P, Peng S, Lawrence MS, Fox C, Stewart C, et al. Exome and whole-genome sequencing of esophageal adenocarcinoma identifies recurrent driver events and mutational complexity. *Nat Genet*. 2013 May;45(5):478-86.
327. Giannakis M, Mu XJ, Shukla SA, Qian ZR, Cohen O, Nishihara R, et al. Genomic Correlates of Immune-Cell Infiltrates in Colorectal Carcinoma. *Cell Rep*. 2016 Apr 14.
328. Zhang L, Fan S, Liu H, Huang C. Targeting SMARCA1 as a novel strategy for cancer therapy. *Biochem Biophys Res Commun*. 2012 Oct 19;427(2):232-5.
329. Kwok M, Davies N, Agathangelou A, Smith E, Oldreive C, Petermann E, et al. ATR inhibition induces synthetic lethality and overcomes chemoresistance in TP53- or ATM-defective chronic lymphocytic leukemia cells. *Blood*. 2016 Feb 4;127(5):582-95.
330. Morin RD, Mendez-Lago M, Mungall AJ, Goya R, Mungall KL, Corbett RD, et al. Frequent mutation of histone-modifying genes in non-Hodgkin lymphoma. *Nature*. 2011 Jul 27;476(7360):298-303.
331. Neuman LL, Ward R, Arnold D, Combs DL, Gruver D, Hill W, et al. First-in-Human Phase 1a Study of the Safety, Pharmacokinetics, and Pharmacodynamics of the Noncovalent Bruton Tyrosine Kinase (BTK) Inhibitor SNS-062 in Healthy Subjects. *Blood*. 2016 DEC 2;128(22).
332. Ahn IE, Underbayev C, Albitar A, Herman SE, Tian X, Maric I, et al. Clonal evolution leading to ibrutinib resistance in chronic lymphocytic leukemia. *Blood*. 2017 Mar 16;129(11):1469-79.
333. Gustafsson MO, Hussain A, Mohammad DK, Mohamed AJ, Nguyen V, Metalnikov P, et al. Regulation of nucleocytoplasmic shuttling of Bruton's tyrosine kinase (Btk) through a novel SH3-dependent interaction with ankyrin repeat domain 54 (ANKRD54). *Mol Cell Biol*. 2012 Jul;32(13):2440-53.
334. Nore BF, Vargas L, Mohamed AJ, Branden LJ, Backesjo CM, Islam TC, et al. Redistribution of Bruton's tyrosine kinase by activation of phosphatidylinositol 3-kinase and Rho-family GTPases. *Eur J Immunol*. 2000 Jan;30(1):145-54.

335. Mohamed AJ, Vargas L, Nore BF, Backesjo CM, Christensson B, Smith CI. Nucleocytoplasmic shuttling of Bruton's tyrosine kinase. *J Biol Chem.* 2000 Dec 22;275(51):40614-9.
336. Dyer MJ, Lillington DM, Bastard C, Tilly H, Lens D, Heward JM, et al. Concurrent activation of MYC and BCL2 in B cell non-Hodgkin lymphoma cell lines by translocation of both oncogenes to the same immunoglobulin heavy chain locus. *Leukemia.* 1996 Jul;10(7):1198-208.
337. Afar DE, Park H, Howell BW, Rawlings DJ, Cooper J, Witte ON. Regulation of Btk by Src family tyrosine kinases. *Mol Cell Biol.* 1996 Jul;16(7):3465-71.
338. Young RM, Wu T, Schmitz R, Dawood M, Xiao W, Phelan JD, et al. Survival of human lymphoma cells requires B-cell receptor engagement by self-antigens. *Proc Natl Acad Sci U S A.* 2015 Nov 3;112(44):13447-54.
339. Craxton A, Jiang A, Kurosaki T, Clark EA. Syk and Bruton's tyrosine kinase are required for B cell antigen receptor-mediated activation of the kinase Akt. *J Biol Chem.* 1999 Oct 22;274(43):30644-50.
340. Chiron D, Di Liberto M, Martin P, Huang X, Sharman J, Bleucia P, et al. Cell-cycle reprogramming for PI3K inhibition overrides a relapse-specific C481S BTK mutation revealed by longitudinal functional genomics in mantle cell lymphoma. *Cancer Discov.* 2014 Sep;4(9):1022-35.
341. Paulus A, Akhtar S, Yousaf H, Manna A, Paulus SM, Bashir Y, et al. Waldenstrom macroglobulinemia cells devoid of BTK(C481S) or CXCR4(WHIM-like) mutations acquire resistance to ibrutinib through upregulation of Bcl-2 and AKT resulting in vulnerability towards venetoclax or MK2206 treatment. *Blood Cancer J.* 2017 May 26;7(5):e565.
342. Ma J, Xing W, Coffey G, Dresser K, Lu K, Guo A, et al. Cerdulatinib, a novel dual SYK/JAK kinase inhibitor, has broad anti-tumor activity in both ABC and GCB types of diffuse large B cell lymphoma. *Oncotarget.* 2015 Dec 22;6(41):43881-96.
343. Rolli V, Gallwitz M, Wossning T, Flemming A, Schamel WW, Zurn C, et al. Amplification of B cell antigen receptor signaling by a Syk/ITAM positive feedback loop. *Mol Cell.* 2002 Nov;10(5):1057-69.
344. Egloff AM, Desiderio S. Identification of phosphorylation sites for Bruton's tyrosine kinase within the transcriptional regulator BAP/TFII-I. *J Biol Chem.* 2001 Jul 27;276(30):27806-15.
345. Valdez BC, Henning D, So RB, Dixon J, Dixon MJ. The Treacher Collins syndrome (TCOF1) gene product is involved in ribosomal DNA gene transcription by

- interacting with upstream binding factor. *Proc Natl Acad Sci U S A*. 2004 Jul 20;101(29):10709-14.
346. Spiess C, Meyer AS, Reissmann S, Frydman J. Mechanism of the eukaryotic chaperonin: protein folding in the chamber of secrets. *Trends Cell Biol*. 2004 Nov;14(11):598-604.
347. Schmidt C, Kim D, Ippolito GC, Naqvi HR, Probst L, Mathur S, et al. Signalling of the BCR is regulated by a lipid rafts-localised transcription factor, Bright. *EMBO J*. 2009 Mar 18;28(6):711-24.
348. Martin F, Malergue F, Pitari G, Philippe JM, Philips S, Chabret C, et al. Vanin genes are clustered (human 6q22-24 and mouse 10A2B1) and encode isoforms of pantetheinase ectoenzymes. *Immunogenetics*. 2001;53(4):296-306.
349. Barrera G. Oxidative stress and lipid peroxidation products in cancer progression and therapy. *ISRN Oncol*. 2012;2012:137289.
350. Wang Q, Holst J. L-type amino acid transport and cancer: targeting the mTORC1 pathway to inhibit neoplasia. *Am J Cancer Res*. 2015 Mar 15;5(4):1281-94.
351. Lan Pham, Zhang L, Tao W, Zhao D, Zhang H, Xie J, et al. Developing Novel Therapeutic Strategies to Overcome Ibrutinib Resistance in Mantle Cell Lymphoma. *Blood*. 2015 DEC 3;126(23).
352. Wang J, Zhang V, Bell T, Liu Y, Guo H, Zhang L. The Effects of PI3K- δ/γ Inhibitor, Duvelisib, in Mantle Cell Lymphoma in Vitro and in Patient-Derived Xenograft Studies. *Blood*. 2016 December;128(22):3016.
353. Dong S, Guinn D, Dubovsky JA, Zhong Y, Lehman A, Kutok J, et al. IPI-145 antagonizes intrinsic and extrinsic survival signals in chronic lymphocytic leukemia cells. *Blood*. 2014 Dec 4;124(24):3583-6.
354. Porcu P, Flinn I, Kahl BS, Horwitz SM, Oki Y, Byrd JC, et al. Clinical Activity of Duvelisib (IPI-145), a Phosphoinositide-3-Kinase-delta, gamma Inhibitor, in Patients Previously Treated with Ibrutinib. *Blood*. 2014 DEC 6;124(21).
355. Anthony R Mato, Chadi Nabhan, Paul M Barr, Chaitra S Ujjani, Brian T Hill, Nicole Lamanna, et al. Outcomes of CLL patients treated with sequential kinase inhibitor therapy: a real world experience. *Blood*. 2016 Nov 3;128(18):2199-205.
356. Kim YM, Kim J, Heo SC, Shin SH, Do EK, Suh DS, et al. Proteomic identification of ADAM12 as a regulator for TGF-beta1-induced differentiation of human mesenchymal stem cells to smooth muscle cells. *PLoS One*. 2012;7(7):e40820.

357. Marteijs JA, van der Meer, L T, Smit JJ, Noordermeer SM, Wissink W, Jansen P, et al. The ubiquitin ligase Triad1 inhibits myelopoiesis through UbcH7 and Ubc13 interacting domains. *Leukemia*. 2009 Aug;23(8):1480-9.
358. Liu S, Chen ZJ. Expanding role of ubiquitination in NF-kappaB signaling. *Cell Res*. 2011 Jan;21(1):6-21.
359. Wertz IE, Dixit VM. Signaling to NF-kappaB: regulation by ubiquitination. *Cold Spring Harb Perspect Biol*. 2010 Mar;2(3):a003350.
360. Ye Y, Rape M. Building ubiquitin chains: E2 enzymes at work. *Nat Rev Mol Cell Biol*. 2009 Nov;10(11):755-64.
361. Panier S, Durocher D. Regulatory ubiquitylation in response to DNA double-strand breaks. *DNA Repair (Amst)*. 2009 Apr 5;8(4):436-43.
362. Yamamoto M, Okamoto T, Takeda K, Sato S, Sanjo H, Uematsu S, et al. Key function for the Ubc13 E2 ubiquitin-conjugating enzyme in immune receptor signaling. *Nat Immunol*. 2006 Sep;7(9):962-70.
363. Laine A, Topisirovic I, Zhai D, Reed JC, Borden KL, Ronai Z. Regulation of p53 localization and activity by Ubc13. *Mol Cell Biol*. 2006 Dec;26(23):8901-13.
364. Pulvino M, Liang Y, Oleksyn D, DeRan M, Van Pelt E, Shapiro J, et al. Inhibition of proliferation and survival of diffuse large B-cell lymphoma cells by a small-molecule inhibitor of the ubiquitin-conjugating enzyme Ubc13-Uev1A. *Blood*. 2012 Aug 23;120(8):1668-77.
365. Foster LJ, Chan QW. Lipid raft proteomics: more than just detergent-resistant membranes. *Subcell Biochem*. 2007;43:35-47.
366. Subramaniam S, Fahy E, Gupta S, Sud M, Byrnes RW, Cotter D, et al. Bioinformatics and systems biology of the lipidome. *Chem Rev*. 2011 Oct 12;111(10):6452-90.
367. Baruthio F, Quadroni M, Ruegg C, Mariotti A. Proteomic analysis of membrane rafts of melanoma cells identifies protein patterns characteristic of the tumor progression stage. *Proteomics*. 2008 Nov;8(22):4733-47.
368. Arielly SS, Ariel M, Yehuda R, Scigelova M, Yehezkel G, Khalaila I. Quantitative analysis of caveolin-rich lipid raft proteins from primary and metastatic colorectal cancer clones. *J Proteomics*. 2012 May 17;75(9):2629-37.
369. Alomari M, Mactier S, Kaufman KL, Best OG, Mulligan SP, Christopherson RI. Profiling the Lipid Raft Proteome from Human MEC1 Chronic Lymphocytic Leukemia Cells. *Journal of Proteomics & Bioinformatics*. 2014 Jan 1,(S7):1.

370. Foster LJ. Moving closer to the lipid raft proteome using quantitative proteomics. *Methods Mol Biol.* 2009;528:189-99.
371. Cao MY, Shinjo F, Heinrichs S, Soh JW, Jongstra-Bilen J, Jongstra J. Inhibition of anti-IgM-induced translocation of protein kinase C beta I inhibits ERK2 activation and increases apoptosis. *J Biol Chem.* 2001 Jul 6;276(27):24506-10.
372. Jongstra-Bilen J, Wielowieyski A, Misener V, Jongstra J. LSP1 regulates anti-IgM induced apoptosis in WEHI-231 cells and normal immature B-cells. *Mol Immunol.* 1999 Apr;36(6):349-59.
373. Brown JR, Hillmen P, O'Brien S, Barrientos JC, Reddy NM, Coutre SE, et al. Extended follow-up and impact of high-risk prognostic factors from the phase 3 RESONATE study in patients with previously treated CLL/SLL. *Leukemia.* 2018 Jan;32(1):83-91.
374. Cunningham D, Hawkes EA, Jack A, Qian W, Smith P, Mouncey P, et al. Rituximab plus cyclophosphamide, doxorubicin, vincristine, and prednisolone in patients with newly diagnosed diffuse large B-cell non-Hodgkin lymphoma: a phase 3 comparison of dose intensification with 14-day versus 21-day cycles. *Lancet.* 2013 May 25;381(9880):1817-26.
375. Wilson WH, Sin-Ho J, Pitcher BN, Hsi ED, Friedberg J, Cheson B, et al. Phase III Randomized Study of R-CHOP Versus DA-EPOCH-R and Molecular Analysis of Untreated Diffuse Large B-Cell Lymphoma: CALGB/Alliance 50303. *Blood.* 2016 DEC 2;128(22).
376. Goede V, Fischer K, Engelke A, Schlag R, Lepretre S, Montero LF, et al. Obinutuzumab as frontline treatment of chronic lymphocytic leukemia: updated results of the CLL11 study. *Leukemia.* 2015 Jul;29(7):1602-4.
377. Vitolo U, Trneny M, Belada D, Burke JM, Carella AM, Chua N, et al. Obinutuzumab or Rituximab Plus Cyclophosphamide, Doxorubicin, Vincristine, and Prednisone in Previously Untreated Diffuse Large B-Cell Lymphoma. *J Clin Oncol.* 2017 Nov 1;35(31):3529-37.
378. Davies AJ, Caddy J, Maishman T, Barrans S, Mamot C, Care M, et al. A Prospective Randomised Trial of Targeted Therapy for Diffuse Large B-Cell Lymphoma (DLBCL) Based upon Real-Time Gene Expression Profiling: The Remodl-B Study of the UK NCRI and SAKK Lymphoma Groups (ISRCTN51837425). *Blood.* 2015 DEC 3;126(23).
379. Cheson BD, Horning SJ, Coiffier B, Shipp MA, Fisher RI, Connors JM, et al. Report of an international workshop to standardize response criteria for non-Hodgkin's

lymphomas. NCI Sponsored International Working Group. J Clin Oncol. 1999 Apr;17(4):1244.